



**MONASH** University

**Effect of *Helicobacter pylori* Interactions with Host  
Epithelial Cells on Inflammation and Disease**

**Kimberley Natalie D'Costa**

*Bachelor of Biotechnology (with Honours)*

A thesis submitted for the degree of *Doctor of Philosophy* at  
Monash University in 2017

Hudson Institute of Medical Research  
Faculty of Medicine, Nursing and Health Sciences

## **Copyright notice**

© Kimberley Natalie D’Costa (2018)

I certify that I have made all reasonable efforts to secure copyright permissions for third-party content included in this thesis and have not knowingly added copyright content to my work without the owner's permission.



# TABLE OF CONTENTS

Table of contents.....	iii
Publications.....	v
Thesis Declaration 1.....	vi
Thesis Declaration 2.....	viii
Acknowledgements.....	ix
List of Abbreviations.....	xi
Thesis Summary.....	xv

## Chapter 1: Introduction

1.1. <i>Helicobacter pylori</i> .....	1
1.2. <i>Bacterial factors contributing to colonization and virulence</i> .....	2
1.2.1. Colonization and adherence.....	2
1.2.2. <i>cag</i> Pathogenicity Island ( <i>cag</i> PAI).....	3
1.2.3. Cytotoxin-associated gene A (CagA).....	5
1.2.4. Peptidoglycan (PG).....	5
1.2.5. Vacuolating cytotoxin A (VacA).....	7
1.3. <i>Cholesterol-rich microdomains in eukaryotes and prokaryotes</i> .....	9
1.4. <i>Alternate host-pathogen interactions affecting bacterial colonization and H. pylori-associated disease</i> .....	12
1.5. <i>NOD-like receptors (NLRs)</i> .....	14
1.6. <i>Roles for NOD1 in the host beyond mediating anti-bacterial immunity</i> .....	19
1.7. <i>Aims of this study</i> .....	21

## Chapter 2: A *Helicobacter pylori* homolog of eukaryotic flotillin is involved in cholesterol accumulation, epithelial cell responses and host colonization

2.1. <i>Summary</i> .....	23
2.2. <i>Manuscript - A Helicobacter pylori homolog of eukaryotic flotillin is involved in cholesterol accumulation, epithelial cell responses and host colonization</i> .....	25
2.3. <i>Discussion</i> .....	45

**Chapter 3: Modifications of *Helicobacter pylori* peptidoglycan during host adaptation affect NOD1-mediated gastric epithelial cell responses**

3.1. <i>Summary</i> .....	47
3.2. <i>Manuscript</i> - Modifications in muropeptide composition arising from mouse adaptation of a human <i>Helicobacter pylori</i> isolate have an impact on host-specific NOD1 responses.....	49
3.3. <i>Discussion</i> .....	100

**Chapter 4: Novel host responses triggered by the NOD1 signaling pathway during long-term *Helicobacter pylori* infection favors bacterial persistence *in vivo***

4.1. <i>Introduction</i> .....	102
4.2. <i>Materials and Methods</i> .....	104
4.3. <i>Results</i> .....	112
4.4. <i>Discussion</i> .....	124

**Chapter 5: Final Discussion and Future Directions.....128**

**Appendix 1.....136**

**Appendix 2.....152**

**References.....169**

## **PUBLICATIONS**

### **Chapter 2**

M.L. Hutton\*, K. D’Costa\*, A.E. Rossiter, L. Wang, L. Turner, D.L. Steer, S.L. Masters, B.A. Croker, M. Kaparakis-Liaskos, R.L. Ferrero. *A Helicobacter pylori homolog of eukaryotic flotillin is involved in cholesterol accumulation, epithelial cell responses and host colonization.* – **Published, 08 June 2017, Frontiers in Cellular and Infection Microbiology.**

*\*co-first authors*

### **Chapter 3**

K. D’Costa, L.S. Tran, C. Ecobichon, S. Hicham, A. Guanizo, T.P. Stinear, R. Legaie, R. Wheeler, A. De Paoli, H. Tye, C.C. Allison, D.L. Steer, J. Ferrand, S.E. Girardin, I.G. Boneca & R.L. Ferrero. *Modifications in muropeptide composition arising from mouse adaptation of a human Helicobacter pylori isolate have an impact on host-specific NOD1 responses.* – **Prepared for submission, May 2018, mBio.**

### **Appendix 1**

K. D’Costa, M. Chonwerawong, L.S. Tran & R.L. Ferrero. *Mouse models of Helicobacter infection and gastric pathologies.* – **Accepted for publication, 02 May 2018, Journal of Visualized Experiments.**

### **Appendix 2**

L.S. Tran, D. Tran, A. De Paoli, K. D’Costa, S.J. Creed, G.Z. Ng, L. Le, P. Sutton, J. Silke, U. Nachbur & R.L. Ferrero. *NOD1 is required for Helicobacter pylori induction of IL-33 responses in gastric epithelial cells.* - **Published, 02 February 2018, Cellular Microbiology.**

## THESIS DECLARATION - 1

I hereby declare that this thesis contains no material which has been accepted for the award of any other degree or diploma at any university or equivalent institution and that, to the best of my knowledge and belief, this thesis contains no material previously published or written by another person, except where due reference is made in the text of the thesis.

This thesis includes **1** original paper published in a peer-reviewed journal. The core theme of the thesis is the characterization of novel host-pathogen interactions in *Helicobacter pylori* infection. The ideas, development and writing up of all the papers in the thesis were the principal responsibility of myself, the student, working within the Hudson Institute of Medical Research, Faculty of Medicine, Nursing and Health Sciences under the supervision of A/Prof. Richard Ferrero and Dr. Le Son Tran.

The inclusion of co-authors reflects the fact that the work came from active collaboration between researchers and acknowledges input into team-based research.

In the case of **Chapter 2**, my contribution to the work involved the following:

Thesis Chapter	Publication Title	Status	Nature and % of student contribution	Co-author name(s) Nature and % of Co-author's contribution*	Co-author(s), Monash student
<b>2</b>	A <i>Helicobacter pylori</i> homolog of eukaryotic flotillin is involved in cholesterol accumulation, epithelial cell responses and host colonization	<b>Published</b>	Involved in project conception, designed and performed experiments, interpreted the data and revised manuscript, <b>50%</b>	<ol style="list-style-type: none"> <li>1. Dr. Melanie L. Hutton – Involved in project conception, designed and performed initial experiments, interpreted the data and drafted initial manuscript, <b>39.5%</b></li> <li>2. Dr. Amanda E. Rossiter – provided expertise in bacterial mutagenesis, <b>0.25%</b></li> <li>3. Ms. Lin Wang – performed in vitro co-culture assays, <b>0.25%</b></li> <li>4. Dr. Lorinda Turner – assisted with generation of <i>H. pylori</i> mutants, <b>0.5%</b></li> <li>5. Dr. David L. Steer – performed mass spectrometric analysis, <b>0.5%</b></li> <li>6. Dr. Seth Masters – provided expertise with isolating primary BMDMs, <b>0.25%</b></li> <li>7. Dr. Ben L. Croker - provided expertise with isolating primary BMDMs, <b>0.25%</b></li> <li>8. Dr. Maria Kaparakis-Liaskos –</li> </ol>	<b>No</b>

				involved in project conception and provided input into manuscript, <b>1%</b>	
				9. <i>A/Prof. Richard Ferrero</i> – developed original project concept, provided research direction and revised manuscript, <b>7.5%</b>	

I have not renumbered sections of submitted or published papers in order to generate a consistent presentation within the thesis.

**Student signature:**



**Date:** 06/05/2018

The undersigned hereby certify that the above declaration correctly reflects the nature and extent of the student's and co-authors' contributions to this work. In instances where I am not the responsible author I have consulted with the responsible author to agree on the respective contributions of the authors.

**Main Supervisor signature:**

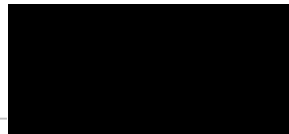


**Date:** 06/05/2018

## **THESIS DECLARATION - 2**

This thesis contains no material which has been accepted for the award of any other degree or diploma at any university or equivalent institution and that, to the best of my knowledge and belief, this thesis contains no material previously published or written by another person, except where due reference is made in the text of the thesis.

**Signature:**

A solid black rectangular box used to redact the signature of the author.

**Print Name:** Kimberley Natalie D'Costa

**Date:** 06/05/2018

## ACKNOWLEDGEMENTS

First and foremost, I would like to extend my sincere gratitude to my supervisor, A/Prof. Richard Ferrero, for your patience and advice during my PhD. You have been an excellent mentor (and sometimes a laboratory “dad”) for the past 4 years. Your constant enthusiasm and encouragement were crucial to the success of the project and the completion of this thesis. I am thankful for all the opportunities that have enabled me to learn and grow not only as an independent and capable scientist, but also as a confident young woman.

I would also like to express my gratitude to my co-supervisor, Dr. Le Son Tran, whose dedication to Science is inspiring. Thank you for your constant motivation and help in the lab - I would have never survived those numerous mouse sacrifices and failed western blots without you. I will miss our long conversations about publications, future experiments and research in general.

A special shout out to Dr. Maria Kaparakis-Liaskos, who first recognized my passion for medical research and introduced me to the fascinating world of *Helicobacter pylori* and NOD1. Thank you also to Dr. Melanie Hutton, for all your valuable help with the flotillin manuscript and for sharing the many tears involved with the publication process.

To all the present and past members of the Gastrointestinal Infection and Inflammation laboratory - especially Jo, Amanda, Julia and Michelle; I would like to thank you all for your scientific help and more importantly making life in the lab a little more tolerable. Thanks also to the Centre for Innate Immunity and Infectious Diseases and Prof. Paul Hertzog, for providing valuable feedback, answering my numerous stupid questions, sharing reagents and always creating a positive work environment. It has been a joy to be part of CiiiD!

The support and encouragement of my family and friends around the world has been indispensable. I would like to particularly acknowledge my closest friend, Viroshi, who has always made time to listen to me rant. Our many coffee and dinner dates have been key to keeping me sane. A special thank you also to Alison and Hendrika,

who always understood what I was going through and whose advice and encouragement, has meant the world to me.

To Rukan, thank you for your patience and forbearance during my PhD journey. I am so glad that you had my back and never let me give up, even when I thought it was too hard. This thesis would probably never exist without you.

Finally, I cannot express my love and gratitude enough to my parents, for always believing in me and supporting my choices. Mum and Dad, without you I would have never made it this far. This thesis is dedicated to you - I hope I have made you proud!



## LIST OF ABBREVIATIONS

<b>AGS</b>	Human adenocarcinoma cell line (ATCC CRL-1739)
<b>APC</b>	Antigen presenting cell
<b>APAF1</b>	Apoptotic protease activation factor 1
<b>ASC</b>	Apoptosis-associated speck-like protein
<b>BabA</b>	Blood group antigen binding adhesin
<b><i>B. burgdorferi</i></b>	<i>Borrelia burgdorferi</i>
<b>BIR</b>	Baculovirus inhibitor of apoptosis protein repeat
<b><i>B. halodurans</i></b>	<i>Bacillus halodurans</i>
<b>BHI</b>	Brain heart infusion
<b><i>B. subtilis</i></b>	<i>Bacillus subtilis</i>
<b>CagA</b>	Cytotoxin-associated gene A
<b><i>cagPAI</i></b>	<i>cag</i> Pathogenicity island
<b>CARD</b>	Caspase activation and recruitment domain
<b>cfu</b>	Colony forming units
<b>CO<sub>2</sub></b>	Carbon dioxide
<b>ConA</b>	Concanavalin A
<b>COX-2</b>	Cyclooxygenase-2
<b><i>C. trachomatis</i></b>	<i>Chlamydia trachomatis</i>
<b>Cxcl1/KC</b>	C-X-C motif ligand 1
<b>Cxcl2/MIP-2</b>	C-X-C motif ligand 2
<b>DAB</b>	3,3'- Diaminobenzidine
<b>°C</b>	° Celsius
<b>DMEM</b>	Dulbecco's modified eagle medium
<b>DRM</b>	Detergent-resistant microdomain
<b><i>E. coli</i></b>	<i>Escherichia coli</i>
<b>EDTA</b>	Ethylenediaminetetraacetic acid
<b>EGFR</b>	Epidermal growth factor receptor
<b>EPIYA</b>	Glu-Pro-Ile-Tyr-Ala
<b>ERK</b>	Extracellular signal-related kinase 1
<b>FACS</b>	Fluorescence-activated cell sorting
<b>FCS</b>	Foetal calf serum
<b>g</b>	Gram (s)

<b>GEC</b>	Gastric epithelial cell (s)
<b>GM</b>	GlcNAc-(anhydro)MurNAc
<b>GPI</b>	Glycosylphosphatidylinositol
<b>h</b>	Hour (s)
<b>H&amp;E</b>	Haematoxylin and Eosin
<b>HBA</b>	Horse Blood Agar
<b>hBD2</b>	Human beta defensin 2
<b>HBSS</b>	Hank's Balanced Salt Solution
<b>hNOD1</b>	Human NOD1
<b><i>H. pylori</i></b>	<i>Helicobacter pylori</i>
<b>Hsp60</b>	Heat shock protein 60
<b>iE-DAP</b>	$\gamma$ -D-glutamyl- <i>meso</i> -diaminopimelic acid
<b>IFN-<math>\gamma</math></b>	Interferon- $\gamma$
<b>IHC</b>	Immunohistochemistry
<b>IL-1<math>\beta</math></b>	Interleukin-1 beta
<b>IL-2</b>	Interleukin-2
<b>IL-6</b>	Interleukin-6
<b>IL-8</b>	Interleukin-8
<b>IL-10</b>	Interleukin-10
<b>IL-17</b>	Interleukin-17
<b>IL-18</b>	Interleukin-18
<b>iNOS</b>	Nitric oxide synthase pathway
<b>JNK</b>	c-Jun N-terminal kinase
<b>kb</b>	Kilobase
<b>KO</b>	Knock-out animal
<b>LPS</b>	Lipopolysaccharide
<b>LRR</b>	Leucine Rich Repeat
<b><math>\mu</math></b>	Micro
<b>m</b>	Milli
<b>M</b>	Molar
<b>MAMP</b>	Microbial-associated molecular pattern (s)
<b>MAPK</b>	Mitogen-activated protein kinase
<b>MDP</b>	Muramyl dipeptide

<b>min</b>	Minute (s)
<b>MIP-1<math>\alpha</math></b>	Macrophage inflammatory protein-1 $\alpha$
<b>nNod1</b>	Mouse Nod1
<b>ml</b>	Millilitre (s)
<b>MOI</b>	Multiplicity of infection
<b>n</b>	Nano
<b>NF-<math>\kappa</math>B</b>	Nuclear Factor–kappa B
<b>NLR</b>	NOD-Like Receptor (s)
<b>NOD1</b>	Nucleotide-binding oligomerization domain 1
<b>OipA</b>	Outer inflammatory protein A
<b>OMV</b>	Outer membrane vesicle (s)
<b>PACAP</b>	Pituitary adenylate cyclase-activating polypeptide
<b>PaCS</b>	Particle-rich cytoplasmic structure
<b>PBS</b>	Phosphate buffered saline
<b>PBST</b>	PBS + 0.05% Tween
<b>PG</b>	Peptidoglycan
<b>PGE<sub>2</sub></b>	Prostaglandin E2
<b>PI</b>	Propium iodide
<b>PMN</b>	Polymorphoneutrophil/ Polymorphonuclear leukocyte
<b>pmol</b>	Picomole (s)
<b>PRR</b>	Pathogen recognition receptor
<b>PYD</b>	Pyrin-containing domain
<b>RIPK2</b>	Receptor interacting serine/threonine-protein kinase 2
<b>RPMI</b>	Roswell Park Memorial Institute 1640 cell culture medium
<b>RT</b>	Room temperature
<b>sec</b>	Second (s)
<b>SabA</b>	Sialic acid binding adhesin
<b><i>S. flexneri</i></b>	<i>Shigella flexneri</i>
<b>SNP</b>	Single nucleotide polymorphism (s)
<b>SPFH</b>	Stomatin, Prohibitin, Flotillin, and HflK/C
<b><i>S. typhimurium</i></b>	<i>Salmonella</i> subspecies <i>enterica</i> serovar Typhimurium
<b>T4SS</b>	Type 4 Secretion System

<b>TCT</b>	Tracheal cytotoxin
<b>Th</b>	T helper cell
<b>TLR</b>	Toll-like receptor
<b>TNF-<math>\alpha</math></b>	Tumor necrosis factor $\alpha$
<b>TUNEL</b>	Terminal deoxynucleotidyl transferase dUTP nick end labeling
<b>u</b>	Units
<b>v</b>	Volume
<b>VacA</b>	Vacuolating cytotoxin-A
<b>w</b>	Weight
<b>WT</b>	Wild-type
<b>x</b>	Times

## THESIS SUMMARY

The pathogen *Helicobacter pylori* (*H. pylori*) is highly adapted to the human stomach and has developed various strategies to enable its chronic persistence in this site. *H. pylori* has a demonstrated ability to acquire cholesterol from host epithelial cells and subsequently incorporate it into its own cell membrane, similar to the cholesterol-enriched microdomains in eukaryotic cells, commonly known as “lipid rafts”. However, the potential role for this *H. pylori* membrane cholesterol in host-pathogen interactions not been described. In Chapter 2, we demonstrate that *H. pylori* bacteria contain lipid raft-like structures and the raft-associated flotillin-like protein, HP0248. *H. pylori* HP0248 was observed to facilitate the association of exogenous cholesterol with the bacterial cell membrane. Eukaryotic flotillin-like proteins have been identified in other bacterial species, however, this is the first report to investigate the functions of one of these proteins in bacterial pathogenesis. Importantly, we showed that HP0248 is involved in *H. pylori* interactions with host cells, specifically playing a role in the induction in gastric epithelial cells of cytoskeletal rearrangements and pro-inflammatory responses via the *H. pylori* *cag* type IV secretion system (T4SS). *H. pylori* *hp0248* mutants were also affected in their ability to establish a chronic infection in mice. Taken together, the data demonstrate important roles for *H. pylori* flotillin in host-pathogen interactions and suggest that HP0248 may be required for the organization of virulence proteins into membrane raft-like structures in this pathogen.

The *H. pylori* *cag* T4SS is a major virulence factor that is encoded by a 40 kilobase [1] locus known as the *cag* pathogenicity island (*cag*PAI). It is well established that infection with *cag*PAI-positive *H. pylori* strains is associated with higher levels of Interleukin-8 (IL-8) production in gastric epithelial cells, more severe inflammation and tissue damage, leading to an increased risk of gastric cancer. These effects on epithelial cells are mediated by the actions of the T4SS, which is responsible for the delivery of the bacterial effectors, cytotoxin-associated gene A (CagA) and peptidoglycan (PG), into the host cell cytoplasm. It has been shown that *H. pylori* interactions with host epithelial cells via the T4SS result in activation of a pro-inflammatory signaling cascade mediated by the intracellular pattern recognition receptor (PRR), Nucleotide-binding oligomerization domain 1 (NOD1). NOD1 in turn

activates the transcription factor, Nuclear Factor- $\kappa$ B (NF- $\kappa$ B), which ultimately results in the production of pro-inflammatory responses. Interestingly, human and mouse NOD1 have evolved to detect slightly different side chains of bacterial PG. In Chapter 3, we investigated host-specific NOD1 signaling using a human *cagPAI*<sup>+</sup> *H. pylori* isolate, strain 245, and its mouse-adapted variant, 245m3. Prior to the inception of this project, it was observed that sequential passage of *H. pylori* 245 resulted in the generation of a mouse-adapted variant, 245m3, which was impaired in its ability to induce NF- $\kappa$ B responses in human gastric epithelial cells. Based on the implications of PG composition on NOD1 signaling, we hypothesized that reduced NF- $\kappa$ B activation by *H. pylori* 245m3 in human cells may be associated with modifications in its cell wall PG composition. Indeed, we showed that *H. pylori* 245m3 retained a functional T4SS, but interestingly, displayed a 2.6-fold increase in murine Nod1-specific GM-Tetra<sub>DAP</sub> relative to the human NOD1-specific GM-Tri<sub>DAP</sub> in its cell wall. We further demonstrated that *H. pylori* 245m3 was affected in its ability to induce NOD1-dependent pro-inflammatory responses in human gastric epithelial cells. In contrast, this strain induced higher chemokine production in murine epithelial cells and embryonic fibroblasts, compared to the human clinical isolate, 245. This is the first study to demonstrate that a modification in peptidoglycan composition during host adaptation renders *H. pylori* more detectable by the host immune system.

Finally, Chapter 4 describes investigations towards an understanding of the functions of the NOD1 signaling pathway during long-term *H. pylori* infection. Previous studies established a central role for the NOD1 receptor in promoting protective immunity in the host and bacterial clearance in response to acute *H. pylori* infection *in vivo*, yet its role in chronic infection had yet to be explored. Furthermore, while NOD1 has been described as a mediator of apoptosis and cell survival responses in cancer models, similar functions in response to microbial infection currently remain unknown. In the present study, we observed reduced bacterial loads in *Nod1*<sup>-/-</sup> mice during chronic infection with *H. pylori* (8 weeks post-infection), an observation that is in contrast to the established role for NOD1 in host defense. These *Nod1*<sup>-/-</sup> mice displayed significantly increased pro-inflammatory gastric cytokine as well as splenocyte T cell responses, when compared to wild type animals. However, interestingly, we also observed decreased inflammation and immune cell infiltration to the gastric mucosa

in these animals. In addition, the stomachs of these *Nod1*<sup>-/-</sup> mice exhibited a significant increase in TUNEL positive cells, thus suggesting a role for NOD1 in suppressing cell death via apoptosis *in vivo*.

Overall, this thesis describes a characterization of the novel mechanisms by which *H. pylori* interacts with host cells and the roles of these interactions in its establishment of infection and persistence in the human gastric mucosa. The knowledge gained from these studies enables us to better understand, manage and prevent disease caused by *H. pylori*, and potentially other Gram-negative pathogens detected by the NOD1 signaling pathway. Furthermore, our findings also highlight the need for improved therapies that target lipid raft-like structures and/or cell wall biosynthesis in *H. pylori*.

## **Chapter 1: Introduction**

### ***1.1. Helicobacter pylori***

*Helicobacter pylori* (*H. pylori*) is a spiral shaped, Gram-negative, human pathogen prevalent in all societies around the world. Although it was first identified *in vitro* in 1982, the bacterium is thought to have been in humans since their migration out of East Africa approximately 58,000 years ago [2]. *H. pylori* colonizes the harsh environment of the stomach and is unable to survive outside the human body for long periods [3]. Transmission of the bacterium thus occurs predominantly by close person-to-person contact via either oral-oral, gastric-oral and/or fecal-oral routes [4]. *H. pylori* is non-invasive and usually found in the gastric mucus layer, where it creates a highly oxidative state on interaction with phagocytic cells like macrophages [5]. It is thought that the bacterium obtains nutrients diffusing from the intercellular junctions of normal, metaplastic and neoplastic gastric epithelium and utilizes these compounds for its growth and metabolism [5, 6]. As such, *H. pylori* is a fastidious bacterium, requiring a microaerobic atmosphere and the presence of serum, blood or other supplements in the laboratory growth medium [7-9]. The bacteria also rapidly lose viability in the stationary phase of growth, as a result of cell lysis, as well as prolonged exposure to atmospheric levels of oxygen.

Although most individuals infected with *H. pylori* are asymptomatic and display chronic gastritis, some develop more severe disease, including peptic and duodenal ulcers [10]. Importantly, *H. pylori* has also been implicated as the strongest known risk factor in 75% of the cases of gastric cancer and hence is classified as a Type 1 carcinogen [11, 12]. *H. pylori*-dependent gastric cancer can be classified into two broad groups: gastric adenocarcinoma and gastric mucosa-associated lymphoid tissue (MALT), affecting gastric epithelial cells (GECs) or extra-nodal lymphoid tissue sites, respectively [10]. Interestingly, while it is generally thought that the host immune responses generated to combat *H. pylori* infection contribute to gastric cancer development, the precise mechanisms contributing to the chronic persistence of this pathogen, as well as to gastric carcinogenesis, remain ill-defined.



*H. pylori* has a relatively small genome (1.6-1.7 Megabases) and a high mutation frequency, making it one of the most diverse species of bacteria [13, 14]. The prevalence of *H. pylori* infections in developing countries is in the order of approximately 80%, compared to only 15.5% in Australia [15, 16]. This discrepancy is likely due to a range of factors, including differences in hygiene and sanitation levels, use of antimicrobials and genetic predisposition to disease [4]. The severity and incidence of *H. pylori* associated disease continues to rise due to low patient compliance with antimicrobial therapy, as well as increasing rates of antimicrobial resistance in the pathogen [17-19].

## ***1.2. Bacterial factors contributing to colonization and virulence***

The ability of the bacterium to survive in the harsh ecological niche of the stomach indicates the presence of well-adapted virulence factors and mechanisms facilitating adherence, growth and metabolism. Consequently, numerous host, environmental and pathogenic factors, as well as interactions between the three, allow *H. pylori* to colonize humans and cause disease [20].

### **1.2.1. Colonization and adherence**

*H. pylori* contains multiple unipolar flagella that are vital for initial colonization and the establishment of infection [21]. Upon colonization of the gastric mucosa, *H. pylori* facilitates the neutralization of the surrounding pH via the secretion of urease, which hydrolyzes urea to carbon dioxide and ammonia, and thus protects itself from the harsh acidic environment of the stomach [22, 23]. Furthermore, at least 30 outer membrane proteins [24] have been identified by genome sequencing as potentially playing a role in facilitating adherence of the bacterium to host cells [25]. The bacterial adhesion factors blood group antigen binding adhesin (BabA), sialic acid binding adhesin (SabA), outer membrane protein 4 (OmpB) and outer inflammatory protein (OipA) bind to cell surface receptors and thereby initiate contact with the host cell [26]. Adherence to host epithelial cells then allows the bacterium access to nutrients, triggers expression of certain bacterial genes involved in the formation of the Type IV Secretion System (T4SS), and ensures the delivery of other virulence factors [26, 27].

### 1.2.2. *cag* Pathogenicity Island (*cag*PAI)

Virulent strains of *H. pylori* possess the 40 kb *cag* Pathogenicity Island (*cag*PAI) which encodes, approximately 30 genes, most of which are required for the production of a T4SS (Figure 1.1.) [25]. It is estimated that 100% of East Asian *H. pylori* strains and 60% of Western strains possess a *cag*PAI [28, 29]. *cag*PAI positive strains of *H. pylori* are associated with production of higher levels of the pro-inflammatory chemokine, Interleukin-8 (IL-8), in the infected host, thus leading to increased polymorphonuclear (PMN) recruitment, which subsequently results in greater tissue damage and more severe disease [20, 30, 31]. Interestingly, it is this chronic inflammation generated as part of the host immune response directed at controlling *H. pylori* infection that has been implicated as an essential precursor of gastric adenocarcinoma [11].

The T4SS of *H. pylori* is a filamentous surface organelle with a pilus-like structure and comprises of several proteins with homology to the prototype T4SS model seen in *Agrobacterium tumefaciens* (Figure 1.1) [32]. *H. pylori* T4SS attachment to the  $\alpha 5\beta 1$  integrin on GECs facilitates the translocation of bacterial effector molecules, including the highly virulent cytotoxin-associated gene A (CagA) and peptidoglycan (PG), into the host cell [33-36]. Engagement of the bacterial T4SS with the GEC results in the production of pro-inflammatory chemokines and cytokines, including IL-8, via the activation of various transcription factors. The major factors involved in these processes are nuclear factor-kappa B (NF- $\kappa$ B) and mitogen-activated protein kinase (MAPK) members, c-Jun N-terminal kinase (JNK) and extracellular signal-related kinase (ERK) – 1 and 2. Furthermore, the up-regulation of gastrin, a known growth factor and hormone affecting gastric acid secretion in the stomach, allows for the generation of a favorable niche thus enabling bacterial colonization [37-39].

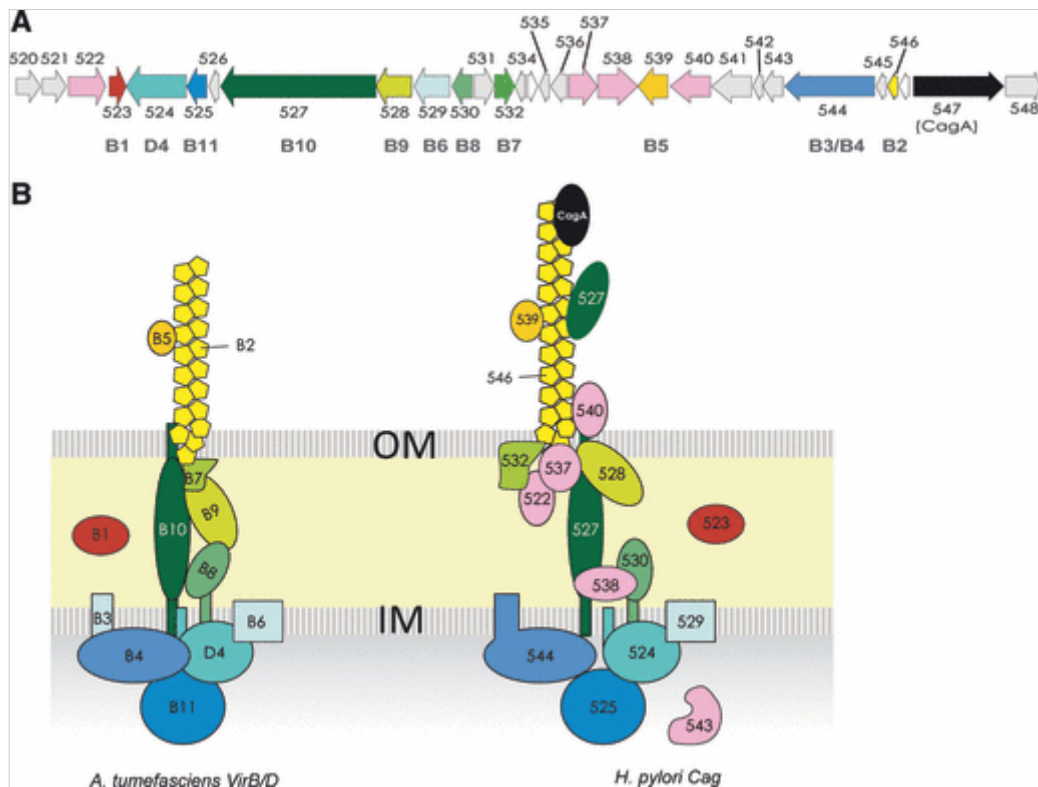


**Figure 1.1: Architecture of the T4SS encoded by the *cagPAI* present in *H. pylori*.**

(A) Graphical representation of the *cagPAI* encoded by the *H. pylori* reference strain, 26695. Each arrow indicates a separate gene labeled with the corresponding “*HP0XXX*” gene numbers identified in the ORF. (B) Comparison of the prototypical T4SS of *A. tumefaciens* with the T4SS encoded by the *H. pylori cagPAI*. The T4SS consists of cytoplasmic proteins (colored in blue), transmembrane proteins (colored in green) and extracellular, pilus proteins (colored in yellow). Proteins labeled in pink are additional components known to associate with the *cag*-T4SS of *H. pylori*. Figure reprinted from Terradot & Waksman, 2011 [40].

### 1.2.3. Cytotoxin-associated gene A (CagA)

CagA is a 120-140 kDa immunogenic protein encoded by the *HP0527/cag26/cagA* gene located on the *cagPAI* [41]. Translocation of CagA via the T4SS has been shown to be dependent on host cholesterol-enriched microdomains or lipid rafts [42]. Upon delivery to the cytoplasm of GECs, CagA is tyrosine phosphorylated by the host kinases, Src and Abl, at multiple sites containing “Glu-Pro-Ile-Tyr-Ala” (EPIYA) motifs (Figure 1.2) [43]. Phosphorylation of CagA results in disruption of cell adhesion and tight junctions, as well as the induction of cell elongation and scattering via actin rearrangement (Figure 1.2) [44]. The latter phenomenon is commonly termed the “hummingbird phenotype” and is typically observed following co-culture of GECs with CagA-positive *H. pylori* strains [45]. CagA has also been shown to enhance chronic inflammation and carcinogenesis via the induction of elevated cell proliferation and expression of host matrix metalloproteinases, activation of anti-apoptotic pathways, loss of cell polarity and genetic instability [46-49]. CagA has thus been classified as a bacterial oncoprotein [50].

### 1.2.4. Peptidoglycan (PG)

Apart from the highly virulent protein, CagA, the *H. pylori* T4SS also delivers bacterial PG to host GECs (Figure 1.2) [35]. PG from *H. pylori* cell walls is brought to be delivered into the host cell as low molecular weight fragments, known as muropeptides. Approximately 15% of the polymeric PG from Gram-negative bacteria is released as muropeptides [51]. Muropeptides have been shown to have a higher biological activity than intact cell walls and trigger a broad range of pro-inflammatory and cytotoxic effects on mammalian host cells, including tissue damage, organ morphogenesis and antimicrobial resistance [52-54].

In addition to the T4SS, PG from the *H. pylori* cell wall can be delivered into host epithelial cells by outer membrane vesicles (OMVs) in a *cagPAI*-independent manner (Figure 1.2) [55]. OMVs are spherical, bi-layered structures spontaneously released from the outer membranes of Gram-negative bacteria and usually range between a size of 20 and 300 nm in diameter [56]. The composition of OMVs varies depending on the bacterial strain, stage of growth and environmental conditions, but usually comprise cell wall constituents, including lipopolysaccharide and PG, in addition to DNA and specific virulence factors, such as toxins [56-58]. The biological roles of

OMVs include toxin delivery, transfer of antibiotic resistance between bacteria and induction of autophagy, hence making them important vehicles in the activation of host innate immune responses [59, 60].

Once internalized, bacterial PG is recognized by the host cytosolic receptor, Nucleotide-binding oligomerization domain- 1 (NOD1), which detects  $\gamma$ -D-glutamyl-*meso*-diaminopimelic acid (iE-DAP), a motif almost exclusively found in the cell walls of Gram-negative bacteria [61]. Upon detection of PG delivered by *H. pylori*, NOD1 initiates a pro-inflammatory signaling cascade via the association with receptor interacting serine/threonine-protein kinase 2 (RIPK2), and the subsequent activation of the NF- $\kappa$ B and MAPK pathways, leading to the downstream production of IL-8 (Figure 1.2) [62-64]. In addition to the canonical signaling pathway, *H. pylori* infection of GECs can also result in the generation of NOD1-dependent type 1-interferon responses [65, 66]. These pro-inflammatory chemokines and cytokines act as chemo-attractants that facilitate the recruitment of immune cells to the site of infection in the gastric mucosa, where bacterial clearance as well as further tissue damage is initiated [20]. NOD1 has also been shown to regulate direct killing of *H. pylori* bacteria in GECs via the production of the antimicrobial peptide, human beta-defensin 2 (hBD-2) [67]. Importantly, these events occur independently of CagA translocation into host cells [35, 55]. *Nod1*<sup>-/-</sup> mice have also been shown to be more susceptible to *H. pylori* infection and colonization, thus establishing the central role of this receptor in promoting protective responses in the host and bacterial clearance *in vivo* [35, 65].

*H. pylori* also utilizes several enzymes that mediate varying PG modifications which may affect bacterial colonization and immune recognition by the host. The PG hydrolase, AmiA, was revealed to mediate the morphological transition of the bacterium from spiral into coccoid shape, thus affecting motility and colonization capacity [68]. Similar functions were elucidated for Csd4, a D, L-carboxypeptidase of PG tripeptide monomers [69]. An additional enzyme, Csd6, was also shown to function in sequence with Csd4, whereby GlcNAc-(anhydro)MurNAc [70]-tripeptide fragments catalyzed by Csd6 are further cleaved into GM-dipeptide structure by Csd4 [69]. These endogenous enzymes thus enable the bacterium to escape detection by NOD1 via reduced production of GM-Tri<sub>DAP</sub>, which subsequently results in enhanced

bacterial colonization in the stomach. Furthermore, N-deacetylase (Pgda) and O-acetyltransferase (PatA) have been shown to protect *H. pylori* from lysozyme degradation, hence conferring a survival advantage to the bacterium [71]. Interestingly, the *H. pylori* lytic transglycosylases, MltD and Slt, which are both lytic transglycosylases or PG cleaving enzymes with muramidase activity, were observed to exhibit no effect on bacterial shape or the expression of flagella, however these proteins were essential for motility and colonization of mice [72, 73]. While non-redundant functions of *H. pylori* MltD and Slt involving PG metabolism have been demonstrated, of importance, is additional data highlighting the strain-specific effects of these enzymes on bacterial growth and function [72, 73].

#### **1.2.5. Vacuolating cytotoxin A (VacA)**

An additional virulence factor present in all *H. pylori* strains is the exotoxin, vacuolating cytotoxin A (VacA). This exotoxin is initially produced as a 140 kDa autotransporter precursor protein that is later cleaved to produce an 88 kDa subunit of mature VacA protein [74, 75]. Furthermore, different allelic variants in the N-terminal (s1a, s1b or s2), intermediate (i1, i2 or i3) and middle (m1 or m2) regions of the *H. pylori vacA* gene have been described. The type of genetic structure present determines the quantity and activity of VacA cytotoxin produced, as well as its clinical relevance [76-79]. Mature VacA enters host cells via cholesterol-rich membrane domains or lipid rafts, where it stimulates vacuolation and affects mitochondrial membrane permeability thus resulting in gastric cell apoptosis [80]. Additionally, it was previously demonstrated that both *H. pylori* toxins, VacA and CagA, interact antagonistically and thereby affect immune responses and disease severity in infected patients [81-83]. VacA also stimulates immunosuppression and inhibits specific T cell proliferation [84]. The toxin functions as a trans-membrane pore to make GECs permeable to urea [85], and is thus thought to aid urease, the aforementioned bacterial virulence factor which neutralizes stomach acidity [86]. The combined actions of VacA and urease ensure the development of chronic *H. pylori* infection by establishing favorable conditions for its growth and evasion of the adaptive immune response.

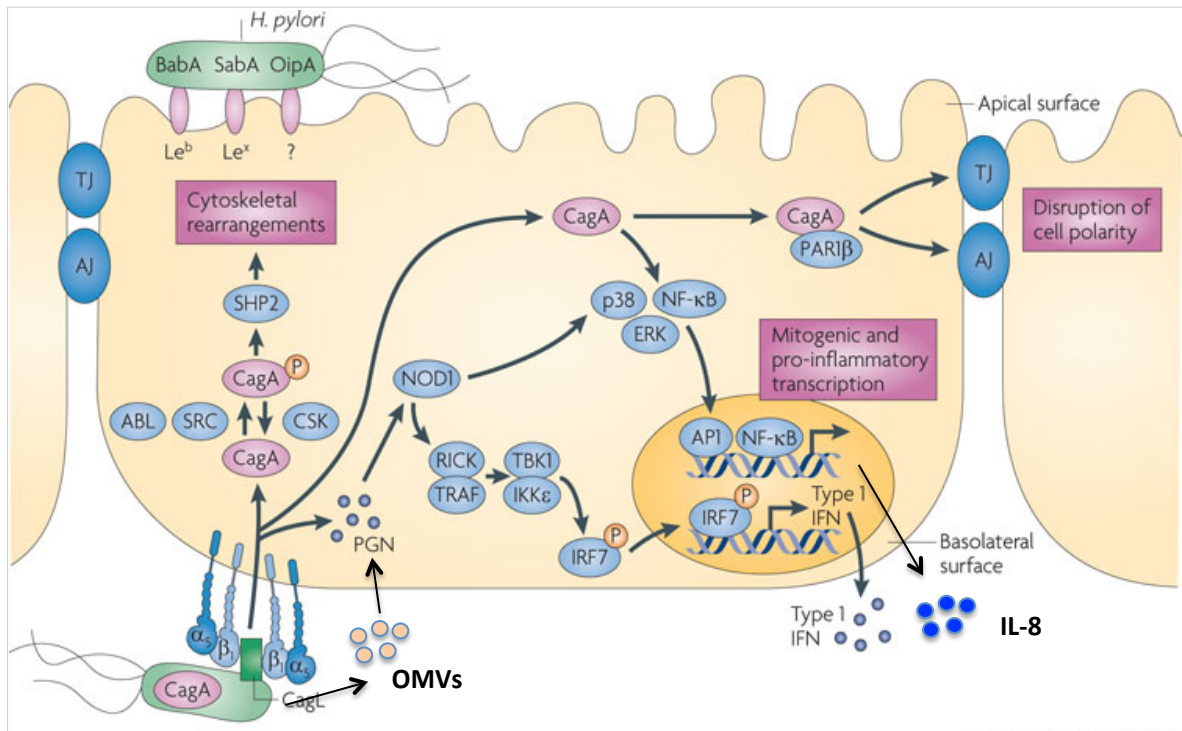


**Figure 1.2: Intracellular host cell interactions initiated by the delivery of the *H. pylori* virulence factors, CagA and Peptidoglycan.**

Several adhesins including BabA, SabA and OipA mediate binding of *H. pylori* to gastric epithelial cells. The bacterium associates with the basolateral integrin  $\alpha_5\beta_1$  to enable translocation of the effector molecules, cagA and PG into the host cell via its T4SS or OMVs. PG is sensed by the cytosolic innate immune receptor NOD1, which subsequently activates the NF- $\kappa$ B, MAPK (via p38, ERK, AP1) and interferon (via IRF7) signaling pathways to induce the release of pro-inflammatory cytokines including IL-8. Translocated CagA is tyrosine phosphorylated and activated by SRC and ABL kinases, leading to cytoskeletal rearrangements. Non-phosphorylated CagA can also trigger the activation of NF- $\kappa$ B and the disruption of cell-cell junctions, which may contribute to the loss of epithelial barrier function. Figure adapted from Polk & Peek, 2010 [11]. AJ, adherens junction; CSK, c-src tyrosine kinase; IFN, interferon; IRF7, interferon regulatory factor 7; RICK, receptor-interacting serine-threonine kinase 2; TJ, tight junction.

### ***1.3. Cholesterol-rich microdomains in eukaryotes and prokaryotes***

It is well established that *H. pylori* exploits various mechanisms involving its cell wall or plasma membrane to facilitate interactions with host epithelial cell cholesterol-rich microdomains, so as to adhere, enter or induce pro-inflammatory signaling cascades in target cells [34, 42, 87]. A study by Inamoto *et al* [88] found that *H. pylori* contained a number of different fatty acids and lipids in its cell membrane. These include cholesterol esters, triglycerides, free fatty acids, cholesterol, diacylglycerols, monoacylglycerols and some glycolipids. Importantly, cholesteryl glucosides account for 25% of the total lipids present in *H. pylori*, including 1.6% of unmodified cholesterol [89-91]. However, *H. pylori* lacks the genes required for the *de novo* synthesis of cholesterol and hence it is likely that the bacterium must obtain this component from an external source, such as the infected host or the growth medium [92, 93].

Wunder and colleagues [90] showed that *H. pylori* follows a cholesterol gradient both *in vitro* and *in vivo*, and can extract cholesterol from the intercellular tight junctions via cholesterol-enriched microdomains, also known as lipid rafts or membrane rafts. Besides containing cholesterol, lipid rafts located on epithelial cell membranes contain large amounts of sphingolipids and proteins (Figure 1.3) [94]. Bacteria use these lipid rafts to attach to host cells and/or as a port of entry into the host [42]. The cholesterol acquired from these domains by *H. pylori* is then converted to cholesterol- $\alpha$ -glucoside by the enzyme cholesterol- $\alpha$ -glucosyltransferase (encoded by the gene *HP0421*), through alpha glucosylation of the free hydroxyl group on the cholesterol steroid nucleus [88]. Cholesterol- $\alpha$ -glucosyltransferase is synthesized as an inactive form in the cytoplasm and is then transported to the membrane where it is then activated [95].

The presence of cholesteryl glucosides in cell membranes of bacteria is a rare occurrence and is seemingly unique to *H. pylori* [89]. Acquisition of host cholesterol is also observed in bacterial species, such as *Chlamydia trachomatis* (*C. trachomatis*) [96], *Salmonella* subspecies *enterica* serovar Typhimurium (*S. typhimurium*) and *Shigella flexneri* (*S. flexneri*) [97]. It is likely that, the inclusion of a host component, such as cholesterol, in the bacterial cell membrane, reduces the ability of the host



immune system to recognize the bacteria as being foreign and thus developing a response against them. Indeed, it was recently demonstrated that the  $\alpha$ -glucosylation of cholesterol enabled *H. pylori* to escape phagocytosis, T cell activation and bacterial clearance *in vivo* [90]. Importantly, *H. pylori* is also able to up-regulate cholesterol gene expression in gastric epithelial cells *in vitro* [98]. Thus, cholesterol acquisition may contribute to a form of molecular mimicry in this pathogen and enhance bacterial pathogenesis.

In eukaryotes, cholesterol is an indispensable constituent of the plasma membrane and is required for many functions in eukaryotic cells, including cell viability, proliferation and for the formation of membrane rafts [99, 100]. Membrane rafts are detergent-resistant microdomains (DRMs) that contain a different assembly of lipids and cholesterol in comparison to the surrounding lipid bilayer (Figure 1.3) [94]. Cholesterol plays an important role in maintaining raft integrity and structure. Indeed, it has been observed that the removal of this constituent by the use of compounds, such as methyl- $\beta$ -cyclodextrin, leads to the dissociation of most proteins and renders membrane rafts non-functional [94, 101].

Membrane rafts control numerous protein-protein and lipid-protein interactions at the cell surface and have been implicated in protein sorting, membrane trafficking, cholesterol metabolism, and signal transduction events [101, 102]. Furthermore, these microdomains further have the unique ability to selectively include or exclude proteins and thus control the interactions at the cell surface [94, 102]. To date, over 100 proteins are known to associate with membrane rafts, including glycosylphosphatidylinositol (GPI) anchored proteins, the Src family of tyrosine kinases and myristoylated or palmitoylated proteins, such as flotillins or reggie proteins (Figure 1.3) [94, 101, 103, 104]. There are two known flotillin proteins: flotillin-1 (reggie-2) and flotillin-2 (reggie-1), both of which associate with membrane rafts [101, 105]. Flotillins belong to the Stomatin, Prohibitin, Flotillin, and HflK/C (SPFH) protein superfamily, whose members share an SPFH domain at their N-terminus [106]. Flotillins also contain a flotillin domain at the C terminus, which is predicted to form coil-coil structures [106]. Importantly, a transmembrane domain was found to be absent from flotillin proteins, which instead interact with the plasma membrane via a hydrophobic region [106].

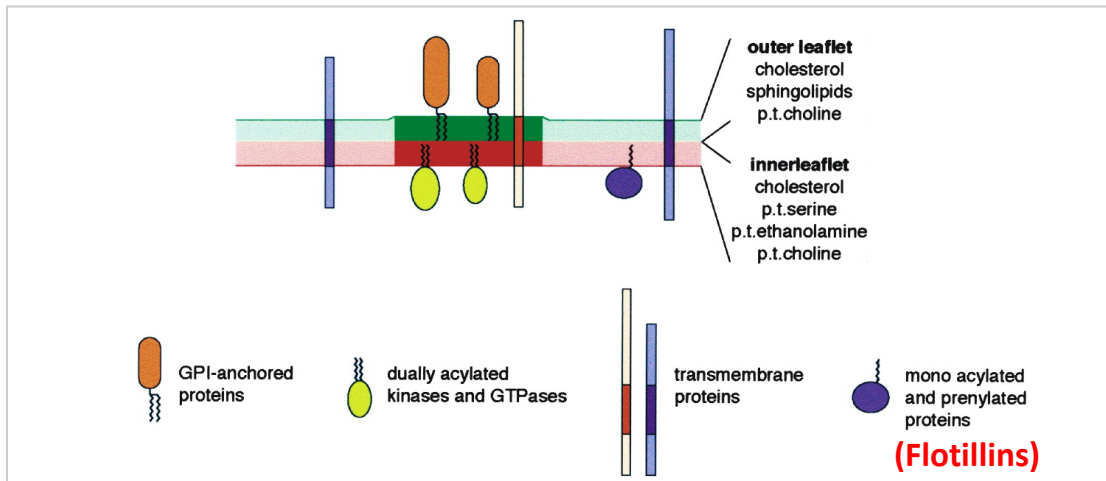


**Figure 1.3: Schematic representation of the typical arrangement and composition of membrane or lipid rafts.**

This diagram depicts the organization of membrane rafts into dynamic assemblies of sphingolipids, cholesterol and proteins, such as GPI-anchored proteins and flotillins, which are located within the exoplasmic leaflet of the phospholipid bilayer of the plasma membrane. Figure adapted from Munro, 2003 [107].

Interestingly, flotillin proteins are highly conserved across human and animal species and also exist in some bacteria, plants and fungi [106]. Bioinformatics analyses indicate that multiple bacterial genomes encode proteins with similarity to flotillin-1 [108]. The best characterized of these bacterial flotillins is the YuaG protein of *Bacillus subtilis* (*B. subtilis*). This flotillin homolog was reported to play roles in a diverse range of cellular functions, including cell division, the maintenance of bacterial shape, and sporulation [109-111]. It has been suggested that bacterial flotillins, such as YuaG, maybe involved in membrane order or organization and are likely to guide the recruitment of specific proteins to defined areas within the membrane [110]. Consistent with this suggestion, *B. subtilis* YuaG was observed to form punctate immunofluorescent staining patterns along the cell membranes of the bacterium [108, 109]. It was further seen to interact with proteins involved in various functions, including protein secretion, cell wall metabolism and signaling processes [110].

The existence of lipid rafts in bacterial cell membranes has also been described in other species including *Bacillus halodurans* (*B. halodurans*), *Staphylococcus aureus* (*S. aureus*) and *Borrelia burgdorferi* (*B. burgdorferi*) [108, 109, 112-114]. From these studies, a further association between bacterial DRMs and proteins required for biofilm formation, signaling, adherence and virulence has been established. Cholesterol thus appears to be not only a key metabolite required for *H. pylori* physiology, but also plays a role in host immune modulation, and ultimately enables survival in the stomach. However, the presence of flotillin-like homologs and membrane rafts in *H. pylori* remains to be elucidated and characterized [115].

#### ***1.4. Alternate host-pathogen interactions affecting bacterial colonization and H. pylori-associated disease***

Bacterial infection of the host is typically detected via the recognition of microbial-associated molecular patterns (MAMPs) by pattern recognition receptors (PRRs) of the innate immune system [116]. This results in the initiation of intracellular signaling cascades, that stimulate pro-inflammatory cytokine and chemokine production by epithelial cells and induce the recruitment of antigen presenting cells (APCs) and lymphocytes, to the site of infection to enable bacterial clearance [6, 117].

*H. pylori* is an extracellular pathogen that is associated with lifelong persistence in infected individuals, thus suggesting the evolution of multiple immune evasion strategies in the bacterium [118]. Following infection of the host, 1% of *H. pylori* bacteria attach to GECs [119]. *H. pylori*-associated ligands, including lipopolysaccharide (LPS) and flagellin, are recognized by toll-like receptors (TLR)-2, 4 and 5 located on host cells [6]. However, interestingly, *H. pylori* LPS is observed to have >100-fold lower biological activity in comparison to LPS from *Escherichia coli* (*E. coli*) [1, 120]. Furthermore, flagellin from *H. pylori* was also shown to exhibit no significant effect on TLR5-mediated pro-inflammatory signaling [121]. Together, these data demonstrate the inefficiency of TLR-driven immunity in response to *H. pylori* infection, and provide evidence for the need to further investigate other immune sensing pathways such as the NOD1-PG signaling axis.

The host defense roles administered by GECs are in contrast to the central role established for tissue macrophages in the development and persistence of *H. pylori*-associated inflammatory disease [122, 123]. Monocytes and other immune cell populations enter the gastric mucosa in response to the production of pro-inflammatory cytokines and chemokines by GECs [6, 124]. Numerous studies have provided evidence for the phagocytosis and survival of *H. pylori* in macrophages, indicating that this may represent an immune evasion mechanism in the bacterium [125, 126]. Formation of autophagosomes has been suggested as being one strategy by which *H. pylori* can survive and multiply in macrophages [125]. Impairment of the nitric oxide synthase pathway (iNOS) in macrophages due to competition from *H. pylori* arginase is another mechanism by which the bacterium is able to resist immune clearance [127]. However, no correlations between *H. pylori* *cag*PAI, VacA and urease, and the evasion of phagocyte killing have been discovered. This finding is indicative of the presence of alternate bacterial factors enabling immune evasion [128]. Thus, while interactions with macrophages contribute to the persistence of *H. pylori* *in vivo*, factors and mechanisms influencing these interactions have yet to be discovered.

*H. pylori* invasion of macrophages also activates the NF- $\kappa$ B signaling pathway via recognition of various bacterial proteins including heat shock protein 60 (Hsp60) [129] and urease [130]. The activation of the NF- $\kappa$ B pathway causes an up-regulation of interleukin-6 (IL-6), tumor necrosis factor- $\alpha$  (TNF- $\alpha$ ), interleukin-1 $\beta$  (IL-1 $\beta$ ), interleukin-18 (IL-18), interferon- $\gamma$  (IFN- $\gamma$ ) and macrophage inflammatory protein-1 $\alpha$  (MIP-1 $\alpha$ ) [6, 131-133]. Production of the immuno-regulatory cytokine interleukin-10 (IL-10) by activated macrophages has also been observed [134]. Release of inflammatory cytokines by macrophages results in gastric inflammation associated with *H. pylori* infection as well as serving as a chemo-attractant for the recruitment of greater numbers of monocytes, macrophages, neutrophils and lymphocytes to the gastric mucosa [123, 128]. *In vitro* studies have also provided evidence for the role of MIP-1 $\alpha$ , and hence mucosal macrophages in the perpetuation of inflammation in *H. pylori* positive patients [131]. Thus, the response by host macrophages appears to promote more destructive tissue damage and chronic disease in the gastric mucosa through initiation of pro-inflammatory signaling cascades.

### ***1.5. NOD-Like Receptors (NLRs)***

NLRs constitute a family of cytosolic innate immune receptors and are characterized by the presence of: a NH<sub>2</sub>-terminal effector binding domain, required for interaction with downstream effector molecules; a central NOD, facilitating self-oligomerization; and a COOH-terminal leucine-rich repeat (LRR) region, responsible for ligand recognition [117, 135]. Members of the NLR family have been identified in varying numbers in animals, plants, bacteria and fungi [136]. In addition to sensing invading pathogens and generating pro-inflammatory responses, NLRs have also been shown to play important roles in the regulation of antigen presentation, detection of intracellular metabolic changes, autophagy, embryo development, cell death, and differentiation of the adaptive immune response [136-139].

The NLR family is further categorized into four subfamilies—NLRA, NLRB, NLRC and NLRP—each characterized by N-terminal structures comprising either: an acidic transactivation domain; a baculovirus inhibitor of apoptosis protein repeat (BIR); a caspase-activation and recruitment domain (CARD); or a Pyrin domain (PYD), respectively [140]. Members of the NLRP group (NLRP1-14) are widely involved in the establishment of multi-protein complexes known as inflammasomes [141]. Stimulation of the inflammasome typically requires two signals: the first of which primes the pathway via NF- $\kappa$ B activation; while the second results in the dimerization of the NLR proteins and the subsequent binding of this dimer to pro-caspase 1, via CARD interactions between pro-caspase 1 and the adaptor protein, apoptosis associated speck-like protein (ASC) [142, 143]. Activation of these cytoplasmic caspase-1 activating platforms results in the processing and release of the pro-inflammatory cytokines, IL-1 $\beta$  and IL-18, as well as the induction of pyroptosis, a form of cell death [144]. NLRP3, the most widely studied NLRP receptor, has been reported to be a major activator of the inflammasome-signaling pathway in innate immune cells (neutrophils, macrophages and dendritic cells) following *H. pylori* infection [145-147]. Infection studies also demonstrated that the critical inflammasome adaptor molecule, ASC, was required for *H. pylori*-mediated production of IL-1 $\beta$  and IL-18 in macrophages and epithelial cells present in the stomach [148, 149]. Furthermore, caspase-1 was shown to have both pro-inflammatory and protective roles during *H. pylori* infection, by modulating T cell

responses via IL-1 $\beta$  and IL-18, respectively [150]. Importantly, gene polymorphisms in *IL1 $\beta$*  and *IL18* are shown to correlate with an enhanced risk of *H. pylori*-associated diseases, including gastric carcinogenesis [151].

NOD1 and NOD2 are the most well characterized members of the NLRC subfamily and differ in the number of central CARD domains present in the receptor (Figure 1.4) [152]. The NOD receptors were first discovered in apoptotic protease activation factor 1 (APAF1) and its nematode homologue (CED-4), both of which are central regulators of programmed cell death [140, 153, 154]. The two proteins also differ in their ligand specificity- NOD1 recognizes an iE-DAP acid residue primarily expressed in peptidoglycan fragments from Gram-negative bacteria and some Gram-positive species, such as *Listeria* and *Mycobacterium tuberculosis* [155, 156], whereas NOD2 detects a muramyl dipeptide (MDP) motif commonly found in peptidoglycan of both Gram-negative and Gram-positive bacteria (Figure 1.4) [157]. Both receptors are expressed in a variety of haemopoietic and non-haemopoietic cell types in the gut and hence play important roles in promoting host defense and the maintenance of homeostasis [158].

Interestingly, human and murine NOD1 have further evolved to sense slightly different forms of muropeptides, namely a tri-peptide stem structure (Tri<sub>DAP</sub>) and a tetra-peptide stem structure (Tetra<sub>DAP</sub>), respectively (Figure 1.5) [155, 159]. Gram-negative pathogens exhibit varying Tri<sub>DAP</sub> versus Tetra<sub>DAP</sub> ratios both within and between bacterial species [51, 68, 72]. The tracheal toxin (TCT) produced by *Bordetella pertussis* is a muropeptide fragment enriched with a GlcNAc-(anhydro)MurNAc [70]-Tetra<sub>DAP</sub> motif, which preferentially activates mouse Nod1 (mNod1) [155, 159]. NOD1-dependent detection of TCT resulted in the initiation of inflammatory responses that subsequently induced maturation and migration of macrophages into the bloodstream [155]. However, this biological activity was shown to be host specific, as mNod1 efficiently recognized TCT, whereas human NOD1 (hNOD1) responded poorly; thus confirming the specificity of NOD1 recognition [155]. Of further significance is data presented by Zarantonelli *et al.*, demonstrating how changes in the muropeptide composition of *Neisseria meningitidis* associated with the development of penicillin resistance, impact on NOD1-dependent responses and bacterial fitness during human infection [160]. Similarly, the Gram-negative

bacterium, *B. subtilis*, has been reported to be a weak inducer of Nod1 activation in mice due to the presence of a higher percentage of amidated GM-Tri<sub>DAP</sub> in its peptidoglycan [61]. Activation of NOD1 signaling also varies between different strains of *H. pylori* (Table 1). As discussed earlier, modifications in *H. pylori* PG have demonstrated effects on cell shape, osmotic stability, immune recognition and thus the overall colonization capacity of the bacterium *in vivo* [69, 161-163]. Repeated passage in mice of a human *cagPAI*<sup>+</sup> strain, *H. pylori* 245, generated a mouse-adapted variant, 245m3, which displayed reduced NF-κB responses in human gastric epithelial cells [164]. Based on the implications of peptidoglycan composition on NOD1 signaling, it is tempting to speculate if reduced NOD1 activation by *H. pylori* 245m3 in human cells may be associated with modifications in its cell wall peptidoglycan. To date, there have been no reports confirming the ability of pathogenic bacteria to alter their peptidoglycan composition during host adaptation, thereby rendering it more detectable by the host innate immune system.

**Table 1: Proportions of Tri- and Tetra-peptides measured by HPLC analysis in different *H. pylori* strains after 24 h of incubation**

<i>H. pylori</i> strain	% of mucopeptides - GM-Tri <sub>DAP</sub>	% of mucopeptides - GM-Tetra <sub>DAP</sub>
26695 [72]	18.9	47.8
N6 [163]	7.4	4.7
B128 [73]	4.6	10.1
NSH57 [161]	9.35	4.87

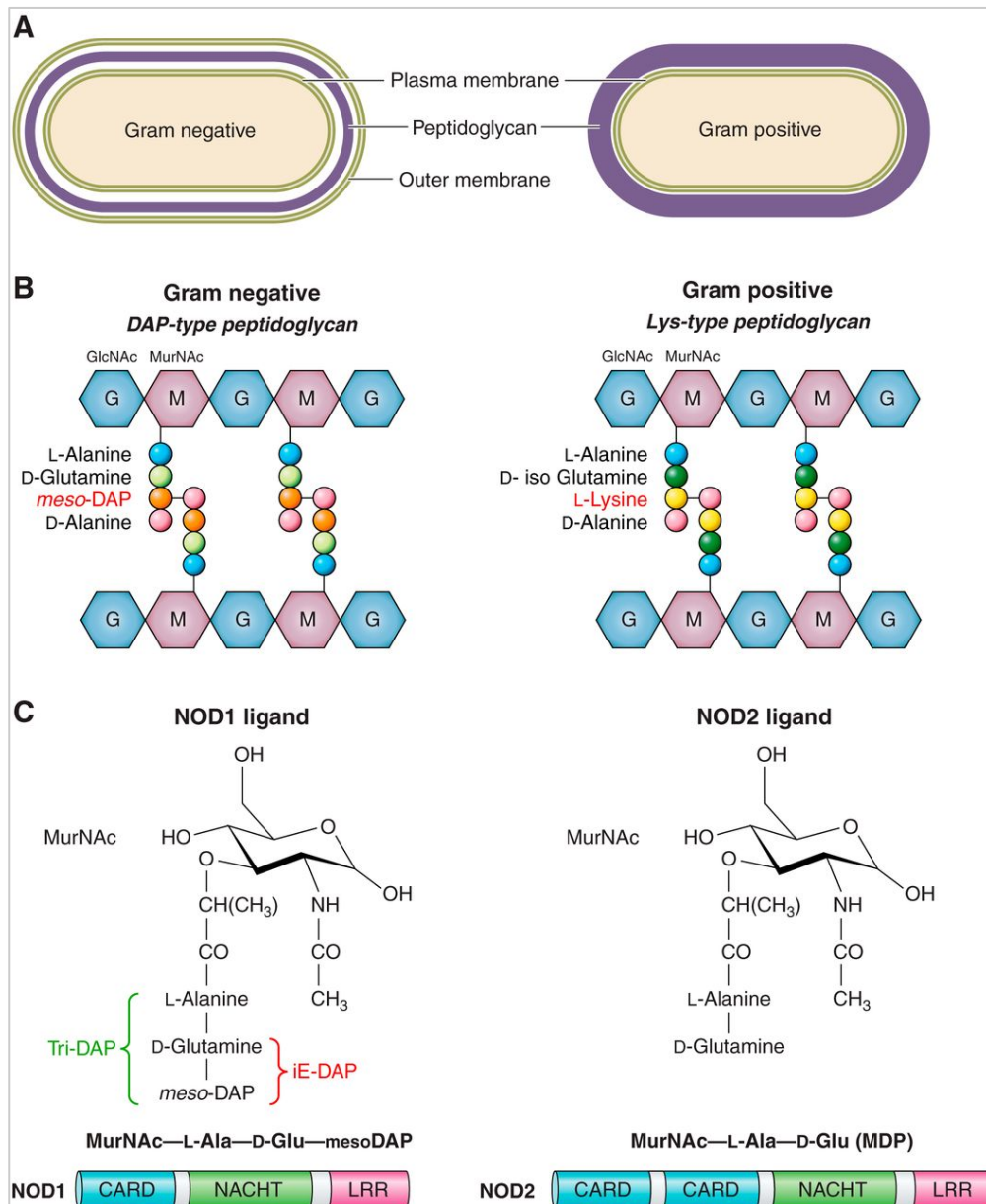


**Figure 1.4: NOD1 and NOD2 recognize bacterial peptidoglycan.**

(A) Composition of the cell walls of Gram-negative and Gram-positive bacteria; (B) Illustration of the basic structure of PG found in Gram-negative (DAP-type PG) and Gram-positive (Lys-type PG) bacteria; (C) NOD1 and NOD2 differ in their ligand specificity – NOD1 detects an *iE*-DAP motif primarily expressed by Gram-negative bacteria; whereas, NOD2 recognized a MDP side chain present in both Gram-positive and Gram-negative bacterial species. Figure reprinted from Motta *et al*, 2015 [136]. *Tri*-DAP, *l*-Ala-*d*-Glu-*meso*-diaminopimelic acid; *iE*-DAP, *d*-Glu-*meso*-diaminopimelic acid; MDP, muramyl dipeptide; GlcNAc, *N*-acetyl-*d*-glucosamine; MurNAc, *N*-acetylmuramic acid.



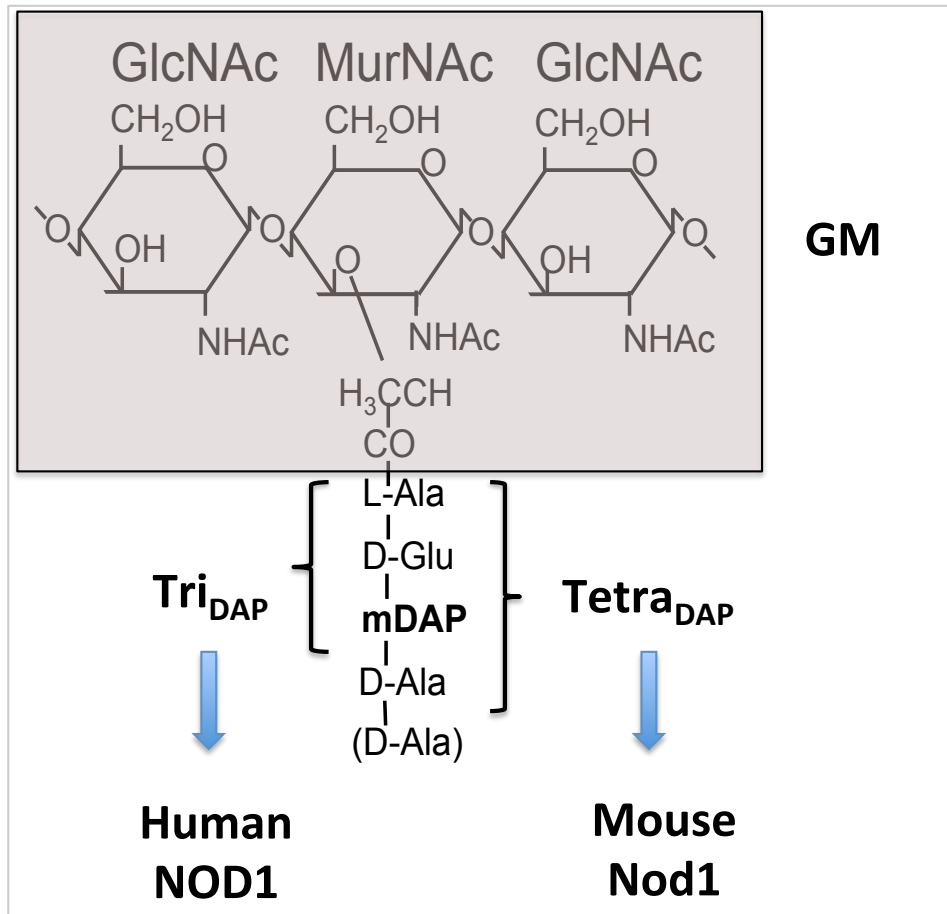


**Figure 1.5: Human and mouse NOD1 recognize different PG ligands**

Human and murine NOD1 have evolved to detect forms of PG from Gram-negative bacteria. Human NOD1 recognizes Tri<sub>DAP</sub>, while mouse Nod1 recognizes Tetra<sub>DAP</sub> which contains an additional alanine motif in its side chain. Figure adapted from Girardin *et al*, 2005 [155].

### ***1.6. Roles for NOD1 in the host beyond mediating anti-bacterial immunity***

Aside from its regulatory role in host defense and inflammation following bacterial infection, current studies indicate additional PG-independent roles for NOD1 via the detection of viruses and parasites, such as Hepatitis C virus and *Trypanosoma cruzi*, respectively [165-167]. Additionally, this intracellular receptor has been implicated in the sensing of altered Rho-GTPase activity and actin cytoskeleton remodeling following microbial infection [168-170].

Increasing evidence also supports a role for NOD1 in mediating transactivation and antigen presentation by dendritic cells, as well as adaptive immune responses via T helper (Th) cell differentiation to a Th2-like phenotype [139, 171, 172]. NOD1 has been shown to induce autophagy in a RIPK2-dependent manner [60], or alternatively by recruiting ATG16L1, a component of the autophagosome, to the plasma membrane at the site of bacterial entry [173]. NOD1 thus has key functions in modulating the fine-tuning of the immune response and maintenance of homeostasis.

As discussed above, NOD1 was originally described as a mediator of apoptosis or cell death [153]. Contradictory studies have subsequently been reported, where on the one hand it is suggested that NOD1 promotes cell proliferation and survival in intestinal tumor and head and neck carcinoma models, whereas it mediated apoptosis in a breast cancer model [174-176]. Nevertheless, while the role of NOD1 in the regulation of cell survival responses in cancer models warrants further investigation, similar functions in response to microbial infection currently remain unknown. This is likely to be important as most bacterial pathogens, including *H. pylori*, have evolved to subvert cell death pathways to ensure persistence in the host [47]. One mechanism by which *H. pylori* has been proposed to prevent apoptosis is via epidermal growth factor (EGFR) activation of cyclooxygenase-2 (COX-2) enzyme and its product, prostaglandin E2 (PGE<sub>2</sub>) [177]. Interestingly, COX-2-dependent production of PGE<sub>2</sub> is shown to also dampen Th1 responses, resulting in increases in bacterial colonization *in vivo* [178].

Studies have also demonstrated a link between NOD1 and the initiation and progression of gastric cancer. Allison and his co-workers showed increased *NOD1* expression in gastric biopsies with severe gastritis versus no gastritis as well as in gastric tumor tissues versus paired non-tumor tissues [64]. Furthermore, numerous groups have provided evidence for a correlation between polymorphisms in *NOD1* and an increased risk for gastric cancer in different populations [179-181]. A recent report by Necchi *et al.* is also of interest as they described the discovery of a particle-rich cytoplasmic structure (PaCS) in gastric epithelium infected with *H. pylori* [182]. This PaCS was found to be associated with metaplastic foci and consisted of numerous molecules including CagA, NOD1, components of the proteasome and in particular, the oncogenic proteins, SHP-2 and ERK [182]. Together, these data establish a potential role for NOD1 in modulating gastric tumorigenesis in response to *H. pylori* infection. In addition to gastric cancer, NOD1 has been implicated in the progression of colon cancer and chronic pancreatitis [174, 183, 184], while gene polymorphisms in *NOD1* have been associated with altered risk profiles for numerous malignancies, including ovarian and lung cancers [185].

Overall, it appears that NOD1 is a versatile intracellular receptor that has crucial functions in a wide variety of biological and disease processes, beyond bacterial sensing and modulation of host-pathogen interactions. It is thus imperative to broaden our understanding of the extended functions of the NOD1 signaling pathway during *H. pylori* infection and the development of subsequent inflammation in order to develop novel therapeutic strategies.

### 1.7. Aims of this study

Previous work in our laboratory established that cholesterol-rich domains, or lipid rafts, in the cell membranes of epithelial cells are required for *H. pylori* delivery of PG to NOD1 [34]. A unique characteristic of *H. pylori* bacteria is the acquisition and incorporation of cholesterol into its cell membrane [88, 89]. However, an interesting yet poorly understood characteristic is the mechanism of accumulation of cholesterol within the bacterial cell wall and its effect on host-pathogen interactions. Furthermore, genomic analyses conducted in our laboratory identified a predicted protein of *H. pylori* (HP0248) with homology to the lipid raft-associated protein, flotillin, in eukaryotic cells. **Thus, the first aim of this project was to determine if this putative flotillin-like protein (HP0248) constituted a novel bacterial virulence factor required for cholesterol acquisition, interactions with host epithelial cells, induction of pro-inflammatory responses and host colonization (Chapter 2).**

The pathogenicity of *H. pylori* is reliant on the interplay between bacterial virulence factors and the pro-inflammatory immune responses generated upon pathogen detection in GECs, which represent the first point of contact in the host [186]. NOD1 is known to be important for epithelial cell sensing of *H. pylori* bacteria via the recognition of the typical iE-DAP motif [61]. Interestingly, human and murine NOD1 have further evolved to sense slightly different forms of muropeptides, namely a tri-peptide stem structure (GM-Tri<sub>DAP</sub>) and a tetra-peptide stem structure (GM-Tetra<sub>DAP</sub>), respectively [155, 159]. Prior to the inception of the present study, it was found that “mouse adaptation” of a clinical isolate of *H. pylori* (245) generated a variant (245m3), which was affected in its ability to induce pro-inflammatory responses in human GECs [164]. **As the second aim of this study, we wished to elucidate if *H. pylori* might modulate its PG composition during host adaptation in mice to actively engage the NOD1 signaling pathway, thereby initiating responses that favor host colonization and bacterial persistence *in vivo* (Chapter 3).**

Finally, although it is known that *Nod1*<sup>-/-</sup> mice are more susceptible to *H. pylori* infection and colonization at 1-4 weeks post infection [35], there is limited evidence for the function of the NOD1 signaling pathway during long-term *H. pylori* infection

(> 4 weeks). **Therefore, the third aim of this project was to investigate the role for NOD1 in the establishment and maintenance of chronic *H. pylori* infection in the host, whilst also elucidating additional roles for this receptor in mediating host cell survival responses during *H. pylori* infection *in vivo* (Chapter 4).**

Collectively, this PhD project has characterized and demonstrated the importance of cholesterol-rich membrane domains and PG in mediating *H. pylori* interactions with host epithelial cells, bacterial virulence and colonization of mice. Furthermore, these data suggest broader implications for the NOD1 signaling pathway during *H. pylori* infection. Our results suggest that NOD1 sensing of *H. pylori* PG generates an initial inflammatory response in which the host controls infection during the acute phase; and a secondary immune response affecting cell survival that potentially benefits persistence of the bacterium, but which may be detrimental to the host. Overall, this study has presented new insights into the cellular and molecular mechanisms involved in *H. pylori* infection and chronic persistence, which may provide new strategies for early diagnosis and contribute to the development of targeted therapies.

## **Chapter 2: A *Helicobacter pylori* homolog of eukaryotic flotillin is involved in cholesterol accumulation, epithelial cell responses and host colonization**

### ***2. 1. Summary***

*H. pylori* is highly adapted to the human stomach and has developed various strategies to enable its chronic persistence in this site [187]. One such mechanism is the inclusion of unique cholesteryl glucoside forms within the bacterial cell membrane, which account for 25% of the total lipids present in *H. pylori* [89, 91]. However, interestingly, *H. pylori* lacks the genes for the *de novo* synthesis of cholesterol and hence it is likely that the bacterium must obtain this component from an external source, usually the infected host or the growth medium [87, 92, 93]. Wunder *et al.* showed that *H. pylori* follows a cholesterol gradient both *in vitro* and *in vivo*, and can extract cholesterol from the intercellular tight junctions via eukaryotic cholesterol-enriched domains (lipid rafts) [90], however the exact mechanisms involved require further investigation. Bacteria use these lipid rafts to attach to host cells and/or as a port of entry into the host [42]. The cholesterol acquired from these domains by *H. pylori* is then chemically modified and converted to cholesterol- $\alpha$ -glucoside [88], which aids in the evasion of immune detection by the pathogen, thus contributing to *H. pylori* persistence and pathogenesis [90]. Cholesterol-rich lipid rafts also augment adherence by bacteria and enable the translocation of *H. pylori* virulence factors, CagA and PG, into epithelial cells; resulting in cytoskeletal rearrangements in the cells and the activation of NF- $\kappa$ B signaling pathway via NOD1, respectively [34, 35, 42]. However, the role of *H. pylori* membrane-associated cholesterol in the induction of pro-inflammatory responses in host cells remains unclear.

Furthermore, it has been recently discovered that prokaryotes may also contain lipid-rich membrane domains with the characteristic structural and functional features of membrane rafts [108]. Indeed, via bioinformatics analyses of the *H. pylori* genome, we discovered a conserved hypothetical protein (HP0248), which displays significant homology to the flotillin-like protein in *B. subtilis* (YuaG). In turn, YuaG is known to share some similarity to Flotillin-1, a typical constituent of eukaryotic lipid rafts

[108]. Bacterial lipid rafts have been shown to harbor and organize proteins involved in small molecule translocation, secretion and signal transduction; as well as to contribute to bacterial pathogenesis [108, 109, 112]. Overall, the presence of both, cholesterol and a bacterial homologue of eukaryotic flotillin, provide evidence for the potential existence of lipid raft-like structures within the cell membrane of *H. pylori*. However, the characteristics of these putative cholesterol-enriched microdomains and their effects on *H. pylori* pathogenesis and virulence remain to be elucidated. This is of importance as bacterial membrane-associated cholesterol has been shown to confer resistance to a range of antibiotics including polymyxin, beta defensins and LL-37 [19]. Taken together, membrane-associated cholesterol appears to be required not only to maintain *H. pylori* physiology and membrane structure, but also to enable host immune modulation, and ultimately, survival within the gastric mucosa.

The following experiments were therefore designed to **firstly** demonstrate the existence of lipid raft-like structures in *H. pylori* containing the flotillin-like protein, HP0248. **Secondly**, we wished to examine the role for HP0248 in cholesterol acquisition and the subsequent stabilization of *H. pylori* lipid raft-like structures. The **final aim** of this project was to characterize the importance of HP0248 in mediating *H. pylori* interactions with host epithelial cells and macrophages, bacterial virulence and colonization of mice.



# A *Helicobacter pylori* Homolog of Eukaryotic Flotillin Is Involved in Cholesterol Accumulation, Epithelial Cell Responses and Host Colonization

Melanie L. Hutton<sup>1†‡</sup>, Kimberley D'Costa<sup>1‡</sup>, Amanda E. Rossiter<sup>1†</sup>, Lin Wang<sup>1</sup>, Lorinda Turner<sup>1†</sup>, David L. Steer<sup>2</sup>, Seth L. Masters<sup>3</sup>, Ben A. Croker<sup>3†</sup>, Maria Kaparakis-Liaskos<sup>1</sup> and Richard L. Ferrero<sup>1,4\*</sup>

## OPEN ACCESS

### Edited by:

D. Scott Merrell,  
Uniformed Services University,  
United States

### Reviewed by:

David J. McGee,  
LSU Health Sciences Center  
Shreveport, United States  
Timothy Cover,  
Vanderbilt University, United States  
Chih-Ho Lai,  
Chang Gung University, Taiwan

### \*Correspondence:

Richard L. Ferrero  
richard.ferrero@hudson.org.au

### †Present Address:

Melanie L. Hutton,  
Infection and Immunity Program,  
Monash Biomedicine Discovery  
Institute and Department of  
Microbiology, Monash University,  
Melbourne, VIC, Australia  
Amanda E. Rossiter,  
School of Immunity and Infection,  
Institute of Microbiology and Infection,  
University of Birmingham,  
Birmingham, United Kingdom  
Lorinda Turner,  
Department of Psychiatry, Cambridge  
Institute for Medical Research,  
Cambridge University, Cambridge,  
United Kingdom  
Ben A. Croker,  
Division of Hematology/Oncology,  
Boston Children's Hospital, Harvard  
Medical School, Dana-Farber/Boston  
Children's Cancer and Blood  
Disorders Centre, Boston, MA,  
United States

‡These authors have contributed  
equally to this work.

<sup>1</sup> Centre for Innate Immunity and Infectious Diseases, Hudson Institute of Medical Research, Melbourne, VIC, Australia, <sup>2</sup> Monash Biomedical Proteomics Facility, Monash University, Melbourne, VIC, Australia, <sup>3</sup> Inflammation Division, The Walter and Eliza Hall Institute, Melbourne, VIC, Australia, <sup>4</sup> Infection and Immunity Program, Monash Biomedicine Discovery Institute and Department of Microbiology, Monash University, Melbourne, VIC, Australia

The human pathogen *Helicobacter pylori* acquires cholesterol from membrane raft domains in eukaryotic cells, commonly known as “lipid rafts.” Incorporation of this cholesterol into the *H. pylori* cell membrane allows the bacterium to avoid clearance by the host immune system and to resist the effects of antibiotics and antimicrobial peptides. The presence of cholesterol in *H. pylori* bacteria suggested that this pathogen may have cholesterol-enriched domains within its membrane. Consistent with this suggestion, we identified a hypothetical *H. pylori* protein (HP0248) with homology to the flotillin proteins normally found in the cholesterol-enriched domains of eukaryotic cells. As shown for eukaryotic flotillin proteins, HP0248 was detected in detergent-resistant membrane fractions of *H. pylori*. Importantly, *H. pylori* HP0248 mutants contained lower levels of cholesterol than wild-type bacteria ( $P < 0.01$ ). HP0248 mutant bacteria also exhibited defects in type IV secretion functions, as indicated by reduced IL-8 responses and CagA translocation in epithelial cells ( $P < 0.05$ ), and were less able to establish a chronic infection in mice than wild-type bacteria ( $P < 0.05$ ). Thus, we have identified an *H. pylori* flotillin protein and shown its importance for bacterial virulence. Taken together, the data demonstrate important roles for *H. pylori* flotillin in host-pathogen interactions. We propose that *H. pylori* flotillin may be required for the organization of virulence proteins into membrane raft-like structures in this pathogen.

**Keywords:** *Helicobacter pylori*, lipid rafts, membrane raft domains, cholesterol, bacterial flotillins, type IV secretion system, CagA

## INTRODUCTION

The human gastric pathogen *Helicobacter pylori* induces chronic gastric inflammation that usually remains asymptomatic. In 10–20% of infections, however, individuals develop either peptic ulceration or gastric cancer (The EUROGAST Study Group, 1993). These severe forms of disease are more commonly associated with infection by *H. pylori* strains which harbor a *cag* pathogenicity



island (*cagPAI*), encoding a type IV secretion system (T4SS) (Montecucco and Rappuoli, 2001). The *H. pylori* T4SS system mediates the induction of pro-inflammatory (e.g., interleukin-8, IL-8) responses (Viala et al., 2004) and a cell scattering or so-called “hummingbird” phenotype in epithelial cells (Segal et al., 1999). These responses are mediated by the T4SS-dependent delivery of cell wall peptidoglycan (Viala et al., 2004) and the effector protein, CagA (Odenbreit et al., 2000), respectively. In contrast, the *H. pylori* T4SS appears to be dispensable for the induction of cytokine responses in macrophages and monocytes (Maeda et al., 2001; Gobert et al., 2004; Koch et al., 2016).

*H. pylori* T4SS functionality depends on cholesterol-rich microdomains in the plasma membrane of epithelial cells (Lai et al., 2008; Hutton et al., 2010). These microdomains are known as membrane rafts, also commonly referred to as lipid rafts. Interestingly, cholesterol is an important factor for *H. pylori* chemotaxis and adherence (Ansorg et al., 1992). *H. pylori* has a specific affinity for cholesterol (Trampenau and Muller, 2003) and is able to grow in cholesterol-supplemented media (Testerman et al., 2001). This is consistent with the fact that *H. pylori* does not appear to carry cholesterol biosynthesis genes critical for *de novo* sterol synthesis (Testerman et al., 2001) and must obtain the cholesterol from an exogenous source. Indeed, *H. pylori* is able to up-regulate cholesterol gene expression in gastric epithelial cells *in vitro* (Guillemin et al., 2002), suggesting one mechanism by which the bacterium may ensure an abundance of cholesterol is present in its environment. *H. pylori* can acquire cholesterol from membrane raft domains in host cells for incorporation into its own membrane (Wunder et al., 2006). Once incorporated, cholesterol is  $\alpha$ -glucosylated by a cholesterol  $\alpha$ -glucosyltransferase (Wunder et al., 2006), resulting in glycolipid forms called cholesteryl glucosides. This  $\alpha$ -glucosylation of cholesterol allows *H. pylori* to escape phagocytosis, T-cell activation and bacterial clearance *in vivo* (Wunder et al., 2006), thereby providing a novel mechanism for persistence within the host.

Cholesterol is an indispensable constituent of the plasma membrane and is required for many functions in eukaryotic cells, including cell viability, proliferation (Goluszko and Nowicki, 2005), and for the formation of membrane rafts (Simons and Ikonen, 1997). Membrane rafts control numerous protein-protein and lipid-protein interactions at the cell surface and have been implicated in protein sorting, membrane trafficking, cholesterol metabolism, and signal transduction events (Simons and Toomre, 2000; Manes et al., 2003). Prokaryotes may also contain membrane domains with the characteristic structural and functional features of membrane rafts (Lopez and Kolter, 2010). The membrane raft domains in bacteria are likely to harbor and organize proteins involved in small molecule translocation, protein secretion and signal transduction. These membrane raft-like domains have been identified in the human pathogen *Borrelia burgdorferi* and are thought to contribute to the pathogenesis of Lyme disease (Larocca et al., 2010; Toledo et al., 2014).

Eukaryotic membrane rafts typically contain many proteins, including a prominent raft-associated protein called flotillin, also known as reggie (Simons and Toomre, 2000). There

are two known flotillin proteins: flotillin-1 (reggie-2) and flotillin-2 (reggie-1), both of which associate with membrane rafts (Lang et al., 1998). Flotillin-1 is involved in a variety of cellular processes, including vesicle trafficking, cytoskeletal rearrangement, and signal transduction (Langhorst et al., 2005). Flotillin proteins also play key roles in cell-cell adhesion (Otto and Nichols, 2011), clathrin-independent endocytosis (Otto and Nichols, 2011), and the uptake of dietary cholesterol via vesicular endocytosis (Ge et al., 2011).

Flotillins belong to the Stomatin, Prohibitin, Flotillin, and HflK/C (SPFH) protein superfamily, whose members share an SPFH domain at their N-terminus. These proteins are highly conserved across human and animal species and also exist in some bacteria, plants and fungi (Langhorst et al., 2005). Bioinformatic analyses indicate that most bacterial genomes encode proteins with similarity to Flotillin-1 (Lopez and Kolter, 2010). The best characterized of these bacterial flotillins is the YuaG protein of the gut commensal, *Bacillus subtilis*. This flotillin homolog was reported to play roles in a diverse range of cellular functions, including cell division, the maintenance of bacterial shape, and sporulation (Donovan and Bramkamp, 2009; Bach and Bramkamp, 2013; Mielich-Suss et al., 2013). It has been suggested that bacterial flotillins, such as YuaG, may be involved in membrane order or organization and are likely to guide the recruitment of specific proteins to defined areas within the membrane (Bach and Bramkamp, 2013). Consistent with this suggestion, *B. subtilis* YuaG forms punctate staining patterns along the cell membranes of the bacterium (Donovan and Bramkamp, 2009; Lopez and Kolter, 2010) and interacts with proteins involved in various functions, including protein secretion, cell wall metabolism and signaling processes (Bach and Bramkamp, 2013). Although a flotillin homolog has been cloned from the human pathogen, *Staphylococcus aureus* (Lopez and Kolter, 2010), the role(s) of flotillin proteins in bacterial pathogenesis have yet to be investigated.

Herein, we present the first characterization of a flotillin-like protein in the virulence of a human pathogen, *H. pylori*. This protein (HP0248) was shown to be involved in the accumulation of cholesterol within *H. pylori* cell membranes. Importantly, we show that *H. pylori* HP0248 mutants were affected in their abilities to induce T4SS-dependent responses in gastric epithelial cells and to establish chronic infection in mice. Collectively, the data demonstrate that the *H. pylori* flotillin-like protein, HP0248, is involved in the accumulation of bacterial membrane cholesterol, thereby contributing to *H. pylori* pathogenesis.

## MATERIALS AND METHODS

### Bacterial Strains, Media, and Culture Conditions

*H. pylori* 251 and 26695 are *cagPAI*<sup>+</sup>/T4SS<sup>+</sup> laboratory strains (Viala et al., 2004), whereas SS1 (*cagPAI*<sup>+</sup>/T4SS<sup>−</sup>) and X47-2AL (*cagPAI*<sup>−</sup>/T4SS<sup>−</sup>) are mouse colonizing strains (Grubman et al., 2010). The *H. pylori* 251Δ*cagA* mutant was described previously (Hutton et al., 2010). *H. pylori* strains were routinely cultured on either blood agar or brain heart infusion

broth (BHI; Oxoid) containing a modified Skirrow's selective supplement (comprising vancomycin, 10 µg/ml; polymyxin B, 25 ng/ml; trimethoprim, 5 µg/ml; and amphotericin B, 2.5 µg/ml), according to standard procedures (Ferrero et al., 1998). *Escherichia coli* BL21 was propagated on Luria-Bertani (LB) agar or broth with the appropriate antibiotic. *H. pylori* was incubated with epithelial cells at a multiplicity of infection (MOI) of 10 (Hutton et al., 2010). Viable counts of *H. pylori* were determined by serial dilution and plating. The cholesterol content of the bacteria was determined using the Amplex red cholesterol detection kit, according to the manufacturer's instructions (Molecular Probes, OR, USA).

## Cell Culture

Human gastric adenocarcinoma cells (AGS) and murine macrophages (RAW 264.7) were routinely cultured in RPMI medium, supplemented with 10% FCS, 50 units/ml penicillin, 50 µg/ml streptomycin and 1% (v/v) L-glutamine (all reagents from Life Technologies, CA, USA). Cells were seeded at  $1 \times 10^5$  cells/ml and incubated at 37°C in 5% CO<sub>2</sub>. For co-culture assays, cells were serum-starved overnight in antibiotic-free RPMI medium, then washed 2–3 times in antibiotic-free RPMI medium prior to the addition of *H. pylori* bacteria.

## In vitro Adherence Assay

Bacterial adherence was assessed using modifications to a previously described method (Chionh et al., 2009). Briefly, AGS cells were seeded at  $1 \times 10^4$  cells in duplicate sets of triplicate wells in 96-well plates (Falcon) and incubated for 24 h at 37°C in 5% CO<sub>2</sub>. Cells were serum-starved overnight and co-cultured with *H. pylori* bacteria for 6 h. One set of the duplicate wells was washed three times with PBS to remove any unattached bacteria. Both sets of wells were fixed for 20 min in a final concentration of 4% paraformaldehyde and then blocked in 1% BSA in PBS for 30 min at room temperature. Cells were incubated for 1 h at room temperature with rabbit anti-*H. pylori* antiserum (diluted 1:500 in PBS; Ferrero et al., 1994). A horseradish peroxidase (HRP)-conjugated goat anti-rabbit antibody (diluted 1:2,000 in PBS; Dako, Glostrup, Denmark) was then added, prior to color development with 3,3', 5,5'-tetramethylbenzidine (TMB) (Pierce, Thermochemical, Rockford, IL, USA). The reaction was stopped by adding 0.5 M H<sub>2</sub>SO<sub>4</sub>. Absorbance was read at 450 nm and the percentages of adherent bacteria were calculated by dividing the average OD of the washed set of samples by the average OD of the unwashed set.

## Cytokine Responses

Serum-starved cells were stimulated with either live *H. pylori* (MOI = 10) or bacterial lysates (20 µg protein/ml), prepared by freeze-thawing, and incubated at 55°C for 20 min. Following incubation for 1 h, the culture medium was replaced and the cells washed 2–3 times to remove bacteria. Cells were then placed in fresh antibiotic-free medium and incubated a further 5 or 23 h, respectively. IL-8 and IL-6 levels in culture supernatants were determined by sandwich ELISA, according to the manufacturer's instructions (BD Biosciences).

## Isolation of H. pylori Detergent-Resistant Membranes (DRMs)

*H. pylori* DRMs were isolated using modifications to a previously described method (Lopez and Kolter, 2010). Briefly, *H. pylori* bacteria ( $\sim 1\text{--}5 \times 10^9$  bacteria) were pelleted after 16 h of growth in BHI liquid culture medium, washed three times with 20 mM Tris-HCL (pH 7.5) and resuspended in 20 mM Tris-HCL containing protease inhibitors. Bacterial cells were sheared using a French press and cell debris was eliminated by centrifugation. Membrane fractions were precipitated from supernatants by ultracentrifugation ( $40,000 \times g$  for 30 min at 4°C) using a Sorvall RC90 ultracentrifuge (Kendro, NC). Proteins that associated with hydrophobic DRM fractions were separated from hydrophilic DSM fractions by phase separation, using the CellLytic MEM protein extraction kit (Sigma) (Lopez and Kolter, 2010).

## Cloning the SPFH Domain of HP0248

The Gateway® Cloning System (Life Technologies) was used to generate an expression vector for the production of a His-tag-labeled 163 amino acid region internal to the predicted SPFH domain of *H. pylori* HP0248 (deduced total length 362 amino acids). Primers MH9 and MH10 (Supplementary Table 1) were used to amplify a 487 bp fragment, containing attB1 and attB2 sites, from the HP0248 gene of *H. pylori* 26695. The resulting PCR product was cloned into the entry clone, pDONR 221. The PCR amplicon was then recombined into the destination vector pDEST17 using LR clonase. Final destination plasmids were confirmed by sequence analysis using the T7 promoter and terminator primers. The pDEST17 expression vector was transformed into *E. coli* BL21 cells for expression.

## Expression and Purification of Recombinant HP0248

The SPFH domain of *H. pylori* HP0248 was expressed in *E. coli* using standard techniques (see Supplementary Methods for details). Briefly, expression was induced by the addition of 0.4 mM isopropyl β-D-1-thiogalactopyranoside (IPTG; Promega) and the bacterial suspensions pelleted, lysed by both sonication and 0.1 mg/ml lysozyme (Sigma) treatment. The insoluble pellets were sonicated and the proteins solubilized using 6 M guanidine hydrochloride (Amresco, Ohio, USA). The solubilized proteins were loaded onto a HisTrap HP column (GE Healthcare, Uppsala, Sweden) and recombinant HP0248 purified by immobilized metal ion affinity chromatography. Polyclonal antibodies to HP0248 were generated by administering the purified recombinant protein to a New Zealand White rabbit (Walter and Eliza Hall Institute of Medical Research Antibody Facility; Bundoora, Melbourne, Australia). This anti-HP0248 serum (diluted 1:1,000) was used in Western blot analyses.

## SDS-Page and Western Blotting

Whole cell lysates, DRM or DSM fractions were resuspended in solubilization buffer, separated in either 12.5% (v/v) acrylamide or 4–12% (v/v) NuPAGE® Bis-tris (Life Technologies) gels and transferred to nitrocellulose. *H. pylori* proteins were reacted with rabbit anti-HP0248 serum (diluted 1:1,000) or anti-UreA

antibody (1:5,000; Ferrero et al., 1994), followed by addition of a goat anti-rabbit-HRP conjugated antibody (1:1,000 dilution; Dako). Antigen-antibody complexes were detected using ECL detection reagent (Pierce).

### *H. pylori* Mutagenesis

Mutagenesis was performed using the Gateway® Cloning System (Life Technologies). Primer combinations and DNA fragments for cloning were as follows: MH1 and MH3 (Supplementary Table 1), a 299 bp fragment from the 5' end of the *hp0248* of *H. pylori* 26695; GmB4rF and GmB3rR, the gentamicin resistance cassette (Gm<sup>R</sup>) from the pUC1813*apra* vector (Bury-Mone et al., 2003); and MH4 and MH2, a 368 bp fragment from the 3' end of the *hp0248* gene. PCR products were cloned into three entry clones and integration confirmed by sequence analysis using the M13 primer pair (Supplementary Table 1). Recombination was performed in the destination vector pDEST17 using LR clonase and the final destination plasmid confirmed by sequencing using the T7 promoter and terminator primers (Supplementary Table 1). *H. pylori*  $\Delta$ HP0248 mutants were created by natural transformation and selected on horse blood agar (HBA) containing apramycin (30 µg/mL; Sigma) (Grubman et al., 2010). Apramycin-resistant transformants in each strain of *H. pylori* were verified by sequencing using primers MH5, MH6, and GmFwd or GmRvs (Supplementary Table 1). Mutant bacteria were characterized by a 263-amino acid deletion in HP0248. This truncated form of HP0248 included a 185-amino acid deletion within the 231 amino acid SPFH domain.

### Complementation of *H. pylori* HP0248 Mutants

Primer combinations and DNA fragments for cloning were as follows: LT8F and LT8R (Supplementary Table 1), a 301 bp fragment from the 5' end of the *H. pylori* 26695 *rdxA* locus; LT9F and LT9R, a 191 bp fragment, encompassing the *H. pylori* 26695 *ureA* promoter sequence; MH11 and MH12, *H. pylori* *hp0248* from *H. pylori* 26695; and LT10F and LT10R, the 3' end of *rdxA*. The four PCR products were cloned into the pDEST17 destination vector and confirmed as above. *H. pylori*  $\Delta$ HP0248 mutants, in which an exogenous copy of *hp0248* was inserted into the *rdxA* locus (Smeets et al., 2000), were selected by natural transformation and cultured on HBA plates supplemented with metronidazole (8–32 µg/mL; Sigma). Mutants were verified by sequencing using the primers AG1F, MH5, MH6, and MH13R (Supplementary Table 1).

### Densitometric Analysis of HP0248 Abundance in DRM and DRM Fractions

Western blots of DRM and DSM fractions from *H. pylori* 251 WT,  $\Delta$ FLOT, or FLOT (FLOT+) strains were analyzed using ImageJ software. The percentage area for HP0248 in each fraction was quantified relative to that for the non-specific protein band in the corresponding fraction. All values were then normalized to the wild-type DRM fraction.

### Proteomic Analysis of *H. pylori* DRM and DSM Fractions

Coomassie-stained protein bands in DRM samples from *H. pylori* 251 WT were excised from preparative SDS-PAGE gels (4–12% NuPAGE® Bis-tris; Life Technologies) and trypsin digested prior to identification by Matrix Assisted Laser Desorption/Ionization Time-of-Flight (MALDI-TOF) and Liquid Chromatography/Mass Spectrometry (LC-MS/MS). For MALDI-TOF, digested samples were co-spotted onto the MALDI target plate and analyzed on an Applied Biosystems (Foster City, CA, USA) 4700 Proteomics Analyser MALDI TOF/TOF in reflectron mode (see Supplementary Methods for details). Data were searched against an in-house database compiled from *H. pylori* genomes downloaded from the ExPASy FTP site (ftp.expasy.org) using the MASCOT search engine (version 1.9, Matrix Science Inc., London, UK) with all taxonomy selected. The following search parameters were used: missed cleavages, 1; peptide mass tolerance,  $\pm 50$  ppm; peptide fragment tolerance,  $\pm 0.1$  Da; peptide charge, 1+; fixed modifications, carbamidomethyl; variable modification, oxidation (Met), and the top five matches reported. Scores were considered significant when above the MASCOT-generated probability-based Mowse score minimum threshold.

LC-MS/MS was performed using an HCT ULTRA ion trap mass spectrometer (Bruker Daltonics, Bremen, Germany), coupled online with an RSLC nano HPLC (Ultimate 3000, Dionex Corporation, Sunnybrook, CA, USA; see Supplementary Methods for details). Data from LC-MS/MS analysis were exported in the Mascot generic file format (\*.mgf) and searched against an in-house database, as above. The following search parameters were used: enzyme specificity, trypsin; missed cleavages, 1; peptide mass tolerance,  $\pm 0.6$  Da; peptide fragment tolerance,  $\pm 0.3$  Da; peptide charge, 2+ and 3+; fixed modifications, carbamidomethyl; variable modification, oxidation (Met).

To identify proteins in DRM and DSM fractions from *H. pylori* WT,  $\Delta$ FLOT, and  $\Delta$ FLOT (FLOT+) bacteria, sections of SDS-PAGE gel corresponding to a molecular weight of  $\sim 40$  kDa were excised. These sections of gel ( $\sim 1$  cm high and spanning the width of the gel) were sliced into six pieces and each trypsin digested prior to analysis. In this case, LC-MS/MS was performed using the QExactive mass spectrometer (Thermo Scientific, Bremen, Germany) coupled online with an RSLC nano HPLC (Ultimate 3000, Thermo Scientific, Bremen, Germany; see Supplementary Methods for details). For each sample, pooled data from six gel slices were exported in the Mascot generic file format (\*.mgf) and analyzed as above.

### Quantitation of Cell Scattering Responses by High Throughput Analysis

AGS cells were seeded on coverslips at  $1 \times 10^5$  cells/ml and incubated for 24 h at 37°C in 5% CO<sub>2</sub>. Cells were then serum-starved overnight prior to co-culture with *H. pylori* for 6 h. Immunofluorescence staining of cellular actin using Alexa



Fluor® 488 phalloidin (1:40 dilution; Molecular Probes) was performed as described previously (Hutton et al., 2010). For staining of bacteria, co-cultured cells or *H. pylori* that had been air dried and fixed onto microscope slides (Polysine™, Menzel-Glaser, Braunschweig, Germany) were incubated with rabbit anti-*H. pylori* sera (diluted 1:5,000 in PBS) for 1 h at room temperature, followed by incubation with an anti-rabbit Alexa Fluor® 568 conjugated antibody (1:1,000 dilution; Molecular Probes). The stained bacteria were examined using a Nikon C1 confocal microscope. Actin staining in cells was viewed using the Celloomics ArrayScan VTI HCS Reader (Thermo Scientific), capturing 20 fields per well with the 20 x objective.

### Quantification of CagA Translocation by Immunofluorescence

AGS cells were seeded in  $\mu$ -slide eight well-chambers (Ibidi) at  $3 \times 10^4$  cells/ml and incubated for 24 h at 37°C in 5% CO<sub>2</sub>. Cells were then serum-starved overnight prior to co-culture with *H. pylori* for 6 h. Cells were subsequently fixed using 4% paraformaldehyde and their nuclei stained with DAPI (diluted 1:1,000 in PBS; Molecular Probes). Extracellular CagA was detected using a rabbit anti-CagA (b-300) antibody (1:100; sc-25766, Santa-Cruz Biotechnology), followed by incubation with an anti-rabbit Alexa Fluor 488 conjugated antibody (1:1,000 dilution; Molecular Probes). Cells were then re-fixed and permeabilized using 1% Triton-X. Intracellular CagA was probed using the same rabbit anti-CagA antibody, followed by incubation with an anti-rabbit Alexa Fluor 647 conjugated antibody (1:1,000 dilution; Molecular Probes). Cells were imaged with the same background intensity settings on a Deltavision API wide-field microscope (60 x objective). Image analysis was performed using ImageJ, where relative intensities of A<sub>647</sub>/A<sub>488</sub> were quantified for five cells per field viewed (five fields viewed per sample;  $n = 2$  experiments).

### Mouse Infection

Animal handling and experimentation was performed in accordance with Victorian State Government regulations and approved by the Monash University Animal Ethics Committee (ethics no. MMCA 2010/18). *H. pylori* suspensions for mouse inoculation were prepared by harvesting bacteria from HBA plates using BHI broth (Ferrero et al., 1998). Six- to eight-week-old female specific pathogen/*Helicobacter*-free C57BL/6 mice were each intragastrically administered a single 100- $\mu$ l aliquot of the inoculating suspension ( $10^7$  cfu/mouse) using polyethylene catheters (Ferrero et al., 1998). The presence of *H. pylori* infection in mice was determined after 30 days of infection by quantitative culture as described previously (Ferrero et al., 1998).

### Statistical Analysis

Data were analyzed using the Student's *t*-test, Mann-Whitney *U*-test or ANOVA, as appropriate. Differences in data values were considered significant at a  $P < 0.05$ .

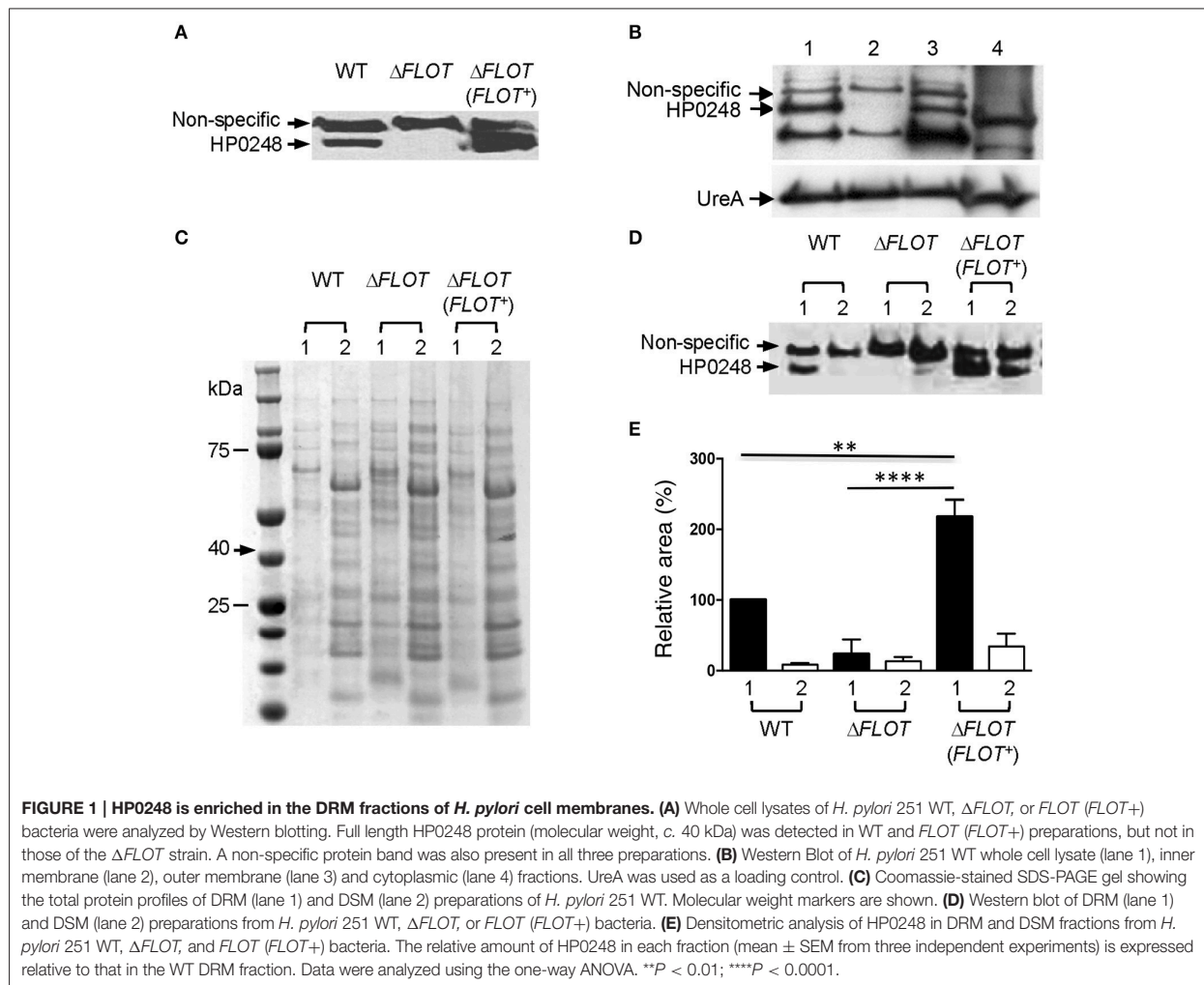
## RESULTS

### *H. pylori* Has a Flotillin-Like Protein (HP0248) That Partitions to Membrane Raft-Like Domains in Its Cell Membrane

Studies have recently described the presence of membrane raft-like domains within the cell membranes of a pathogenic bacterium, *B. burgdorferi*, suggesting that membrane rafts may be conserved amongst both prokaryotic and eukaryotic organisms (Larocca et al., 2010; Toledo et al., 2014). Consistent with this suggestion, the commensal bacterium *B. subtilis* was reported to contain a protein, YuaG, with homology to flotillins, a family of membrane raft-associated proteins (Donovan and Bramkamp, 2009). A flotillin-like protein was identified in the bacterial species, *S. aureus*, but this protein was not characterized (Lopez and Kolter, 2010). Given that *H. pylori* cell membranes are highly enriched in cholesterol, a feature of membrane rafts, we speculated that *H. pylori* may have a flotillin-like protein. To address this question, we used the primary amino acid sequence of *B. subtilis* YuaG (Donovan and Bramkamp, 2009; Lopez and Kolter, 2010) to perform BLAST analyses on the order *Campylobacterales*. We first identified homologs in *Helicobacter hepaticus* (HH0856) and several *Campylobacter* spp. These proteins were, in turn, used to identify the presence of a hypothetical protein, HP0248, in the *H. pylori* 26695 strain. *hp0248* and its predicted protein in this *H. pylori* strain have accession numbers NC\_000915.1 (257084-258172) and NP\_207046.1, respectively. We identified a 231 amino acid region in *H. pylori* HP0248, which when subjected to CLUSTALW analysis, exhibited 14.7% identity and 42.7% similarity with the SPFH domain of human flotillin-1 (Supplementary Figure 1) (Langhorst et al., 2005). The SPFH domain of *H. pylori* HP0248 shares a similar level of identity with that of human flotillin-2 (data not shown). Homologs of HP0248 are present in other *H. pylori* strains (e.g., J99, B128, G27), as well as in various human and animal *Helicobacter* spp. e.g., *Helicobacter acinonychis*, *Helicobacter felis*, *Helicobacter mustelae* (data not shown). This highlights the likely importance of HP0248 in *Helicobacter* biology. On the basis of the findings, we have named the *H. pylori* HP0248 protein, “flotillin-like protein” or “FLOT.”

In order to characterize the biological functions of the *H. pylori* flotillin-like protein, we generated  $\Delta$ hp0248 deletion mutants ( $\Delta$ FLOT) in *H. pylori* 26695 and 251, both of which have functional T4SSs (Viala et al., 2004), as well as in two strains that do not i.e., X47-2AL and SS1 (Grubman et al., 2010). We also generated a complemented mutant ( $\Delta$ FLOT (FLOT+)) in the 251 strain. Western blot analyses using a polyclonal rabbit antibody raised against the HP0248 SPFH domain confirmed the production of HP0248 in *H. pylori* 251 wild-type (WT) and  $\Delta$ FLOT (FLOT+) strains, but not in a  $\Delta$ FLOT mutant (Figure 1A).

To determine the cellular localization of *H. pylori* HP0248, whole bacteria were fractionated into cytoplasmic, inner and outer membrane compartments (Voss et al., 2014). By Western blotting, HP0248 was shown to be present in the outer but not inner membrane (Figure 1B). The *H. pylori* urease A subunit (UreA), which is present in both cytoplasmic and membrane



fractions (Phadnis et al., 1996), was used a sample loading control. Given that flotillins normally partition to membrane rafts, we next sought to determine whether *H. pylori* HP0248 might also localize to membrane raft-like structures within the bacterial membrane. To do this, we exploited the known property of raft-associated proteins to partition to detergent-resistant membrane (DRM) fractions. This approach has been used previously to isolate hydrophobic proteins from membrane rafts in other bacteria (Larocca et al., 2010; Lopez and Kolter, 2010). As shown in **Figure 1C**, DRM fractions of *H. pylori* membranes exhibited markedly different SDS-PAGE profiles to those of detergent-sensitive membrane (DSM) fractions, consistent with the separation of hydrophobic raft-associated proteins from hydrophilic proteins. Importantly, HP0248 was detected in the DRM fractions of WT and  $\Delta$ FLOT (FLOT+), but not in those of  $\Delta$ FLOT bacteria (**Figures 1D,E**). The presence of HP0248 in the DSM of the  $\Delta$ FLOT (FLOT+) mutant can be attributed to over-expression of this protein in the strain due to the use of the strong ureA promoter for complementation (Grubman et al., 2010). Using two different biochemical approaches, we showed

that the *H. pylori* FLOT protein associates with the bacterial membrane.

### Proteomic Analyses Identify *H. pylori* HP0248 within DRM Fractions

Proteomic analyses of the total DRM fractions of WT bacteria identified 29 putative and five hypothetical proteins (**Table 1**). Amongst the putative proteins, 19 were proven experimentally to associate with membranes (Baik et al., 2004; Carlsohn et al., 2006), with an additional four predicted by the PSORTb program to be membrane-associated (**Table 1**, **Figure 1B**). Although the six remaining putative proteins are defined as cytoplasmic (**Table 1**, Supplementary Table 2), five of these have actually been shown to associate with *H. pylori* membranes i.e., HP0072, HP0073, HP0248, HP1462, HP1563. Amongst these predicted cytoplasmic proteins are HP0248 and UreA (HP0073) (**Figure 1B**, Phadnis et al., 1996). Similar findings were reported in a proteomic study on *B. burgdorferi* DRMs in which the majority (63%) of the proteins found in those fractions were predicted to be associated with the bacterial membrane, however,

some cytoplasmic proteins were also detected (Toledo et al., 2015).

To directly compare the protein composition of DRM and DSM fractions, we performed LC/MS-MS analysis on DRM and DSM fractions from *H. pylori* WT,  $\Delta FLOT$  and  $\Delta FLOT$  ( $FLOT+$ ) bacteria. Proteins in the molecular weight range of HP0248 i.e., 40 kDa were selectively analyzed by LC-MS/MS using the QExactive mass spectrometer. This analysis yielded a larger number of protein “hits” than that acquired on the HCT ULTRA ion trap mass spectrometer (Table 1). This is most likely due to the greater level of sensitivity of the former. Most importantly, however, HP0248 was again detected in the DRM but not DSM fractions of WT and  $\Delta FLOT$  ( $FLOT+$ ) bacteria (Supplementary Table 3). Additionally, 50 proteins were identified within the DRM fractions from all three *H. pylori* strains (Supplementary Figure 2), of which 31 were not detected in any of the DSM fractions (Supplementary Tables 3, 4). The latter were considered to be putative membrane raft-associated proteins. In addition to HP0248, several outer membrane proteins (OMPs) were found to partition to the DRM fractions (Table 1, Supplementary Tables 3, 4), suggesting that proteins involved in host-pathogen interactions may selectively localize to the membrane raft-like structures in *H. pylori* membranes. Taken together, the data demonstrate that *H. pylori* HP0248 preferentially associates with a fraction enriched in membrane rafts.

### *H. pylori* HP0248 Is Important for Cholesterol Accumulation and Induction of IL-8 Responses

The *H. pylori* 251  $\Delta FLOT$  and  $\Delta FLOT$  ( $FLOT+$ ) strains grew as well as the WT strain in BHI broth medium supplemented or not with cholesterol (data not shown). Importantly, however, the *H. pylori* 251  $\Delta FLOT$  mutant strain possessed significantly lower cholesterol levels, when compared with WT bacteria (Figure 2A;  $P < 0.01$ ). Similar findings were obtained for  $\Delta FLOT$  mutants on the *H. pylori* 26695, X47-2AL, and SS1 backgrounds, with these mutants consistently displaying 40% less cholesterol than the respective WT strains (data not shown). Finally, the *H. pylori* 251  $\Delta FLOT$  ( $FLOT+$ ) complemented strain exhibited WT levels of cholesterol (Figure 2A), thereby confirming the important function of HP0248 in *H. pylori* cholesterol accumulation.

Given the importance of *H. pylori*-associated cholesterol for the induction of cellular responses, we next examined interactions between *H. pylori* WT,  $\Delta FLOT$ , or  $\Delta FLOT$  ( $FLOT+$ ) bacteria and host epithelial cells. As shown in Figure 2B, *H. pylori*  $\Delta FLOT$  26695 and 251 mutants adhered as well to AGS cells as the corresponding WT strains, suggesting that adhesion occurs independently of the flotillin-like protein. In contrast, *H. pylori*  $\Delta FLOT$  mutant strains on both 26695 and 251 backgrounds induced significantly lower IL-8 responses, when compared with WT strains (Figure 2C;  $P < 0.05$  and  $P < 0.001$ , respectively).  $\Delta FLOT$  ( $FLOT+$ ) bacteria induced significantly increased IL-8 responses when compared with  $\Delta FLOT$  organisms, however, these responses were only partially restored with respect to those induced by WT bacteria (Figure 2C;  $P < 0.001$  and

**TABLE 1 | Proteins identified in DRM fractions of *H. pylori* 251 WT bacteria.**

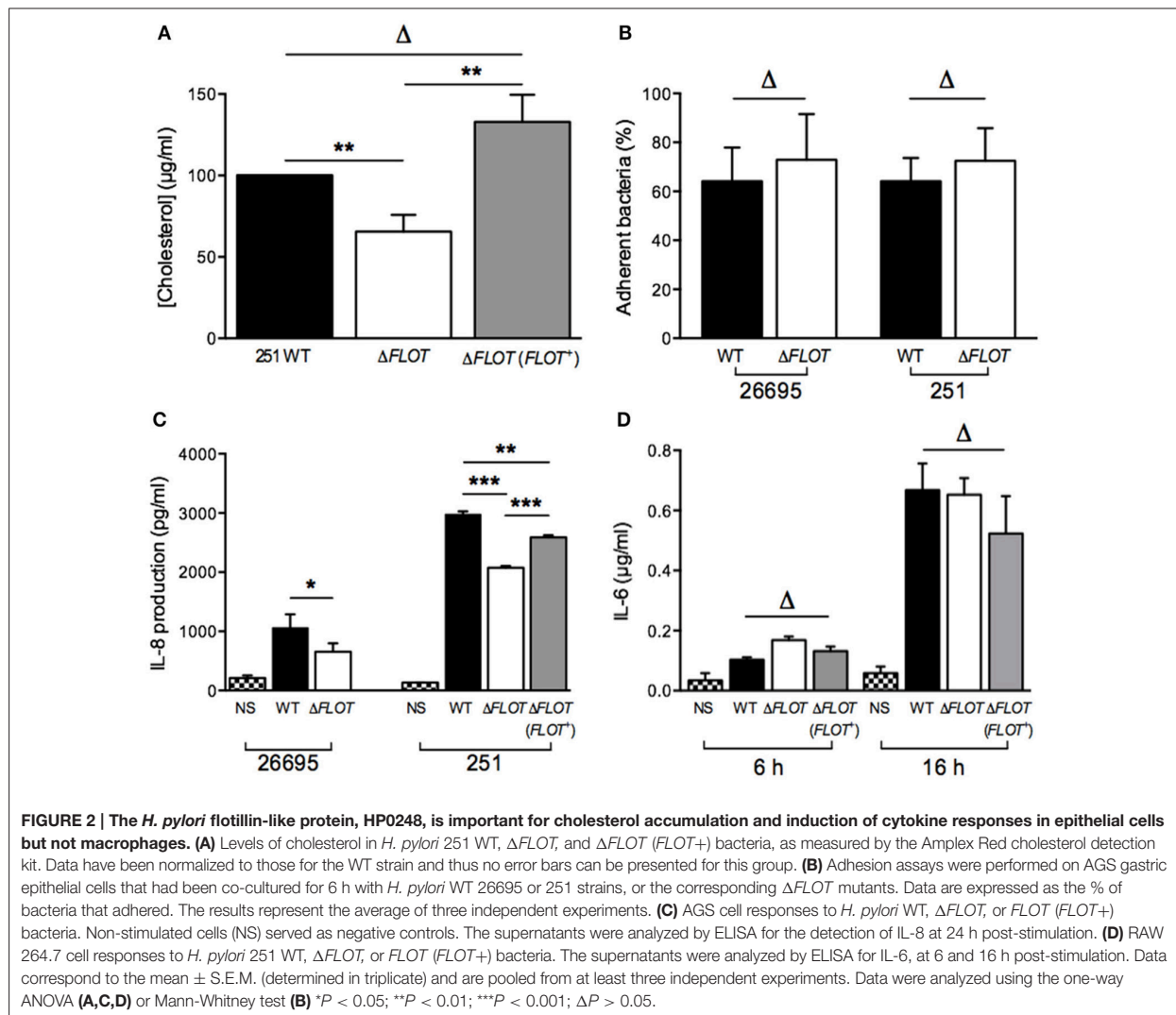
HP number	Protein	Predicted protein location <sup>a</sup>
HP0025	OMP2	Membrane-associated <sup>b,c</sup>
HP0072	Urease subunit beta (UreB)	Cytoplasmic <sup>b,c</sup>
HP0073	Urease subunit alpha (UreA)	Cytoplasmic <sup>b,c</sup>
HP0097	Hypothetical protein	Unknown
HP0127	OMP4 (HofB)	Membrane-associated <sup>b,c</sup>
HP0130	Hypothetical protein	Unknown
HP0185	Hypothetical protein	Cytoplasmic
HP0229	OMP6 (HopA)	Membrane-associated <sup>b,c</sup>
HP0248	Flotillin-like protein	Cytoplasmic
HP0252	OMP7 (HopF)	Membrane-associated <sup>b</sup>
HP0317	OMP9 (HopU or BabC)	Membrane-associated <sup>b</sup>
HP0377	Thiol:Disulphide interchange protein (DsbE)	Membrane-associated
HP0472	OMP11	Membrane-associated <sup>b,c</sup>
HP0486	OMP (HofC)	Periplasmic <sup>b</sup>
HP0606	Membrane fusion protein (MtrC)	Membrane-associated <sup>c</sup>
HP0671	OMP14 (HofF)	Membrane-associated <sup>b,c</sup>
HP0706	OMP15 (HopE)	Membrane-associated <sup>b,c</sup>
HP0797	Lipoprotein (HpaA)	Membrane-associated <sup>b</sup>
HP0896	OMP19 (BabB or HopT)	Membrane-associated <sup>b,c</sup>
HP0912	OMP20 (HopC, AlpA)	Membrane-associated <sup>b,c</sup>
HP0913	OMP21 (HopB, AlpB)	Membrane-associated <sup>b,c</sup>
HP1069	ATP-dependent zinc metalloprotease	Membrane-associated
HP1125	OMP18 (Peptidoglycan-associated lipoprotein precursor)	Membrane-associated <sup>b</sup>
HP1132	ATP synthase F1, subunit beta	Cytoplasmic
HP1173	Hypothetical protein	Cytoplasmic <sup>c</sup>
HP1177	OMP27 (HopQ)	Membrane-associated <sup>b,c</sup>
HP1243	OMP28 (HopS, BabA)	Membrane-associated
HP1395	OMP30 (HofL)	Membrane-associated <sup>b</sup>
HP1462	Secreted protein involved in motility	Cytoplasmic <sup>b</sup>
HP1463	Hypothetical protein	Unknown
HP1469	OMP31 (HopV)	Membrane-associated <sup>b,c</sup>
HP1488	36 kDa antigen	Membrane-associated
HP1540	Ubiquinol cytochrome c oxidoreductase	Membrane-associated
HP1563	Alkyl hydroperoxide reductase (TsaA)	Cytoplasmic <sup>c</sup>

<sup>a</sup>Determined using the PSORTb prediction program (<http://www.psorth.org/psorth/>).

<sup>b</sup>Membrane association proved experimentally (Carlsohn et al., 2006).

<sup>c</sup>Membrane association proved experimentally (Baik et al., 2004).

$P < 0.01$ , respectively). As observed for cholesterol-enriched and cholesterol-depleted bacteria, *H. pylori*  $\Delta FLOT$  mutants induced similar IL-6 and TNF- $\alpha$  responses in macrophages as WT organisms (Figure 2D; data not shown). Cumulatively, these data indicate that *H. pylori* HP0248 is involved in cholesterol accumulation in the bacterial cell membrane and induction of IL-8 responses in epithelial cells. We speculate that the absence of HP0248 may destabilize membrane raft domains in the *H. pylori* cell membrane, thereby affecting T4SS-dependent functions.



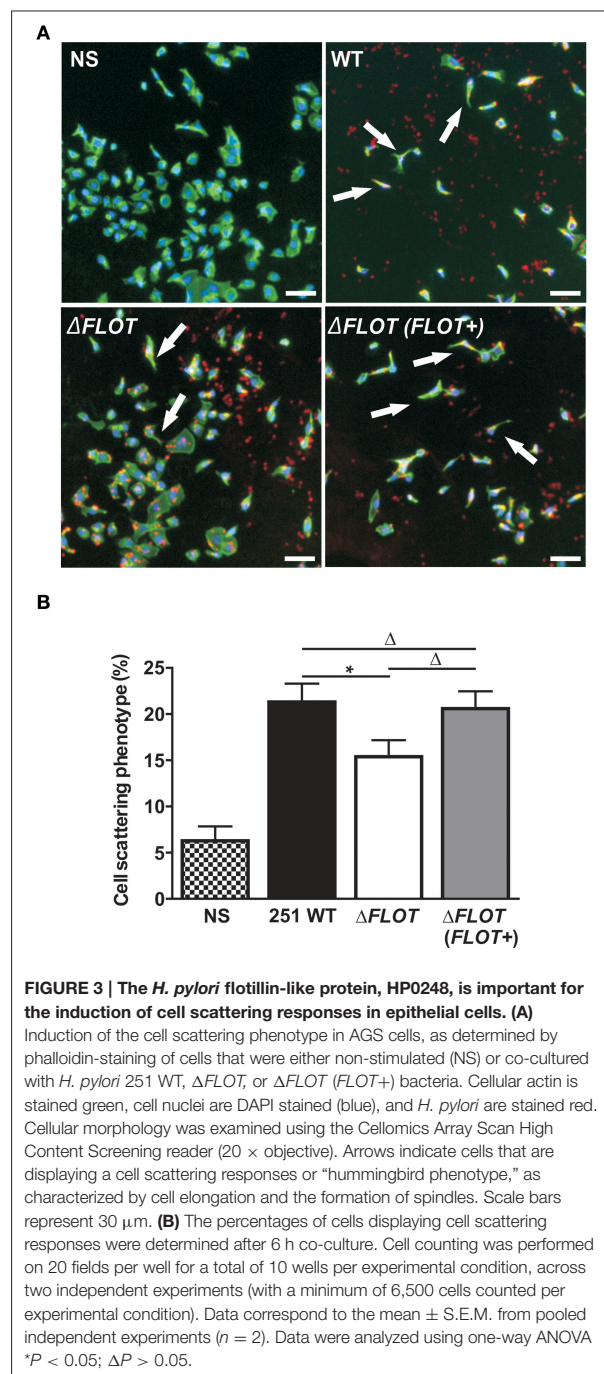
### *H. pylori* HP0248 Is Important for T4SS-Induced Cell Scattering Responses and CagA Translocation in Epithelial Cells

In addition to the induction of IL-8 production in epithelial cells, the *H. pylori* T4SS mediates delivery of the effector molecule, CagA, which causes rearrangement of the host cell actin cytoskeleton and results in cell scattering (Segal et al., 1999; Odenbreit et al., 2000; Backert et al., 2001). To further investigate the importance of *H. pylori* HP0248 in T4SS-dependent functions, we co-cultured AGS cells with *H. pylori* WT,  $\Delta$ FLOT, or  $\Delta$ FLOT (FLOT+) bacteria, and used a high throughput imaging technique to quantify the proportions of cells displaying a cell scattering response (Figure 3A). Consistent with the IL-8 data (Figure 2C), AGS cells that had been co-cultured with an *H. pylori*  $\Delta$ FLOT mutant strain displayed weaker cell scattering responses, when compared with cells

co-cultured with either the WT or complemented mutant strains (Figure 3B;  $P < 0.05$  and  $P > 0.05$ , respectively).

We also confirmed that the reduced levels of cell scattering induced in AGS cells by *H. pylori*  $\Delta$ FLOT bacteria were due to reduced translocation of the CagA effector protein, a functional read-out of T4SS activity. Using an immunofluorescence-based technique to detect both extracellular and intracellular CagA, we observed that the levels of intracellular CagA were significantly reduced in AGS cells that had been co-cultured with *H. pylori*  $\Delta$ FLOT or  $\Delta$ cagA bacteria, when compared with cells co-cultured with either WT or  $\Delta$ FLOT (FLOT+) bacteria (Figure 4;  $P < 0.02$  and  $P < 0.008$ , respectively). Together, the data show that *H. pylori*  $\Delta$ FLOT bacteria are significantly affected in their ability to induce CagA-dependent cell scattering and IL-8 responses in gastric epithelial cells, thereby confirming the importance of the *H. pylori* flotillin-like protein, HP0248, in T4SS functionality.





### *H. pylori* HP0248 Is Important for Establishment of a Chronic Infection in Mice

Finally, mouse infection studies were performed with *H. pylori*  $\Delta$ FLOT mutants that had been generated in the SS1 and X47-2AL mouse-colonizing strains (Grubman et al., 2010). A dramatic

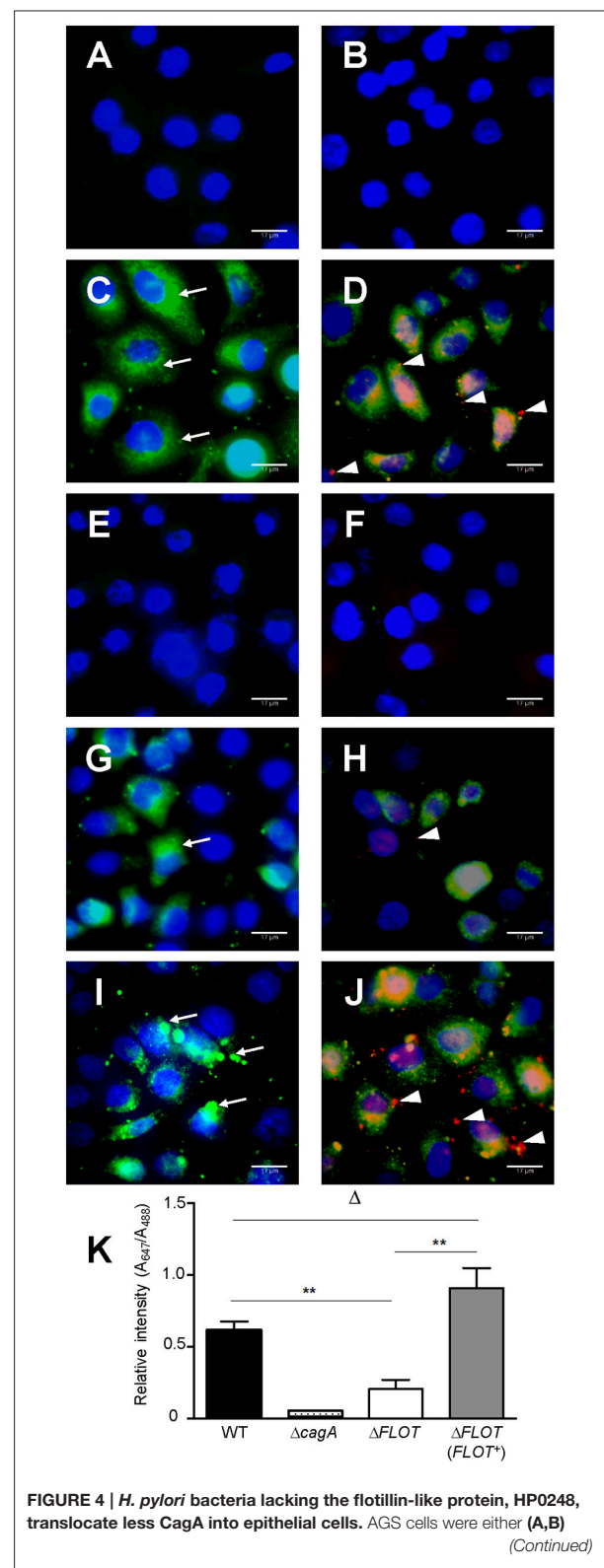




**FIGURE 4 | Continued**

non-stimulated or co-cultured with (C,D) *H. pylori* 251 WT, (E,F)  $\Delta$ cagA, (G,H)  $\Delta$ FLOT, or (I,J)  $\Delta$ FLOT (FLOT+) bacteria. CagA was detected using a rabbit anti-CagA antibody. Panels (A,C,E,G,I) show cells that had been incubated with anti-rabbit Alexa Fluor 488-conjugated secondary antibody. Panels (B,D,F,H,J) show cells that had been incubated with anti-rabbit Alexa Fluor 488-conjugated secondary antibody, permeabilized with 1% Triton-X and then incubated with anti-rabbit Alexa Fluor 647-conjugated antibody. Nuclei (blue) were stained using DAPI. Extracellular CagA molecules (thin arrows) appear as green diffuse areas of staining and were detected using a rabbit anti-CagA (b-300) primary antibody and an Alexa Fluor 488 anti-rabbit conjugate as the secondary antibody. Intracellular CagA molecules (arrow heads) appear as red mainly punctate areas of staining that were detected using the rabbit anti-CagA and Alexa Fluor 647-conjugated anti-rabbit antibodies. Scale bars, 17  $\mu$ m. K, Quantification of Alexa Fluor 647 and Alexa Fluor 488 staining (expressed as relative intensities) in AGS cells that had been co-cultured with either *H. pylori* 251 WT,  $\Delta$ cagA,  $\Delta$ FLOT, or  $\Delta$ FLOT (FLOT+) bacteria. The data represent the mean  $\pm$  SEM for two independent experiments. Data were analyzed using the Mann-Whitney U test. \*\* $P < 0.008$ ;  $\Delta P > 0.05$ .

and highly significant effect on colonization was observed for *H. pylori* SS1  $\Delta$ FLOT mutants, with no bacteria cultured from the gastric tissues of these mice at 30 days post-infection (Figure 5;  $P < 0.0001$ ). Although we were unable to complement the FLOT mutation in *H. pylori* SS1 (data not shown), we were able to do so in another mouse-colonizing strain, *H. pylori* X47-2AL. Bacterial loads in X47-2AL  $\Delta$ FLOT-infected mice were significantly reduced with respect to those in WT-infected mice, albeit less strikingly than for SS1 (Figure 5;  $P = 0.039$ ). Additionally, mice that were infected with the X47-2AL  $\Delta$ FLOT (FLOT+) strain exhibited significantly higher bacterial loads than animals infected with the  $\Delta$ FLOT mutant ( $P = 0.01$ ), but similar loads to those infected with the WT strain ( $P = 0.549$ ). The fact that the FLOT mutation had a more dramatic effect on colonization in SS1 than in X47-2AL is similar to the findings of a previous study (Grubman et al., 2010), indicating likely strain-dependent differences. Taken together, the data demonstrate that HP0248 plays a role in chronic colonization of the mouse gastric mucosa.

## DISCUSSION

It has been known for some time that *H. pylori* obtains host cell-derived cholesterol to generate cholesteryl glucosides which the bacterium incorporates into its own membrane (Ansorg et al., 1992; Hirai et al., 1995). These cholesteryl glucosides allow *H. pylori* to evade phagocytosis, the activation of a T-cell response and thus bacterial clearance (Wunder et al., 2006). We now know that cholesterol plays multiple roles in *H. pylori* pathogenesis. This compound is required during the initial phase of colonization by *H. pylori* (Hildebrandt and McGee, 2009), as well as in bacterial resistance to antibiotics, antimicrobial peptides and bile salts (McGee et al., 2011; Trainor et al., 2011). In the present study, we have identified an *H. pylori* homolog of eukaryotic flotillin proteins that localizes to the cholesterol-enriched cell membranes of the bacterium. We propose that this *H. pylori* flotillin represents a new virulence factor involved in host-pathogen interactions.

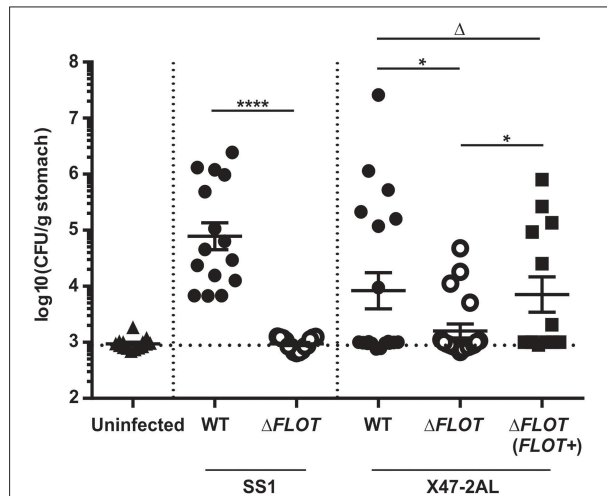


**FIGURE 5 | The *H. pylori* flotillin-like protein, HP0248, is required for mouse colonization.** C57BL/6 mice were inoculated with  $10^7$  CFU of *H. pylori* by intragastric gavage. Quantitative culture assays were performed at 30 days post-infection. Data are presented as Log<sub>10</sub> colony forming units (CFU)/g stomach, with each point representing the mean of two estimations for a single mouse. Horizontal bars represent the geometric means of viable cell count determinations. The limit of detection for the assay is approximately 1,000 CFU/gram. Data for *H. pylori* SS1 are pooled from three independent experiments, whereas those for X47-2AL are from 2 (WT,  $\Delta$ FLOT) and 1 experiment ( $\Delta$ FLOT (FLOT+)), respectively. Data were analyzed using the Mann-Whitney test \* $P < 0.05$ ; \*\*\*\* $P < 0.0001$ ;  $\Delta P > 0.05$ .

It is well-established that cholesterol accumulates within membrane raft microdomains of eukaryotic cells. An important property of membrane rafts is that they can selectively include or exclude proteins to control interactions at the cell surface (Manes et al., 2003). It is becoming apparent that some bacteria possess domains analogous to eukaryotic membrane rafts in their outer membranes (Larocca et al., 2010; Lopez and Kolter, 2010). Additionally, it has been reported that homologs of the archetypal membrane raft molecule, flotillin, can be found in certain bacteria (Donovan and Bramkamp, 2009; Lopez and Kolter, 2010). For the first time, we have characterized a flotillin-like protein in a human bacterial pathogen and demonstrated its importance in pathogenesis. This protein, encoded by the *hp0248* gene in *H. pylori* 26695, was originally annotated as a hypothetical protein. Consistent with this finding, a recent review article reported *H. pylori* *hp0248* as being a putative flotillin-encoding gene, however, no evidence for this conclusion was provided (Bramkamp and Lopez, 2015). Interestingly, although we used the amino acid sequence of the *B. subtilis* flotillin-like protein YuaG (also known as FloT) to identify *H. pylori* HP0248, it was suggested that HP0248 was likely to be more similar to the *B. subtilis* flotillin-like protein YqfA (or FloA) (Bramkamp and Lopez, 2015). It is therefore possible that in common with *B. subtilis* and other bacteria, *H. pylori* has two flotillin-like proteins, a fact that may explain the significant but relatively modest differences observed between the *H. pylori* WT and  $\Delta$ FLOT mutants observed here. CLUSTALW analysis of *H. pylori*

HP0248 (Supplementary Figure 1) showed that it has a predicted SPFH domain, characteristic of flotillin family members. By homologous recombination, we were able to generate *H. pylori* HP0248 mutants lacking all but 47 amino acids in the N-terminal region of the SPFH domain. In contrast, and despite two different mutagenesis approaches, all attempts to generate *H. pylori* HP0248 mutants lacking the entire SPFH domain were unsuccessful (data not shown). The precise reason for this observation remains unclear. One possibility is that the downstream gene, *hp0249*, which was used as a homology arm for recombination, may be an essential gene for *H. pylori*. The start codon of *hp0249* is situated only seven base pairs from the stop codon of *hp0248* and the two genes are likely to be part of the same transcriptional unit. Thus, any perturbation in *hp0249* expression may be lethal for the bacterium.

*H. pylori* can incorporate cholesterol into its cell membrane (Wunder et al., 2006) and thus it appeared likely that the bacterium may have membrane raft-like structures in its outer membrane. Based on the known property of membrane raft components to partition to DRM fractions, our data indicate that *H. pylori* HP0248 is a membrane raft-associated protein (Figure 1, Supplementary Tables 3, 4). Bioinformatic analyses suggest that this protein does not have a signal sequence but does have the predicted transmembrane region (data not shown) required for the association of SPFH proteins with the bacterial membrane (Bramkamp and Lopez, 2015). Proteomic analyses of the DRM preparations (Table 1, Supplementary Tables 3, 4) also revealed a selective enrichment of OMPs, including several of which are important for adhesion e.g., BabA, HopB, HopC, HopQ. In *S. aureus*, DRMs were reported to contain proteins required for biofilm formation, signaling, attachment, and virulence (Lopez and Kolter, 2010). Similarly, selective packaging of outer surface lipoproteins into membrane rafts has been reported in *B. burgdorferi* (Toledo et al., 2014). We hypothesize that specific proteins, required for *H. pylori* interactions with target cells and/or colonization, may compartmentalize within the membrane raft domains of this pathogen.

Eukaryotic flotillin is found within membrane raft domains and is important for various cellular functions (Simons and Ikonen, 1997). We therefore speculated whether the flotillin-like protein, HP0248, renamed here as FLOT, may hold a similar importance for *H. pylori* physiology. Indeed, *H. pylori*  $\Delta$ FLOT mutants displayed ~40% less cholesterol in their membranes (Figure 2A), thus indicating that the protein is involved in cholesterol accumulation by the bacterium. Although a cholesterol receptor has yet to be identified in *H. pylori*, previous experimental evidence suggested that cholesterol uptake in the bacterium is protein-mediated (Trampenau and Muller, 2003). It is therefore possible that *H. pylori* FLOT may be one protein required for the uptake of cholesterol within the *H. pylori* cell membrane. We hypothesize that through its stabilization of membrane raft domains, *H. pylori* FLOT may be important for cholesterol accumulation within its cell membrane. In turn, these domains may be required for the proper formation and functioning of the T4SS apparatus. Consistent with this hypothesis, we demonstrated that T4SS-dependent functions, as determined by cell scattering responses

and CagA translocation, were significantly affected in *H. pylori*  $\Delta$ FLOT mutants (Figures 3, 4, respectively). Furthermore, we showed that these mutants were also significantly affected in their ability to colonize mice in a bacterial strain-dependent manner (Figure 5). Similar strain-dependent effects on colonization have been reported for other *H. pylori* mutants (Grubman et al., 2010) and are most likely reflective of the enormous genetic diversity in this bacterial species (Falush et al., 2003).

In conclusion, the flotillin-like protein, HP0248 appears to be critical for *H. pylori* pathogenesis, as not only is this protein important for the induction of T4SS-mediated host cell responses, but also for colonization. Although we have shown that HP0248 is involved in the optimal delivery of CagA into host cells and complete induction of IL-8 immune responses, it would be of interest to directly show whether T4SS-dependent delivery of peptidoglycan to host cells is reduced in the absence of HP0248. Furthermore, it remains to be elucidated whether the reduced amounts of cholesterol in the *H. pylori*  $\Delta$ FLOT bacteria, or a combination of reduced cholesterol and the absence of FLOT, account for the lower host cell responses and decreased colonization levels observed. The difficulty in separating the contribution of cholesterol and FLOT to the phenotypes observed during this study has raised further questions that will form the basis of future investigations. Are the observed HP0248-dependent phenotypes a result of lost interactions between FLOT and other *H. pylori* proteins that might complex within the membrane raft domain? Are these phenotypes an indirect effect of the reduction in membrane cholesterol, rather than through the direct loss of FLOT? Finally, is FLOT itself responsible for controlling integration of cholesterol into membrane microdomains? Whatever the relative contributions of cholesterol and FLOT, the fact that both have an association with DRMs identifies *H. pylori* membrane raft-like structures as critical to host-pathogen interactions during *H. pylori* infection. Finally, as cholesterol is a key metabolite in *H. pylori* physiology and plays a critical role in bacterial survival within the stomach, we propose that the biological pathways involved in accumulation of this sterol or its derivatives may be attractive targets for the design of new treatments against infection. Interestingly, *H. pylori*-infected subjects with high serum levels of total cholesterol and low-density lipoprotein cholesterol exhibited increased gastritis scores (Kucukazman et al., 2009). It is tempting to speculate whether increased levels of cholesterol within the gastric niche of these subjects might render *H. pylori* bacteria more pathogenic.

## AUTHOR CONTRIBUTIONS

MH and KD performed and analyzed experiments and drafted initial versions of the manuscript. AR designed and constructed suicide vectors for construction of mutants and analyzed the SPFH domain of HP0248. LW, SM, and BC assisted with acquisition and interpretation of data. LT assisted with the construction of vectors for expression of FLOT protein and generation of FLOT mutants. DS performed and analyzed all proteomic analyses. MK assisted with the design of experiments.

RF conceived and coordinated the study and drafted the final version of the manuscript. All authors reviewed the results and approved the final version of the manuscript.

## FUNDING

This project was supported by funding from the National Health and Medical Research Council (NHMRC) to RF and BC (project APP1030243). Research at the Hudson Institute of Medical Research is supported by the Victorian Government's Operational Infrastructure Support Program. RF and AR are supported by fellowships from the NHMRC (SRF GTN606476 and APP1079904) and Wellcome Trust (Sir Henry Postdoctoral Fellow), respectively. MH was supported by a Monash University Graduate Scholarship and Australian Postgraduate Award (APA). KD is supported by an International Postgraduate Scholarship (Monash University Faculty of Medicine, Nursing and Health Sciences) and by the Centre for Innate Immunity and Infectious Diseases. LT was funded by an APA and a Monash

University Faculty of Medicine, Nursing, and Health Sciences Excellence Award.

## ACKNOWLEDGMENTS

The authors thank: Dr. S. Sgouras (Hellenic Pasteur Institute, Greece), for sharing his expertise regarding CagA translocation assays; Dr. C. Lo, for imaging expertise; Dr. A. McAlister, for advice on the expression of His-tagged proteins; Danqing Yin (Hudson Institute of Medical Research), for performing the Venn analysis; Dr. A. Grubman, for assistance with construction of the cloning vectors; and S. Panckridge (Hudson Institute of Medical Research) and C. Ferrero for graphics expertise.

## SUPPLEMENTARY MATERIAL

The Supplementary Material for this article can be found online at: <http://journal.frontiersin.org/article/10.3389/fcimb.2017.00219/full#supplementary-material>

## REFERENCES

- Ansorg, R., Muller, K. D., Von Recklinghausen, G., and Nalik, H. P. (1992). Cholesterol binding of *Helicobacter pylori*. *Zentralbl. Bakteriol.* 276, 323–329. doi: 10.1016/S0934-8840(11)80538-4
- Bach, J. N., and Bramkamp, M. (2013). Flotillins functionally organize the bacterial membrane. *Mol. Microbiol.* 88, 1205–1217. doi: 10.1111/mmi.12252
- Backert, S., Moese, S., Selbach, M., Brinkmann, V., and Meyer, T. F. (2001). Phosphorylation of tyrosine 972 of the *Helicobacter pylori* CagA protein is essential for induction of a scattering phenotype in gastric epithelial cells. *Mol. Microbiol.* 42, 631–644. doi: 10.1046/j.1365-2958.2001.02649
- Baik, S. C., Kim, K. M., Song, S. M., Kim, D. S., Jun, J. S., Lee, S. G., et al. (2004). Proteomic analysis of the sarcosine-insoluble outer membrane fraction of *Helicobacter pylori* strain 26695. *J. Bacteriol.* 186, 949–955. doi: 10.1128/JB.186.4.949-955.2004
- Bramkamp, M., and Lopez, D. (2015). Exploring the existence of lipid rafts in bacteria. *Microbiol. Mol. Biol. Rev.* 79, 81–100. doi: 10.1128/MMBR.00036-14
- Bury-Mone, S., Skouloubris, S., Dauga, C., Thiberge, J. M., Dailidiene, D., Berg, D. E., et al. (2003). Presence of active aliphatic amidases in *Helicobacter* species able to colonize the stomach. *Infect. Immun.* 71, 5613–5622. doi: 10.1128/IAI.71.10.5613-5622.2003
- Carlssohn, E., Nystrom, J., Karlsson, H., Svennerholm, A. M., and Nilsson, C. L. (2006). Characterization of the outer membrane protein profile from disease-related *Helicobacter pylori* isolates by subcellular fractionation and nano-LC FT-ICR MS analysis. *J. Prot. Res.* 5, 3197–3204. doi: 10.1021/pr060181p
- Chionh, Y. T., Walduck, A. K., Mitchell, H. M., and Sutton, P. (2009). A comparison of glycan expression and adhesion of mouse-adapted strains and clinical isolates of *Helicobacter pylori*. *FEMS Immunol. Med. Microbiol.* 57, 25–31. doi: 10.1111/j.1574-695X.2009.00578
- Donovan, C., and Bramkamp, M. (2009). Characterization and subcellular localization of a bacterial flotillin homologue. *Microbiology* 155, 1786–1799. doi: 10.1099/mic.0.025312-0
- Falush, D., Wirth, T., Linz, B., Pritchard, J. K., Stephens, M., Kidd, M., et al. (2003). Traces of human migrations in *Helicobacter pylori* populations. *Science* 299, 1582–1585. doi: 10.1126/science.1080857
- Ferrero, R. L., Thiberge, J. M., Huerre, M., and Labigne, A. (1994). Recombinant antigens prepared from the urease subunits of *Helicobacter* spp.: evidence of protection in a mouse model of gastric infection. *Infect. Immun.* 62, 4981–4989.
- Ferrero, R. L., Thiberge, J. M., Huerre, M., and Labigne, A. (1998). Immune responses of specific-pathogen-free mice to chronic *Helicobacter pylori* (strain SS1) infection. *Infect. Immun.* 66, 1349–1355.
- Ge, L., Qi, W., Wang, L. J., Miao, H. H., Qu, Y. X., Li, B. L., et al. (2011). Flotillins play an essential role in Niemann-Pick C1-like 1-mediated cholesterol uptake. *Proc. Natl. Acad. Sci. U.S.A.* 108, 551–556. doi: 10.1073/pnas.1014434108
- Gobert, A. P., Bambou, J. C., Werts, C., Balloy, V., Chignard, M., Moran, A. P., et al. (2004). *Helicobacter pylori* heat shock protein 60 mediates interleukin-6 production by macrophages via a toll-like receptor (TLR)-2-, TLR-4-, and myeloid differentiation factor 88-independent mechanism. *J. Biol. Chem.* 279, 245–250. doi: 10.1074/jbc.M307858200
- Goluszko, P., and Nowicki, B. (2005). Membrane cholesterol: a crucial molecule affecting interactions of microbial pathogens with mammalian cells. *Infect. Immun.* 73, 7791–7796. doi: 10.1128/IAI.73.12.7791-7796.2005
- Grubman, A., Phillips, A., Thibonnier, M., Kaparakis-Liaskos, M., Johnson, C., Thiberge, J. M., et al. (2010). Vitamin B(6) Is Required for Full Motility and Virulence in *Helicobacter pylori*. *mBio* 1:e00112-10. doi: 10.1128/mBio.00112-10
- Guillemin, K., Salama, N. R., Tompkins, L. S., and Falkow, S. (2002). Cag pathogenicity island-specific responses of gastric epithelial cells to *Helicobacter pylori* infection. *Proc. Natl. Acad. Sci. U.S.A.* 99, 15136–15141. doi: 10.1073/pnas.182558799
- Hildebrandt, E., and Mcgee, D. J. (2009). *Helicobacter pylori* lipopolysaccharide modification, Lewis antigen expression, and gastric colonization are cholesterol-dependent. *BMC Microbiol.* 9:258. doi: 10.1186/1471-2180-9-258
- Hirai, Y., Haque, M., Yoshida, T., Yokota, K., Yasuda, T., and Oguma, K. (1995). Unique cholesteryl glucosides in *Helicobacter pylori*: composition and structural analysis. *J. Bacteriol.* 177, 5327–5333. doi: 10.1128/jb.177.18.5327-5333.1995
- Hutton, M. L., Kaparakis-Liaskos, M., Turner, L., Cardona, A., Kwok, T., and Ferrero, R. L. (2010). *Helicobacter pylori* exploits cholesterol-rich microdomains for induction of NF- $\kappa$ B-dependent responses and peptidoglycan delivery in epithelial cells. *Infect. Immun.* 78, 4523–4531. doi: 10.1128/IAI.00439-10
- Koch, M., Mollenkopf, H. J., and Meyer, T. F. (2016). Macrophages recognize the *Helicobacter pylori* type IV secretion system in the absence of toll-like receptor signalling. *Cell. Microbiol.* 18, 137–147. doi: 10.1111/cmi.12492
- Kucukazman, M., Yavuz, B., Sacikara, M., Asilturk, Z., Ata, N., Ertugrul, D. T., et al. (2009). The relationship between updated sydney system score and LDL cholesterol levels in patients infected with *Helicobacter pylori*. *Digest. Dis. Sci.* 54, 604–607. doi: 10.1007/s10620-008-0391-y
- Lai, C. H., Chang, Y. C., Du, S. Y., Wang, H. J., Kuo, C. H., Fang, S. H., et al. (2008). Cholesterol depletion reduces *Helicobacter pylori* CagA translocation and CagA-induced responses in AGS cells. *Infect. Immun.* 76, 3293–3303. doi: 10.1128/IAI.00365-08

- Lang, D. M., Lommel, S., Jung, M., Ankerhold, R., Petrusch, B., Laessing, U., et al. (1998). Identification of reggie-1 and reggie-2 as plasmamembrane-associated proteins which cocluster with activated GPI-anchored cell adhesion molecules in non-caveolar micropatches in neurons. *J. Neurobiol.* 37, 502–523. doi: 10.1002/(SICI)1097-4695(199812)37:4<502::AID-NEU2>3.0.CO;2-S
- Langhorst, M. F., Reuter, A., and Stuermer, C. A. (2005). Scaffolding microdomains and beyond: the function of reggie/flotillin proteins. *Cell. Mol. Life Sci.* 62, 2228–2240. doi: 10.1007/s00018-005-5166-4
- Larocca, T. J., Crowley, J. T., Cusack, B. J., Pathak, P., Benach, J., London, E., et al. (2010). Cholesterol lipids of *Borrelia burgdorferi* form lipid rafts and are required for the bactericidal activity of a complement-independent antibody. *Cell Host Microbes* 8, 331–342. doi: 10.1016/j.chom.2010.09.001
- Lopez, D., and Kolter, R. (2010). Functional microdomains in bacterial membranes. *Genes Dev.* 24, 1893–1902. doi: 10.1101/gad.1945010
- Maeda, S., Akanuma, M., Mitsuno, Y., Hirata, Y., Ogura, K., Yoshida, H., et al. (2001). Distinct mechanism of *Helicobacter pylori*-mediated NF- $\kappa$ B activation between gastric cancer cells and monocytic cells. *J. Biol. Chem.* 276, 44856–44864. doi: 10.1074/jbc.M105381200
- Manes, S., Del Real, G., and Martinez, A. C. (2003). Pathogens: raft hijackers. *Nat. Rev. Immunol.* 3, 557–568. doi: 10.1038/nri1129
- Mcgee, D. J., George, A. E., Trainor, E. A., Horton, K. E., Hildebrandt, E., and Testerman, T. L. (2011). Cholesterol enhances *Helicobacter pylori* resistance to antibiotics and LL-37. *Antimicrob. Agents Chemother.* 55, 2897–2904. doi: 10.1128/AAC.00016-11
- Mielich-Suss, B., Schneider, J., and Lopez, D. (2013). Overproduction of flotillin influences cell differentiation and shape in *Bacillus subtilis*. *mBio* 4, e00719–e00713. doi: 10.1128/mBio.00719-13
- Montecucco, C., and Rappuoli, R. (2001). Living dangerously: how *Helicobacter pylori* survives in the human stomach. *Nat. Rev. Mol. Cell. Biol.* 2, 457–466. doi: 10.1038/35073084
- Odenbreit, S., Puls, J., Sedlmaier, B., Gerland, E., Fischer, W., and Haas, R. (2000). Translocation of *Helicobacter pylori* CagA into gastric epithelial cells by type IV secretion. *Science* 287, 1497–1500. doi: 10.1126/science.287.5457.1497
- Otto, G. P., and Nichols, B. J. (2011). The roles of flotillin microdomains–endocytosis and beyond. *J. Cell. Sci.* 124, 3933–3940. doi: 10.1242/jcs.092015
- Phadnis, S. H., Parlow, M. H., Levy, M., Ilver, D., Caulkins, C. M., Connors, J. B., et al. (1996). Surface localization of *Helicobacter pylori* urease and a heat shock protein homolog requires bacterial autolysis. *Infect. Immun.* 64, 905–912.
- Segal, E. D., Cha, J., Lo, J., Falkow, S., and Tompkins, L. S. (1999). Altered states: involvement of phosphorylated CagA in the induction of host cellular growth changes by *Helicobacter pylori*. *Proc. Natl. Acad. Sci. U.S.A.* 96, 14559–14564. doi: 10.1073/pnas.96.25.14559
- Simons, K., and Ikonen, E. (1997). Functional rafts in cell membranes. *Nature* 387, 569–572. doi: 10.1038/42408
- Simons, K., and Toomre, D. (2000). Lipid rafts and signal transduction. *Nat. Rev. Mol. Cell. Biol.* 1, 31–39. doi: 10.1038/35036052
- Smeets, L. C., Bijlsma, J. J., Boomkens, S. Y., Vandenbroucke-Grauls, C. M., and Kusters, J. G. (2000). *comH*, a novel gene essential for natural transformation of *Helicobacter pylori*. *J. Bacteriol.* 182, 3948–3954. doi: 10.1128/JB.182.14.3948-3954.2000
- Testerman, T. L., Mcgee, D. J., and Mobley, H. L. (2001). *Helicobacter pylori* growth and urease detection in the chemically defined medium Ham's F-12 nutrient mixture. *J. Clin. Microbiol.* 39, 3842–3850. doi: 10.1128/JCM.39.11.3842-3850.2001
- The EUROGAST Study Group (1993). An international association between *Helicobacter pylori* infection and gastric cancer. *Lancet* 341, 1359–1362. doi: 10.1016/0140-6736(93)90938-D
- Toledo, A., Crowley, J. T., Coleman, J. L., Larocca, T. J., Chiantia, S., London, E., et al. (2014). Selective association of outer surface lipoproteins with the lipid rafts of *Borrelia burgdorferi*. *mBio* 5, e00899–e00814. doi: 10.1128/mBio.00899-14
- Toledo, A., Pérez, A., Coleman, J. L., and Benach, J. L. (2015). The lipid raft proteome of *Borrelia burgdorferi*. *Proteomics* 15, 3662–3675. doi: 10.1002/pmic.201500093
- Trainor, E. A., Horton, K. E., Savage, P. B., Testerman, T. L., and Mcgee, D. J. (2011). Role of the HefC efflux pump in *Helicobacter pylori* cholesterol-dependent resistance to ceragenins and bile salts. *Infect. Immun.* 79, 88–97. doi: 10.1128/IAI.00974-09
- Trampenau, C., and Muller, K. D. (2003). Affinity of *Helicobacter pylori* to cholesterol and other steroids. *Microbes Infect.* 5, 13–17. doi: 10.1016/S1286-4579(02)00054-0
- Viala, J., Chaput, C., Boneca, I. G., Cardona, A., Girardin, S. E., Moran, A. P., et al. (2004). Nod1 responds to peptidoglycan delivered by the *Helicobacter pylori* cag pathogenicity island. *Nat. Immunol.* 5, 1166–1174. doi: 10.1038/nl1131
- Voss, B. J., Gaddy, J. A., McDonald, W. H., and Cover, T. L. (2014). Analysis of surface-exposed outer membrane proteins in *Helicobacter pylori*. *J. Bacteriol.* 196, 2455–2471. doi: 10.1128/JB.01768-14
- Wunder, C., Churin, Y., Winau, F., Warnecke, D., Vieth, M., Lindner, B., et al. (2006). Cholesterol glucosylation promotes immune evasion by *Helicobacter pylori*. *Nat. Med.* 12, 1030–1038. doi: 10.1038/nm1480

**Conflict of Interest Statement:** The authors declare that the research was conducted in the absence of any commercial or financial relationships that could be construed as a potential conflict of interest.

Received: 15 January 2017; Accepted: 11 May 2017; Published: 06 June 2017

Citation: Hutton ML, D'Costa K, Rossiter AE, Wang L, Turner L, Steer DL, Masters SL, Croker BA, Kaparakis-Liaskos M and Ferrero RL (2017) A *Helicobacter pylori* Homolog of Eukaryotic Flotillin Is Involved in Cholesterol Accumulation, Epithelial Cell Responses and Host Colonization. *Front. Cell. Infect. Microbiol.* 7:219. doi: 10.3389/fcimb.2017.00219

Copyright © 2017 Hutton, D'Costa, Rossiter, Wang, Turner, Steer, Masters, Croker, Kaparakis-Liaskos and Ferrero. This is an open-access article distributed under the terms of the Creative Commons Attribution License (CC BY). The use, distribution or reproduction in other forums is permitted, provided the original author(s) or licensor are credited and that the original publication in this journal is cited, in accordance with accepted academic practice. No use, distribution or reproduction is permitted which does not comply with these terms.

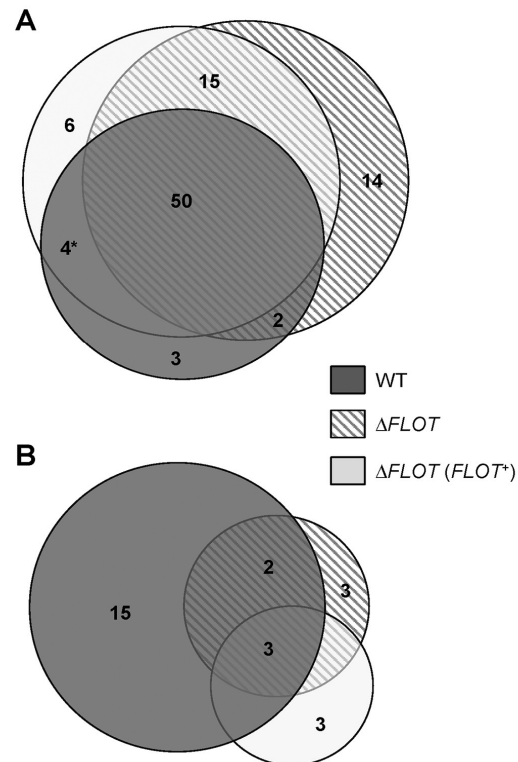


```

sp|075955|FLOT1_HUMAN      30 FVLPCIQQIQRISLNTLTLNVKS---EKVYTRHGVPISVTGIAQVKIQGQ 76
tr|025030|O25030_HELPY   53 VIAFLAKPFEVISSGEIGIKITAGKYEPTPLQPGIHFFVPIIQDILIVDT 102
      : : : : * : : : : : * : : * : * : :
      -----
sp|075955|FLOT1_HUMAN      123 ---NKEMLAAACQMF LGKTEAEIAHIALETLEGHQRAIMAHMTVEEIKD 123
tr|025030|O25030_HELPY   150 RIRNINFSRTEDMGVAGKNQGIFRNDAINVMD--SRGLTVSIELTVQYRL 150
      * : : : . ** : : : * : : : . * : : :
      -----
sp|075955|FLOT1_HUMAN      173 RQKFSEQVFKVASSDLVNMGISVVSYTLKDIHDDQDYLHSLGKARTAQVQ 173
tr|025030|O25030_HELPY   194 NPQTTPQTIATYG---LSWEQKIINPVVRDVVRS---VVG RYPAEDLPK 194
      . : : * : . . : . : . : . : * : . : . * . : :
      -----
sp|075955|FLOT1_HUMAN      288 KDQVAKTKQQIEEQRVQVQVVERAQQVAVQEQEIARREKELEARVRKPAE 288
tr|025030|O25030_HELPY   239 RNEIAALINSGIN-----KEVSKLPNTPVELSSIQLREIVLPKIKEQIE 239
      : : : * : . : : : * : : : : . * ** * * : : : *
      -----
sp|075955|FLOT1_HUMAN      338 AERYKLERLAEAEKSQLIMQAEAEAAASVRMRGEAEFAIGARARAEAEQM 338
tr|025030|O25030_HELPY   284 KVQIARQESERVKYEVERSKQEAQKQAALAKGEADANRIKAQGVA----- 284
      : : . : . : : * : : : : * : * * : . *
      -----
sp|075955|FLOT1_HUMAN      AKKAEAFQL 347
tr|025030|O25030_HELPY   -----

```

**Supplementary Figure 1. CLUSTALW alignment of the SPFH domain human flotillin-1 with that of HP0248.** The SPFH domain of *H. pylori* HP0248 is 231 amino acids in length. The thick line corresponds to the consensus sequence for the SPFH/Band 7 family domain, as determined using MiST2.2 software (<http://mistdb.com/>). Asterisks, colons and dots indicate identical, conserved and semi-conserved amino acid residues, respectively. Numbers refer to amino acid residue positions for human flotillin-1 (total length, 427 amino acids) and *H. pylori* HP0248 (total length, 362 amino acids), respectively.



**Supplementary Figure 2. Venn diagrams showing the distribution of protein “hits” identified by LC-MS/MS analysis of proteins with molecular weights in the 40 kDa range. (A) DRM and (B) DSM fractions of *H. pylori* 251 wild-type (WT), ΔFLOT or FLOT (FLOT<sup>+</sup>) strains were separated by SDS-PAGE and gel digests analyzed by LC-MS/MS. Vennt software (<http://www.vicbioinformatics.com/software/vennt.shtml>) was used to generate Venn diagrams showing the numbers of DRM- and DSM-associated proteins in all *H. pylori* strains. Asterisk indicates HP0248 was amongst the four proteins identified in the DRM fractions from WT and FLOT (FLOT<sup>+</sup>) strains, but not from those of ΔFLOT bacteria.**

**Supplementary Table 1. Primers used in this study**

<b>Primer name</b>	<b>Primer sequence</b>
MH9	GGGGACAAGTTTGTACAAAAAAGCAGGCTTAaggatccacttctttgtgcct atc
MH10	GGGGACCACTTTGTACAAGAAAGCTGGGTAtcattcttggcgcgcgatttgga c
MH1	GGGGACAAGTTTGTACAAAAAAGCAGGCTTAATGCCCATTGAT TTGAACGAACAT
MH3	GGGGACAACCTTTGTATAGAAAAGTTGGGTGCCACAATGAGAAT GTCTTGAATGA
GmB4rF	GGGGACAACCTTTTCTATACAAAGTTGCTGGTACCCGGGTGACTA AC
GmB3rR	GGGGACAACCTTTATTATACAAAGTTGTGGATCCCCGTGTCATTA TTCC
MH4	GGGGACAACCTTTGTATAATAAAGTTGCTAAAAGTCCAAATCGC GCGCCAAGA
MH2	GGGGACCACTTTGTACAAGAAAGCTGGGTACTATTAAGGCTCTT TAGTCTCGGCAAT
M13	TGTAACACGACGGCCAGT (f) TCACACAGGAAACAGCTATGAC (r)
T7	TAATACGACTCACTATAGGG (promoter) GCTAGTTATTGCTCAGCGG (terminator)
MH5	CCTAATACGCCTAATAATGGG
MH6	GGCTCTTTAGTCTCGGCAAT
GmFwd	gacacgatgccaacacgacg
GmRvs	agggcctcgatcagccaag
LT8F	GGGGACAAGTTTGTACAAAAAAGCAGGCTCAATGAAATTTTTG GATCAAG
LT8R	GGGGACAACCTTTTGTATACAAAGTTGTATTTGAGCAAAAGAGG GGATC
LT9F	GGGGACAACCTTTGTATACAAAGTTGCATTAGTTAATGAACGCT

	TCTG
LT9R	GGGGACAACCTTTGTATAGAAAAGTTGGGTGTTTTGGGGTGAGTT TCATCTC
MH11	GGGGACAACCTTTTCTATACAAAGTTGCAATGCCCATTGATTTGA ACGAAC
MH12	GGGGACAACCTTTATTATACAAAGTTGTTTAAGGCTCTTTAGTCT CGGC
LT10F	GGGGACAACCTTTGTATAATAAAGTTGCAGAGATTCAACCACAG CATGC
LT10R	GGGGACCACTTTGTACAAGAAAGCTGGGTATCACAACCAAGTA ATCGCATC
AG1F	ACCACACGGCCACTACATGC
MH13R	ACCACACGGCCACTACATGC



**Supplementary Table 2. Cellular locations of cytoplasmic proteins as predicted by the PSORTb program.**

<b>HP No.</b>	<b>Protein</b>	<b>Cytoplasmic</b>	<b>Cytoplasmic Membrane</b>	<b>Periplasmic</b>	<b>Outer Membrane</b>	<b>Extra-cellular</b>
0072	Urease subunit B (UreB)	100 <sup>a</sup>	0	0	0	0
0073	Urease subunit A (UreA)	100	0	0	0	0
0248	Flotillin-like protein	89.6	5.1	2.6	0.1	2.6
1132	ATP synthase F1, subunit beta	91.2	8.8	0	0	0
1462	Secreted protein involved in motility	89.6	5.1	2.6	0.1	2.6
1563	Alkyl hydroperoxide reductase (TsaA)	100	0	0	0	0

<sup>a</sup> Predicted locations are reported as percentages.

**Supplementary Table 4. List of proteins migrating in the 40 kDa molecular weight range and common to DRM fractions from *H. pylori* WT,  $\Delta FLOT$  and  $\Delta FLOT$  (*FLOT+*) bacteria but absent from all DSM fractions.** <sup>1</sup>

<b>HP number</b>	<b>Protein name</b>	<b>Accession number</b>	<b>Da</b>	<b>Mascot search score</b>	<b>Total peptides matched</b>
HP0010	60 kDa Heat shock protein, chaperone (GroEL/HspB)	P42383	58285	108	10
HP0019	Chemotaxis protein (CheV1)	O24864	36735	30	2
HP0045	Nodulation protein (NolK)	O24886	35075	93	7
HP0106	Cystathionine g-synthase (MetB)	P56069	41320	52	2
HP0118	Hypothetical protein	O24937	45336	20	1
HP0176	Fructose-biphosphate aldolase (Fba/Tsr)	P56109	33865	230	15
HP0197	S-adenosylmethionine synthase (MetK)	P56460	42678	40	2
HP0254	Outer membrane protein 8 (OMP8, HopG)	O25036	47526	38	5
HP0267	Adenosine deaminase	O25046	45798	68	3
HP0393	Chemotaxis protein (CheV3)	O25154	35665	51	1
HP0554	Hypothetical protein	O25280	37202	81	4
HP0569	GTP-binding protein (Gtp1)	O25293	40834	53	2
HP0570	Cytosol aminopeptidase (PepA)	O25294	54969	41	1
HP0582	Hypothetical periplasmic protein (TonB homolog)	O25304	37359	47	5
HP0589	2-oxoglutarate-acceptor oxidoreductase subunit (OorA)	O25311	41596	26	2
HP0631	Hydrogenase (NiFe) small subunit (HydA)	O25348	42954	50	2
HP0656	Dehypoxanthine futalosine cyclase	O25370	43738	47	2

HP0694	Hypothetical protein	O25401	29996	150	5
HP0825	Thioredoxin reductase (TrxB)	P56431	34030	287	13
HP0913	OMP21 (HopB, AlpB)	O25571	57141	19	2
HP1110	Pyruvate ferredoxin oxidoreductase, a subunit (PorA)	O25738	45000	26	1
HP1111	Pyruvate ferredoxin oxidoreductase, b subunit (PorB)	O25739	35390	31	3
HP1118	g-glutamyltranspeptidase (GGT)	O25743	61113	62	4
HP1133	ATP synthase g chain (AtpG)	P56082	34221	121	4
HP1177	OMP27 (HopQ)	O25791	69991	55	4
HP1335	Predicted tRNA-specific 2- thiouridylase (MnmA)	O25893	38508	71	5
HP1345	Phosphoglycerate kinase (Pgk)	P56154	44915	60	4
HP1349	Hypothetical periplasmic protein	O25904	44538	37	1
HP1373	Rod shape-determining actin- like protein (MreB)	O25925	37488	220	7
HP1398	Alanine dehydrogenase (Ald)	O25948	41256	196	8
HP1554	30S ribosomal protein S2 (RpsB)	P56009	30839	61	2

<sup>1</sup> Proteins were identified by LC-MS/MS using the QExactive mass spectrometer.

### 2.3. Discussion

The findings of this chapter have demonstrated the existence and characteristics of a novel flotillin-like protein, HP0248, in a bacterial pathogen. Furthermore, we have provided convincing evidence for the presence lipid raft-like structures in the human pathogen, *H. pylori*. Although this is not the first report of lipid rafts and flotillin-like proteins in prokaryotes [108, 109, 113, 115, 188], we have demonstrated for the first time a role for bacterial membrane cholesterol in the stabilization of bacterial raft-like structures as well as the incorporation of specific proteins important for adherence, virulence and colonization into these cholesterol-rich domains present in *H. pylori*. These observations are consistent with an important property of eukaryotic membrane rafts to selectively include or exclude proteins that influence interactions at the cell surface [102]. Furthermore, DRMs in *S. aureus* were reported to contain proteins required for biofilm formation, signaling, attachment, and virulence [108]. Similar findings were also reported for lipid raft-like structures from other bacterial pathogens such as *B. burgdorferi* [112].

Interestingly, this study has also determined a role for the *H. pylori* flotillin-like protein, HP0248, in the induction of pro-inflammatory cytokine and chemokine responses in host epithelial cells. In addition, we found that HP0248 was required for the T4SS-dependent delivery of CagA to target cells and mouse colonization *in vivo*. However, the most striking finding is the association between the flotillin-like protein, HP0248, and the presence of cholesterol in the cell membrane of the bacterium, making this is the first example of a specific protein that may be involved in cholesterol acquisition/retention in *H. pylori*. Taken together, these data suggest that HP0248 and the associated membrane rafts are critical for *H. pylori* pathogenesis and virulence.

Overall, we have identified a novel *H. pylori* homolog of eukaryotic flotillin that localizes to the cholesterol-enriched cell membrane domains of the bacterium. We propose that this bacterial protein constitutes a new class of bacterial virulence factors involved in host-pathogen interactions. Given that the deletion of HP0248 did not completely abrogate pro-inflammatory chemokine responses in host epithelial cells, it is possible that *H. pylori* encodes for additional flotillin-like proteins, as is common in

other bacterial species such as *B. subtilis* [115]. Indeed, recent findings suggest HP0248 is likely to be more similar to the flotillin-like protein YqfA (or FloA) from *B. subtilis*, rather than the YuaG (or FloT) protein used to identify HP0248 in this study [115]. Furthermore, since our results have shown that HP0248 is required in the optimal delivery of CagA into host cells, it would be of interest to demonstrate if the T4SS-dependent translocation of PG and subsequent induction of NOD1-dependent pro-inflammatory responses are also affected in the absence of this bacterial flotillin-like protein. Finally, this study recognizes cholesterol-rich membrane domains as a novel therapeutic target to combat persistent *H. pylori* infection, and thus provides additional evidence to support emerging data identifying the use of statins as a feasible approach to alleviate *H. pylori*-mediated inflammation [189, 190].

## **Chapter 3: Modifications of *Helicobacter pylori* peptidoglycan during host adaptation affect NOD1-mediated gastric epithelial cell responses**

### ***3.1. Summary***

The intracellular innate immune receptor, NOD1, recognizes a conserved structure present in Gram-negative bacterial PG [61]. Human and murine NOD1 have further evolved to preferentially sense two distinct forms of PG that differ solely in the lengths of their side chains – being GM-Tri<sub>DAP</sub> and GM-Tetra<sub>DAP</sub>, respectively [155, 159]. Ratios of Tri/Tetra<sub>DAP</sub> have been shown to vary not only between bacterial species, but also between different strains within the same bacterial species [51, 161, 191, 192]. However, interestingly, the biological significance of these observations remains unclear. *Helicobacter pylori*, a non-invasive gastric pathogen, activates NOD1 signaling by delivering PG fragments into host cells via the T4SS encoded by the *cagPAI* or OMVs [35, 55]. NOD1 detection of *H. pylori* typically initiates host defense mechanisms resulting in NF- $\kappa$ B activation and production of the CXC chemokine, IL-8, by epithelial cells [35, 65]. Thus, NOD1 is an important mediator of epithelial cell sensing of *H. pylori* infection.

Gram-negative pathogens have, however, evolved various strategies to modify their PG and thus avoid NOD1 detection [68, 160, 193]. Indeed, *H. pylori* also utilizes several enzymes that mediate cell wall PG modifications which, in turn, affects bacterial colonization and immune recognition by the host [68, 72, 73]. Bacterial PG is thus an important virulence factor required for the establishment and persistence of infection in the host.

Studies have previously reported how the sequential passage of a clinical *cagPAI*<sup>+</sup> *H. pylori* isolate (245) through mice resulted in a “mouse-adapted” variant (245m3) that colonized the mouse in high numbers, but which had lost the ability to induce NF- $\kappa$ B and IL-8 responses in a human gastric epithelial cell line [164]. The mouse-adapted *H. pylori* 245m3 variant was further observed to retain a genetically intact *cagPAI* [164]. Based on the implications of PG composition on NOD1 recognition,

we hypothesized that the reduced NF- $\kappa$ B activation by *H. pylori* 245m3 in human cells may be associated with modifications in its cell wall PG composition. We speculate that NOD1 signaling may confer a selective advantage to *H. pylori in vivo*, a finding that would have broader implications for other bacterial pathogens detected by this cytosolic receptor.

The following experiments were therefore designed to: **firstly**, identify any genomic differences between the mouse-adapted *H. pylori* strain, 245m3, and its human clinical progenitor isolate, *H. pylori* 245; **secondly**, we wished to characterize the PG muropeptide composition of the aforementioned human and mouse-adapted isolates of *H. pylori* as well as other paired human and mouse-adapted *H. pylori* strains; **finally**, we sought to determine the impact of bacterial PG modifications on NOD1-dependent host responses and colonization *in vitro* and *in vivo*, respectively.

**Modifications in Muropeptide Composition Arising From Mouse Adaptation of a Human *Helicobacter pylori* Isolate Have an Impact on Host-Specific NOD1 Responses<sup>#</sup>**

Kimberley D'Costa<sup>a</sup>, Le Son Tran<sup>a</sup>, Chantal Ecobichon<sup>b,c</sup>, Samia Hicham<sup>b,c</sup>, Aleks Guanizo<sup>a</sup>, Timothy P. Stinear<sup>d</sup>, Roxane Legaie<sup>e</sup>, Richard Wheeler<sup>b,c</sup>, Amanda De Paoli<sup>a\*</sup>, Hazel Tye<sup>a</sup>, Cody C. Allison<sup>a\*</sup>, David L. Steer<sup>f</sup>, Jonathan Ferrand<sup>a</sup>, Stephen E. Girardin<sup>h</sup>, Ivo G. Boneca<sup>b,c</sup>, Richard L. Ferrero<sup>a,i</sup>

Centre for Innate Immunity and Infectious Diseases, Hudson Institute of Medical Research, Monash University, Clayton, Victoria, Australia <sup>a</sup>; Unit of Biology and Genetics of the Bacterial Cell Wall, Institut Pasteur, Paris, France <sup>b</sup>; INSERM, Groupe Avenir, Paris, France <sup>c</sup>; Doherty Applied Microbial Genomics, Department of Microbiology and Immunology, University of Melbourne at the Doherty Institute for Infection & Immunity, Melbourne, Victoria, Australia <sup>d</sup>; Monash Bioinformatics Platform, Monash University, Clayton, Victoria, Australia <sup>e</sup>; Monash Biomedical Proteomics Facility, Monash University, Clayton, Victoria, Australia <sup>f</sup>; Department of Immunology, University of Toronto, Toronto, Canada <sup>g</sup>; Department of Laboratory Medicine and Pathobiology, University of Toronto, Toronto, Canada <sup>h</sup>; Biomedicine Discovery Institute, Department of Microbiology, Monash University, Clayton, Victoria, Australia <sup>i</sup>.

<sup>#</sup> Running title: Changes to *H. pylori* peptidoglycan during host adaptation

Address correspondence to: Richard L. Ferrero, [REDACTED]

\* Present Address: Amanda De Paoli, Department of Biochemistry and Molecular Biology Drug Delivery Disposition and Dynamics, Monash Institute of Pharmaceutical Sciences, Monash University, Parkville, Victoria, Australia; Cody Allison, The Walter and Eliza Hall



- 26 Institute of Medical Research, Melbourne, Australia and Department of Medical Biology,  
27 The University of Melbourne, Melbourne, Australia.
- 28 Abstract word count: **254**
- 29 Total word count: **9,275**

## ABSTRACT

The intracellular innate immune receptor, NOD1, recognizes a conserved structure present in the degradation products (muropeptides) of Gram-negative bacterial peptidoglycan (PG). Human and mouse NOD1 preferentially detect two distinct forms of muropeptides, namely GM-Tri<sub>DAP</sub> and GM-Tetra<sub>DAP</sub>, respectively. The non-invasive gastric pathogen, *Helicobacter pylori*, activates NOD1 signaling by delivering muropeptides into host epithelial cells via a type IV secretion system. Here, we investigated whether changes in cell wall PG occurred during host adaptation of *H. pylori* and if these modifications may subsequently affect NOD1 signaling in host cells. For this, we used a clinical isolate, *H. pylori* 245, and its mouse-adapted variant, 245m3, which colonizes mice in higher numbers. We showed that *H. pylori* 245m3 displayed a 2.6-fold increase in murine Nod1-specific GM-Tetra<sub>DAP</sub> relative to the human NOD1-specific GM-Tri<sub>DAP</sub> in its cell wall. In comparison to the clinical isolate, 245, *H. pylori* 245m3 was affected in its ability to induce pro-inflammatory responses in human gastric epithelial cells. These differences appeared to be independent of T4SS functions. Interestingly, however, *H. pylori* 245m3 induced higher chemokine production in mouse epithelial cells and embryonic fibroblasts. Analyses of additional pairs of clinical and mouse-adapted *H. pylori* strains suggested that the modifications in PG muropeptide composition arising from host adaptation have an impact on NOD1 responses in host cells, but these changes may be strain-dependent. Taken together, our findings demonstrate that the human gastric pathogen, *H. pylori*, modulates its muropeptide composition to enable detection by the NOD1 signaling pathway, which may be important for bacterial colonization and persistence *in vivo*.

## 52    **IMPORTANCE**

53    The stomach pathogen *Helicobacter pylori* has been associated with humans for over 100,000  
54    years. This Gram-negative bacterium is highly adapted to the human stomach, where it can  
55    persist for decades. The cytosolic molecule NOD1 is important for epithelial cell sensing of  
56    Gram-negative peptidoglycan and host defense responses against infection. Interestingly,  
57    human and mouse NOD1 have evolved to detect slightly different structures within Gram-  
58    negative peptidoglycan, yet the biological significance of this specificity remains undefined.  
59    We have shown that “mouse-adaptation” of a clinical *H. pylori* isolate (245) generated a  
60    variant (245m3) that exhibited an increased proportion of the murine Nod1 agonist, GM-  
61    Tetra<sub>DAP</sub>. We confirmed the specificity of NOD1 recognition of *H. pylori* 245 and 245m3 in  
62    *in vitro* cell culture models. This study demonstrates that modifications in peptidoglycan  
63    composition arising from host adaptation may render bacteria more detectable by NOD1,  
64    thereby potentially promoting their persistence *in vivo*.

## INTRODUCTION

During cell division, Gram-negative bacteria remodel their cell walls, resulting in the release of low molecular weight, soluble fragments of degraded peptidoglycan (PG), known as muropeptides (1). These muropeptides have been shown to have a higher biological activity than intact cell walls and to induce multiple pro-inflammatory and cytotoxic effects on mammalian host cells (1-3).

Bacterial muropeptides are recognized by the cytoplasmic innate immune sensor, Nucleotide-binding Oligomerisation Domain 1 (NOD1) in mammalian cells (4, 5). NOD1 specifically senses  $\gamma$ -D-glutamyl-meso-diaminopimelic acid (iE-DAP), a motif almost exclusively found in the cell walls of Gram-negative bacteria (6). Interestingly, human and murine NOD1 have been shown to preferentially detect slightly differently forms of muropeptides, namely a tri-peptide stem structure (GM-Tri<sub>DAP</sub>) and a tetra-peptide stem structure (GM-Tetra<sub>DAP</sub>), respectively (7, 8). Gram-negative pathogens exhibit varying GM-Tri<sub>DAP</sub> versus GM-Tetra<sub>DAP</sub> ratios both within and between bacterial species (9, 10). Indeed, the tracheal toxin produced by *Bordetella pertussis*, a muropeptide fragment enriched with a GlcNAc-(anhydro)MurNAc (11) -Tetra<sub>DAP</sub> motif, is observed to preferentially activate mouse Nod1 (7, 8). In contrast, *Bacillus subtilis* has been reported to be a weak inducer of Nod1 activation in mice due to the presence of a higher percentage of amidated GM-Tri<sub>DAP</sub> muropeptides in its PG (12). Bacteria have thus evolved various strategies to modify their PG and evade NOD1 detection (13, 14). Indeed, bacteria possess a variety of PG-modifying enzymes that can modify PG muropeptide composition thereby affecting both innate immune recognition and bacterial colonization in the host (10, 13-18). Of significance are recent data reported by Zarantonelli *et al.*, demonstrating how modifications in the muropeptide composition of *Neisseria meningitidis* had compound effects on its resistance to penicillin, induction of NOD1-

dependent responses and fitness in an *in vivo* infection model (18). Nevertheless, the biological significance of differential NOD1 agonist specificity and PG muropeptide composition in bacteria remains poorly understood.

*Helicobacter pylori* is a Gram-negative human pathogen that infects half of the world's population. It is classified as a Type 1 carcinogen and is the leading risk factor associated with 75% cases of gastric cancer (19, 20). *H. pylori* is highly adapted to the human stomach and has developed numerous mechanisms to enable its chronic persistence in this site. In particular, virulent strains of *H. pylori* possess a 40 kb *cag* pathogenicity island (*cagPAI*), which encodes genes required for the production of a Type 4 Secretion System (T4SS) (21, 22). Interactions between the CagL protein on the exterior of the *H. pylori* T4SS and  $\alpha_5\beta_1$  integrins on gastric epithelial cells facilitate the translocation of bacterial effector molecules, cytotoxin-associated gene A (CagA) and PG, into host cells (23-26). In addition to the delivery of PG via the T4SS, this *H. pylori* cell wall component can be delivered into host epithelial cells by outer membrane vesicles (OMVs) in a *cagPAI*-independent manner (27). It has been shown that *H. pylori* interactions with host epithelial cells, involving either the T4SS or OMVs, result in activation of a pro-inflammatory signaling cascade mediated by NOD1 (5, 27). Upon detection of PG delivered by *H. pylori*, NOD1 associates with the adaptor molecule, receptor interacting serine/threonine-protein kinase 2 (RIPK2), and subsequently activates the nuclear factor-kappa B (NF- $\kappa$ B) and mitogen-activated protein kinase (MAPK) pathways resulting in the production of the pro-inflammatory chemokine, Interleukin-8 (IL-8) (5, 28-30).

Previous work from our group described how the repeated passage through mice of a human *H. pylori* *cagPAI*<sup>+</sup> isolate, strain 245, resulted in the generation of a mouse-adapted variant,

115 245m3, which was impaired in its ability to induce NF- $\kappa$ B-dependent responses in human  
116 gastric epithelial cells (31). In the current study, we have used these paired *H. pylori* isolates  
117 to investigate the dual impact of host adaptation on PG mucopeptide composition and  
118 recognition by the host innate immune system. We found that the mouse-adapted *H. pylori*  
119 245m3 variant exhibited an increased proportion of GM-Tetra<sub>DAP</sub> relative to GM-Tri<sub>DAP</sub>  
120 mucopeptides, when compared with the progenitor clinical isolate. This alteration in  
121 mucopeptide composition resulted in reduced NOD1-dependent CXC chemokine responses in  
122 human epithelial cells. Importantly, we showed that while other mouse-adapted *H. pylori*  
123 strains displayed modifications to their PG composition, others retained a similar profile to  
124 their parental isolates. From genomic analyses, we also identified a predicted protein  
125 truncation in the PG-modifying lytic transglycosylase enzyme, MltD (HP0527), in the  
126 mouse-adapted variant, 245m3. We hypothesize that the human gastric pathogen, *H. pylori*,  
127 modulates its mucopeptide composition via MltD, or other PG- modifying enzymes, to  
128 actively engage the NOD1 signaling pathway.

## RESULTS

**Host specificity in NOD1-mediated host defense against *H. pylori* infection in mice.** In a previous study (31), we showed that the repeated passage of a clinical isolate, *H. pylori* 245, resulted in a generation of a mouse-adapted variant, 245m3, which colonized the stomachs of wild-type mice in high numbers. In the present study, we sought to investigate the effect of the NOD1 signaling pathway on the colonization of the *H. pylori* strains, 245 and 245m3, *in vivo*. For this, *Nod1*<sup>+/+</sup> and *Nod1*<sup>-/-</sup> mice were infected with *H. pylori* strains, 245 and 245m3, and then sacrificed at either 7 (Fig.1A) or 30 (Fig. 1C) days post-infection. Consistent with previous findings (31), 2-fold higher bacterial loads were recovered from *Nod1*<sup>+/+</sup> mice infected with *H. pylori* 245m3 compared to 245, at both time points (Fig.1A, C). Interestingly, both the human (1.5 fold increase) and mouse-adapted (0.5 fold increase) *H. pylori* strains were able to colonize *Nod1*<sup>-/-</sup> animals with greater efficiency at 7 days post-infection (Fig.1A); however, at 30 days post-infection, only *H. pylori* 245m3 bacteria were recovered at significantly higher numbers (1.2 fold increase; Fig. 1C). These data suggested that mouse Nod1 may have a greater impact on chronic infection by the mouse-adapted strain.

As human and mouse NOD1 preferentially recognize different PG side chains (7), we next infected transgenic mice that specifically express human NOD1 but not its murine equivalent (hTghNOD1<sup>+/+</sup>) (18). At 7 days post-infection, hTghNOD1<sup>+/+</sup> animals infected with the human clinical isolate, 245, exhibited lower bacterial loads when compared with their *Nod1*<sup>-/-</sup> counterparts, though these differences did not reach statistical significance (Fig. 1B). Interestingly, no differences were observed in animals gavaged with the *H. pylori* 245m3 strain (Fig. 1B). Collectively, these data demonstrate host-specificity in NOD1-mediated host defense against infection by *H. pylori* strains.

**Identification of genetic polymorphisms arising from mouse adaptation of a human**

***H. pylori* isolate.** Strain-specific genetic diversity has been proposed to affect the ability of *H. pylori* to colonize and persist in a host (32). Therefore, we wished to first ascertain whether the mouse-adapted *H. pylori* variant, 245m3, was indeed derived from the progenitor human clinical isolate, *H. pylori* 245. Using paired-end whole genome sequencing and subsequent mapping/bioinformatics analyses, we demonstrated that both *H. pylori* 245 and 245m3 displayed >90% similarity to the genome of the reference strain, *H. pylori* 26695. In addition, both strains shared >95% similarity with each other (Fig. 2A). We further confirmed this result via sequencing of the well-conserved housekeeping gene, *glmM*, (33) as well as CagA genotyping both strains (SF.1). Interestingly, 300 single nucleotide polymorphisms (SNPs) were also identified in the genome of the mouse-adapted variant, when compared with the genome of the parental clinical isolate (Fig. 2B). Of these, approximately 63.3% were predicted to induce missense mutations in the genome, whereas 1.3% were predicted to induce premature stop codons in the open reading frames of genes (Fig. 2B, Table 1). Importantly, three of the nonsense mutations were detected in *cagPAI*- and PG metabolism-associated genes, namely: *cag3* (HP0522), *cag7* (HP0527) and *mltD/dniR* (HP1572) (Fig. 2C, Table 1).

**Mouse-adapted *H. pylori* 245m3 has a functional T4SS.** Having identified the presence of SNPs in the genome of *H. pylori* 245m3, it was imperative to confirm the presence of an intact *cagPAI* in both *H. pylori* strains via Western blotting for Cag3, Cag7 and CagA (Figure 3A; SF.2). Full-length CagA and Cag7 proteins were observed in whole cell lysates obtained from *H. pylori* 245m3, however, no Cag3 protein production was detected (Figure 3A; SF.2). We subsequently examined the translocation of the CagA effector protein to confirm the presence of a functional T4SS in *H. pylori* 245 and 245m3 bacteria. Using an



immunofluorescence-based technique to detect both extracellular and intracellular CagA (34), we observed that the levels of intracellular CagA were unchanged in AGS cells that had been co-cultured with *H. pylori* 245 or 245m3 bacteria (Fig. 3B;  $P > 0.05$ ). Together, these data indicate that *H. pylori* 245m3, appears to retain a genetically intact *cagPAI* and is still able to translocate CagA into host cells, suggesting the presence of a functional T4SS.

**Mouse-adapted *H. pylori* strains exhibit an increased proportion of murine Nod1-specific GM-Tetra<sub>DAP</sub> relative to the human NOD1 agonist, GM-Tri<sub>DAP</sub>.** To investigate whether changes in cell wall PG muropeptides could account for the differential detection of *H. pylori* 245 and 245m3 by NOD1 in mice (Fig. 1), we performed HPLC/MALDI-MS analyses on the digested PG from both strains (Fig. 4A). Strikingly, the PG from *H. pylori* 245m3 displayed a 2.6-fold increase in mouse Nod1-specific Tetra<sub>DAP</sub> muropeptides relative to the human NOD1-specific Tri<sub>DAP</sub> form, when compared with *H. pylori* 245 (Fig. 4A, B). To corroborate these findings, we also analyzed alternate pairs of *H. pylori* clinical (10700, 256) and mouse-adapted (SS1, 256m1, 256m2) strains (31, 35, 36). Similar to the results obtained for *H. pylori* 245 and 245m3, HPLC/MALDI-MS analyses revealed a 1.53-fold increase in Tetra<sub>DAP</sub> muropeptides relative to the Tri<sub>DAP</sub> form in the mouse-adapted *H. pylori* SS1 strain, when compared with its clinical progenitor, 10700 (also known as PMSS1) (37) (SF. 3A, B). Significantly higher (1.1 fold increase) bacterial loads were also recovered at 7 days post-infection from *Nod1*<sup>-/-</sup> mice infected with *H. pylori* SS1 but not 10700, when compared with *Nod1*<sup>+/+</sup> animals (SF. 3D). In contrast, no changes in the muropeptide composition were observed in the mouse-adapted strains, 256m1 and 256m2, when compared with the clinical isolate, 256 (5, 31) (SF. 4A, B). Interestingly, it was shown that although *H. pylori* SS1, like *H. pylori* 245m3, was affected in its ability to induce NF-κB-dependent responses in human epithelial cells, both *H. pylori* 256m1 and 256m2 were unaffected in this

regard (31). Thus, the data suggest that the acquisition of modifications in PG mucopeptide composition during host adaptation is a strain-specific phenomenon and that these changes may have an impact on host cell responses.

***H. pylori* 245m3 is affected in its ability to induce NOD1-dependent cytokine responses in human gastric epithelial cells, but not cells of murine origin.**

Given the importance of *H. pylori* detection by NOD1 for the generation of pro-inflammatory responses in host gastric epithelial cells (5), we next examined interactions between *H. pylori* 245/245m3 and host cells *in vitro*. Using AGS human cell lines stably expressing short hairpin RNA (shRNA) to either *NOD1* or an irrelevant gene (23, 29, 38), we found that the 245m3 strain induced significantly lower NF- $\kappa$ B p65 subunit translocation (Fig. 5A), *CXCL8* gene expression (Fig. 5B) and CXCL8/IL-8 cytokine production (Fig. 5C), compared with the 245 strain. These responses were further abrogated in the AGS *NOD1* knockdown cell line infected with both *H. pylori* strains (Fig. 5A-C). We also corroborated our observations relating to IL-8 chemokine production using AGS control and *NOD1* knockout cell lines generated using the CRISPR-Cas9 technology, thereby confirming a role for NOD1 in mediating altered cytokine responses upon infection with human and mouse-adapted *H. pylori* bacteria (Fig. 2D).

Finally, to investigate whether the altered pro-inflammatory responses observed in gastric epithelial cells were *cagPAI*-independent effects, OMVs from *H. pylori* 245 and 245m3 were added to AGS control and NOD1 knockdown cell lines (Fig. 6A). As hypothesized, we observed significantly reduced IL-8 responses in AGS control cells stimulated with 245m3 OMVs in comparison to those stimulated with 245 OMVs, as well as an additional significant decline in IL-8 responses in stimulated AGS *NOD1* knockdown cells (Fig. 6A). In contrast, murine epithelial cells (GSM06) and immortalized murine embryonic fibroblasts (MEFs) stimulated with 245m3 OMVs produced higher levels of Cxcl2/MIP-2, a murine IL-8

homologue (39) (Fig. 6B, C). Importantly, a significant decrease in Cxcl2/MIP-2 responses was observed in immortalized *Nod1*<sup>-/-</sup> MEFs stimulated with 245m3 OMVs, when compared with those from *Nod1*<sup>+/+</sup> mice (Fig. 6C). In summary, we identified that *H. pylori* 245m3 was significantly impaired in its ability to induce NOD1-dependent responses in human gastric epithelial cells, when compared with the progenitor strain, 245. However, these trends were reversed in epithelial cells and embryonic fibroblasts of murine origin, thus further confirming the host specificity of *H. pylori*-NOD1 signaling axis.

#### ***H. pylori* 245m3 has a SNP in the gene encoding the PG-modification enzyme, MltD.**

*H. pylori* MltD (encoded by *HP1572*) has previously been established to function as a key factor involved in the modulation of PG composition in *H. pylori* in a strain-specific manner (10, 15). Having identified the introduction of a SNP in the *mltD* gene of *H. pylori* 245m3 by comparative genomics (Fig. 2C), we confirmed the presence of this SNP via Sanger sequencing (SF. 5A). Next, we investigated its expression in *H. pylori* 245 and 245m3 via RT-PCR (SF. 5B). Interestingly, while the genome sequencing analysis predicted a premature truncation of the *mltD* gene truncation in *H. pylori* 245m3 (SF. 5A), our RT-PCR data indicate that this gene is expressed in both clinical and mouse-adapted *H. pylori* strains of interest, with only a slight reduction in the latter (SF. 5B). Although published findings by Roure *et al* (15) reported that the inactivation of *mltD* resulted in a motility defect in *H. pylori*, semi-solid agar tests conducted in our laboratory indicated that the observed SNP in *mltD* had no significant effect on the motility of *H. pylori* 245m3 (SF. 5D, E). Taken together, these results indicate that the phenotypic and pathogenic changes observed in *H. pylori* 245m3 post-host adaptation could be attributed to genetic changes in *mltD*, a known PG modification enzyme.

## DISCUSSION

The innate immune receptor, NOD1, is present in the cytoplasm of various cell types and tissues and has key functions in immune surveillance, host responses against infection and regulation of cell death (4). It is well established that NOD1 sensing of *H. pylori* PG, delivered via the T4SS or OMVs, results in the generation of pro-inflammatory immune responses required for bacterial clearance and host defense (5, 27). Furthermore, the NOD1 receptor from human and murine hosts has been shown to preferentially recognize different motifs (GM-Tri<sub>DAP</sub> versus GM-Tetra<sub>DAP</sub>) in bacterial PG (7, 8). Importantly, the reasons contributing to this evolution and its biological repercussions remain ill-defined. Many Gram-negative human pathogens, such as *N. meningitidis*, produce significantly more GM-Tetra<sub>DAP</sub> than GM-Tri<sub>DAP</sub> muropeptides (40-42). In contrast, *H. pylori* strains seem to contain similar proportions of GM-Tri<sub>DAP</sub> versus GM-Tetra<sub>DAP</sub> forms (10, 13, 15, 43, 44). Interestingly, however, examination of published data (15, 17) suggest that laboratory *H. pylori* strains contain more GM-Tri<sub>DAP</sub>, whereas host-adapted isolates that colonize mice in high numbers seem to display a higher ratio of GM-Tetra<sub>DAP</sub>. In the present study, we have demonstrated that changes in GM-Tetra<sub>DAP</sub>/GM-Tri<sub>DAP</sub> ratios are a common occurrence in *H. pylori* strains that have been adapted to colonize the murine host. In addition, we have shown that these modifications in muropeptide composition impact on NOD1 signaling in the host, thereby possibly providing a selective advantage to the bacterium *in vivo*.

In agreement with an earlier study (31), we showed that the mouse-adapted strain, *H. pylori* 245m3, colonized wild-type mice with greater efficiency at 7 and 30 days post-infection, in comparison to its parental human clinical isolate, *H. pylori* 245 (Figure 1). Importantly, higher bacterial loads were recovered from *Nod1*<sup>-/-</sup> mice infected with both *H. pylori* 245 and

245m3 at 7 days post-infection, with only the latter mouse-adapted variant displaying a colonization advantage at the later time point assessed (Figure 1).

We next performed whole genome sequencing of both *H. pylori* 245 and 245m3 strains in order to confirm the genetic similarity between both isolates. We corroborated that *H. pylori* 245m3 was indeed a variant of its parental human isolate, but additionally identified 300 SNPs in its genome (Figure 2, SF.1, Table 1). Significantly, 3 of the identified SNPs were predicted to induce premature stop codons in *cagPAI*- and PG metabolism-associated genes (i.e. *cag3*, *cag7* and *mltD*) (Figure 2, Table 1). From previous work (5), it appears that NOD1 sensing of *H. pylori* is affected by both the *cagPAI* and PG-status of the bacterium. Interestingly, we determined by Western blotting a loss of Cag3 protein expression, but no change in Cag7 expression in the mouse-adapted strain, 245m3 (SF.2). As Cag3 has previously been shown to be essential for T4SS function in *H. pylori* (45, 46), it is possible that the 245m3 variant contained a non-functional T4SS. However, CagA expression and T4SS-dependent CagA translocation appeared to be unaffected (Figure 3). Hence, the effect of Cag3 loss in the mouse-adapted *H. pylori* strain, 245m3, remains to be elucidated.

Importantly, from HPLC/MALDI analyses of digested PG from *H. pylori* 245 and 245m3, we demonstrated that the latter mouse-adapted variant displayed a 2.6-fold increase in the murine Nod1 agonist, GM-Tetra<sub>DAP</sub> compared with GM-Tri<sub>DAP</sub>, which is preferentially recognized by human NOD1 (Figure 4). This would enable us to explain the findings reported by Philpott *et al.* (31), as well as the differences in colonization efficiencies between *H. pylori* 245 and 245m3 observed in Figure 1. Furthermore, we confirmed our results of changes in PG composition during host adaptation, as well as the resulting effects on NOD1-recognition *in vivo*, using an additional pair of human- and mouse-adapted strains, 10700 and SS1,

respectively (SF.3). However, similar results were not obtained when an alternate set of parental and adapted strains, 256 and 256m1/m2 respectively, were investigated (SF.4). This suggests that the modification of muropeptide composition during host adaptation is strain-dependent.

Finally, using both live bacteria and OMVs as mechanisms for the delivery of PG into cells, we have been able to confirm the reduced ability of the 245m3 strain to induce pro-inflammatory responses in human epithelial cells (Figure 5, 6). In contrast, murine epithelial cells and fibroblasts infected with *H. pylori* 245m3 displayed increased cytokine and chemokine production, in comparison with those stimulated with either bacteria or OMVs of the progenitor strain, 245, thus confirming the specificity of NOD1 recognition (Figure 6).

*H. pylori* MltD, (also known as dniR), is a lytic transglycosylase or PG-cleaving enzyme with previously established functions involving PG metabolism, modifications to muropeptide composition and bacterial motility (10, 15). Having identified a SNP in *hp0527 (mltD)* (Table 1, SF.5), conferring a putative truncated protein, we hypothesized that *H. pylori* may modulate its PG composition via MltD during host adaptation to actively engage the NOD1 signaling pathway, thereby initiating responses that favor bacterial persistence *in vivo*. However, RT-PCR analyses only revealed a partial reduction in the expression of *mltD* in *H. pylori* 245m3, in comparison with the progenitor strain, 245 (SF.5). Furthermore, in contrast to a previous study (15), the SNP in *mltD* had no effect on motility of *H. pylori* 245m3 bacteria; indeed, this strain seemed to be even more motile than the clinical isolate (SF.5). The increased motility observed in *H. pylori* 245m3 could partly account for its greater colonization potential *in vivo* (47). It will therefore be important to confirm our gene expression results with future experiments investigating protein expression of MltD via

327 Western blotting. Further investigations are also warranted to determine if MltD is directly  
328 responsible for the change in GM-Tetra<sub>DAP</sub>-GM-Tri<sub>DAP</sub> ratios observed in the mouse-adapted  
329 *H. pylori* strains 245m3 and SS1.

330

331 In conclusion, our data suggest a novel adaptation mechanism employed by *H. pylori* to  
332 enable robust infection in the human host. We have demonstrated how subtle changes in the  
333 PG muropeptide composition of the Gram-negative pathogen, *H. pylori*, affect NOD1  
334 signaling and hence favor bacterial colonization *in vivo*. However, future investigations are  
335 required to demonstrate whether MltD, or other PG modification enzyme(s), are responsible  
336 for the changes in muropeptide composition observed in *H. pylori* 245m3. Given the strain-  
337 dependent occurrence of PG modifications observed in the study, it would be of interest to  
338 show if these PG modification enzymes are solely responsible for host adaptation of *H. pylori*  
339 strains or if there exists an additional virulence factor that confers a selective advantage to the  
340 bacterium. This would enable us to explain why some mouse-adapted variants investigated  
341 altered their muropeptide composition, while others did not.

## MATERIALS AND METHODS

**Bacterial strains, media and culture conditions.** Clinical *cagPAI*<sup>+</sup> isolates (*H. pylori* 245, 256, 10700, P1, P1  $\Delta$ *cagPAI*) and mouse-adapted variants (*H. pylori* 245m3, 256m2, SS1) have been described previously (26, 31, 38). *H. pylori* strains were routinely cultured on either blood agar or in brain heart infusion broth (BHI; Oxoid), according to standard procedures (36). Viable counts of *H. pylori* were determined by serial dilution and plating.

**Mouse Infection.** Animal experimentation was performed in accordance with institutional guidelines (Monash University AEC no. MMCA 2015/43). *H. pylori* suspensions for mouse inoculation were prepared by harvesting bacteria from HBA plates using BHI broth (36). Six- to eight-week-old specific pathogen/*Helicobacter*-free *NodI*<sup>+/+</sup>, *NodI*<sup>-/-</sup> and transgenic *hNODI*<sup>+/+</sup>/*NodI*<sup>-/-</sup> C57BL/6 (5, 8, 18) mice were each intra-gastrically administered a single 100  $\mu$ l aliquot of the inoculating suspension ( $10^7$  cfu/mouse) using polyethylene catheters (36). The presence of *H. pylori* infection in mice was determined after 7 or 30 days of infection by quantitative culture as described previously (36, 48).

**Whole Genome Sequencing and Analysis.** Genomic DNA was extracted using a PureLink Genomic DNA mini kit (Thermo Fisher Scientific) from overnight cultures of *H. pylori* 245 and 245m3 grown on HBA plates. Whole-genome sequencing was performed using a paired-end 250 bp protocol on the Illumina MiSeq sequencer. Raw reads from the two RNAseq libraries were quality checked using the fastQC tool and subsequently trimmed using the Trimmomatic tool (49) and a sliding window approach, to ensure the highest quality of sequences for downstream mapping and variant calling steps. Remaining good quality read pairs were then mapped to the reference *Helicobacter* genome (*Helicobacter pylori* 26695-gi15644634) using the BWA tool (50). Before proceeding with variant calling, the mapping



files were sorted on coordinates using the Samtools (51) and duplicated reads were marked using the Picard toolkit. The FreeBayes tool was then used to identify variation between each strain and the reference genome, including SNPs and Insertions/Deletions (In/Dels). Parameters were set such as at any position in the genome covered by at least 10 reads, a variant would be reported if the alternative nucleotide was present in at least 70% of the reads. Variants that were not in common between those two lists were then identified as the differences between the two strains of interest.

**Western Blotting.** Whole cell lysates from various *H. pylori* strains were collected in solubilization buffer, separated in 4-12% (v/v) NuPAGE® Bis-tris (LifeTechnologies) gels and transferred to nitrocellulose. *H. pylori* proteins were reacted with either rabbit anti-CagA (diluted 1:1000; b-300, Santa-Cruz Biotechnology), rabbit anti-Cag3 (diluted 1:10,000) (46) or rabbit anti-Cag7 (diluted 1:10,000) (52). A goat anti-rabbit-HRP conjugated antibody (1:2000 dilution; Dako) was added and antigen-antibody complexes detected using ECL detection reagent (Cell Signaling Technologies).

**Quantification of CagA translocation by immunofluorescence.** AGS cells were seeded in  $\mu$ -slide 8 well chambers (Ibidi) at  $3 \times 10^4$  cells/ml and incubated for 24 hours at 37 °C in 5% CO<sub>2</sub>. Cells were then serum-starved overnight prior to co-culture with *H. pylori* 245 and 245m3 for 6 h. *H. pylori* P1 and P1  $\Delta$ cagPAI were used as positive and negative control strains (26), respectively. Cells were subsequently washed, fixed, stained and analyzed as described previously (5 fields viewed per sample; data pooled from n=3 experiments) (34).

**PG extraction and analysis.** The PG from *H. pylori* was extracted from 1 L of exponentially growing liquid cultures. The isolated PG was subsequently purified, digested and analyzed as described previously (10, 53).

**OMV purification.** *H. pylori* OMVs were purified using standard techniques (27). OMV protein concentrations were determined by Bradford Protein Assay (Bio-Rad).

**Cell culture.** Human gastric adenocarcinoma cell line (AGS) (54), either wild type or stably transfected with an expression vector containing shRNA directed to either *NodI* or a control gene (*EGFP*) (38), as well as immortalized *NodI*<sup>+/+</sup> and *NodI*<sup>-/-</sup> murine embryonic fibroblasts (27), were routinely cultured in RPMI medium, supplemented with 10 % FCS, 50 units/ml penicillin, 50 µg/ml streptomycin and 1% (v/v) L-glutamine (all reagents from Life Technologies, CA, USA). Generation and maintenance of human epithelial AGS cell lines harboring CRISPR/Cas9 mediated control or *NODI* gene knockout have been described previously (Tran *et al*, manuscript under revision at *Cell Microbiology*). Cells were seeded at 1 X 10<sup>5</sup> cells/ml and incubated at 37 °C in 5 % CO<sub>2</sub>. The mouse gastric epithelial cell line, GSM06 (55), was maintained in Dulbecco's modified Eagle medium–nutrient mixture/F-12 medium, supplemented with 10% FCS, 1% (w/v) insulin/transferring/selenite (Gibco) and 10 ng/ml epidermal growth factor. Cells were grown in 5% CO<sub>2</sub> at 33°C, then moved to 37°C prior to experiments.

**Electrophoretic mobility shift assay (EMSA).** Nuclear extracts were prepared from AGS cells stably transfected with an expression vector containing shRNA directed to either *NodI* or a control gene (*EGFP*) at 4 h post-stimulation, as described previously (31). The nuclear

translocation of the p65 sub-unit of NF- $\kappa$ B was subsequently detected according to a previously published protocol (55).

**Gene Expression.** RNA from cell lines post-stimulation, was extracted using the PureLink® RNA mini kit (Thermo Fisher Scientific). cDNA was generated from 500  $\mu$ g of RNA using the SuperScript® kit (Thermo Fisher Scientific), as per the manufacturer's instructions. qPCR reactions consisted of 4  $\mu$ l of diluted synthesized cDNA (1:10), 5  $\mu$ l of SYBR® Green qPCR MasterMix (Thermo Fisher Scientific) and 1  $\mu$ l of oligonucleotide primers (1  $\mu$ M) for the tested genes. Sterile nuclease-free water was used as a negative control for all the genes tested. Oligonucleotide sequences were as follows: *RNA18s*: Fwd – CGGCTACCACATCCAAGGAA, Rev- GCTGGAATTACCGCGGCT; *CXCL8*: Fwd- GCTTTCTGATGGAAGAGAGC, Rev- GGCACAGTGGACAAGGAC. qPCR assays were performed in an Applied Biosystems™ 7900 Fast Real-Time PCR machine (Thermo Fisher Scientific), using the following program: 50°C, 2 min, followed by 95°C, 10 min, then 40 successive cycles of amplification (95°C, 15 sec; 60°C, 1 min). Gene expression levels were determined by the Delta-Delta Ct method to measure relative gene expression levels to the *18S rRNA* gene.

**Cytokine responses.** Serum-starved cells were stimulated with either live *H. pylori* (Multiplicity of Infection, MOI=10) (5) or OMVs (50  $\mu$ g of protein/ml). Following incubation with live bacteria for 1 h, the culture medium was replaced and the cells washed 2-3 times to remove bacteria. Cells were then placed in fresh medium and incubated a further 23 h. In co-culture assays with OMVs, cells were left untreated or treated with an equivalent volume of BHI only as negative controls. IL-8 (BD Biosciences) and MIP-2 (R&D Systems)

438 levels in culture supernatants were determined by sandwich ELISA, according to the  
439 manufacturer's instructions.

440

441 **Statistical analysis.** Data were analyzed using the non-parametric Mann-Whitney U test  
442 (when two conditions/stimuli were tested) or the parametric one-way ANOVA with Tukey's  
443 multiple testing correction (when three or more conditions/stimuli were present), as  
444 appropriate. Differences in data values were considered significant at a *P* value of  $< 0.05$ .

445    **FUNDING INFORMATION**

446    This project was funded by the National Health and Medical Research Council (NHMRC) to  
447    RLF (project APP1079930). Research at the Hudson Institute of Medical Research is  
448    supported by the Victorian Government's Operational Infrastructure Support Program. RLF  
449    is a Senior Research Fellow of the NHMRC (APP1079904). KDC is supported by an  
450    International Postgraduate Scholarship (Monash University Faculty of Medicine, Nursing and  
451    Health Sciences) and funding from the Centre for Innate Immunity and Infectious Diseases.

452

453    **ACKNOWLEDGEMENTS**

454    The authors thank: the MHTP Genomics Facility, for their assistance with bacterial genome  
455    sequencing; Dr. Nina Salama, for the anti-Cag3 antibody and Prof. Rainer Haas, for the anti-  
456    Cag7 antibody.

457

458    **CONFLICT OF INTEREST**

459    The authors declare that they have no conflicts of interest with the contents of this article.

## REFERENCES

1. **Cloud-Hansen KA, Peterson SB, Stabb EV, Goldman WE, McFall-Ngai MJ, Handelsman J.** 2006. Breaching the great wall: peptidoglycan and microbial interactions. *Nat Rev Microbiol* **4**:710-716.
2. **Luker KE, Collier JL, Kolodziej EW, Marshall GR, Goldman WE.** 1993. *Bordetella pertussis* tracheal cytotoxin and other muramyl peptides: distinct structure-activity relationships for respiratory epithelial cytopathology. *Proceedings of the National Academy of Sciences* **90**:2365-2369.
3. **Burroughs M, Prasad S, Cabellos C, Mendelman PM, Tuomanen E.** 1993. The biologic activities of peptidoglycan in experimental *Haemophilus influenzae* meningitis. *J Infect Dis* **167**:464-468.
4. **Fritz JH, Ferrero RL, Philpott DJ, Girardin SE.** 2006. Nod-like proteins in immunity, inflammation and disease. *Nat Immunol* **7**:1250-1257.
5. **Viala J, Chaput C, Boneca IG, Cardona A, Girardin SE, Moran AP, Athman R, Memet S, Huerre MR, Coyle AJ, DiStefano PS, Sansonetti PJ, Labigne A, Bertin J, Philpott DJ, Ferrero RL.** 2004. Nod1 responds to peptidoglycan delivered by the *Helicobacter pylori* *cag* pathogenicity island. *Nat Immunol* **5**:1166-1174.
6. **Girardin SE, Travassos LH, Herve M, Blanot D, Boneca IG, Philpott DJ, Sansonetti PJ, Mengin-Lecreulx D.** 2003. Peptidoglycan molecular requirements allowing detection by Nod1 and Nod2. *J Biol Chem* **278**:41702-41708.
7. **Girardin SE, Jehanno M, Mengin-Lecreulx D, Sansonetti PJ, Alzari PM, Philpott DJ.** 2005. Identification of the critical residues involved in peptidoglycan detection by Nod1. *J Biol Chem* **280**:38648-38656.
8. **Magalhaes JG, Philpott DJ, Nahori MA, Jehanno M, Fritz J, Le Bourhis L, Viala J, Hugot JP, Giovannini M, Bertin J, Lepoivre M, Mengin-Lecreulx D,**

- 485        **Sansonetti PJ, Girardin SE.** 2005. Murine Nod1 but not its human orthologue  
486        mediates innate immune detection of tracheal cytotoxin. *EMBO Rep* **6**:1201-1207.
- 487    9.        **Woodhams KL, Chan JM, Lenz JD, Hackett KT, Dillard JP.** 2013. Peptidoglycan  
488        fragment release from *Neisseria meningitidis*. *Infect Immun* **81**:3490-3498.
- 489    10.       **Chaput C, Labigne A, Boneca IG.** 2007. Characterization of *Helicobacter pylori*  
490        lytic transglycosylases Slt and MltD. *J Bacteriol* **189**:422-429.
- 491    11.       **Yang Y, Du J, Liu F, Wang X, Li X, Li Y.** 2017. Role of caspase-3/E-cadherin in  
492        *Helicobacter pylori*-induced apoptosis of gastric epithelial cells. *Oncotarget*.  
493        **8**(35):59204-59216. doi:10.18632/oncotarget.19471.
- 494    12.       **Girardin SE, Boneca IG, Carneiro LA, Antignac A, Jehanno M, Viala J, Tedin**  
495        **K, Taha MK, Labigne A, Zahringer U, Coyle AJ, DiStefano PS, Bertin J,**  
496        **Sansonetti PJ, Philpott DJ.** 2003. Nod1 detects a unique muropeptide from Gram-  
497        negative bacterial peptidoglycan. *Science* **300**:1584-1587.
- 498    13.       **Chaput C, Ecobichon C, Cayet N, Girardin SE, Werts C, Guadagnini S, Prevost**  
499        **MC, Mengin-Lecreulx D, Labigne A, Boneca IG.** 2006. Role of AmiA in the  
500        morphological transition of *Helicobacter pylori* and in immune escape. *PLoS Pathog*  
501        **2**:e97.
- 502    14.       **Liu M, Haenssler E, Uehara T, Losick VP, Park JT, Isberg RR.** 2012. The  
503        *Legionella pneumophila* EnhC protein interferes with immunestimulatory muramyl  
504        peptide production to evade innate immunity. *Cell host & microbe* **12**:166-176.
- 505    15.       **Roure S, Bonis M, Chaput C, Ecobichon C, Mattox A, Barrière C, Geldmacher**  
506        **N, Guadagnini S, Schmitt C, Prévost M-C, Labigne A, Backert S, Ferrero RL,**  
507        **Boneca IG.** 2012. Peptidoglycan maturation enzymes affect flagellar functionality in  
508        bacteria. *Molecular Microbiology* **86**:845-856.

- 509 16. **Sycuro LK, Pincus Z, Gutierrez KD, Biboy J, Stern CA, Vollmer W, Salama NR.**  
510 2010. Peptidoglycan Crosslinking Relaxation Promotes *Helicobacter pylori*'s Helical  
511 Shape and Stomach Colonization. *Cell* **141**:822-833.
- 512 17. **Sycuro LK, Wyckoff TJ, Biboy J, Born P, Pincus Z, Vollmer W, Salama NR.**  
513 2012. Multiple peptidoglycan modification networks modulate *Helicobacter pylori*'s  
514 cell shape, motility, and colonization potential. *PLoS Pathog* **8**:e1002603.
- 515 18. **Zarantonelli ML, Skoczynska A, Antignac A, El Ghachi M, Deghmane AE,**  
516 **Szatanik M, Mulet C, Werts C, Peduto L, d'Andon MF, Thouron F, Nato F,**  
517 **Lebourhis L, Philpott DJ, Girardin SE, Vives FL, Sansonetti P, Eberl G, Pedron**  
518 **T, Taha MK, Boneca IG.** 2013. Penicillin resistance compromises Nod1-dependent  
519 proinflammatory activity and virulence fitness of *Neisseria meningitidis*. *Cell Host*  
520 *Microbe* **13**:735-745.
- 521 19. **Gisbert JP.** 2011. *Helicobacter pylori*-related diseases: dyspepsia, ulcers and gastric  
522 cancer. *Gastroenterol Hepatol* **34 Suppl 2**:15-26.
- 523 20. **Polk DB, Peek RM, Jr.** 2010. *Helicobacter pylori*: gastric cancer and beyond. *Nat*  
524 *Rev Cancer* **10**:403-414.
- 525 21. **Tomb JF, White O, Kerlavage AR, Clayton RA, Sutton GG, Fleischmann RD,**  
526 **Ketchum KA, Klenk HP, Gill S, Dougherty BA, Nelson K, Quackenbush J, Zhou**  
527 **L, Kirkness EF, Peterson S, Loftus B, Richardson D, Dodson R, Khalak HG,**  
528 **Glodek A, McKenney K, Fitzgerald LM, Lee N, Adams MD, Hickey EK, Berg**  
529 **DE, Gocayne JD, Utterback TR, Peterson JD, Kelley JM, Cotton MD, Weidman**  
530 **JM, Fujii C, Bowman C, Watthey L, Wallin E, Hayes WS, Borodovsky M, Karp**  
531 **PD, Smith HO, Fraser CM, Venter JC.** 1997. The complete genome sequence of  
532 the gastric pathogen *Helicobacter pylori*. *Nature* **388**:539-547.



- 533 22. **Montecucco C, Rappuoli R.** 2001. Living dangerously: how *Helicobacter pylori*  
534 survives in the human stomach. *Nat Rev Mol Cell Biol* **2**:457-466.
- 535 23. **Hutton ML, Kaparakis-Liaskos M, Turner L, Cardona A, Kwok T, Ferrero RL.**  
536 2010. *Helicobacter pylori* exploits cholesterol-rich microdomains for induction of  
537 NF-kappaB-dependent responses and peptidoglycan delivery in epithelial cells. *Infect*  
538 *Immun* **78**:4523-4531.
- 539 24. **Backert S, Selbach M.** 2008. Role of type IV secretion in *Helicobacter pylori*  
540 pathogenesis. *Cell Microbiol* **10**:1573-1581.
- 541 25. **Kwok T, Zabler D, Urman S, Rohde M, Hartig R, Wessler S, Misselwitz R,**  
542 **Berger J, Sewald N, Konig W, Backert S.** 2007. *Helicobacter* exploits integrin for  
543 type IV secretion and kinase activation. *Nature* **449**:862-866.
- 544 26. **Gorrell RJ, Guan J, Xin Y, Tafreshi MA, Hutton ML, McGuckin MA, Ferrero**  
545 **RL, Kwok T.** 2013. A novel NOD1- and CagA-independent pathway of interleukin-8  
546 induction mediated by the *Helicobacter pylori* type IV secretion system. *Cell*  
547 *Microbiol* **15**:554-570.
- 548 27. **Kaparakis M, Turnbull L, Carneiro L, Firth S, Coleman HA, Parkinson HC,**  
549 **Le Bourhis L, Karrar A, Viala J, Mak J, Hutton ML, Davies JK, Crack PJ,**  
550 **Hertzog PJ, Philpott DJ, Girardin SE, Whitchurch CB, Ferrero RL.** 2010.  
551 Bacterial membrane vesicles deliver peptidoglycan to NOD1 in epithelial cells. *Cell*  
552 *Microbiol* **12**:372-385.
- 553 28. **Inohara N, Koseki T, Lin J, del Peso L, Lucas PC, Chen FF, Ogura Y, Nunez G.**  
554 2000. An induced proximity model for NF-kappa B activation in the Nod1/RICK and  
555 RIP signaling pathways. *J Biol Chem* **275**:27823-27831.

- 556 29. **Allison CC, Kufer TA, Kremmer E, Kaparakis M, Ferrero RL.** 2009.  
557 *Helicobacter pylori* induces MAPK phosphorylation and AP-1 activation via a  
558 NOD1-dependent mechanism. *J Immunol* **183**:8099-8109.
- 559 30. **Kobayashi K, Inohara N, Hernandez LD, Galan JE, Nunez G, Janeway CA,**  
560 **Medzhitov R, Flavell RA.** 2002. RICK/Rip2/CARDIAK mediates signalling for  
561 receptors of the innate and adaptive immune systems. *Nature* **416**:194-199.
- 562 31. **Philpott DJ, Belaid D, Troubadour P, Thiberge JM, Tankovic J, Labigne A,**  
563 **Ferrero RL.** 2002. Reduced activation of inflammatory responses in host cells by  
564 mouse-adapted *Helicobacter pylori* isolates. *Cell Microbiol* **4**:285-296.
- 565 32. **Blaser MJ, Berg DE.** 2001. *Helicobacter pylori* genetic diversity and risk of human  
566 disease. *Journal of Clinical Investigation* **107**:767-773.
- 567 33. **Kansau I, Raymond J, Bingen E, Courcoux P, Kalach N, Bergeret M, Braimi N,**  
568 **Dupont C, Labigne A.** 1996. Genotyping of *Helicobacter pylori* isolates by  
569 sequencing of PCR products and comparison with the RAPD technique. *Res*  
570 *Microbiol* **147**:661-669.
- 571 34. **Hutton ML, D'Costa K, Rossiter AE, Wang L, Turner L, Steer DL, Masters SL,**  
572 **Crocker BA, Kaparakis-Liaskos M, Ferrero RL.** 2017. A *Helicobacter pylori*  
573 Homolog of Eukaryotic Flotillin Is Involved in Cholesterol Accumulation, Epithelial  
574 Cell Responses and Host Colonization. *Frontiers in Cellular and Infection*  
575 *Microbiology* **7**:219.
- 576 35. **Lee A, O'Rourke J, De Ungria MC, Robertson B, Daskalopoulos G, Dixon MF.**  
577 1997. A standardized mouse model of *Helicobacter pylori* infection: introducing the  
578 Sydney strain. *Gastroenterology* **112**:1386-1397.

- 579 36. **Ferrero RL, Thiberge JM, Huerre M, Labigne A.** 1998. Immune Responses of  
580 Specific-Pathogen-Free Mice to Chronic *Helicobacter pylori* (Strain SS1) Infection.  
581 Infection and Immunity **66**:1349-1355.
- 582 37. **Lee A, O'Rourke J, De Ungria MC, Robertson B, Daskalopoulos G, Dixon MF.**  
583 1997. A standardized mouse model of *Helicobacter pylori* infection: introducing the  
584 Sydney strain. Gastroenterology **112**:1386-1397.
- 585 38. **Grubman A, Kaparakis M, Viala J, Allison C, Badea L, Karrar A, Boneca IG,**  
586 **Le Bourhis L, Reeve S, Smith IA, Hartland EL, Philpott DJ, Ferrero RL.** 2010.  
587 The innate immune molecule, NOD1, regulates direct killing of *Helicobacter pylori*  
588 by antimicrobial peptides. Cell Microbiol **12**:626-639.
- 589 39. **Watanabe K, Iida M, Takaishi K, Suzuki T, Hamada Y, Iizuka Y, Tsurufuji S.**  
590 1993. Chemoattractants for neutrophils in lipopolysaccharide-induced inflammatory  
591 exudate from rats are not interleukin-8 counterparts but gro-gene-product/melanoma-  
592 growth-stimulating-activity-related factors. Eur J Biochem **214**:267-270.
- 593 40. **Folkening WJ, Nogami W, Martin SA, Rosenthal RS.** 1987. Structure of  
594 *Bordetella pertussis* peptidoglycan. J Bacteriol **169**:4223-4227.
- 595 41. **Burroughs MH, Chang YS, Gage DA, Tuomanen EI.** 1993. Composition of the  
596 peptidoglycan of *Haemophilus influenzae*. J Biol Chem **268**:11594-11598.
- 597 42. **Antignac A, Rousselle JC, Namane A, Labigne A, Taha MK, Boneca IG.** 2003.  
598 Detailed structural analysis of the peptidoglycan of the human pathogen *Neisseria*  
599 *meningitidis*. J Biol Chem **278**:31521-31528.
- 600 43. **Bonis M, Ecobichon C, Guadagnini S, Prevost MC, Boneca IG.** 2010. A M23B  
601 family metallopeptidase of *Helicobacter pylori* required for cell shape, pole formation  
602 and virulence. Mol Microbiol **78**:809-819.

- 603 44. **Wang G, Lo LF, Forsberg LS, Maier RJ.** 2012. *Helicobacter pylori* peptidoglycan  
604 modifications confer lysozyme resistance and contribute to survival in the host. MBio  
605 3:e00409-00412.
- 606 45. **Smart J, Fouillen A, Casu B, Nanci A, Baron C.** 2017. Cag-delta (Cag3) protein  
607 from the *Helicobacter pylori* 26695 cag type IV secretion system forms ring-like  
608 supramolecular assemblies. FEMS Microbiol Lett **364**.
- 609 46. **Pinto-Santini DM, Salama NR.** 2009. Cag3 is a novel essential component of the  
610 *Helicobacter pylori* Cag type IV secretion system outer membrane subcomplex. J  
611 Bacteriol **191**:7343-7352.
- 612 47. **Aihara E, Closson C, Matthis AL, Schumacher MA, Engevik AC, Zavros Y,**  
613 **Ottemann KM, Montrose MH.** 2014. Motility and Chemotaxis Mediate the  
614 Preferential Colonization of Gastric Injury Sites by *Helicobacter pylori*. PLoS  
615 Pathogens **10**:e1004275.
- 616 48. **Ferrero RL, Wilson JE, Sutton P.** 2012. Mouse models of *Helicobacter*-induced  
617 gastric cancer: use of cocarcinogens. Methods Mol Biol **921**:157-173.
- 618 49. **Bolger AM, Lohse M, Usadel B.** 2014. Trimmomatic: a flexible trimmer for  
619 Illumina sequence data. Bioinformatics **30**:2114-2120.
- 620 50. **Li H, Durbin R.** 2010. Fast and accurate long-read alignment with Burrows-Wheeler  
621 transform. Bioinformatics **26**:589-595.
- 622 51. **Li H.** 2011. A statistical framework for SNP calling, mutation discovery, association  
623 mapping and population genetical parameter estimation from sequencing data.  
624 Bioinformatics **27**:2987-2993.
- 625 52. **Rohde M, Puls J, Buhrdorf R, Fischer W, Haas R.** 2003. A novel sheathed surface  
626 organelle of the *Helicobacter pylori* cag type IV secretion system. Mol Microbiol  
627 **49**:219-234.

- 628 53. **Glauner B.** 1988. Separation and quantification of mucopeptides with high-  
629 performance liquid chromatography. *Analytical Biochemistry* **172**:451-464.
- 630 54. **Keenan J, Day T, Neal S, Cook B, Perez-Perez G, Allardyce R, Bagshaw P.** 2000.  
631 A role for the bacterial outer membrane in the pathogenesis of *Helicobacter pylori*  
632 infection. *FEMS Microbiol Lett* **182**:259-264.
- 633 55. **Ferrero RL, Avé P, Ndiaye D, Bambou J-C, Huerre MR, Philpott DJ, Mémet S.**  
634 2008. NF- $\kappa$ B Activation during Acute *Helicobacter pylori* Infection in Mice.  
635 *Infection and Immunity* **76**:551-561.
- 636 56. **Gobert AP, McGee DJ, Akhtar M, Mendz GL, Newton JC, Cheng Y, Mobley**  
637 **HL, Wilson KT.** 2001. *Helicobacter pylori* arginase inhibits nitric oxide production  
638 by eukaryotic cells: a strategy for bacterial survival. *Proc Natl Acad Sci U S A*  
639 **98**:13844-13849.
- 640 57. **Wiedemann T, Hofbaur S, Tegtmeyer N, Huber S, Sewald N, Wessler S, Backert**  
641 **S, Rieder G.** 2012. *Helicobacter pylori* CagL dependent induction of gastrin  
642 expression via a novel  $\alpha$ v $\beta$ 5-integrin-integrin linked kinase signalling complex.  
643 *Gut* **61**:986-996.  
644

## FIGURE LEGENDS

**Fig. 1. NOD1-mediated host defense responses generated against *H. pylori* infection are host-specific.** *Nod1*<sup>+/+</sup> and *Nod1*<sup>-/-</sup> mice (minimum n=5 per group per *H. pylori* strain tested) were inoculated intra-gastrically with 10<sup>7</sup> CFU of *H. pylori* 245 and 245m3 and sacrificed either 7 (A) or 30 (C) days post-infection. (B) *Nod1*<sup>-/-</sup> mice (n=12 per *H. pylori* strain tested) and BAC-transgenic mice expressing human *NOD1* (hTg*NOD1*<sup>+/+</sup>) (n=5 per *H. pylori* strain tested) were also inoculated with both *H. pylori* strains and culled 7 days post infection. Bacterial loads in mice were determined by quantitative culture of gastric tissue samples and are pooled from at least two independent experiments. Data are presented as Log<sub>10</sub> colony forming units (CFU)/g stomach, with each point representing a single mouse. The limit of detection for the assay was 1,000 CFU/gram. Data were analyzed using a Mann-Whitney U test. \*, *P* < 0.05; \*\*, *P* < 0.01; \*\*\*, *P* < 0.001.

**Fig. 2. Identification of SNPs in the genome of the mouse-adapted *H. pylori* 245m3.** (A) A circular representation of the genomes from *H. pylori* strains, 245 and 245m3, aligned to the reference strain, 26695. (B) Genome analysis revealed the presence of 300 SNPs in the genome of *H. pylori* 245m3 in comparison to the human isolate, 245. The effects on protein translation resulting from each individual SNP was predicted and annotated as “missense”, “synonymous”, “stop-gained” or “unknown” (expressed as percentages of total). (C) Details of SNPs identified in key *cagPAI*- and PG-associated genes.

**Fig. 3. Mouse adaptation of *H. pylori* 245 does not alter its T4SS function.** (A) Whole cell lysates of *H. pylori* P1 wild-type [127] (lane 1), P1  $\Delta$ *cagPAI* (lane 2), 245 (lane 3) or 245m3 (lane 4) strains were analyzed by immunoblotting using an antibody directed against CagA (b-300; Santa Cruz Biotechnology). Full length CagA protein (molecular weight, c. 140 kDa)

was detected in *H. pylori* P1, 245 and 245m3 preparations, but not in those of the  $\Delta$ cagPAI strain. **(B)** AGS cells were either non-stimulated (NS) or co-cultured with *H. pylori* P1 WT, P1  $\Delta$ cagA, 245 or 245m3 bacteria. Panels show cells that had been incubated with Alexa Fluor 488-conjugated secondary antibody, permeabilised with 1% Triton-X and then incubated with Alexa Fluor 647-conjugated antibody. Nuclei (blue) were stained using Hoescht 33342 (Thermo Fisher Scientific). Arrows indicate intracellular CagA molecules, which appear as red mainly punctate areas of staining (detected using Alexa Fluor 647 conjugated antibody). Scale bar, 15  $\mu$ m. Quantification of Alexa Fluor 647 and Alexa Fluor 488 staining (expressed as relative intensities) in AGS cells that had been co-cultured with either *H. pylori* P1 WT, 245 and 245m3 bacteria are represented as a histogram. The data represent the mean  $\pm$  SEM for three independent experiments. Data were analyzed using a Mann-Whitney U test. ns,  $P > 0.05$ .

**Fig. 4. PG muropeptides in *H. pylori* 245m3 are enriched in the murine Nod1 agonist, GM-Tetra<sub>DAP</sub>.** **(A)** Chromatogram of muropeptides from *H. pylori* strains 245 and 245m3, separated by HPLC. Peaks 1 to 4 correspond to G-anhM-tripeptide, G-anhM-tetrapeptide, G-anhM-tetrapeptide-glycine and G-anhM-dipeptide, respectively. **(B)** Proportions of dipeptides, tripeptides, tetrapeptides and tetraglycinepeptides present in *H. pylori* 245 and 245m3.

**Fig. 5. *H. pylori* strain 245m3 is a poor inducer of NOD1-dependent pro-inflammatory responses in human gastric epithelial cells.** **(A)** EMSA showing nuclear translocation of NF- $\kappa$ B p65 in AGS control and *NOD1* knockdown cells. AGS cells stably expressing shRNA to *NOD1* (white bars) or a control gene (black bars) were either left untreated (control) or infected with *H. pylori* 245 or 245m3. **(B)** *CXCL8* expression and **(C)** IL-8 production were

measured 6 h and 24 h post-infection, respectively. **(D)** Control (black bars) or *NOD1* knockout (white bars) AGS cell lines were co-cultured with *H. pylori* strains, 245 and 245m3, for 24 h. The supernatants were then analyzed by ELISA for the detection of IL-8 responses. Data correspond to the mean  $\pm$  S.E.M. (determined in triplicate) and are representative of at least three independent experiments. Data were analyzed using a Mann-Whitney U test or one-way ANOVA. \*,  $P < 0.05$ ; \*\*\*,  $P < 0.001$ .

**Fig. 6. OMVs purified from *H. pylori* 245m3 are affected in their ability to induce NOD1-dependent pro-inflammatory responses in human gastric epithelial cells, but not murine cell lines.** **(A)** Human gastric epithelial AGS cell lines, stably expressing shRNA targeting either *NOD1* or a control gene, were either left untreated or stimulated with a control BHI broth or OMVs (50  $\mu$ g/ml) purified from *H. pylori* strains, 245 and 245m3. IL-8 cytokine production was measured at 24 h p.i. **(B)** GSM06 murine epithelial cells and **(C)** *Nod1*<sup>+/+</sup> (black bars) and *Nod1*<sup>-/-</sup> (white bars) immortalized murine embryonic fibroblasts were stimulated with OMVs. Production of the murine IL-8 homologue, Cxcl2/MIP2, was measured 24 h p.i. Figures show means  $\pm$  SEM and are pooled from three independent experiments. Data was analyzed using a one-way ANOVA. \*\*,  $p < 0.01$ ; \*\*\*\*,  $p < 0.0001$ .



712 **Table 1: Single nucleotide polymorphisms identified in the genome of the mouse-**  
713 **adapted *H. pylori* 245m3 strain.**

Gene	Position	Sequence in <i>H. pylori</i> 245	Sequence in <i>H. pylori</i> 245m3	Effect
hp0009 ( <i>hopZ</i> )	6791	C	T	Predicted change from Asn to Asp
hp0289 ( <i>imaA</i> )	298963	G	A	Predicted change from Val to Thr
hp0289 ( <i>imaA</i> )	304659	C	T	Predicted change from Thr to Ala
hp0289 ( <i>imaA</i> )	304994	C	T	Predicted change from Ala to Val
hp0317 ( <i>hopU/babc</i> )	332799	C	G	Predicted change from Ser to Thr
hp0373 ( <i>homC</i> )	382150	C	T	Predicted change from Arg to Cys
hp0407 ( <i>bisC</i> )	421174	G	T	Predicted premature stop codon
hp0477 ( <i>hopJ</i> )	500023	G	A	Predicted change from Met to Val
hp0522 ( <i>cag3</i> )	548226	CATTAAG	TATTAAGAAG	Predicted premature stop codon
hp0527 ( <i>cag7</i> )	554776	C	T	Predicted premature stop codon
hp0527 ( <i>cag7</i> )	557650	TTT	ATC	Predicted premature stop codon
hp0527 ( <i>cag7</i> )	558280	G	A	Predicted premature stop codon
hp0527 ( <i>cag7</i> )	559029	CTC	ATT	Predicted premature stop codon
hp0725 ( <i>sabA</i> )	779058- 779069	GTAATTGAGTGC	CCAGTTTGGTGT	Predicted change from Gly-Thr-Gln- Leu-Gln to Asp-Thr-Lys-Leu-Glu
hp0725 ( <i>sabA</i> )	779112	T	C	Predicted change from Ile to Val
hp0887 ( <i>vacA</i> )	940144	A	G	Predicted change from Arg to His
hp0887 ( <i>vacA</i> )	940465	G	A	Predicted change from Gly to Asp

hp0896 ( <i>babB</i> )	949053- 949054	TT	GC	Predicted change from Lys To Ser
hp0912 ( <i>hopB</i> )	965469	G	T	Predicted change from Gly to Ile
hp0913 ( <i>hopC</i> )	967112- 967113	AG	CA	Predicted change from His to Ser
hp1083 [38]	1142062	C	A	Predicted change from Trp to Leu
hp1157 ( <i>hopL</i> )	1224192	A	G	Predicted change from Ala to Thr
hp1177 ( <i>hopQ</i> )	1244610- 1244615	GCGGCA	ATAGCG	Predicted change from Ser-Ala-Ala to Ser-Ala-Ile
hp1177 ( <i>hopQ</i> )	1244634- 1244638	GTCGC	ACACT	Predicted change from Cys-Ala-Thr to Cys-Ser-Val
hp1243 ( <i>hopS/babB</i> )	1319279	G	A	Predicted change from Ser to Leu
hp1243 ( <i>hopS/babB</i> )	1319562	A	G	Predicted change from Asn-Gly-His- Lys to Asn-Gly-Tyr-Thr
hp1243 ( <i>hopS/babB</i> )	1319874- 1319876	AAC	GCT	Predicted change from Asn-Leu-Asn to Lys-Leu-Ser
hp1243 ( <i>hopS/babB</i> )	1319885- 1319887	CGA	TTG	Predicted change from Asp-Asn to Asp-Arg
hp1243 ( <i>hopS/babB</i> )	1319898	C	G	Predicted change from Gln to Glu
hp1403 ( <i>hsdM</i> )	1469837	G	T	Predicted premature stop codon gained
hp1512 ( <i>frpB</i> )	1584934	C	T	Predicted change from Ala to Val
hp1512 ( <i>frpB</i> )	1586656	G	A	Predicted change from Arg to Lys
hp1560 ( <i>ftsW</i> )	1642176	ATTTC	GTTTT	Predicted change from Ile-Ser to Val- Leu
hp1565 ( <i>pbp2</i> )	1648503	T	C	Predicted change from Glu to Lys
hp1569 ( <i>lptC</i> )	1651016	T	C	Predicted change from Asp-His to Asn-Tyr
hp1572 ( <i>mltD/DniR</i> )	1653734	G	A	Predicted premature stop codon

714

715

## SUPPLEMENTAL MATERIALS AND METHODS

**Capillary Sequencing of *H. pylori* genes.** Genomic DNA was isolated from *H. pylori* 245 and 245m3, using a PureLink Genomic DNA mini kit (Thermo Fisher Scientific). *H. pylori* *glmM* (HP0075), *cagA* (HP0547) and *mltD* (HP1572) were amplified and sequenced using the primers listed in ST1. Sequences were aligned using the ClustalW program.

**qRT-PCR.** RNA (200 ng to 2 µg) was reverse transcribed using random hexamers and SuperScript III (Invitrogen). Primers (described in ST1) were designed based on the *H. pylori* 245 genomic DNA sequence and directed to the 5' and 3' regions of the *mltD* gene. qRT-PCR was performed as previously described [67]. Expression of the housekeeping gene, *ureB* was used as a positive control [86].

**Motility testing.** Bacterial motility was determined using semisolid agar plates. Motility assays were performed in 0.35% agar Brain Heart Infusion medium (Oxoid) complemented with 1% of heat inactivated FCS and Skirrow's Selective Supplement [73, 213].

## SUPPLEMENTAL REFERENCES

1. **Grubman A, Kaparakis M, Viala J, Allison C, Badea L, Karrar A, Boneca IG, Le Bourhis L, Reeve S, Smith IA, Hartland EL, Philpott DJ, Ferrero RL.** 2010. The innate immune molecule, NOD1, regulates direct killing of *Helicobacter pylori* by antimicrobial peptides. *Cell Microbiol* **12**:626-639.
2. **Schoep TD, Fulurija A, Good F, Lu W, Himbeck RP, Schwan C, Choi SS, Berg DE, Mittl PR, Benghezal M, Marshall BJ.** 2010. Surface properties of *Helicobacter pylori* urease complex are essential for persistence. *PLoS One* **5**:e15042.
3. **Schirm M, Soo Ec Fau - Aubry AJ, Aubry Aj Fau - Austin J, Austin J Fau - Thibault P, Thibault P Fau - Logan SM, Logan SM.** 2003. Structural, genetic and functional characterization of the flagellin glycosylation process in *Helicobacter pylori*. *Molecular Microbiology* **48**:1579-92.
4. **Roure S, Bonis M, Chaput C, Ecobichon C, Mattox A, Barrière C, Geldmacher N, Guadagnini S, Schmitt C, Prévost M-C, Labigne A, Backert S, Ferrero RL, Boneca IG.** 2012. Peptidoglycan maturation enzymes affect flagellar functionality in bacteria. *Molecular Microbiology* **86**:845-856.

748 **SUPPLEMENTAL FIGURE LEGENDS**

749 **SF. 1. ClustalW alignment of *glmM* and *cagA* sequences in *H. pylori* 245 and 245m3.**

750 Alignment of the genomic DNA sequences of (A) *glmM* and predicted amino acid sequences  
751 of (B) CagA from *H. pylori* 245 and 245m3. The CagA type exhibited by each strain was  
752 determined using the “Glu-Pro-Ile-Tyr-Ala” (EPIYA) motifs (highlighted in red) and the  
753 surrounding amino acid sequences (highlighted in blue).

754

755 **SF. 2. *H. pylori* 245m3 displays Cag7, but not Cag3 expression.** Whole cell lysates of  
756 *H. pylori* P1 wild-type (lane 1), P1  $\Delta$ cagPAI (lane 2), 245 (lane 3) or 245m3 (lane 4) strains  
757 were analyzed by immunoblotting using an antibody directed against Cag7 or Cag3. Full  
758 length Cag7 protein (molecular weight, *c.* 120 kDa) was detected in *H. pylori* P1, 245 and  
759 245m3 preparations, but not in those of the  $\Delta$ cagPAI strain. A non-specific band was also  
760 present in all four preparations. Full length Cag3 protein (molecular weight, *c.* 60 kDa) was  
761 present in *H. pylori* P1 and 245 lysates, but absent in lysates from  $\Delta$ cagPAI and 245m3  
762 strains.

763

764 **SF. 3. PG from the mouse-adapted *H. pylori* SS1 strain, is enriched in the murine Nod1**

765 **agonist, Tetra<sub>DAP</sub>.** (A) Chromatogram of muropeptides from *H. pylori* strains 10700 and  
766 SS1, separated by HPLC. Peaks 1 to 4 correspond to G-anhM-tripeptide, G-anhM-  
767 tetrapeptide, G-anhM-tetrapeptide-glycine and G-anhM-dipeptide, respectively. (B)  
768 Proportions of dipeptides, tripeptides, tetrapeptides and tetraglycinepeptides present in  
769 *H. pylori* 10700 and SS1. (C) Control (black bars) or *NOD1* knockout (white bars) AGS cell  
770 lines were either left untreated (NS) or co-cultured with *H. pylori* strains, 10700 and SS1, for  
771 24 hours. The supernatants were then analyzed by ELISA for the detection of IL-8 responses.  
772 (D) *Nod1*<sup>+/+</sup> and *Nod1*<sup>-/-</sup> mice (n = 9 each per *H. pylori* strain tested) were inoculated with 10<sup>7</sup>

CFU of *H. pylori* by intra-gastric gavage. Quantitative culture assays were performed 7 days post-infection. Data are presented as Log<sub>10</sub> colony forming units (CFU)/g stomach, with each point representing a single mouse. The limit of detection for the assay was 1,000 CFU/gram. Samples displaying values lower than this threshold were excluded from the analysis. Data correspond to the mean  $\pm$  S.E.M. (determined in triplicate) and are pooled from at least three independent experiments. Data were analyzed using a Mann-Whitney U test or a one-way ANOVA. \*,  $P < 0.05$ ; \*\*,  $P < 0.01$ .

**SF. 4. The cell wall composition of the mouse-adapted *H. pylori* 256m2 strain remains unchanged from that of the original clinical 256 isolate.** (A) Chromatogram of muropeptides from *H. pylori* strains 256, 256m1 and 256m2, separated by HPLC. Peaks 1 to 4 correspond to G-anhM-tripeptide, G-anhM-tetrapeptide, G-anhM-tetrapeptide-glycine and G-anhM-dipeptide, respectively. (B) Proportions of dipeptides, tripeptides, tetrapeptides and tetraglycinepeptides present in *H. pylori* 256, 256m1 and 256m2.

**SF. 5. The presence of a SNP in *mltD* (HP1572) affects gene expression in *H. pylori* 245m3.** (A) ClustalW alignment of the genomic sequences of *mltD* from *H. pylori* 245 and 245m3 revealed a SNP in the latter strain. (B) Gene expression of the 5' and 3' regions of *mltD* in each strain was analysed using RT-PCR. (C) The expression of the *ureB* gene was tested as a positive control. Genomic DNA isolated from *H. pylori* 26695 was used as a positive control in both (B) and (C). (D) Soft-agar motility testing of *H. pylori* strains 245 and 245m3. (E) The diameters of motility halos were measured for each strain. Data correspond to the mean  $\pm$  S.E.M. (determined in triplicate) and are pooled from at least three independent experiments. Data were analyzed using a Mann-Whitney U test. \*\*\*,  $P < 0.001$ .

797 **ST1. Primers used in this study**

Primer name	Primer sequence
<i>glmM</i> (F)	GGATAAGCTTTTAGGGGTGTTAGGGG
<i>glmM</i> (R)	GCTTGCTTTCTAACACTAACGCGC
<i>cagA</i> (F)	GGGAATTGTCTGATAAACTTG
<i>cagA</i> (R)	GCTATTAATGCGTGTGTGGCT
<i>mltD</i> 5' (F)	GAATGAAGTG TTTTAGTC
<i>mltD</i> 5' (R)	CTCCGGTTTGCTTGTAAGC
<i>mltD</i> 3' (F)	GCTCTACAAG CAAACCGGAG
<i>mltD</i> 3' (R)	CCCTTGTAGCGAGTAATT

798

**Figure 1**

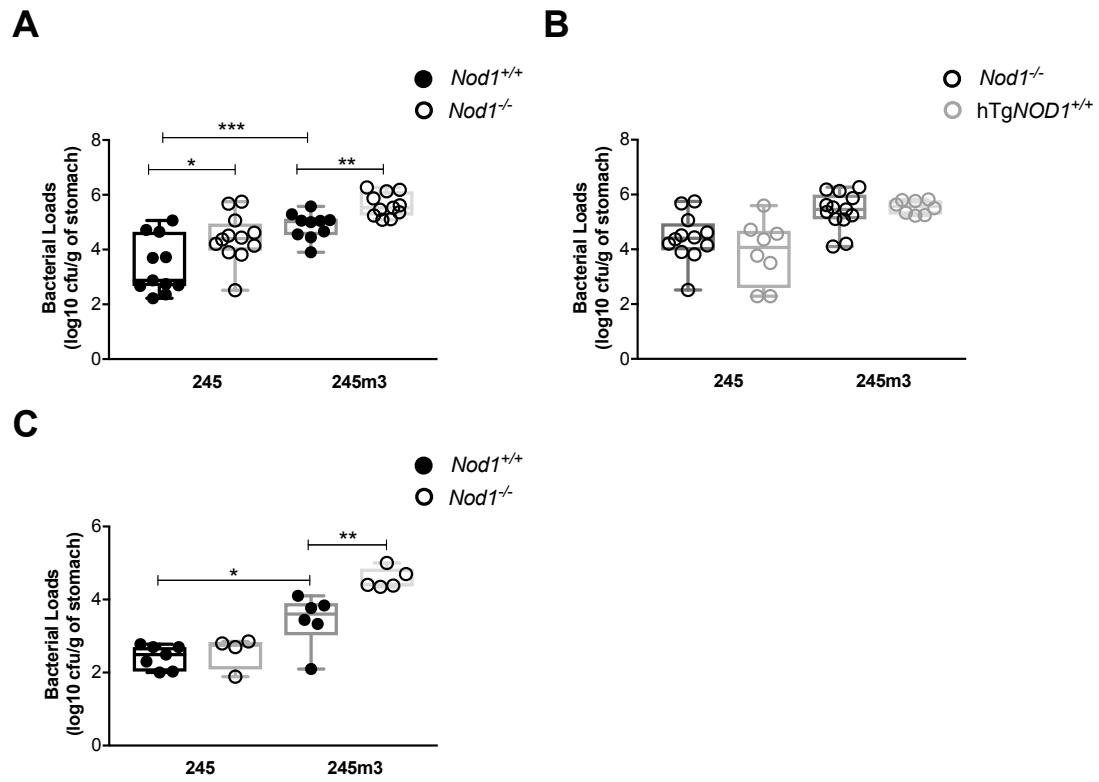




Figure 2

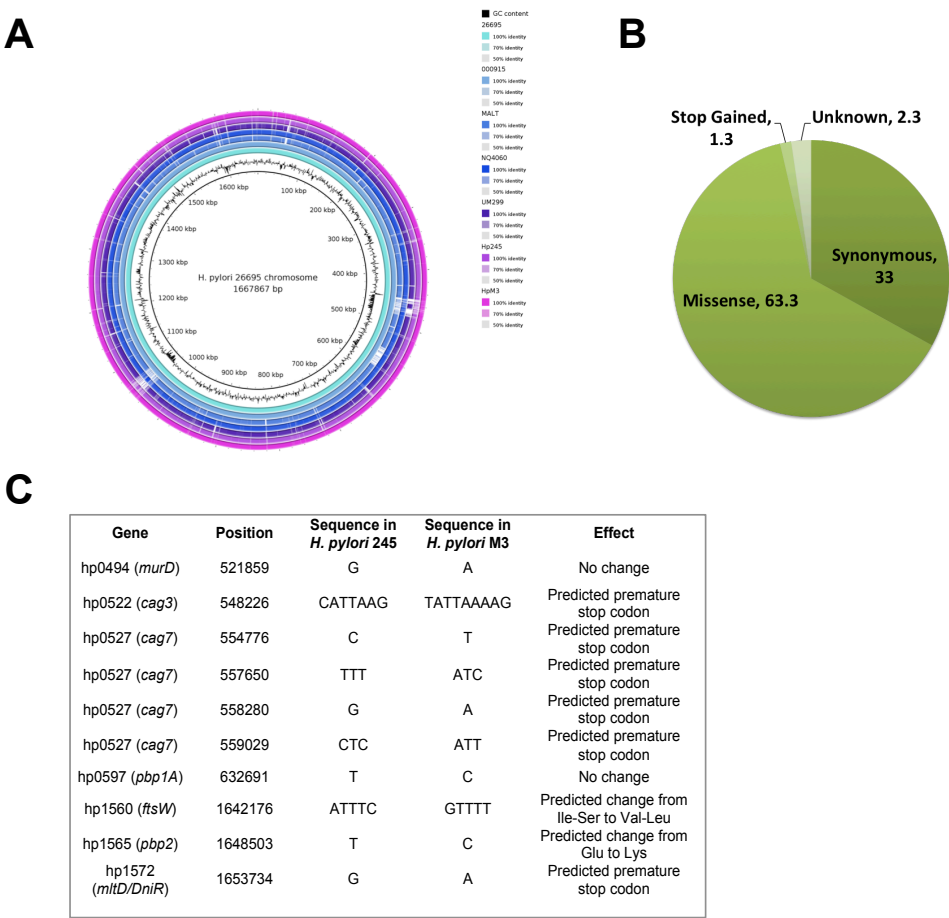
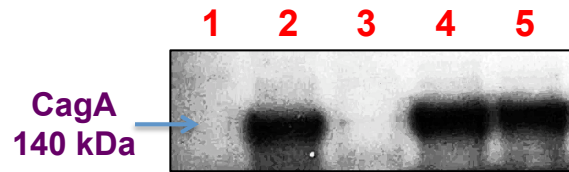
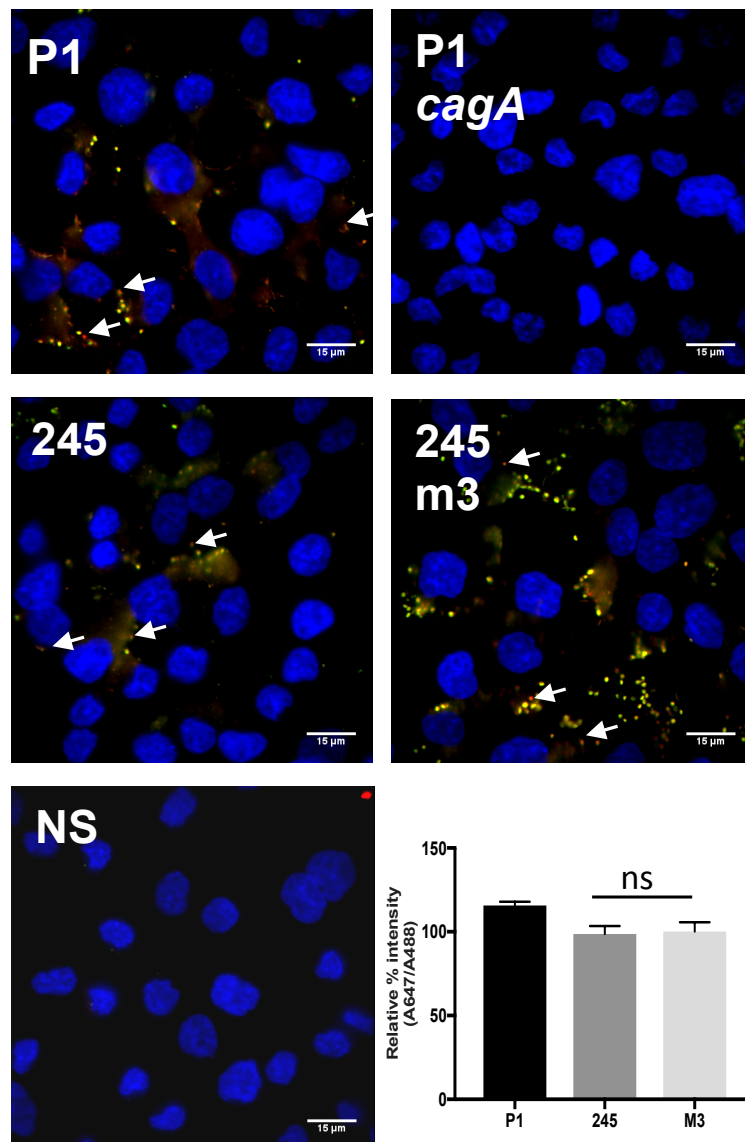


Figure 3

A

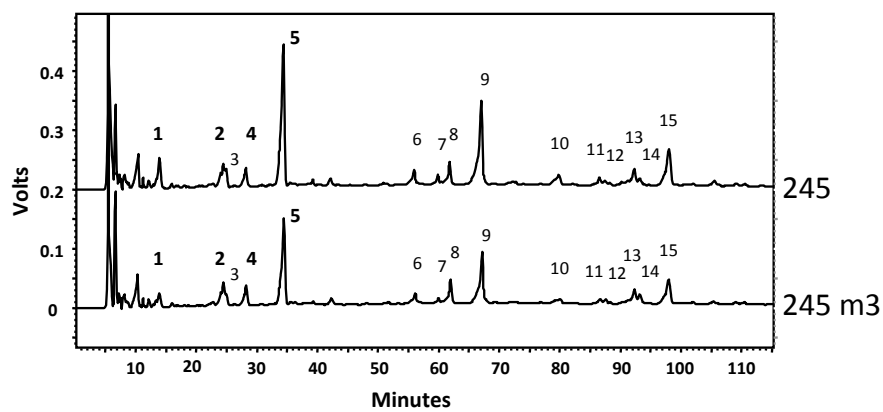


B



# Figure 4

## A

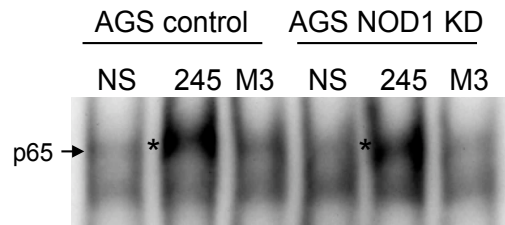


## B

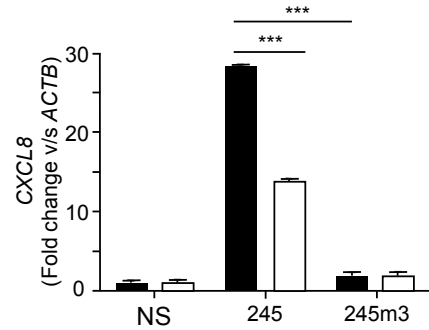
Peaks	Muropeptides	245 (in %)	245m3 (in %)
4	Di	4.29	6.44
1	Tri	5.27	3.06
2	Tetra	5.83	8.75
5	Penta	34.97	30.29
	Tetra/Tri Ratio	1.11	2.86

# Figure 5

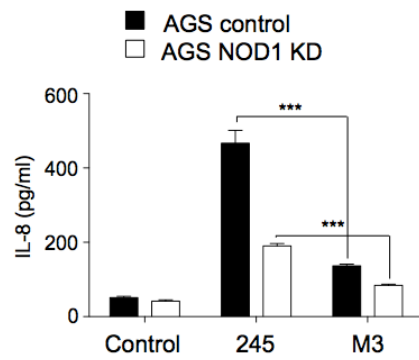
**A**



**B**



**C**



**D**

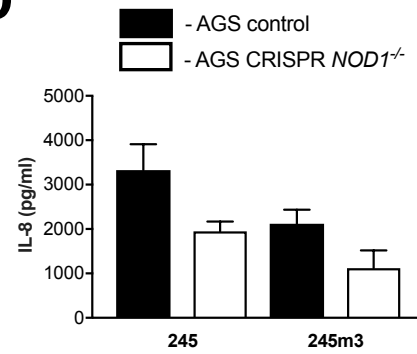
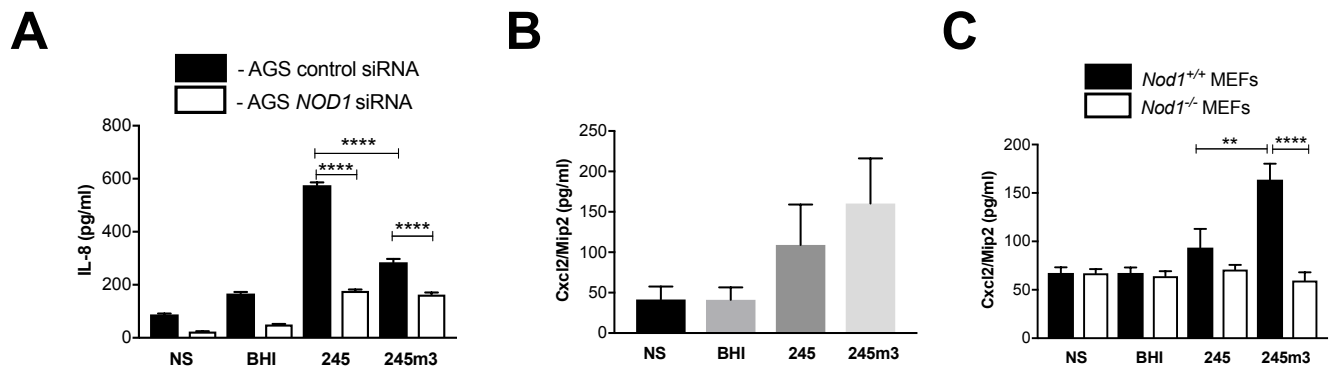


Figure 6



# Supplementary Figure 1

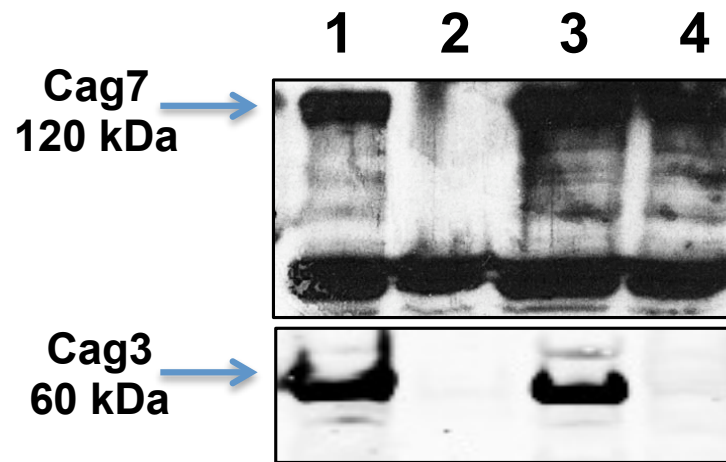
A

245_glmM	GCGATTGTCGCTACAAACATGAGCAATTTAGCCCTTAAAGAATACTTAAATCCCAAGAT
M3_glmM	GCGATTNTCGCTACAAACATGAGCAATTTAGCCCTTAAAGAATACTTAAATCCCAAGAT
	*****
245_glmM	TTGGAATTGAAGCATTGCGCGATTGGGGATAAGTTTGTGAGCGAATGCATGCGATTGAAT
M3_glmM	TTGGAATTGAAGCATTGCGCGATTGGGGATAAGTTTGTGAGCGAATGCATGCGATTGAAT
	*****
245_glmM	AAAGCCAATTTTGGAGGCGAGCAAAGCGGGCATATCATTTTTAGCGATTACGCTAAAACC
M3_glmM	AAAGCCAATTTTGGAGGCGAGCAAAGCGGGCATATCATTTTTAGCGATTACGCTAAAACC
	*****
245_glmM	GGCGATGGTTGGTGTGCGCGTTGCAAGTGAGCGCGTTAG
M3_glmM	GGCGATGGTTGGTGTGCGCGTTGCAAGTGAGCGCGTTAG
	*****

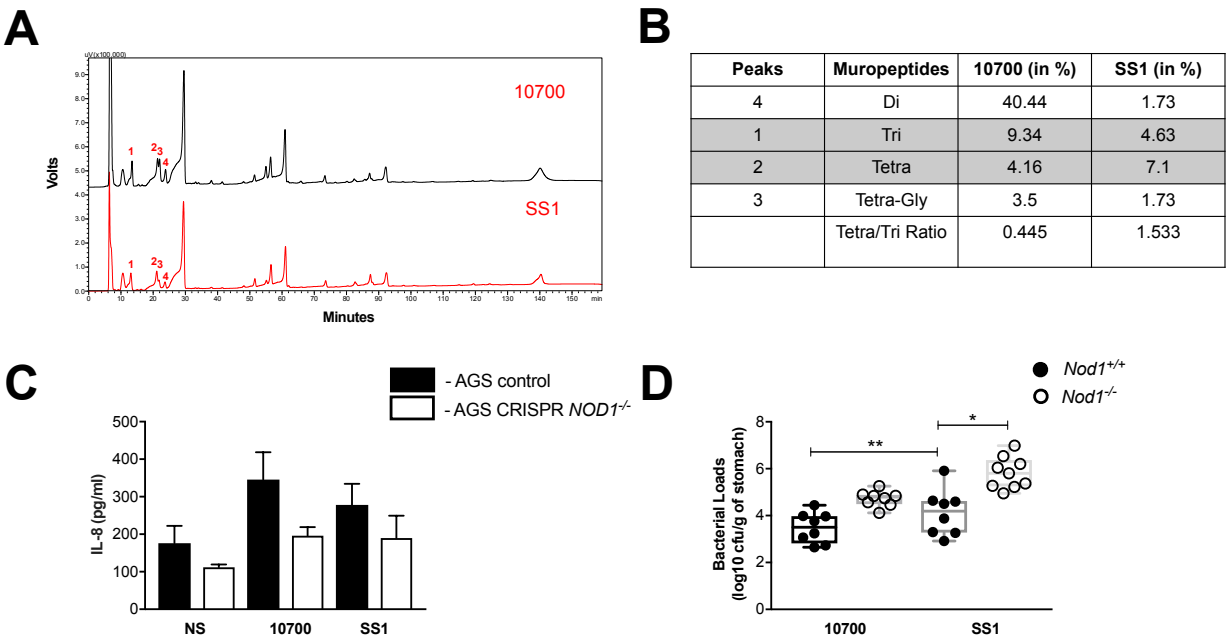
B

245_cagA	SKVENLXAXLNEFXNXNKDLSKVTQAKSDLENSVKDVIINQKVTDKVDNLNQAVSVAKA
M3_cagA	SKVENLNAXLNEFKNGXNKDLSKVTQAKSDLENSVKDVIINQKVTDKVDNLNQAVSVAKA
	*****
245_cagA	TGDFSRVEQALADLNFSKEQLAQQAQKNEDFNTGKNSALYQSVKNGVNGTLVXNGLSGI
M3_cagA	TGDFSRVEQALADLNFSKEQLAQQAQKNEDFNTGKNSALYQSVKNGVNGTLVXNGLSGI
	*****
245_cagA	EATALAKNFSDIKKELNEFKNFNNNNGLKNST <b>EPIY</b> AKVNKKKTGQAASPE <b>EPIYA</b> QV
M3_cagA	EATALAKNFSDIKKELNEFKNFNNNNGLKNST <b>EPIY</b> AKVNKKKTGQAASPE <b>EPIYA</b> QV
	*****
245_cagA	AKKVNAKIDQLNQIASGLGGVGQAAG <b>FPLKR</b> HDKVEDLSKVGRSVSP <b>EPIYA</b> TIDDLGGP
M3_cagA	AKKVNAKIDQLNQIAXGLGGVGQAAG <b>FPLKR</b> HDKVEDLSKVGRSVSP <b>EPIYA</b> TIDDLGGP
	*****
245_cagA	FPLKRHDKVDDL SKVGLSRXQELA---
M3_cagA	FPLKRHDKVDDL SKVGLXRNQELAXKI
	*****

## Supplementary Figure 2



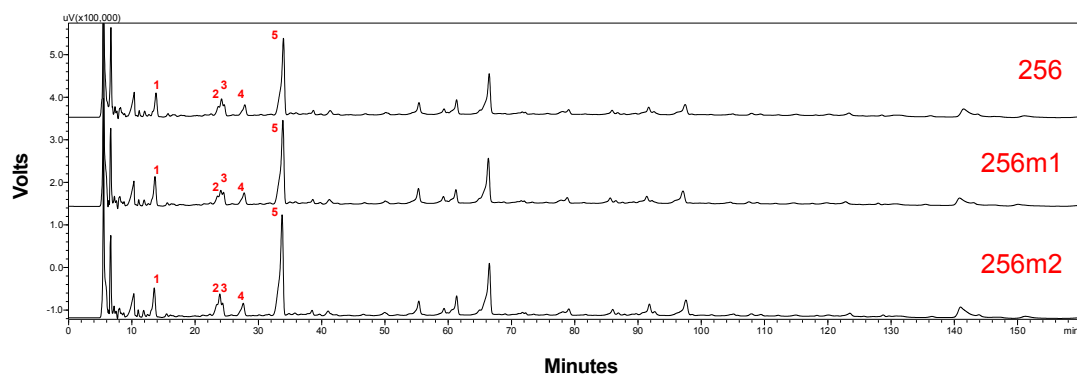
# Supplementary Figure 3





## Supplementary Figure 4

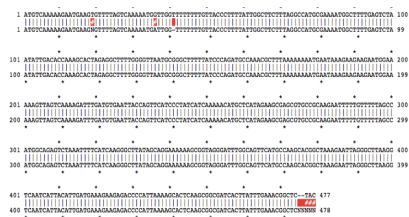
**A**



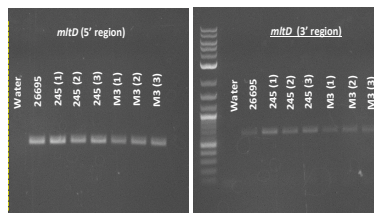
**B**

Peaks	Muropeptides	256 (in %)	256m1 (in %)	256m2 (in %)
4	Di	8.3	8.3	7.6
1	Tri	14.1	15.6	13.0
2	Tetra	19.7	17.1	19.5
5	Penta	57.9	59	59.9
	Tetra/Tri Ratio	1.4	1.01	1.5

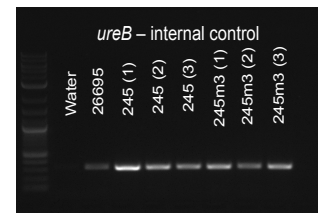
**A**



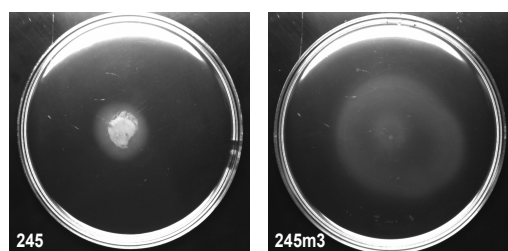
# B



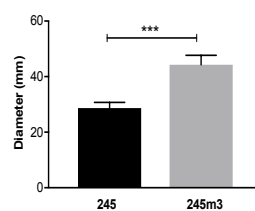
C



D



# E



### 3.3. Discussion

The findings of this chapter have demonstrated for the first time that a modification in peptidoglycan composition, generated during host adaptation, renders *H. pylori* more detectable by a molecule of the host innate immune system. We showed that a *cagPAI*<sup>+</sup> mouse-adapted strain, *H. pylori* 245m3, displayed a 2.6-fold increase in murine Nod1-specific GM-Tetra<sub>DAP</sub> relative to the human NOD1-specific GM-Tri<sub>DAP</sub> [155] in its cell wall. We further demonstrated that this mouse-adapted variant was affected in its ability to induce NOD1-dependent pro-inflammatory responses in human gastric epithelial cells. In contrast, this strain induced higher levels of chemokine production in mouse epithelial cells and embryonic fibroblasts, compared to the human clinical isolate, 245, thereby confirming the host-specificity of the NOD1 molecule.

Importantly, we confirmed via whole genome sequencing that mouse-adapted *H. pylori* 245m3 was indeed derived from the progenitor 245 strain. In addition, bioinformatics analyses identified 300 SNPs in the genome of *H. pylori* 245m3, when compared with that of the 245 strain. These SNPs included a point nonsense mutation in *HP1572* (*mltD/dniR*), which encodes a known PG modification enzyme [72, 73]. Thus, we hypothesize that *H. pylori* may modulate its PG composition via MltD, to actively engage the NOD1 signaling pathway. Future mutagenesis and *in vitro* co-culture studies are warranted to confirm if the lytic transglycosylase activity of MltD is indeed responsible for the changes in cell wall composition observed in *H. pylori* 245m3, as well as its subsequent effects on NOD1-dependent host cell responses.

Muropeptides have been implicated in a diverse array of biological processes, including tissue damage and antimicrobial resistance [52]. Indeed, changes to PG composition in *N. meningitidis* have previously been shown to have an impact on bacterial resistance to penicillin, a  $\beta$ -lactam antibiotic [160]. Therefore, it will be of interest to investigate any potential differences in the antibiotic resistance profiles of the human clinical *H. pylori* 245 isolate and its associated mouse-adapted variant, 245m3. Data from this study will enable us to further understand the mechanisms

contributing to the generation of antibiotic resistance in pathogens and thereby allow the development of novel antimicrobial compounds [163].

Overall, we have demonstrated how subtle changes in PG composition of the Gram-negative pathogen, *H. pylori*, affect NOD1 signaling and hence may favor bacterial persistence *in vivo*. Our data further suggest that bacterial pathogens may be able to customize their PG composition to better interact with the NOD1 receptor of the host, thereby facilitating chronic persistence *in vivo*.

## **Chapter 4: Novel host responses triggered by the NOD1 signaling pathway during long-term *Helicobacter pylori* infection favors bacterial persistence *in vivo***

### ***4.1. Introduction***

The innate immune receptor, NOD1, is ubiquitously expressed in various cell types and tissues, including the gut epithelium [153], where it plays key roles in immune surveillance and host responses against bacterial infection [136]. It is well established that NOD1 sensing of *H. pylori* PG, delivered via the T4SS or OMVs, results in the activation of NF- $\kappa$ B and the subsequent generation of pro-inflammatory responses required for host defense [35, 55]. Bacterial interactions with host epithelial cells also induce the activation and rapid recruitment of immune cells, such as monocytes and neutrophils, to the gastric mucosa thus perpetuating the inflammation associated with *H. pylori* infection [214, 215]. Furthermore, mice lacking functional Nod1 were shown to be more susceptible to *H. pylori* infection, thus establishing a central role for this molecule in promoting bacterial clearance *in vivo* [35, 65]. As such, many Gram-negative pathogens, including *H. pylori*, have evolved the ability to modify their PG and avoid NOD1 detection [68, 162, 193]. However, our findings described in Chapter 3 show that a mouse-adapted *H. pylori* strain had altered its cell wall composition to express relatively higher levels of GM-Tetra<sub>DAP</sub>, a muropeptide preferentially detected by mouse Nod1, as well as exhibited higher colonization levels compared to its human isolate during long-term infection, thereby suggesting that there may be some benefit for the bacterium to engage NOD1. We thus hypothesize that *H. pylori*-dependent activation of the NOD1 signaling pathway may represent a double-edged sword, with certain downstream responses promoting anti-bacterial effects and others enabling bacterial survival.

Interestingly, most previous studies have focused on the role of the NOD1 signaling pathway during short-term *H. pylori* infection [35, 216, 217]; however, the function of this cytosolic receptor during long-term *H. pylori* infection (> 4 weeks), as well as the relationship between NOD1 activation and *H. pylori*-induced disease remains unclear. This is of importance as chronic inflammation caused by persistent *H. pylori*

infection is an essential precursor to gastric carcinogenesis [11]. Furthermore, innate immune recognition of *H. pylori* has been shown to result in pro-inflammatory T helper (Th) 1 and Th17 responses, which in turn, promote the development of gastric immunopathologies [150, 218]. Our developing hypothesis is concurrent with a previous study by Allison and colleagues, which demonstrated an increased expression of *NOD1* in human gastric cancer biopsies [219]. However, in contrast, a recent report by Suarez et al. [214] showed that the pre-activation of NOD1 suppressed the gastric inflammation and injury caused in response to *H. pylori* infection.

Although NOD1 is now recognized mainly for its roles in NF- $\kappa$ B signaling and inflammation, this protein was originally identified due to its similarities to two pro-apoptotic proteins, cell death protein 4 (CED-4) and Apoptotic protease activating factor 1 Apaf-1 (Apaf-1), found in worms and mammals, respectively [153, 220]. NOD1, or CARD4 as it was earlier known, was subsequently observed to interact with the transcription factor, RIPK2, as well the pro-inflammatory caspases -1, -2, -4 and -9 [153, 220-222]. Its role in apoptosis is, however, yet to be fully examined with NOD1 reported to mediate apoptosis in a breast cancer model [176], whereas it promoted cell survival in an intestinal tumor model [174]. Even less is known regarding NOD1 regulation of cell survival and apoptotic functions in response to bacterial infection. Given that bacterial pathogens, including *H. pylori*, have evolved strategies to subvert cell death pathways for their survival in the host [47, 223], we speculate that *H. pylori* may exploit the PG-NOD1 signaling axis to regulate cell death and proliferative responses, thus enhancing its persistence and replication *in vivo*.

In the present chapter, we present primary evidence for the functions of NOD1 during chronic *H. pylori* infection. We found that *Nod1*<sup>-/-</sup> mice had reduced *H. pylori* bacterial loads when compared with their *Nod1*<sup>+/+</sup> counterparts at 8 weeks post-infection, which is in contrast to the established role for NOD1 in host defense. These *Nod1*<sup>-/-</sup> mice also displayed significantly increased gastric chemokine and splenocyte T cell cytokine responses, yet surprisingly had decreased inflammation scores and gastric immune cell infiltration when compared with wild type animals. Interestingly, a significant increase in apoptotic cells was also observed in the stomachs of

*H. pylori*-infected *Nod1*<sup>-/-</sup> mice. Taken together, our findings implicate NOD1 as being an important factor in facilitating the establishment and persistence of *H. pylori* infection in the stomach. We further observed NOD1 to be a regulator of host adaptive immunity as well as gastric epithelial cell survival responses.

## **4.2. Materials and Methods**

### **4.2.1. Bacterial Strains and Culture Conditions.**

The mouse-adapted *H. pylori* 245m3 strain has been described previously in Chapter 3. *H. pylori* bacteria were routinely cultured on either horse blood agar (HBA), according to standard procedures [205]. Viable counts of *H. pylori* were determined by serial dilution and plating.

### **4.2.2. Mouse Infection.**

Animal experimentation was performed in accordance with institutional guidelines (Monash University AEC no. MMCA 2015/43). *H. pylori* suspensions for mouse inoculation were prepared by harvesting bacteria from HBA plates using Brain Heart Infusion (BHI) broth [198]. Six- to eight-week-old specific pathogen/*Helicobacter*-free *Nod1*<sup>+/+</sup> or *Nod1*<sup>-/-</sup> [35] mice on a C57BL/6 background were each intra-gastrically administered a single 100-μl aliquot of the inoculating suspension (10<sup>7</sup> cfu/mouse) or control BHI broth using polyethylene catheters [205]. Mice were sacrificed by carbon-dioxide asphyxiation at 8 weeks post-infection, and subsequently the stomachs and spleens were collected and weighed. The presence of *H. pylori* infection was determined by quantitative culture, as described previously [198, 205].

### **4.2.3. Haematoxylin and Eosin (H&E) Staining.**

Formalin-fixed, paraffin-embedded gastric sections were de-paraffinized in histolene (2 x 5 mins) and re-hydrated in 100% ethanol (2 x 3 mins), followed by 3 mins in 70% ethanol and a 1 min rinse in tap water. Slides were then incubated with Mayer's haematoxylin solution for 5 mins, rinsed thrice in tap water, dipped in Scott's tap water for 1 min and rinsed a further 3 times in tap water. Subsequently, slides were incubated for 3 mins in 1% Eosin. Following a rinse with tap water, sections were dehydrated using the following incubation steps: 1 x 30 sec in 70% ethanol, 2 x 10 sec

in 100% ethanol and 2 x10 sec in histolene. Finally, slides were thoroughly air-dried before being cover-slipped (Menzel-Gläser) using DPX mounting medium (Merck). H&E-stained sections were imaged at 20x magnification using an Olympus BX53 confocal microscope and assessed blindly by an independent researcher for histopathological changes. Inflammatory scores for PMNs and lymphocytes were graded according to a previously described six-point scheme [224, 225] (Table 1)

**Table 1: Histological scoring scheme to grade PMN and lymphocyte infiltration and gastric inflammation [123, 226]**

Score	Criteria	Definition of criteria
0	No inflammation	Absence of immune cells in the mucosa
1	Mild multifocal	Scattered clumps of two or three immune cells
2	Mild widespread OR moderate multifocal	Widespread scattering of two or three immune cells across most of the antrum or fundus OR larger clumps of immune cells seen in a few fields per region
3	Mild widespread AND moderate OR severe multifocal	As per 2, plus large infiltrations of immune cells across the whole width of the mucosa
4	Moderate widespread	Large clumps of immune cells seen throughout the whole width of mucosa
5	Moderate widespread and severe multifocal	As per 4, but also with areas of dense concentrations of immune cells
6	Severe widespread	Dense sheets of immune cells throughout the mucosa

#### 4.2.4 Immunohistochemistry (IHC).

Gastric tissue samples were acquired as formalin-fixed, paraffin-embedded sections. All IHC staining commenced with a de-paraffinization procedure described in 4.2.3. Antigen retrieval was performed by immersion of tissue sections in 10 mM sodium citrate buffer, pH 6 and boiling for 8 mins in a microwave. Slides were then rinsed in tap water and allowed to cool. Endogenous peroxidases were inactivated via incubation with 3% hydrogen peroxide solution diluted in methanol for 30 mins at room temperature (RT), followed by 2 x 5 mins washes in phosphate-buffered saline (PBS). Next, a clear border around each section was drawn with a PapPen (Dako Australia). Sections were blocked in 10% (v/v) normal goat serum (Vector



Laboratories) in 0.05% PBS-Tween 20 (PBST) for 1.5 h at RT, followed by an overnight incubation at 4 °C with either rat anti-mouse F4/80 (ab6640, Abcam) or rat anti-mouse CD45 (550539, BD Pharmingen), each diluted 1 in 100 in blocking buffer. Isotype control antibodies of similar concentrations were also included in each experiment. After 3 x 5 mins washes in PBST, a biotin-conjugated anti-rat secondary antibody (Vector Laboratories) was applied for 1 h at RT. Sections were then washed for 2 x 5 mins in PBST and subsequently incubated with ABC vecta stain reagent (Vector Laboratories), according to the manufacturer's instructions, for 30 mins at RT. Slides were washed twice with PBST before addition of 3,3'-diaminobenzidine (DAB) peroxidase substrate (Vector Laboratories). The development of DAB-specific brown staining was monitored closely under a microscope and the length of incubation was kept consistent within each experiment. At the conclusion of staining, samples were counterstained in Mayer's haematoxylin for approximately 45 sec, "blued" in Scott's water for 1 min and dehydrated in 70% ethanol for 1 min, 100% ethanol for 2 x 1 min and histolene for 2 x 1 min. Sections were then dried prior to the addition of cover-slips (Menzel-Gläser) using DPX mounting medium (Merck). IHC-stained slides were then scanned and captured at 40x magnification using the Aperio Scanscope AT Turbo slide scanner (Leica Biosystems), located at the Monash Histology Platform (Clayton, Victoria, Australia). The numbers of positively-stained cells/total number of cells were analyzed for a minimum of 2 sections per sample using Aperio Imagescope software (Leica Biosystems). Only antral and body sections of the stomach were used for the analysis. The thickness of gastric tissue sections was also measured using this software.

#### **4.2.5. Flow cytometry.**

To isolate lymphocytes, whole stomachs from euthanized mice were first placed in ice-cold sterile PBS (Life Technologies) and their contents removed. Stomachs were then chopped into fine pieces in sterile petri dishes and transferred to 50 ml Falcon tubes (Thermo Fisher Scientific) containing fresh dissociation buffer [2% foetal calf serum (FCS) in Hank's Balanced Salt Solution (HBSS) (Calcium and Magnesium free; Life Technologies) + 5 mM Ethylenediaminetetraacetic acid (EDTA)]. Cell suspensions were incubated at 37°C with shaking at 180 rpm for 30 mins, vortexed for 15 sec and then passed through 70 µm cell strainers (Falcon, Thermo Fisher Scientific) into fresh 50 ml Falcon tubes. The remaining pieces of tissue were

returned to the original Falcon tubes prior to the addition of digestion buffer [2% FCS in RPMI (Life Technologies) + 1 mg/ml collagenase Type 1 (Life Technologies) + 0.4 units dispase (Life Technologies) + 0.4 units DNase (Promega)]. Samples were incubated at 37°C with shaking at 180 rpm for 45 mins and subsequently passed through new cell strainers into the Falcon tubes containing the prior cell filtrates. Tubes were then centrifuged at 630 x g for 10 mins at RT. Following this, supernatants were discarded and the cell pellets resuspended in 40% percoll (GE Healthcare) and diluted in sterile PBS. This cell suspension was then gently added drop-wise to 15 ml Falcon tubes containing 80% Percoll (GE Healthcare). Tubes were centrifuged at 900 x g (with no brake) for 20 mins at RT. Later, the cell debris at the top was removed and the cell suspensions beneath were collected into fresh 15 ml Falcon tubes. This material was centrifuged at 630 x g for 10 mins at RT, resuspended in HBSS and centrifuged once more. Finally, the resulting cell pellets were transferred to fluorescence-activated cell sorting (FACS) tubes (Falcon, Thermo Fisher Scientific), prior to the addition of FACS buffer (2% FCS in PBS) containing Fc block and Propidium-iodide (PI) (Table 2). Tubes were incubated for 15 mins and cells were then washed in fresh FACS buffer. Subsequently, cell pellets were resuspended in FACS buffer containing the antibodies at desired concentrations (Table 2) and incubated for 30 mins. Finally, samples were washed twice in fresh FACS buffer and the stained lymphocytes were ready to be analyzed. Data was acquired on a FACSCanto™ II system (BD Biosciences) and analyzed using Kaluza software (Beckman Coulter). Compensation was set up on the FACSCanto™ II flow cytometer at the beginning of the experiment. The gating and cell identification strategy is shown in Figure 4.5 and is as follows: firstly, cell debris was eliminated and single cell suspensions were gated using a forward versus side scatter (FSC-A/SSC-A) dot plot (data not shown). Total viable leukocytes were then identified based on the expression of CD45 and the simultaneous exclusion of the live/dead dye, PI. Myeloid cells and T cells were distinguished within this CD45<sup>+</sup> cell population by their expression of CD11b, and CD3, respectively. Finally, proportions of neutrophils and macrophages within the gated CD11b<sup>+</sup> cell population were determined based on their expression of the neutrophil-specific marker, Ly6G and F4/80, respectively.

**Table 2: List of antibodies and concentrations used for flow cytometry analysis**

Antibody	Dilution
TruStain FcX (anti-mouse CD16/CD32 antibody) (#101310, Biolegend)	1 in 50
PI (Thermo Fisher Scientific)	1 in 1000
PE/Cy7 anti-mouse CD45 (#103113, Biolegend)	1 in 100
FITC anti-mouse F4/80 (#123107, Biolegend)	1 in 50
PE anti-mouse/human CD11b (#101207, Biolegend)	1 in 100
APC anti-mouse Ly6G (#127613, Biolegend)	1 in 100
Pacific Blue anti-mouse CD3 (#100213, Biolegend)	1 in 100

#### 4.2.6. Gene expression.

RNA was isolated from murine gastric tissues using TRI Reagent (Thermo Fisher Scientific), according to the manufacturer's instructions. cDNA was generated from RNA (1 µg) using the SuperScript® kit (Thermo Fisher Scientific), as per the manufacturer's instructions. qPCR reactions consisted of 4 µl diluted synthesized cDNA (1:10), 5 µl SYBR® Green qPCR MasterMix (Thermo Fisher Scientific) and 1 µl oligonucleotide primers (1 µM) for the tested genes (Table 3). Sterile nuclease-free water was used as a negative control for all the genes tested. Quantitative real-time PCR (qPCR) assays were performed in Applied Biosystems™ 7900 Fast Real-Time PCR machines (Thermo Fisher Scientific), using the following program: 50°C, 2 min, followed by 95°C, 10 min, then 40 successive cycles of amplification (95°C, 15 s; 60°C, 1 min). Gene expression levels were determined by the Delta-Delta Ct method to measure relative gene expression levels to the 18S rRNA gene (*Rn18s*).

#### 4.2.7. Gastric cytokine responses.

Stomachs were homogenized in 1 ml of BHI broth using the gentleMACS™ dissociator (Miltenyi Biotec). Keratinocyte-derived chemokine, KC (CXCL1, R&D Systems), macrophage inflammatory protein 2, MIP-2 (CXCL2, R&D Systems) and C-C motif ligand 2, CCL2 (R&D Systems) cytokine levels in gastric homogenates were determined by sandwich ELISA, according to the manufacturer's instructions.

**Table 3: List of primers used for qPCR**

Primer name	Primer sequence
m18S F	GTAACCCGTTGAACCCATT
m18S R	CCATCCAATCGGTAGTAGCG
mNod1 F	GCCTGACAAGGTCCGAAAGA
mNod1 R	GGTATACCTGCTTACTGGGTCA
mCxcl1 F	CCTTGACCCTGAAGCTCCCT
mCxcl1 R	CAGGTGCCATCAGAGCAGTCT
mCxcl2 F	AACATCCAGAGCTTGAGTGTGA
mCxcl2 R	TTCAGGGTCAAGGCAAACCT
mCcl2 F	AGGTGTCCCAAAGAAGCTGTA
mCcl2 R	ATGTCTGGACCCATTCTCTCT
mMid1 F	CTCCAGTACACCATATTCACCG
mMid1 R	GTGGTTCTGCTTGATGTTGG
mErdr1 F	TCAAGATGTTACCCGCC
mErdr1 R	TGTGCTTTCGTGGGTGAC
mATgfb F	GTCATCCTTGTCCTGCTCTG
mATgfb R	CCTTGGTCTACATAGTGAGTTCC
mBpifb1 F	GTCACCTCTGCTAACATCCTC
mBpifb1 R	TCGGTGCTCATTTGGAACCTC
mAdcyap1r1 F	AAATGAGTCTTCCCCAGGTTG
mAdcyap1r1 R	CCCCTATGGTTTCTGTCATCC

**4.2.8. Splenocyte cytokine responses.**

Spleens were collected from euthanized mice. Single cell suspensions were obtained by grinding tissues through 70  $\mu$ m cell strainers. Splenocytes were recovered in RPMI complete medium (RPMI + 10% FCS + 1% penicillin/streptomycin) and seeded at  $2 \times 10^6$  cells/ml in 24-well plates (Falcon). Cells were left untreated or stimulated with 5  $\mu$ g/ml concanavalin A (ConA; Sigma Aldrich), and then incubated for 3 days at 37°C in 5% CO<sub>2</sub>. Levels of Interferon-gamma (IFN- $\gamma$ ), Interleukin-2 (IL-2), Tumor necrosis factor (TNF) and Interleukin-17 (IL-17) were measured in splenocyte supernatants using a cytometric bead array (BD Biosciences), as per the manufacturer's instructions.

#### **4.2.9. Terminal deoxynucleotidyl transferase dUTP nick end-labeling (TUNEL) assay.**

Apoptotic cells in gastric tissue sections were fluorescently labeled using a Click-iT® Plus TUNEL assay (C10617, Thermo Fisher Scientific), according to the manufacturer's instructions. Stained samples were imaged at 20x magnification using a confocal microscope. The numbers of apoptotic cells (stained green), as well as the total numbers of cells (identified via DNA staining in blue) per sample were analyzed using a custom macro written for Image J software (Dr. Sarah Creed, Monash Micro Imaging).

#### **4.2.10. Microarray analysis.**

RNA was isolated from stomach tissues collected from *Nod1*<sup>+/+</sup> (n=3) and *Nod1*<sup>-/-</sup> (n=4) mice at 8 weeks post-infection. Cyanine-3 (Cy3)-labeled cRNA was then prepared from total RNA (0.2 µg) using the One-Color Low input Quick Amp labeling Kit (Agilent) and RNeasy column purification (Qiagen). Dye incorporation and cRNA yield were determined with a NanoDrop ND-1000 Spectrophotometer. cRNA (600 ng) was labeled with Cy3 (specific activity > 6 pmol Cy3/µg cRNA) and fragmented at 60°C for 30 mins in a reaction volume of 25 µl, containing 1x Agilent fragmentation buffer and 2 x Agilent blocking agent, as per the manufacturer's instructions. On completion, 25 µl of 2x Agilent gene expression hybridization buffer was added and 42 µl of sample hybridized for 17 h at 65°C in a rotating Agilent hybridization oven. After hybridization, microarrays were washed for 1 min at RT with GE wash buffer 1 (Agilent) and again for 1 min with GE wash buffer 2 (Agilent) at 37°C. Slides were scanned immediately after washing on the Agilent C, DNA microarray scanner using one color scan settings for 8 x 60 K array slides and the following parameters: scan area, 61x21.6 mm; scan resolution, 3 µm; dye channel set to Green; and 20 bit Tiff. The scanned images were analyzed with Feature Extraction Software 11.0.1.1 (Agilent) using default parameters (protocol GE1-1100\_Jul11 and Grid: (074809\_D\_F\_20150624) to obtain background subtracted and spatially detrended processed signal intensities.

Microarray data were analyzed using GeneSpring GX software to identify genes displaying differential expression patterns (>= 1.5 fold) between infected *Nod1*<sup>+/+</sup> and *Nod1*<sup>-/-</sup> mice. Genes displaying statistically significant (p < 0.05) expression levels between both groups of animals were identified using Limma software [227]

(Dr. Ross Chapman, Hudson Institute of Medical Research), and subsequently validated via qPCR, as described in section 4.2.6.

#### **4.2.11. Statistical analysis.**

Data were analyzed using the parametric Students' *t*-test or non-parametric Mann-Whitney U test, as appropriate, when two conditions/stimuli were tested. Alternatively, a parametric one-way ANOVA with Tukey's multiple testing correction was employed when three or more conditions/stimuli were present. Differences in data values were considered significant at a *P* value of  $< 0.05$ .

### 4.3. Results

#### 4.3.1. *Nod1*<sup>-/-</sup> mice display reduced susceptibility to infection with *H. pylori* 245m3 at 8 weeks post-infection.

To determine the role of NOD1 during chronic infection, *Nod1*<sup>+/+</sup> and *Nod1*<sup>-/-</sup> mice were gavaged with either *H. pylori* 245m3 bacteria or BHI broth, then sacrificed at 56 days (8 weeks) post-gavage. Interestingly, in contrast to our previous findings at both 7 and 30 days post-infection (Chapter 3), *Nod1* did not seem to protect against chronic infection, with *Nod1*<sup>-/-</sup> mice infected with *H. pylori* 245m3 exhibiting similar, if not reduced, bacterial loads when compared with their *Nod1*<sup>+/+</sup> counterparts (Fig. 4.1. A;  $p = 0.0726$ ). *H. pylori*-infected *Nod1*<sup>+/+</sup> and *Nod1*<sup>-/-</sup> mice had similar stomach and spleen weights (Fig. 4.1. B, C). However, interestingly, spleens from BHI-inoculated *Nod1*<sup>-/-</sup> mice displayed a significantly higher weight in comparison to their *Nod1*<sup>+/+</sup> counterparts (16-fold increase) (Fig. 4.1. C,  $p = 0.0065$ ). No *Helicobacters* were isolated from the stomachs of control animals administered BHI (data not shown).

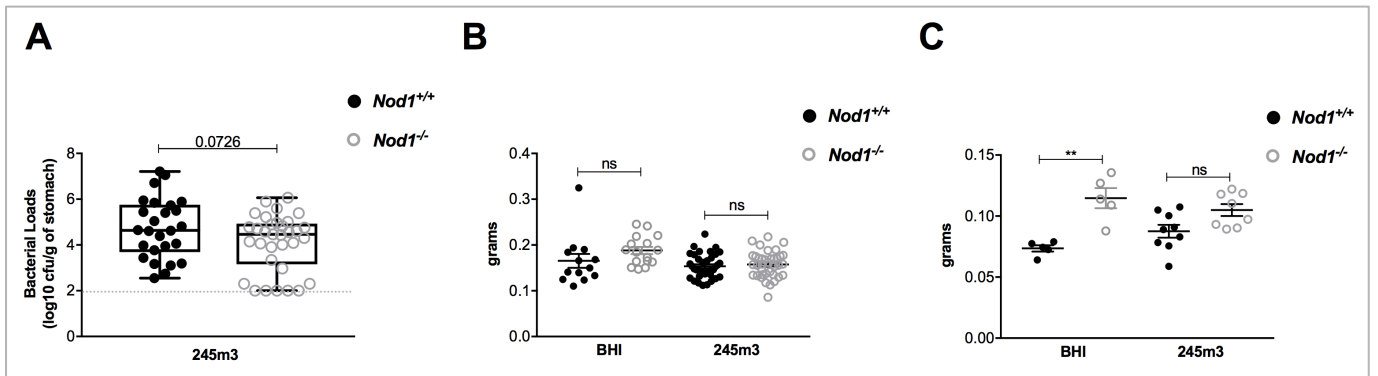


**Figure 4.1: *Nod1*<sup>-/-</sup> mice do not display increased bacterial loads during chronic *H. pylori* infection.** *Nod1*<sup>+/+</sup> and *Nod1*<sup>-/-</sup> mice (n=28 per group) were gavaged with either control BHI broth or 10<sup>7</sup> colony-forming units (CFUs) of *H. pylori* 245m3 and sacrificed 56 days post gavage. **(A)** Bacterial loads in mice were determined by quantitative culture of gastric tissue samples and are pooled from four independent experiments. Data are presented as Log<sub>10</sub> colony forming units (CFU)/g stomach. The limit of detection for the assay is 1,000 CFU/gram. **(B)** Stomachs (n≥8) and **(C)** spleens (n≥5), isolated from control and infected mice, were weighed prior to use in downstream analyses. Each point represents a single mouse. Data were analyzed using a Student's t - test. \*\*  $p < 0.01$ , 'ns'  $p > 0.05$ .

#### **4.3.2. *Nod1*<sup>-/-</sup> mice infected with *H. pylori* 245m3 exhibit extensive gastric hyperplasia and significantly decreased gastric inflammation and mucosal immune cell infiltration.**

It has been previously established that the recognition of Gram-negative bacterial PG by the intracellular NOD1 receptor stimulates a pro-inflammatory signaling cascade, ultimately resulting in the recruitment of immune cells to the gastric mucosa [158, 228, 229]. To investigate the gastric inflammatory phenotype following long-term *H. pylori* infection, we performed histological analyses on gastric antrum and corpus tissues from both *H. pylori*-infected and control *Nod1*<sup>+/+</sup> and *Nod1*<sup>-/-</sup> mice. H&E staining revealed increased gastric mucosal thickening or hyperplasia in *Nod1*<sup>-/-</sup> mice inoculated with BHI at 8 weeks post-infection. This effect was further exacerbated in animals infected with *H. pylori* 245m3 (Fig. 4.2. A, C;  $p = 0.0003$ ). However, surprisingly, in comparison to *Nod1*<sup>+/+</sup> animals infected with *H. pylori* 245m3, these *Nod1*<sup>-/-</sup> mice displayed significantly lower immune cell infiltration and gland atrophy, as well as fewer lymphoid aggregates, thus resulting in decreased overall inflammation scores (Fig. 4.2. A, B;  $p = 0.0571$ ). Furthermore, from immunohistochemical analyses, we observed significantly reduced recruitment of CD45<sup>+</sup> immune cells (Fig. 4.3. A, B;  $p < 0.0001$ ; 1.8 fold decrease) and F4/80<sup>+</sup> macrophages (Fig. 4.4. A, B;  $p < 0.0001$ ; 2.3 fold decrease) to the gastric mucosa of *Nod1*<sup>-/-</sup> mice infected with *H. pylori* 245m3 in comparison with their *Nod1*<sup>+/+</sup> counterparts. Interestingly, however, no differences in CD45<sup>+</sup> immune cell infiltration to the gastric sub-mucosa were observed between infected *Nod1*<sup>+/+</sup> and *Nod1*<sup>-/-</sup> mice (Fig. 4.3. C), thus suggesting that immune cell migration to the gastric mucosa may be impeded in *Nod1*<sup>-/-</sup> mice.

In order to confirm the results obtained via histological analyses, proportions of certain immune cell subsets present in a pool of lymphocytes isolated from *H. pylori*-infected and control *Nod1*<sup>+/+</sup> and *Nod1*<sup>-/-</sup> mice were determined by flow cytometry. We observed a lower overall relative percentage of macrophages and neutrophils in infected *Nod1*<sup>-/-</sup> animals, in comparison to *Nod1*<sup>+/+</sup> mice. In contrast, a higher relative percentage of T cells were seen in these *Nod1*<sup>-/-</sup> mice (Fig. 4.5. A-F). Collectively, our data indicate that while *Nod1*<sup>-/-</sup> mice infected with *H. pylori* 245m3 display extensive gastric hyperplasia, they are characterized by lower inflammation and decreased



immune cell infiltration to the gastric mucosa, when compared with infected *Nod1*<sup>+/+</sup> animals, at 8 weeks post-infection.

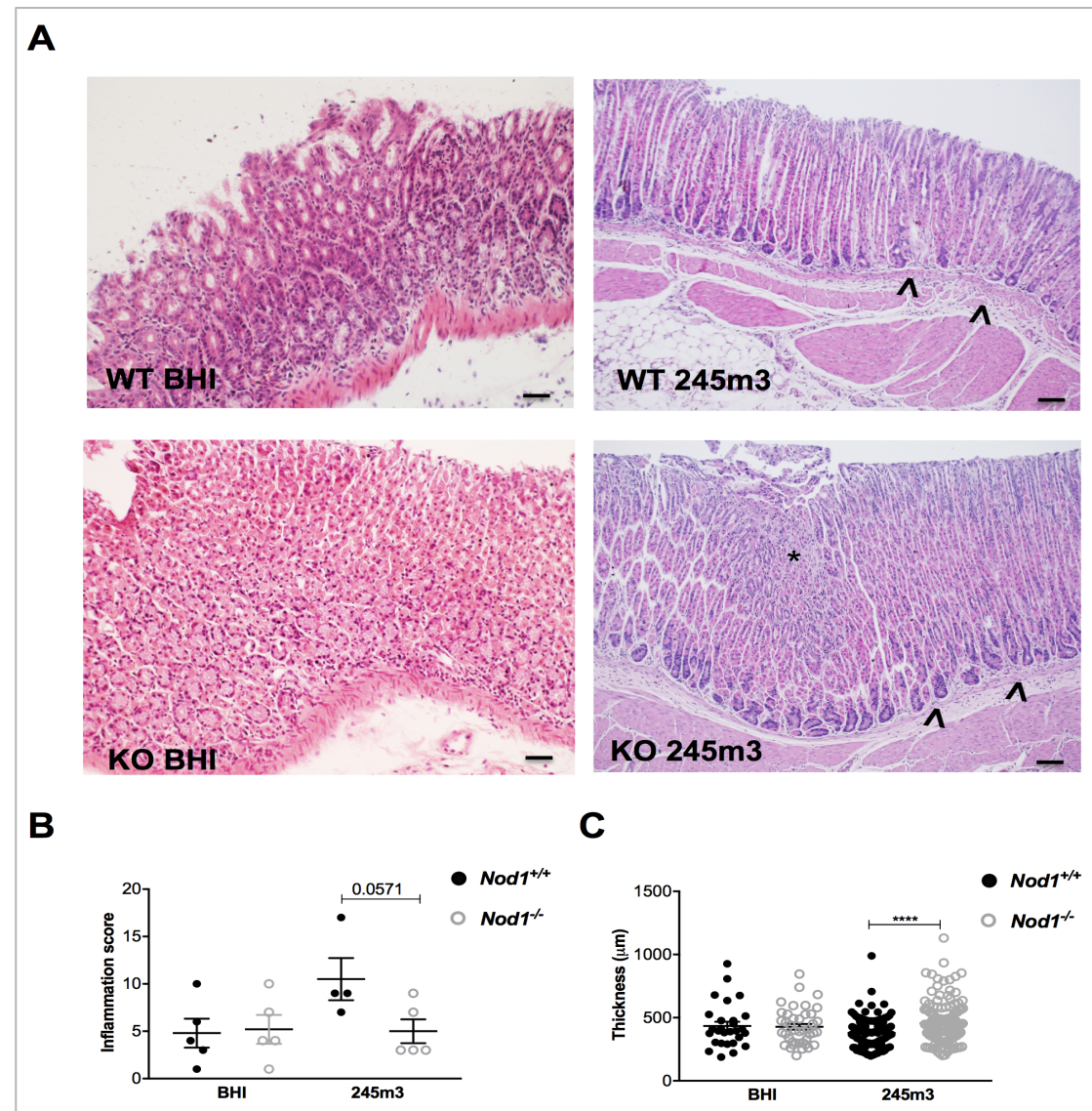


**Fig. 4.2. *Nod1*<sup>-/-</sup> mice infected with *H. pylori* 245m3 exhibit less gastric immunopathology but significantly increased mucosal thickening.** *Nod1*<sup>+/+</sup> (black spots) and *Nod1*<sup>-/-</sup> (grey spots) mice were gavaged with either BHI broth or *H. pylori* 245m3 and sacrificed 8 weeks post-gavage. **(A)** Gastric tissue sections were subsequently stained with H&E to determine overall inflammation, comprising PMNs, mononuclear cells, parietal cell atrophy and lymphoid aggregates/abscesses in the antrum and body of tissues; **(B)** The overall inflammatory scores (see Methods, Table 1) (n=5 per group); **(C)** The mucosal thickness of each gastric tissue section was measured using the Aperio Imagescope software. **(B)** Each data point represents a single mouse or **(C)** a single analyzed field of view from n=20 mice per group. Figures show means ± SEM. Data are pooled from 2 independent experiments and analyzed for statistical significance using a Mann Whitney test. \*\*\*\* *p* < 0.0001. > infiltrating cells, \* cell aggregates, magnification = 20X, Scale bar = 50 μm.

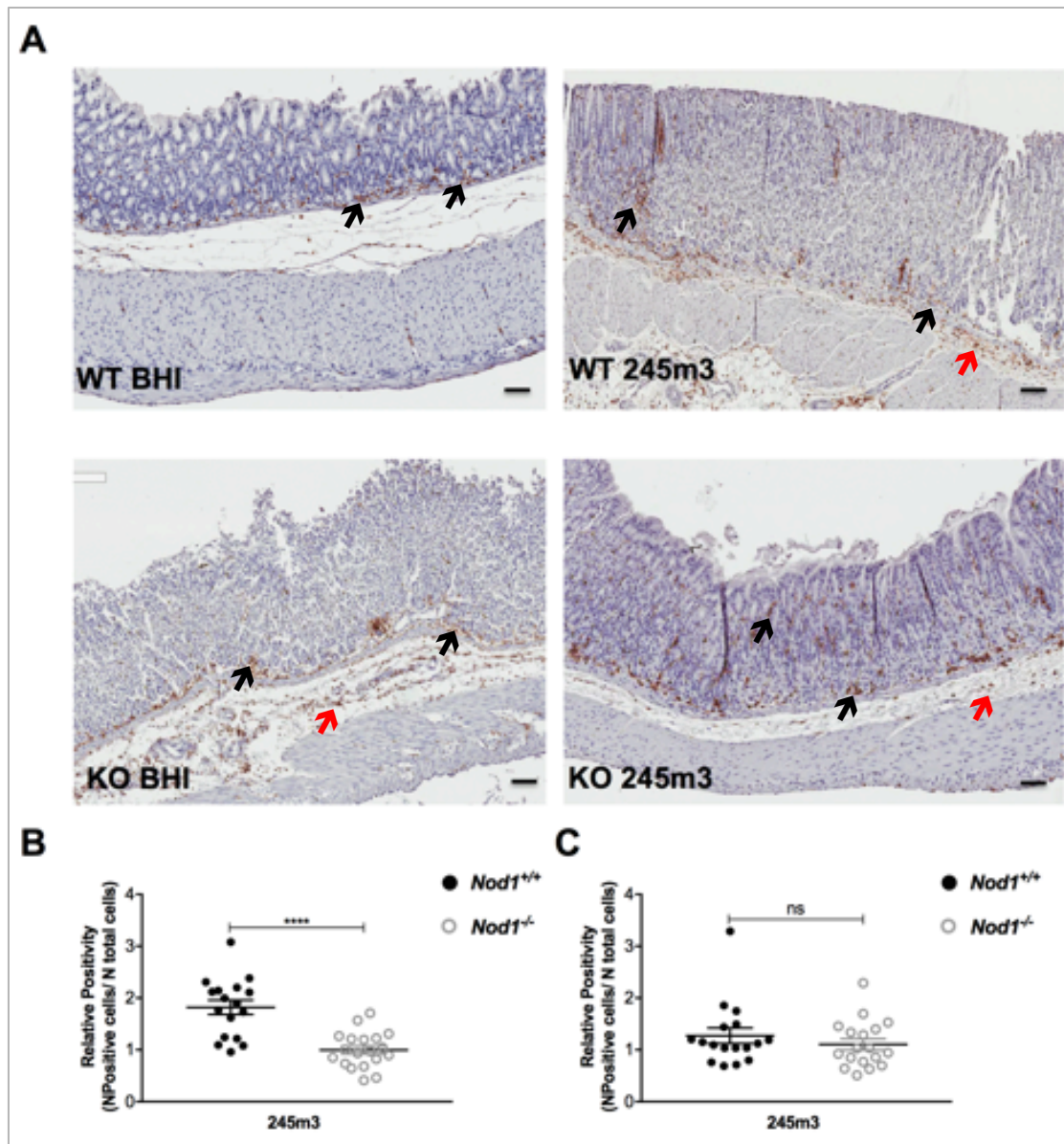


**Fig. 4.3. *Nod1*<sup>-/-</sup> mice infected with *H. pylori* 245m3 display decreased CD45<sup>+</sup> immune cell infiltration to the gastric mucosa.** *Nod1*<sup>+/+</sup> (black spots) and *Nod1*<sup>-/-</sup> (grey spots) mice (n=18 per group) were gavaged with either BHI broth or *H. pylori* 245m3 and sacrificed 8 weeks post-gavage. **(A)** Gastric tissue sections were stained with anti-CD45 antibody to ascertain the recruitment of leukocytes. The proportion of CD45<sup>+</sup> immune cells present in the **(B)** gastric mucosa (indicated by black arrows) and **(C)** gastric sub-mucosa (indicated by red arrows) of infected mice are represented as “relative positivity” or (number of positively stained cells/number of total cells) in *H. pylori*-infected mice relative to control mice on the same genetic background. Data were analyzed using the Aperio Imagescope software. Each data point represents a single mouse. Figures show means ± SEM. Data are pooled from 2 independent experiments and analyzed for statistical significance using a Mann Whitney test. \*\*\*\* *p* < 0.0001, ‘ns’ *p* > 0.05. Magnification = 40X, Scale bar = 400 μm.



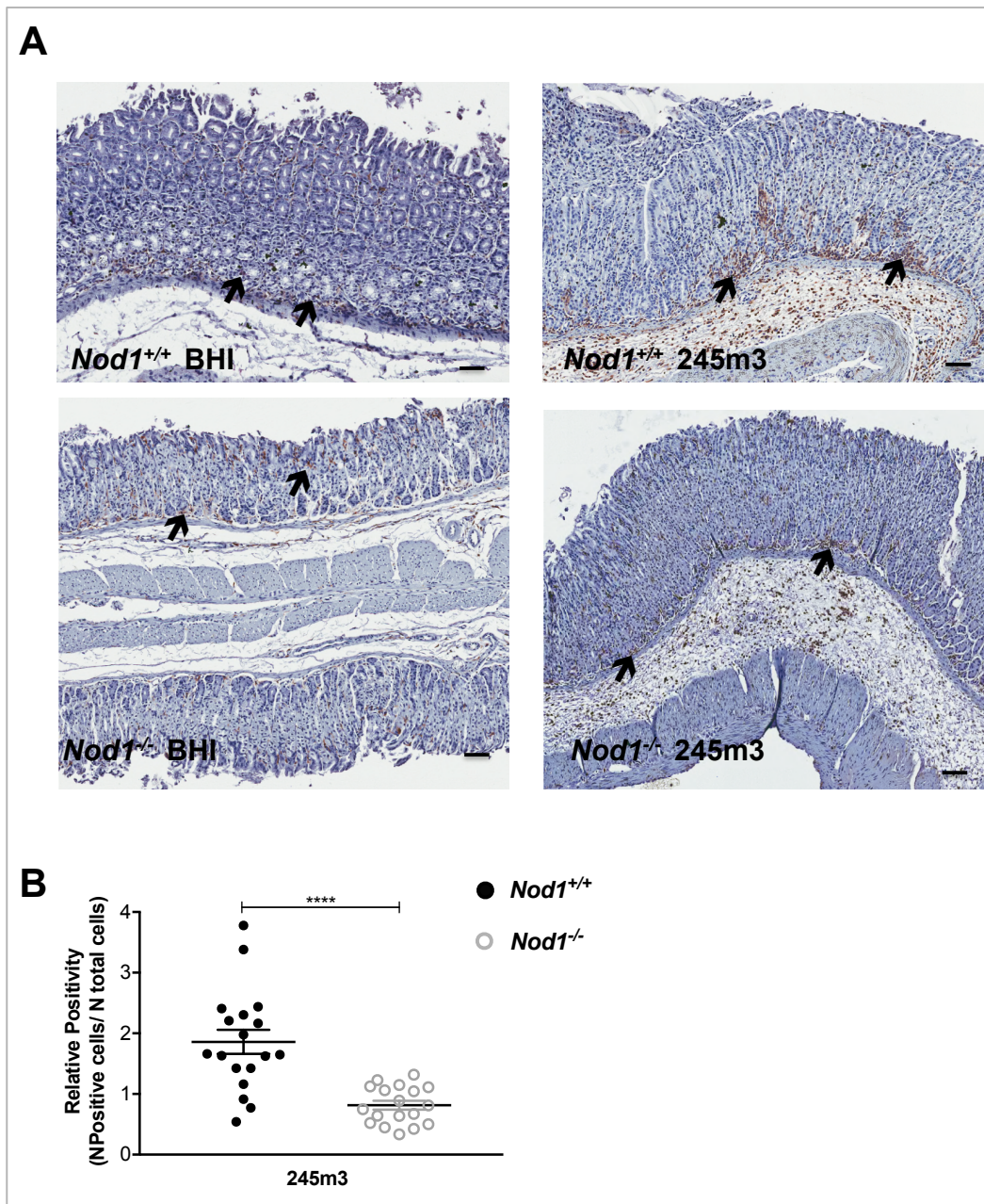


**Fig. 4.4. *Nod1*<sup>-/-</sup> mice infected with *H. pylori* 245m3 display decreased F4/80<sup>+</sup> macrophage infiltration to the gastric mucosa.** *Nod1*<sup>+/+</sup> (black spots) and *Nod1*<sup>-/-</sup> (grey spots) mice (n=18 per group) were gavaged with either BHI broth or *H. pylori* 245m3 and sacrificed 8 weeks post-infection. **(A)** Gastric tissue sections were subsequently stained with anti-F4/80 antibody to ascertain the specific recruitment of macrophages in response to infection; **(B)** The proportion of F4/80<sup>+</sup> immune cells present in the gastric mucosa (indicated by black arrows) of infected mice are represented as “relative positivity” or (number of positively stained cells/number of total cells) in *H. pylori*-infected mice relative to control mice on the same genetic background. Data were analyzed using the Aperio Imagescope software. Each data point represents a single mouse. Figures show means ± SEM. Data are pooled from 2 independent experiments and analyzed for statistical significance using a Mann Whitney test. \*\*\*\*  $p < 0.0001$ . Magnification = 40X, Scale bar = 200  $\mu$ m.

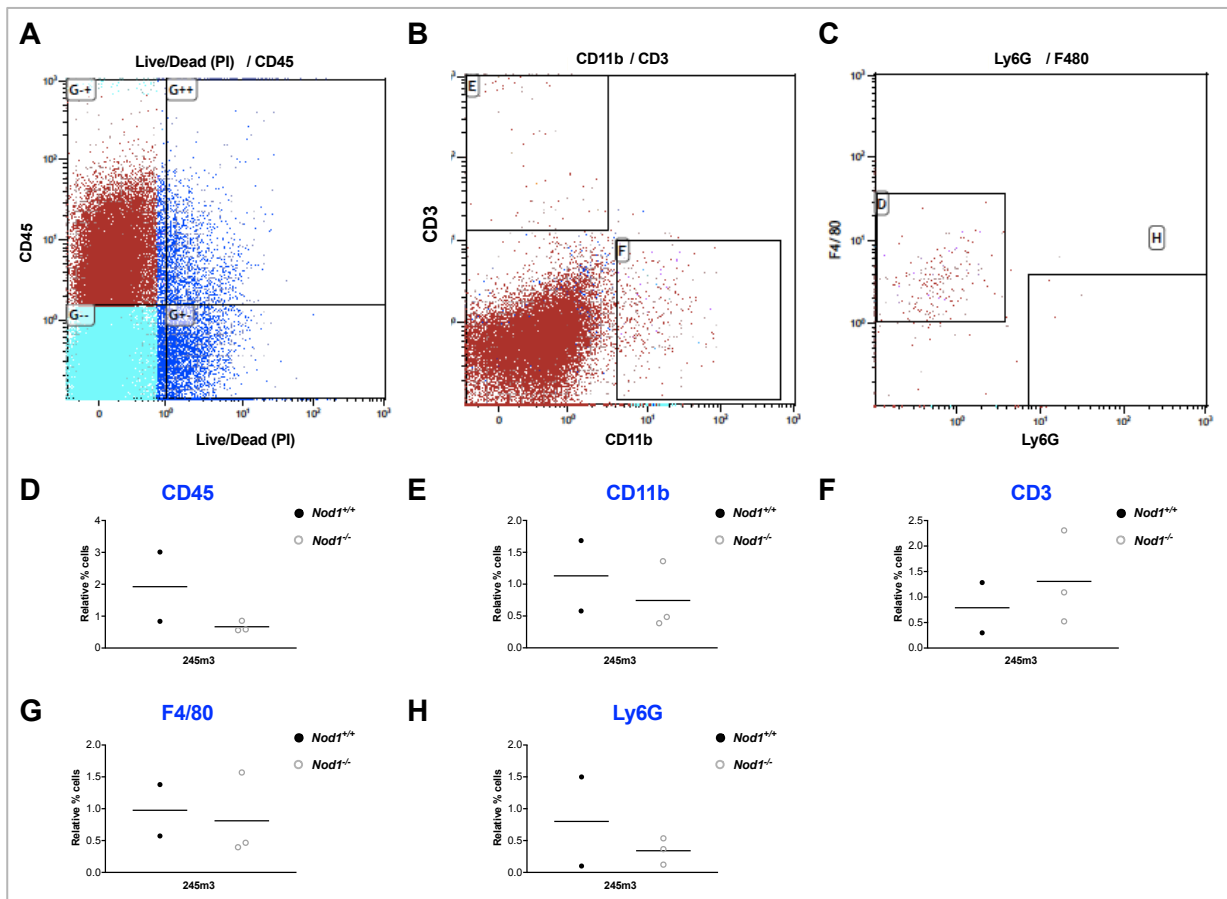


**Fig 4.5. *Nod1*<sup>-/-</sup> mice infected with *H. pylori* 245m3 exhibit reduced T cell, macrophage and neutrophil recruitment to the gastric compartment.** *Nod1*<sup>+/+</sup> (black spots; n=2) and *Nod1*<sup>-/-</sup> (grey spots; n=3) mice were gavaged with either BHI broth or *H. pylori* 245m3 and sacrificed 8 weeks post-infection. Immune cells isolated from murine stomachs were stained using fluorescently labeled antibodies with specificity for viable cells (anti-PI), leukocytes (anti-CD45, anti-CD11b), T cells (anti-CD3), macrophages (anti-F4/80) and neutrophils (anti-Ly6G). (A) To analyze the samples, a rectangular region was initially used to circumscribe viable leukocytes (CD45<sup>+</sup>, PI) in a bivariate histogram of CD45 v/s PI. (B, C) Scatter-inclusive cells were used to evaluate the activation state of each respective measured population. The proportions of (D) CD45<sup>+</sup>, (E) CD11b<sup>+</sup>, (F) CD3<sup>+</sup>, (G) F4/80<sup>+</sup> and (H) Ly6G<sup>+</sup> in the total number of viable cells isolated from *H. pylori*-infected *Nod1*<sup>+/+</sup> and *Nod1*<sup>-/-</sup> mice were normalized to control animals on the same genetic background. Data are represented as means. Each data point represents an independent sample.

#### **4.3.3. *Nod1*<sup>-/-</sup> mice infected with *H. pylori* 245m3 exhibit significantly altered levels of pro-inflammatory chemokines in the stomach.**

Having observed differences in inflammation and gastric architecture in *Nod1*<sup>-/-</sup> mice with chronic *H. pylori* infection, we wished to ascertain if there were concurrent changes in NOD1-dependent pro-inflammatory cytokine production in these mice. Previous studies have demonstrated the ability of the NOD1 signaling pathway to trigger the secretion of murine IL-8 homologues, CXCL1/KC and CXCL2/MIP-2, in *H. pylori*-infected cells [35, 117, 212]. Furthermore, NOD1 stimulation has been shown to enhance the production of CCL2, the murine homologue of monocyte chemo-attractant protein 1 (MCP-1) [228]. Therefore, we analyzed gastric Cxcl1, Cxcl2 and Ccl2 responses by qPCR and ELISA in *H. pylori*-infected and control *Nod1*<sup>+/+</sup> and *Nod1*<sup>-/-</sup> mice. Interestingly, we observed a significant increase in relative gene expression and protein secretion of Cxcl1 (Fig. 4.6. A, D;  $p = 0.0397$  and  $p = 0.0228$ , respectively) in infected *Nod1*<sup>-/-</sup> animals. However, only a significant enhancement of relative Cxcl2 protein production was observed in these mice (Fig. 4.6. B, E;  $p = 0.0166$ ). In agreement with the histological results described earlier (Fig. 4.4), we observed a significant reduction in the relative gene expression of Ccl2 in *H. pylori*-infected *Nod1*<sup>-/-</sup> mice compared to infected *Nod1*<sup>+/+</sup> mice (Fig. 4.6. C, F;  $p = 0.0010$ ). Together, these data indicate that *Nod1*<sup>-/-</sup> mice infected with *H. pylori* for 8 weeks exhibit altered pro-inflammatory cytokine profiles in the stomach, when compared to *Nod1*<sup>+/+</sup> counterparts.

#### **4.3.4. Infection with *H. pylori* 245m3 generates a shift towards a Th-1/Th-17 inflammatory phenotype in *Nod1*<sup>-/-</sup> mice at 8 weeks post-infection.**

In addition to influencing innate immune signaling following *H. pylori* infection, NOD1 activation has also been implicated in the generation of adaptive T cell responses [139, 171]. Hence, we next investigated the cytokine profiles of splenocytes isolated from control and infected *Nod1*<sup>+/+</sup> or *Nod1*<sup>-/-</sup> mice at 8 weeks post-infection. Although splenocytes from *Nod1*<sup>+/+</sup> and *Nod1*<sup>-/-</sup> mice produced similar levels of the Th-2 cytokines, IL-4 and IL-10 (data not shown), splenocytes isolated from *Nod1*<sup>-/-</sup> mice produced significantly higher levels of the Th-1 cytokines, IFN- $\gamma$ , TNF $\alpha$  and IL-2, as compared with *Nod1*<sup>+/+</sup> splenocytes (Fig. 4.7. A-C;  $p = 0.0433$ ,  $p = 0.0159$  and  $p = 0.1255$ , respectively). Significant differences were also observed for the

Th-17-associated cytokine, IL-17 (Fig. 4.7. D,  $p = 0.0159$ ). Thus, our data indicate that during chronic infection with *H. pylori*, NOD1 regulates adaptive immune responses to dampen a pro-inflammatory TH-1 and IL-17 driven phenotype.

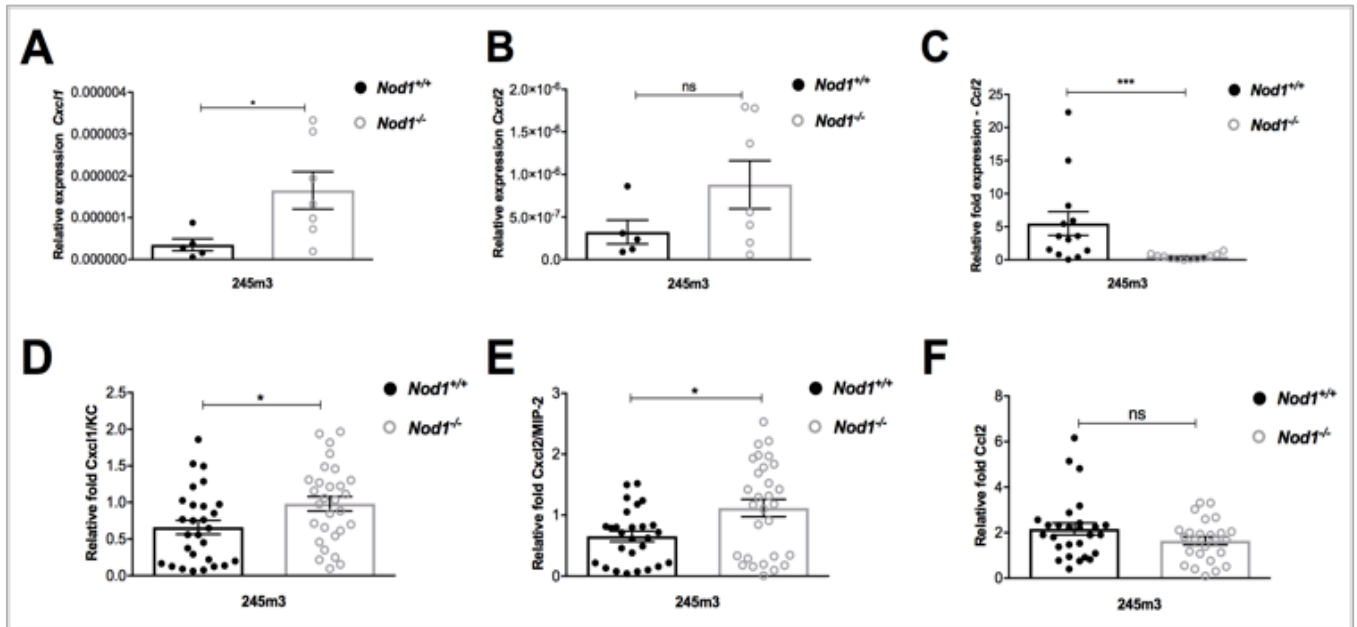


**Fig. 4.6. Stomachs from *Nod1*<sup>-/-</sup> mice infected with *H. pylori* 245m3 display a significantly altered pro-inflammatory chemokine profile at 8 weeks post infection.** *Nod1*<sup>+/+</sup> and *Nod1*<sup>-/-</sup> mice ( $n \geq 8$  per group) were gavaged with *H. pylori* 245m3 and sacrificed 8 weeks post-infection. (A, D) Cxcl1/KC, (B, E) Cxcl2/Mip2 and (C, F) Ccl2, gene expression and cytokine responses were determined from stomach homogenates of *Nod1*<sup>+/+</sup> and *Nod1*<sup>-/-</sup> mice and expressed relative to those of control animals. Figures show means  $\pm$  SEM. Data was pooled from a minimum of 2 independent experiments and was analyzed using a Mann Whitney test. \*  $p < 0.05$ , \*\*\*  $p < 0.001$ , 'ns'  $p > 0.05$ .

#### 4.3.5. *Nod1*<sup>-/-</sup> mice display increased numbers of TUNEL<sup>+</sup> apoptotic cells in the gastric mucosa following long-term *H. pylori* infection.

NOD1 was originally described as a mediator of apoptosis [153], but was reported to have either pro- or anti-apoptotic functions in different mouse tumor models [174-176]. Furthermore, *H. pylori* has been independently shown to affect cell survival pathways in the host to overcome the turnover of gastric epithelial cells and thus establish persistent infection [47]. We therefore sought to investigate a potential role for Nod1 in mediating apoptosis following chronic *H. pylori* infection. In order to visualize and quantify apoptotic cells in the murine stomach following infection, mice

were administered etoposide, an intrinsic apoptosis-inducer, 24 h prior to sacrifice [47]. Gastric tissue sections acquired from control and *H. pylori*-infected *Nod1*<sup>+/+</sup> and *Nod1*<sup>-/-</sup> mice were then examined using the TUNEL assay, to detect DNA fragmentation and cell death via apoptosis. The numbers of TUNEL<sup>+</sup> cells in the gastric tissues of *H. pylori*-infected mice were normalized to control animals. A significant increase in TUNEL<sup>+</sup> apoptotic gastric epithelial cells was observed in *Nod1*<sup>-/-</sup> mice infected with *H. pylori* 245m3 for 8 weeks (Fig. 4.8. A, B;  $p = 0.0158$ ), thereby suggesting that NOD1 may play an anti-apoptotic role during long-term *H. pylori* infection *in vivo*.

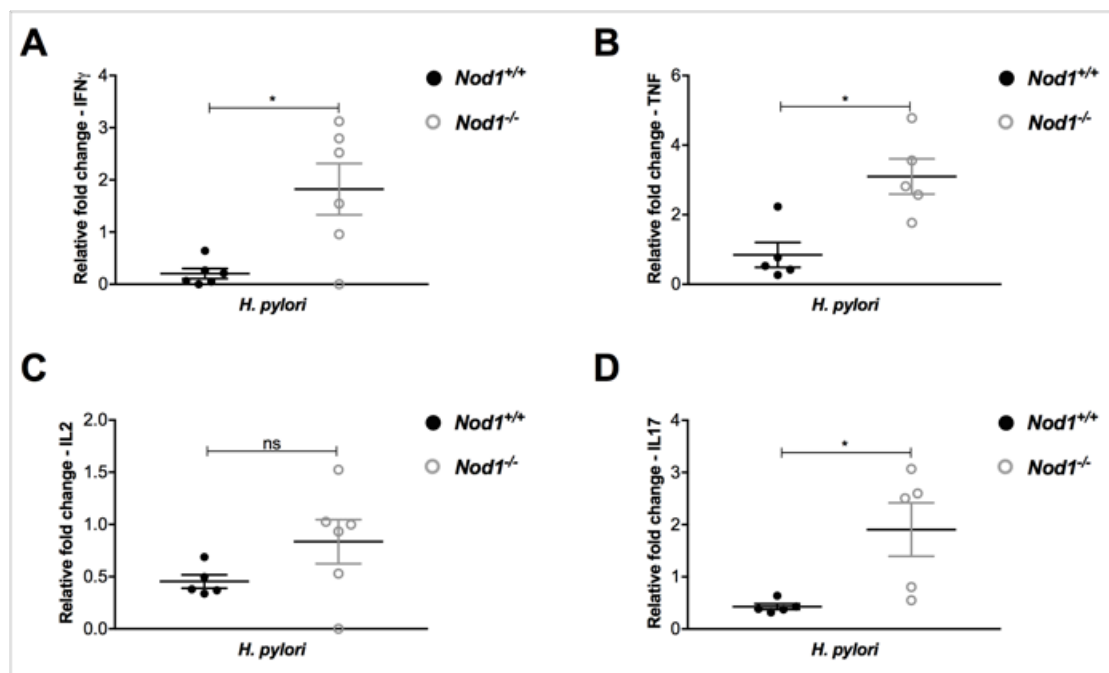


**Fig. 4.7. *H. pylori*-infected *Nod1*<sup>-/-</sup> mice display a Th1-dominant phenotype at 8 weeks post infection.** *Nod1*<sup>+/+</sup> and *Nod1*<sup>-/-</sup> mice (n=6 per group) were gavaged with *H. pylori* 245m3 and sacrificed 8 weeks post-infection. (A) IFN-g, (B) TNF, (C) IL-2 and (D) IL-17 cytokine production in the culture supernatants of ConA-stimulated splenic cells isolated from mice. Data are normalized to control animals and presented as the means  $\pm$  SEM. Data were analyzed using a Mann Whitney test. \*  $p < 0.05$ , 'ns'  $p > 0.05$ .

#### **4.3.6. NOD1 plays a novel role in regulating the gene expression of *Adcyap1r1*, a mediator of gastric acid secretion.**

Finally, in order to corroborate a role for NOD1 in mediating apoptosis, as well as identify the down-stream mediators of this novel function for this receptor during *H. pylori* infection, microarray analyses were performed on stomachs from *Nod1*<sup>+/+</sup> and *Nod1*<sup>-/-</sup> mice that had been infected with *H. pylori* 245m3 for 8 weeks. From this, 248 genes were identified as being differentially expressed and hence to be potentially NOD1-regulated (Fig. 4.9. A). Subsequent bioinformatics and power analyses revealed 10 target genes, whose expression levels were significantly altered in the stomachs of *Nod1*<sup>-/-</sup> mice when compared with those of *Nod1*<sup>+/+</sup> animals (Fig. 4.9. B). One of these genes was *Nod1* itself (Fig. 4.9. B). The differential gene expression of hits displaying greatest significance was validated using qPCR (Fig. 4.10. A-E). From this, we observed a significant down regulation of *Adcyap1r1* (also known as pituitary adenylate cyclase-activating polypeptide type 1 receptor, *Pac1*) (Fig. 4.10. D, *p* = 0.0314). No significant differences were observed for the other genes investigated (*Mid1*, *Erdr1*, *antiTgfb* and *Bpifb1*) (Fig. 4.10. A, B, C, E). Collectively, from this data we have identified a novel NOD1-regulated gene during chronic *H. pylori* infection.



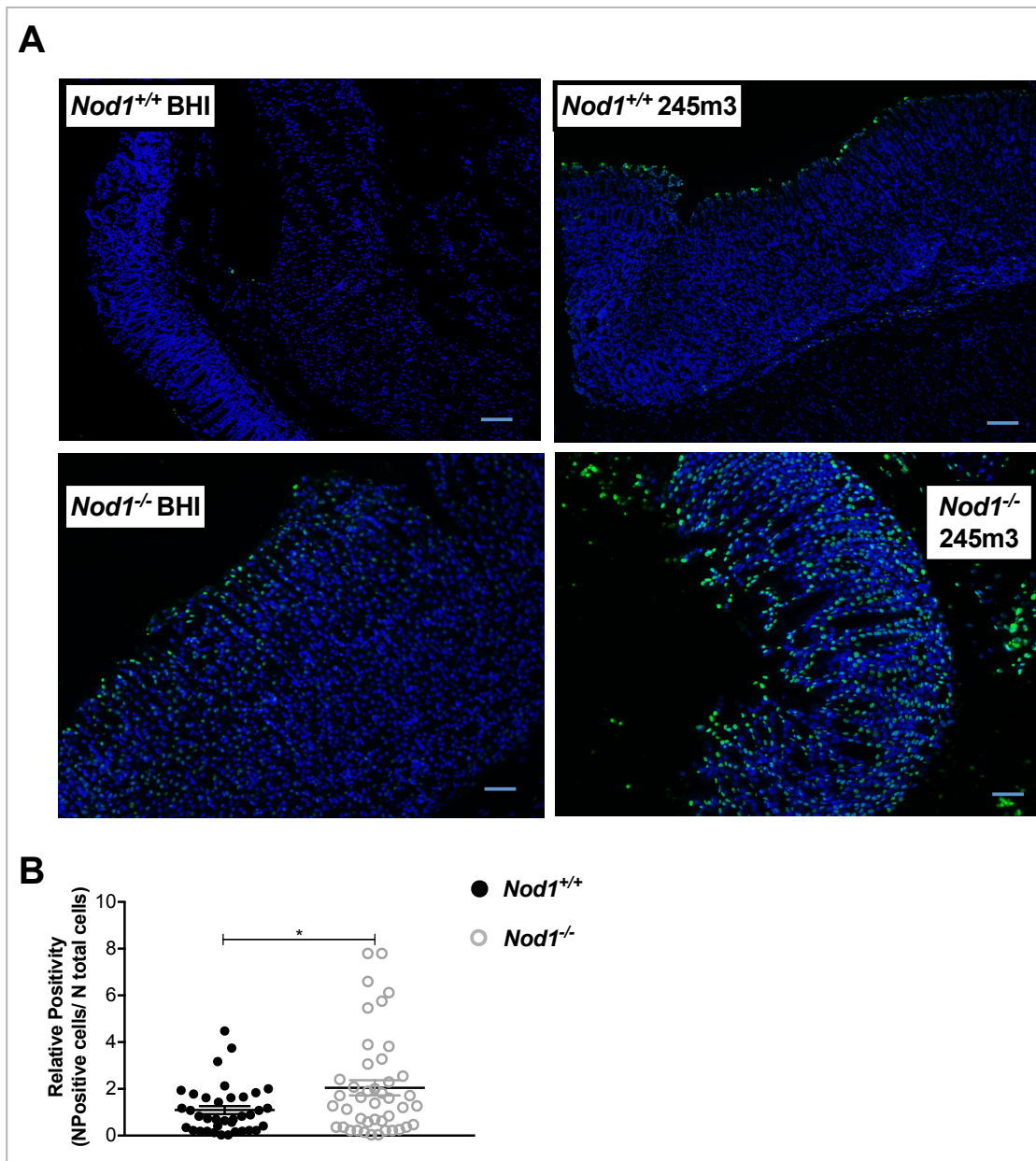


**Fig. 4.8. NOD1 dampens gastric apoptosis during long-term *H. pylori* infection *in vivo*.**

*Nod1*<sup>+/+</sup> (black spots) and *Nod1*<sup>-/-</sup> (clear spots) mice (n=5 per group for BHI infection, n=30 per group for *H. pylori* infection) were gavaged with BHI or *H. pylori* 245m3 and sacrificed 8 weeks post-infection. Twenty-four hours prior to sacrifice, mice were gavaged with etoposide, an apoptosis-inducer. Gastric tissue sections were stained using the Click-IT Plus TUNEL assay to determine apoptosis. Data are pooled from 3 independent experiments and are represented as the means ± SEM of “Relative Positivity” or (number of positive cells/number of total cells) in *H. pylori*-infected mice normalized to control animals. Each data point represents an individual mouse. Figure shows means ± SEM. Data were analyzed using a Mann Whitney test. \* *p* < 0.05.

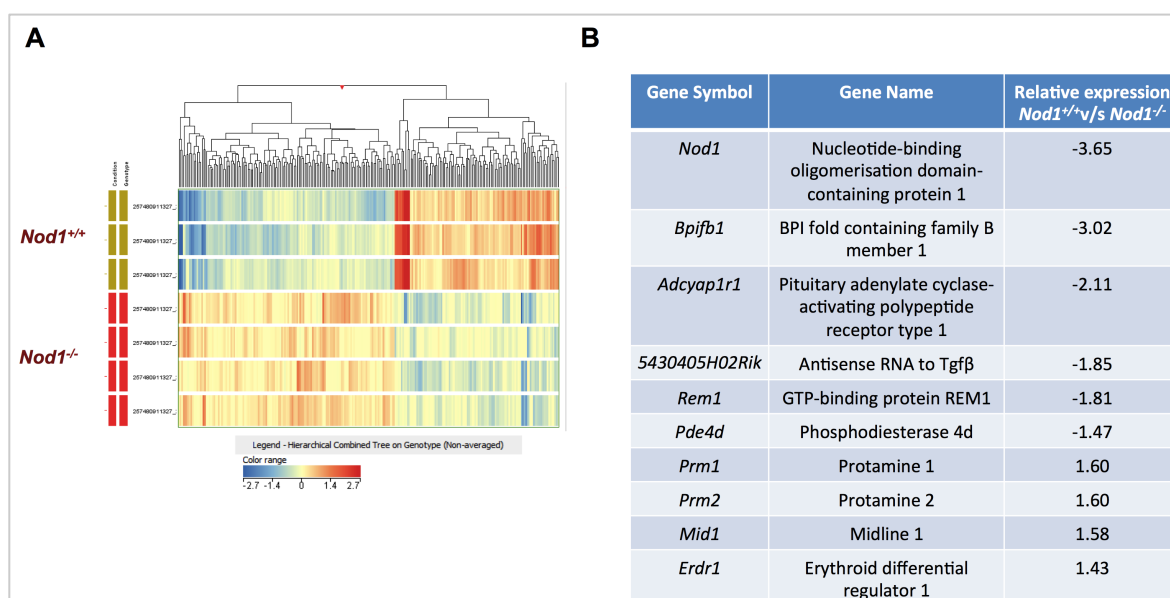


**Fig 4.9. *Nod1* regulates the expression of 248 genes *in vivo* in response to chronic *H. pylori* infection.** *Nod1<sup>+/+</sup>* and *Nod1<sup>-/-</sup>* mice (n=4 per group) were gavaged with *H. pylori* 245m3 and sacrificed 8 weeks post-infection. RNA was extracted from the gastric tissues of these mice. **(A)** Microarray analyses identified 248 genes to be differentially expressed between *Nod1<sup>+/+</sup>* and *Nod1<sup>-/-</sup>* infected mice. These genes are displayed as a cluster heat map, based on fold change. **(B)** The expression levels of 10 of these genes were statistically different between *Nod1<sup>+/+</sup>* and *Nod1<sup>-/-</sup>* mice. Data are pooled from n=4 biological replicates and analyzed using a Student's t test,  $p < 0.05$ , Fold change  $\geq 1.5$ , no multiple testing correction.

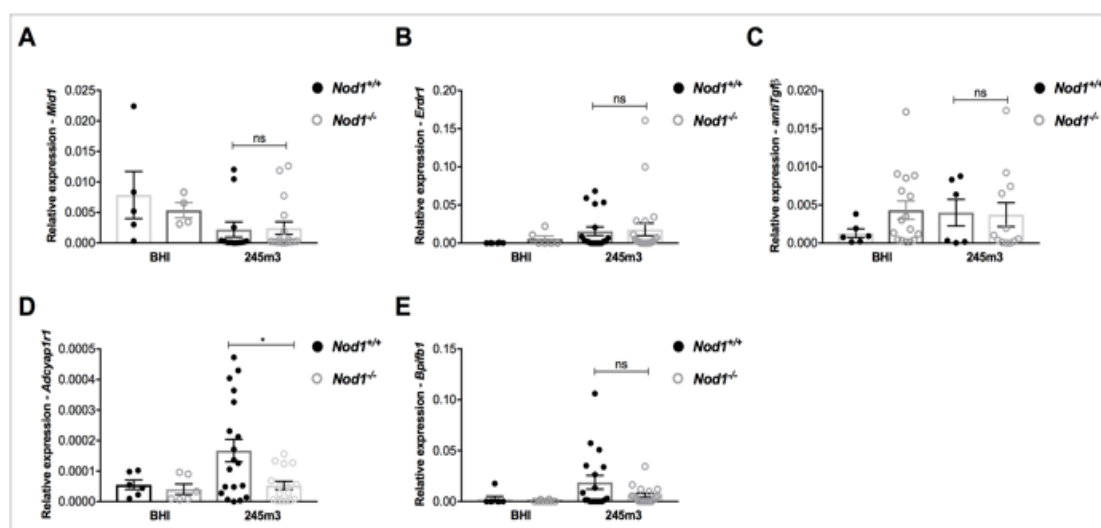


**Fig. 4. 10. *Adcyap1r1* expression is significantly reduced in *H. pylori*-infected *Nod1<sup>-/-</sup>* mice at 8 weeks post-infection.** Gene expression of **(A) *Mid1***, **(B) *Erdr1***, **(C) *antiTgfβ***, **(D) *Adcyap1r1*** and **(E) *Bpifb1*** was validated by qPCR in control (BHI) and *H. pylori*-infected mouse samples at 8 weeks post-infection (at least n $\geq$ 5 per group). Figures show means  $\pm$  SEM. Data are pooled from n=4 independent experiments and analyzed using the Mann Whitney U test. \*  $p < 0.05$ , 'ns'  $p > 0.05$ .

## 4.4. Discussion

The extracellular pathogen, *H. pylori*, is highly adapted to the human stomach and has developed various strategies to enable its chronic persistence in this site [187]. It has been shown that the innate immune receptor NOD1, which recognizes a conserved structure present in Gram-negative bacterial PG [61], has important host defense functions in several infection models, including those caused by *H. pylori* [35, 61, 230]. Activation of NOD1 signaling initiates a pro-inflammatory signaling cascade via the transcription regulator NF- $\kappa$ B, resulting in the production of the chemokine, CXCL8/IL-8 [35]. The majority of the published studies on NOD1 to date have focused on its role in immunity and inflammation during short-term *H. pylori* infection, thus providing firm evidence for the current dogma that NOD1 protects the host against infection by pathogens [35, 64, 65, 67, 219]. However, the findings detailed in Chapter 3 of this thesis indicate that an *H. pylori* strain, that was adapted to colonize mice in higher numbers, exhibited a modified muropeptide composition to potentially actively engage the NOD1 signaling pathway; thereby suggesting that NOD1 may also serve potentially beneficial functions for *H. pylori* during host colonization. In the present study, we have shown that while NOD1 sensing of *H. pylori* PG generates an initial inflammatory response in which the host controls infection, a secondary immune response is generated during chronic infection that potentially benefits persistence of the bacterium. Furthermore, our data suggest a novel role for the PG-NOD1 signaling axis in suppressing cell death via apoptosis in the host.

Although significantly higher bacterial loads were observed in *Nod1*<sup>-/-</sup> mice following infection with *H. pylori* 245m3 for 1-4 weeks (**Chapter 3**), reduced numbers of bacteria were recovered from these mice during chronic infection with the 245m3 strain (8 weeks post-infection) (**Figure 4.1**). Furthermore, the stomachs of these *Nod1*<sup>-/-</sup> mice exhibited extensive gastric mucosal thickening (**Figure 4.2. A, C**), yet surprisingly, also displayed decreased inflammation (**Figure 4.2. A, B**) and significantly impaired recruitment of CD45<sup>+</sup> leukocytes (**Figure 4.3, 4.5**) and F4/80<sup>+</sup> macrophages (**Figure 4.4, 4.5**) to the gastric mucosa, when compared with infected *Nod1*<sup>+/+</sup> counterparts. Interestingly, similar numbers of CD45<sup>+</sup> immune cells were

observed in the gastric sub-mucosa of *H. pylori*-infected *Nod1*<sup>-/-</sup> animals at 8 weeks post-infection, when compared with *Nod1*<sup>+/+</sup> animals (**Figure 4.3. C**). This observation suggests an impairment in the migration of immune cells from the gastric sub-mucosa to mucosal layer and requires further investigation to delineate the reasons or mechanisms resulting in this phenomenon. Future studies are also warranted to investigate the factors contributing to the gastric hyperplasia observed in *Nod1*<sup>-/-</sup> mice with chronic *H. pylori* infection, such as the gastric epithelium proliferation index, gastric pit length and numbers of parietal cells [231, 232]. Furthermore, as we were unable to identify all the individual cell types present in the pool of CD45<sup>+</sup> leukocytes isolated via flow cytometry analyses (**Figure 4.5.A**), it would be of interest to examine the relative proportions of other immune cells known to be recruited to the gastric sub-mucosa and mucosal layers following *H. pylori* infection, including B cells [233], mast cells [234] and dendritic cells [235].

In addition to the infiltration of immune cells to the gastric mucosa, the inflammation associated with *H. pylori* infection is also propagated via the up-regulation in the stomach of the pro-inflammatory cytokines IL-1, IL-6, IL-8, TNF and RANTES [236]. In our current study, we observed a significant increase in the expression and secretion of the functional murine homologues of CXCL8/IL-8, Cxcl1/KC and Cxcl2/Mip2, in gastric homogenates from *H. pylori*-infected *Nod1*<sup>-/-</sup> mice, when compared with *Nod1*<sup>+/+</sup> animals, at 8 weeks post-infection (**Figure 4.6. A-B, D-E**). Based on previous findings, these responses would be expected to accentuate the development of gastric inflammation and thus affect bacterial clearance [218, 237]. In the present study, although we observed lower overall inflammatory scores in *Nod1*<sup>-/-</sup> mice infected with *H. pylori* 245m3 for 8 weeks, we hypothesize that the increased production of pro-inflammatory cytokines is a result of the enhanced gastric hyperplasia described earlier [238]. Additionally, complementary to results obtained via immunohistochemical analyses described earlier (**Figure 4.4**), we observed a significant reduction in the production of the murine macrophage chemo-attractant protein, Ccl2 (**Figure 4.6. C, F**).

Importantly, these altered chemokine responses in gastric homogenates were associated with up-regulation of IFN- $\gamma$ , TNF, IL-2 and IL-17 production in splenic

lymphocytes in *Nod1*<sup>-/-</sup> mice infected with *H. pylori* 245m3 at 8 weeks post-infection (**Figure 4.7. A-D**). NOD1 is thus seen to regulate adaptive immune responses to dampen a pro-inflammatory Th-1 and Th-17 phenotype, which in turn could result in the increased bacterial colonization observed *in vivo* (**Figure 4.1**) [239]. Interestingly, this observation is in contrast to previously published data by Allison and colleagues [219] as well as Kaparakis *et al.* [55], which demonstrated a link between NOD1 activation and the generation of Th-1 responses following acute *H. pylori* infection. Furthermore, enhanced IL-17 secretion is also associated with a greater induction of pro-inflammatory cytokine production *in vivo*, thus validating our results observed in **Figure 4.6**. Taken together, the altered pro-inflammatory cytokine profile observed in the stomachs and splenic lymphocytes of *Nod1*<sup>-/-</sup> mice infected with *H. pylori* 245m3 for 8 weeks is complementary to the histopathological phenotype in the animals described earlier.

Aside from its regulatory role in pro-inflammatory signaling and inflammation, NOD1 was originally described as also regulating apoptotic functions [153, 220]. Indeed, we observed a significant increase in etoposide-induced apoptosis in the stomachs of *Nod1*<sup>-/-</sup> mice at 8 weeks post-infection with *H. pylori* 245m3 (**Figure 4.8. A-B**), thus suggesting that *H. pylori* can regulate host cell death/survival responses *in vivo* via a NOD1-dependent mechanism. However, the mechanistic details of this process remain to be elucidated. One mechanism by which *H. pylori* has previously been proposed to prevent apoptosis is via Epidermal growth factor receptor (EGFR) activation of the cyclooxygenase – 2 (COX-2) enzyme and its product, Prostaglandin E2 (PGE<sub>2</sub>) [177]. Furthermore, NOD1 activation has also been linked to the up-regulation of COX-2 expression and PGE<sub>2</sub> production [240, 241]. Interestingly, COX-2-dependent production of PGE<sub>2</sub> was shown to also dampen Th-1 responses resulting in increases in bacterial colonization *in vivo* [178]. In addition, increased PGE<sub>2</sub> signaling was shown to enhance production of CCL-2 and infiltration of macrophages to the gastric mucosa [242].

Additionally, we also observed a statistically significant down regulation of *Adcyap1r1/Pac1* in infected *Nod1*<sup>-/-</sup> animals at 8 weeks post-infection via microarray analyses and subsequent qPCR validation (**Figure 4.9-4.10**). Previous studies have shown PAC1 is an anti-apoptotic factor and is also essential for the maintenance of

homeostasis of gastric acid secretion [243-245]. Interestingly, it has also been shown that *H. pylori* inhibits gastric acid secretion to enable colonization and cause disease [246-248]. Therefore, it is tempting to speculate that *PAC1* may be a key NOD1-dependent factor required for the establishment of persistent *H. pylori* infection in the stomach. Nonetheless, future studies are warranted to further demonstrate the mechanism by which the PG-NOD1-PAC1 signaling axis stimulates apoptosis and/or generates a favorable niche for the establishment of chronic *H. pylori* infection. Overall, we have demonstrated a role for NOD1 in facilitating the establishment and persistence of *H. pylori* infection in the stomach. Our findings also suggest a novel anti-apoptotic role mediated by NOD1 signaling pathway during long-term *H. pylori* infection.

## **Chapter 5: Final Discussion and Future Directions**

*H. pylori* is a Gram-negative gastric pathogen that infects half of the world's population, commonly resulting in chronic persistence within the host [187]. This bacterium is also classified as a Type 1 carcinogen and is the leading cause of gastric cancer [11], a malignancy that is responsible for the second highest number of deaths due to cancer worldwide [249]. Interestingly, however, the mechanisms contributing to the chronic persistence of *H. pylori* as well as gastric carcinogenesis following infection remain ill-defined. It has been previously demonstrated that infection with virulent *H. pylori* strains harboring the *cagPAI* are more frequently associated with the initiation of gastric cancer [11, 250]. The *cagPAI* encodes approximately 30 genes required for the production of a T4SS, which in turn exploits cholesterol-rich lipid raft microdomains in GECs to facilitate the translocation of bacterial effector molecules, cytotoxin-associated gene A (CagA) and peptidoglycan (PG), into the host cell [33, 34, 36]. In addition to the T4SS, *H. pylori* can deliver factors such as PG, to epithelial cells in a *cagPAI*-independent manner via OMVs [55]. It has been shown that *H. pylori* interactions with host epithelial cells, involving either the T4SS or OMVs, result in activation of a pro-inflammatory signaling cascade mediated by the intracellular PRR, NOD1 [35, 55, 60]. NOD1 in turn activates the transcription factor, NF- $\kappa$ B, which ultimately results in the upregulation of pro-inflammatory genes and production of chemokines, such as IL-8 and type 1-interferons [35, 65, 66, 187]. Mucosal production of IL-8 in response to *H. pylori* infection is associated with greater tissue damage and an increased risk of severe disease [30, 49, 250].

Previous work in our laboratory established that cholesterol-rich domains, or lipid rafts, in the cell membranes of host epithelial cells are required for *H. pylori* delivery of PG to NOD1 [34, 55]. Furthermore, eukaryotic lipid rafts have been shown to be essential for *H. pylori* delivery of CagA and the vacuolating cytotoxin (VacA) into host epithelial cells, thus confirming an essential role for these microdomains in facilitating *H. pylori* interactions with the gastric mucosa [42]. Cholesterol is an indispensable constituent of the plasma membrane and is essential for the formation of lipid rafts in eukaryotic cells [99, 100]. Interestingly, 25% of the total lipids in the *H. pylori* cell wall are also derived from cholesterol, yet the bacterium lacks the genes

required for the *de novo* synthesis of this sterol [89, 92, 93]. Unsurprisingly, it was subsequently demonstrated that *H. pylori* associates with the lipid rafts of host epithelial cells and acquires cholesterol from these microdomains for incorporation into its own cell membrane [90]. However, the mechanism of accumulation of cholesterol within the bacterial cell membrane and furthermore, the potential role for this *H. pylori* membrane cholesterol in host-pathogen interactions had not been described. Furthermore, while the existence of cholesterol-enriched microdomains or lipid rafts had been described in several bacterial species, such as *B. subtilis* and *S. aureus* [108, 113], similar structures had not been investigated in pathogenic bacteria.

From the findings presented in Chapter 2 of this thesis, we have demonstrated the existence and characteristics of a novel flotillin-like protein, HP0248, in the human pathogen, *H. pylori*. In addition, we have provided convincing evidence for the presence of lipid raft-like structures in this bacterium and have shown a role for bacterial membrane cholesterol in the stabilization of these structures, as well as their incorporation of specific proteins important for bacterial virulence. These observations are consistent with an important property of eukaryotic membrane rafts to selectively include or exclude proteins that influence interactions at cell surfaces [102]. Interestingly, the study presented here has also demonstrated a role for the *H. pylori* flotillin-like protein, HP0248, in the induction of pro-inflammatory cytokine and chemokine responses in host epithelial cells. Additionally, we found that HP0248 was required for both the T4SS-dependent delivery of CagA to target cells and mouse colonization *in vivo*. However, the most striking finding is the association between the flotillin-like protein, HP0248, and the presence of cholesterol in the cell membrane of the bacterium, making this is the first example of a specific protein that may be involved in cholesterol acquisition/retention in *H. pylori*. Taken together, these data suggest that HP0248 and the associated membrane rafts serve as platforms for the organization of bacterial proteins that are critical for *H. pylori* pathogenesis. Future studies are warranted to determine if the flotillin-like protein, HP0248, is solely responsible for controlling integration of cholesterol into *H. pylori* membrane microdomains, or if the bacterium possesses additional flotillin-like proteins, as is common in other bacterial species, such as *B. subtilis* [115].



In addition to the role of cholesterol-enriched microdomains in direct interactions with host cells, bacteria release low molecular weight, soluble fragments of cell wall PG, known as muropeptides, which can trigger a broad range of pro-inflammatory and cytotoxic effects on mammalian host cells, thereby mediating tissue damage and organ morphogenesis *in vivo* [52-54]. As described earlier, bacterial muropeptides, consisting of the GlcNAc–MurNAc [70] disaccharide and oligopeptide chains of varying lengths, are recognized via the cytoplasmic innate immune sensor, NOD1 [35, 117]. This host defense protein specifically detects a minimal iE-DAP structure [156] present within muropeptides that are almost exclusively found in the cell walls of Gram-negative bacteria [61]. Interestingly, human and murine NOD1 have further evolved to sense slightly differently forms of muropeptides that differ solely in the lengths of their oligopeptide side chains, namely tri-peptide (GM-Tri<sub>DAP</sub>) and tetra-peptide (GM-Tetra<sub>DAP</sub>) stem structures, respectively [155, 159]. This difference in host-specificity of the NOD1 signaling pathway allowed us to investigate the ability of *H. pylori* bacteria to alter its PG composition during host adaptation. In Chapter 3, we demonstrated that mouse-adapted *H. pylori* bacteria are able to modify their cell wall PG composition to enable preferential detection by the murine Nod1 protein. We found that the mouse-adapted variant of an *H. pylori* clinical isolate, 245m3, displayed a functional T4SS, but interestingly also exhibited an increased proportion of GM-Tetra<sub>DAP</sub>, the murine Nod1 agonist. Consistent with this finding, the mouse-adapted strain, 245m3, induced strong pro-inflammatory responses in mouse epithelial cells, but was significantly affected in its ability to induce NOD1-dependent responses in human cell lines. These primary data suggest that bacterial pathogens may be able to tailor their PG composition to specifically target NOD1 detection by the host. It is tempting to further speculate a potential role for the NOD1 signaling pathway in favoring bacterial replication and survival *in vivo*. Interestingly, in the present study we also observed a strain-specificity in cell wall modification, wherein the mouse-adapted variants, 245m3 and SS1, displayed increased proportions of the murine Nod1 agonist; whereas an additional mouse-adapted bacterial strain, 256m2, showed no difference in PG composition when compared to its progenitor human clinical isolate. Therefore, further analysis of the cell wall PG composition from other pairs of human and host-adapted *H. pylori* strains, such as B128 and B128 7.13 [251], G27 and NSH57 [161], PMSS2000 and SS2000 [252], are required to investigate the frequency of PG modifications and confirm our aforementioned hypothesis.

Importantly, comparative genomic analyses of *H. pylori* 245 and its mouse-adapted 245m3 variant allowed us to identify a predicted premature protein truncation in MltD. *H. pylori* MltD, also referred to as regulatory protein DniR, is encoded by the *HP1572* gene and is a known PG-cleaving enzyme exhibiting muramidase-like activity [72]. Further investigation is warranted to determine if MltD is indeed absent and hence directly responsible for the change in GM-Tetra<sub>DAP</sub>-GM-Tri<sub>DAP</sub> ratios as well as the subsequent effects of *H. pylori* 245m3 on NOD1-dependent cytokine responses in murine versus human non-phagocytic cells. Given that MltD and another PG-cleaving enzyme, Slt, have non-redundant and strain-dependent functions in PG cleavage [72], it will be crucial to demonstrate if these or indeed, other related PG-cleaving enzymes mediate cell wall modifications in other host-adapted *H. pylori* isolates. Interestingly, *H. pylori*  $\Delta$ *slt* mutant bacteria have previously been shown to have a reduced capacity to induce pro-inflammatory signaling due to an impaired release of NOD1-activating ligands [35, 253, 254]. Other relevant examples of PG modification enzymes in *H. pylori* include the cell shape-determining proteins, Csd6 and Csd4, which constitute L, D-carboxypeptidase enzymes that were recently found to play key roles in mediating cross-linking and trimming of PG muropeptides, thereby regulating the levels of GM-Tri<sub>DAP</sub> in the cell wall [69, 255-257]. It is therefore of interest to further investigate the presence of potential morphological differences between *H. pylori* 245 and 245m3 strains. Importantly, PG modification enzymes in *Campylobacter jejuni*, a close relative of *H. pylori*, were also shown to influence bacterial morphology, PG biosynthesis, pathogenesis, NOD1 activation and subsequent inflammatory responses in the host [258-260].

The absence of complete abrogation of cytokine responses in NOD1-deficient cell lines following infection with *H. pylori* 245m3 (Chapter 3) suggests that other bacterial changes may have an effect on host cell responses and/or other host immune pathways involved in detection of Gram-negative bacteria. A proposed alternate innate immune sensor of *H. pylori* infection is tumor necrosis factor receptor-associated factor (TRAF)-interacting protein with forkhead-associated domain (TIFA) [261]. TIFA has been shown to be activated by the cytosolic presence of the bacterial heptose-1,7-bisphosphate (HBP), a metabolic intermediate in LPS biosynthesis [262-266]. Interestingly, it was recently described that T4SS-dependent TIFA activation precedes the NOD1 response during acute *H. pylori* infection [261]. In contrast,

Gaudet and colleagues demonstrated the primary activation of NOD1 followed by TIFA in response to invasive *S. flexneri* infection [264]. Nevertheless, there is currently no experimental evidence to support this sequential activation of NOD1 and TIFA during *H. pylori* infection. Future studies are therefore required to delineate the relative roles of NOD1 and TIFA in mediating host inflammatory responses during *H. pylori* infection.

Finally, since NOD1 has been shown to play key roles in immune surveillance and generation of host responses primarily during acute bacterial infection, we sought to investigate the functions of the NOD1 pathway during chronic *H. pylori* infection (Chapter 4). We found that *Nod1*<sup>-/-</sup> mice had reduced *H. pylori* bacterial loads when compared with their *Nod1*<sup>+/+</sup> counterparts at 8 weeks post-infection, which is in contrast to the established role for NOD1 in host defense. These *Nod1*<sup>-/-</sup> mice also displayed significantly increased gastric chemokine and splenocyte T cell cytokine responses, yet surprisingly had decreased inflammation scores and gastric immune cell infiltration when compared with wild type animals. NOD1 therefore appears to be essential for the maintenance of the gastric niche required for *H. pylori* persistence and the subsequent disease phenotype associated with chronic infection. Interestingly, a significant increase in apoptotic cells was also observed in the stomachs of *H. pylori*-infected *Nod1*<sup>-/-</sup> mice, thereby suggesting a role for NOD1 in suppressing cell death *in vivo*. Taken together, we propose that NOD1 is an important factor in facilitating the persistence of *H. pylori* infection in the stomach. However, the mechanistic details of NOD1-dependent apoptosis following chronic *H. pylori* infection remain to be elucidated. One mechanism by which *H. pylori* has previously been proposed to prevent apoptosis is via EGFR activation of the cyclooxygenase-2 (COX-2) enzyme and its product, Prostaglandin E2 (PGE<sub>2</sub>) [177]. Interestingly, NOD1 activation has been linked to the up-regulation of COX-2 expression and PGE<sub>2</sub> production [240, 241]. Furthermore, recent data suggest that the caspase-3/E-cadherin pathway is also involved in the induction of apoptosis of gastric epithelial cells in response to *H. pylori* [70], hence making it an alternate downstream mediator of NOD1-driven cell survival responses that warrants further experimentation.

Microarray analyses of the gastric mucosa from *Nod1*<sup>+/+</sup> and *Nod1*<sup>-/-</sup> animals revealed a statistically significant down regulation of *Adcyap1r1/Pac1* in *Nod1*<sup>-/-</sup> animals at 8

weeks post-infection (Chapter 4). PAC1 is widely expressed in the gastrointestinal tract and displays specific affinity for Pituitary adenylate cyclase-activating polypeptide (PACAP) [267, 268]. Furthermore, PAC1 has been observed to suppress apoptosis *in vitro* and *in vivo*, as well as to play an essential role in the maintenance of homeostasis of gastric acid secretion [243-245]. Pac1-deficient mice displayed higher basal gastric acid output, increased gastric mucosa thickness and glands height, when compared to wild-type mice [243]. Interestingly, it has been shown that *H. pylori* can inhibit gastric acid secretion to enable colonization and cause disease [246-248]. As gastric acid reduces susceptibility to infection with ingested bacterial pathogens [269], it is tempting to speculate that NOD1-dependent regulation of PAC1 may be a determinant of *H. pylori* colonization. The corollary of this suggestion is that the reduced levels of *Pac1* expression in *Nod1*<sup>-/-</sup> mice may result in increased gastric acidity, thus contributing to the reduced levels of *H. pylori* infection that were observed in the stomachs of these animals. However, preliminary experiments in which we measured the gastric pH of the gastric contents from wild-type and *Nod1* knock-out mice infected with *H. pylori* for 8 weeks, showed no statistically significant differences (data not shown).

A significant limitation of the aforementioned data is the absence of complementary evidence in human samples due to the exclusive use of *in vitro* cell lines and mouse models of *H. pylori* infection to study host-pathogen interactions. Our conclusions describing the novel functions of the *H. pylori*-NOD1 signaling axis could be enhanced and supported by the inclusion of additional experiments using gastric biopsies from human patients or alternatively via the use of human gastric organoids. Gastric organoids refer to three-dimensional culture systems that are grown from gastric stem cells and are organized epithelial structures that comprise all the differentiated cell types of the stomach (Bartfeld, 2015 #360). They can be expanded indefinitely and have been shown to be highly instrumental in revealing new insights into the pathogenesis of *H. pylori* infection as well as the resulting immune responses and histopathological changes associated with disease (Bartfeld, 2015 #362)(Schlaermann, 2016 #364)(Hill, 2017 #361).

In addition to regulating NF- $\kappa$ B signaling and IL-8 secretion in host epithelial cells, the NOD1 pathway was shown to enhance IL-1 $\beta$  production in *Chlamydia*

*trachomatis*-infected trophoblasts [270]. Furthermore, *H. pylori* bacteria have been shown to induce IL-1 $\beta$  and IL-18 responses in epithelial cells and macrophages [148, 271-273]. Interestingly, cholesterol crystals have also been shown to act as danger signals *in vitro*, thereby inducing the production of the aforementioned pro-inflammatory cytokines in phagocytes [274]. A study by Rajamaki *et al* also confirmed that cholesterol crystals present in atherosclerotic lesions induced IL-1 $\beta$  secretion from macrophages in a caspase-1-dependent manner [275]. There have been several reports that NOD1 may be able to interact with caspase-1 [153, 220, 222], however, the findings of those studies were inconclusive and need to be substantiated by further work. It therefore remains to be determined whether the *H. pylori*-NOD1 signaling axis constitutes a novel inflammasome-like pathway and/or represents a potential link between the generation of host immune responses by epithelial and/or phagocytic cells.

Dysregulation of NOD1 functions has been linked to the progression of several inflammatory and auto-inflammatory diseases [276, 277]. For example, insertion-deletion polymorphisms in *NOD1* have been correlated with an increased susceptibility to the development of asthma and inflammatory bowel disease [278, 279]. Controversially, hematopoietic NOD1 has been identified to enhance a high-fat diet-induced metabolic inflammation and insulin intolerance, commonly associated with the onset of Type 2 diabetes [280, 281]. Recent reports also suggest a role for NOD1 in the generation of an infection-induced cytokine storm in pregnant mothers, which results in fetal inflammation and premature births [282]. Overall, these data suggest that NOD1 displays many functions beyond mediating pro-inflammatory signaling, including the maintenance of immune homeostasis, and thus warrant further investigation.

In conclusion, we have demonstrated that the presence of bacterial membrane cholesterol and lipid raft-like domains appears to be important for host immune modulation and ultimately survival of *H. pylori* within the stomach, thus complementing earlier studies in this field [90, 283]. We have also provided evidence for the first time that *H. pylori* is able to modulate its PG composition during host-adaptation to actively engage the NOD1 signaling pathway. Finally, we have shown that NOD1 sensing of *H. pylori* PG generates an initial inflammatory response in

which the host controls infection during the acute phase, and a secondary response in which epithelial cell apoptosis is prevented thus potentially facilitating bacterial persistence. Taken together, these data describe novel mechanisms by which Gram-negative pathogens utilize interactions with host epithelial cells to enable chronic persistence in the host, as well as suggest broader implications for the NOD1 signaling pathway during *H. pylori* infection. The fundamental new information presented here may thus inform the design of novel, improved therapies that target *H. pylori* cell wall structures to eradicate the bacterium or reduce the inflammation associated with this infection.

## Appendix 1

### Mouse Models of *Helicobacter* Infection and Gastric Pathologies

Kimberley D'Costa<sup>1</sup>, Michelle Chonwerawong<sup>1</sup>, Le Son Tran<sup>1</sup>, Richard L. Ferrero<sup>1,2</sup>

<sup>1</sup> Centre for Innate Immunity and Infectious Diseases, Hudson Institute of Medical Research, Melbourne, Australia

<sup>2</sup> Infection and Immunity Program, Monash Biomedicine Discovery Institute and Department of Microbiology, Monash University, Melbourne, Australia

Corresponding Author:

A/Prof. Richard L. Ferrero

Email address: [REDACTED]  
[REDACTED]

Email Addresses of Co-Authors:

Kimberley D'Costa: [REDACTED]

Michelle Chonwerawong: [REDACTED]

Le Son Tran: [REDACTED]

**KEYWORDS:** *Helicobacter pylori*, *Helicobacter felis*, mouse model, MALT lymphoma, inflammation

#### **SHORT ABSTRACT:**

Mice represent an invaluable *in vivo* model to study infection and diseases caused by gastrointestinal microorganisms. Here, we describe the methods used to study bacterial colonisation and histopathological changes in mouse models of *Helicobacter pylori*-related disease.

#### **LONG ABSTRACT:**

*Helicobacter pylori* is a gastric pathogen that is present in half of the global population and is a significant cause of morbidity and mortality in humans. Several mouse models of gastric *Helicobacter* infection have been developed to study the molecular and cellular mechanisms whereby *H. pylori* bacteria colonise the stomach of human hosts and cause disease. Herein, we describe protocols to: 1) prepare bacterial suspensions for the *in vivo* infection of mice via intragastric gavage; 2) determine bacterial colonisation levels in mouse gastric tissues, by polymerase chain reaction and viable counting; and 3) assess pathological changes, by histology. To establish *Helicobacter* infection in mice, specific pathogen-free (SPF) animals are first inoculated with suspensions (containing  $\geq 10^5$  colony-forming units, CFUs) of mouse-colonising strains of either *Helicobacter pylori* or other gastric *Helicobacter* spp. from animals, such as *Helicobacter felis*. At the appropriate time-points post-infection, stomachs are excised and dissected sagittally into two equal tissue fragments, each comprising the antrum and body regions. One of these fragments is then used for either viable counting or DNA extraction, while the other is subjected to histological processing. Bacterial colonisation and histopathological

changes in the stomach may be assessed routinely in gastric tissue sections stained with Warthin-Starry, Giemsa or Haematoxylin and Eosin (H&E) stains, as appropriate. Additional immunological analyses may also be undertaken by immunohistochemistry or immunofluorescence on mouse gastric tissue sections. The protocols described below are specifically designed to enable the assessment in the mice of gastric pathologies resembling those in human-related *H. pylori* disease, including inflammation, gland atrophy and lymphoid follicle formation. The inoculum preparation and intragastric gavage protocols may also be adapted to study the pathogenesis of other enteric human pathogens that colonise mice, such as *Salmonella* Typhimurium or *Citrobacter rodentium*.

## INTRODUCTION:

*Helicobacter pylori* is a spiral-shaped, gram-negative, human gastric pathogen present in all populations across the world, with infection rates in developing countries estimated to be in the order of 80%<sup>1</sup>. Although most *H. pylori*-infected individuals are asymptomatic, some develop more severe disease, ranging from peptic ulceration to gastric cancer<sup>2</sup>. *H. pylori*-associated cancers are broadly characterised either by malignant changes in epithelial cells (GECs) or by the formation of extra-nodal lymphoid tissues in the stomach, resulting in gastric adenocarcinoma or mucosa-associated lymphoid tissue (MALT) lymphoma, respectively. *H. pylori* is highly adapted to survive in the harsh ecological niche of the stomach due to the presence of various virulence factors and mechanisms facilitating its adherence, growth and metabolism in this niche. In particular, virulent strains of *H. pylori* possess the 40 kb *cag* Pathogenicity Island (*cagPAI*) that encodes 30 genes required for the production of a Type 4 secretion system (T4SS)<sup>3</sup>. *cagPAI*-positive *H. pylori* strains are associated with the induction of higher levels of chronic inflammation in the host, which interestingly has been implicated as an essential precursor of gastric adenocarcinoma<sup>4</sup>.

*In vivo* animal models, particularly mice, have been highly informative by allowing researchers to investigate the relative contributions of host, bacterial and environmental factors on *H. pylori* infection and disease outcome<sup>5</sup>. Studies have previously demonstrated that *prolonged H. pylori* infection of mice on the C57BL/6 genetic background results in the development of chronic gastritis and gland atrophy, both hallmarks of *H. pylori* infection<sup>6</sup>. Furthermore, infection with the related feline/canine bacterial species, *Helicobacter felis*, has been shown to induce MALT formation in mice with similar pathology and disease progression as seen in human MALT lymphoma<sup>7,8</sup>. The most commonly used *H. pylori* isolate in mouse colonisation studies is the "Sydney Strain 1" (SS1) strain, which is *cagPAI*<sup>+</sup> but has a non-functional T4SS (T4SS<sup>-</sup>)<sup>9,10</sup>. Other widely used strains include *H. pylori* B128 (*cagPAI*<sup>+</sup>/T4SS<sup>+</sup>)<sup>11</sup> and X47-2AL (*cagPAI*<sup>-</sup>/T4SS<sup>-</sup>)<sup>10,12</sup>. For *H. felis* infections, the strain CS1 ("Cat Spiral 1", *cagPAI*<sup>-</sup>/T4SS<sup>-</sup>) is generally used<sup>13,14</sup>.

Herein, we provide a video protocol describing the preparation of *Helicobacter* inocula for *in vivo* infection, the procedure for intragastric gavage of mice, as well as methods for the processing of tissues for the study of histopathological changes in the stomach. In particular,



this article will focus on the histological methods used to visualise bacterial colonisation and assess histopathological changes, including MALT formation, in the gastric mucosa of infected mice. Some of the methods described here may be adapted to the study of other gut pathogens such as *Salmonella Typhimurium* or *Citrobacter rodentium*.

## PROTOCOL:

### 1. Growth and Preparation of Bacterial Inocula

1. Thaw glycerol stocks of *H. pylori* or *H. felis*<sup>16</sup> from -80 °C and subculture on horse blood agar (HBA) plates comprising: Blood Agar Base No.2; a modified "Skirrow's antibiotic selective supplement" (consisting of vancomycin, 10 µg/ml; polymyxin B, 25 ng/ml; trimethoprim, 5 µg/ml; amphotericin B, 2.5 µg/ml); and 5-10% (v/v) horse blood<sup>15-17</sup>. The bacteria grow well under microaerobic conditions in Oxoid 2.5 or 3.5 L anaerobic jars containing the appropriate CampyGen sachets, at 37 °C.

Note: *H. pylori* strains grown under these conditions must be subcultured after 1-1.5 days' incubation, whereas for *H. felis*, at least 2 days' incubation is generally required. Suitable culture and storage media have been described in detail previously<sup>16</sup>.

2. Prepare bacterial inocula for mouse infection from early-to-mid logarithmic phase cultures. Harvest bacteria gently from agar plates by flooding each plate with 1-2 ml brain heart infusion (BHI) broth and aspirating suspensions with Pasteur pipettes. Inocula can also be prepared from *Helicobacter* bacteria that have been propagated in BHI broth for 16-18 h<sup>16</sup>. In this case, collect bacteria by low speed centrifugation.
3. Assess the viability and motility of the bacteria by examining wet mount preparations under phase contrast microscopy (100 X magnification).

Note: Only use *H. pylori* inocula if the majority of bacteria have a bacillary or spiral shape (the morphology can vary depending on the strain). *H. felis* inocula should primarily contain helical-shaped bacteria. Do not use inocula if a preponderance of the bacteria present have a coccoid morphology, as these forms are not viable and will not establish an infection in mice.

4. Estimate the number of bacteria in the inocula by counting under phase contrast microscopy the approximate number of bacteria per field (100 X magnification) and by using the following guide:  
1 bacterium per field = approximately  $10^6$  colony forming units (CFU) of *Helicobacter*/ml; 10 bacteria per field = approximately  $10^7$  CFU/ml; 100 bacteria per field = approximately  $10^8$  CFU/ml etc.
5. Adjust the bacterial cell density of inocula to approximately  $10^7$ - $10^8$  CFU/ml by dilution in BHI broth, if necessary.

Note: To ensure maximal bacterial viability, use inocula for intragastric gavage as soon as possible after preparation. Always confirm *H. pylori* cell density and viability by performing viable counting of inocula immediately after the gavage procedure (see below). This is not always possible for *H. felis* as it does not usually form

isolated colonies on culture media. The numbers of viable *Helicobacters* in inocula cannot be determined by optical density measurement ( $A_{600}$ ) as this method does not discriminate between viable (*i. e.* bacillary/spiral/helical) and non-viable (*i. e.* coccoid) bacteria.

## 2. Intragastric Gavage of Mice with *Helicobacter*

Note: This method of intragastric gavage can be applied to other bacterial species that colonise the gut *e. g.* *Salmonella Typhimurium*, *Citrobacter rodentium*, *Listeria monocytogenes*.

1. Use 6-8 week old, specific pathogen-free (SPF) and *Helicobacter*-free male or female mice. Animals on a C57BL/6 genetic background are typically used for infection experiments with *H. pylori* or *H. felis*. In the present study, we have used wild-type (WT) and genetically modified C57BL/6 mice lacking a key innate immune receptor (termed knock-out or KO animals).

Note: Mice on other genetic backgrounds can also be used for *Helicobacter* infections, however, colonisation levels and disease severity may be impacted by the type of host background<sup>18,19</sup>.

2. Aspirate the bacterial inocula (Step 1.5) into disposable 1 ml syringes and replace the supplied needles with 23 gauge needles onto which are affixed disposable polyethylene catheters (length, 6-8 cm; internal diameter, 0.58 mm). Catheters are fastened to the needles by the application of small strips of Parafilm M® film. Alternatively, the needle/catheter assembly can be replaced by using sterile plastic feeding tubes (20 gauge x 38 mm).
3. Physically restrain mice by a firm grip at the scruff of the neck and tail.  
Note: This procedure can be performed without anaesthesia, or alternatively, with the use of an inhaled anaesthetic, such as methoxyflurane or isoflurane<sup>16</sup>.
4. Insert catheter into the centre of the open jaw and guide in a caudal direction towards the oesophagus. Extend the neck of the mouse to allow ease of access to the stomach through the oesophagus (and away from the trachea) until most or all of the catheter is no longer visible and a resistance is felt, corresponding to the base of the stomach. Deliver a specific aliquot, usually 100 µl per inoculation (Figure 1).

Note: Mice should be gavaged with  $\geq 10^5$  CFU to ensure optimal colonisation and disease pathology.

5. House mice in an SPF animal facility for the duration of the experiment.  
Note: Severe pathology and adenocarcinoma in WT C57BL/6 mice is only observed at approximately 24 months' post-infection<sup>20</sup>. However, this effect may be accelerated in some genetically modified animals, or in mice with other genetic backgrounds.
6. Upon completion of the gavage procedure, perform a modification of the Miles and Misra technique to determine the numbers of viable *H. pylori* bacteria administered

to mice. For this, inocula are serially diluted (from  $10^{-1}$ - $10^{-5}$ ) in BHI using the method described in detail previously<sup>16</sup>.

Note: HBA plates should be warmed and dried in a sterile fume hood or 37°C incubator for 10-15 mins prior to use.

### 3. Harvesting Tissues from Mice Post-Experiment

1. Euthanize mice by either carbon-dioxide inhalation or cervical dislocation, according to the relevant ethics committee for animal experimentation.
2. Open the abdominal cavity and excise stomachs using fine, curved scissors.  
Note: Sera can also be collected by cardiac puncture to aid in the investigation of systemic responses to *Helicobacter* infection. Additionally, the collection of spleens and paragastric lymph nodes are useful in studying adaptive immune responses.
3. Cut stomachs along the greater curvature and remove residual waste either by scraping with a scalpel or by washing in sterile phosphate buffered saline (PBS).
4. Wash stomachs again in sterile PBS and then record the wet weight using tared 6 cm plastic petri dishes.
5. Flatten stomachs and dissect sagittally into two equal tissue fragments, each comprising the antrum, body and non-glandular forestomach regions (Figure 2). The non-glandular region is removed and one half of each stomach weighed before adding to either 1 ml sterile BHI (for viable counting) or snap freezing in liquid nitrogen (for DNA extraction).  
Note: Eppendorf tubes containing tissue in BHI must be stored on ice until they are ready to be processed. Snap frozen stomach tissues can also be used to extract RNA or proteins for qPCR (quantitative PCR) or Western blotting analyses, respectively.
6. Add the other stomach halves to 15 ml Falcon tubes containing 10% formalin. Immerse tissues in 10% formalin for 10 sec and then flatten to the top side of tubes. Allow tissues to fix before re-immersing in 10% formalin solution for a minimum of 24 h.  
Note: Tissues can remain in 10% formalin for many weeks prior to processing for histology. Prolonged storage of tissue may, however, affect its architecture and/or antigenicity resulting in sub-optimal results in downstream analyses.

### 4. Confirmation of Bacterial Colonisation in the Stomach Post-Infection

1. Viable Counting of *H. pylori* in the Stomach.
  1. Sterile HBA plates are supplemented with additional antibiotics (200 µg/ml bacitracin and 10 µg/ml naladixic acid) prior to performing colony counts from infected mouse stomachs<sup>15</sup>.
  2. Homogenize stomach sections either manually, using autoclavable polypropylene micropestles, or using a mechanical dissociation instrument *e. g.* gentleMACs Dissociator™.



3. Prepare duplicate serial dilutions ( $10^{-1}$ - $10^{-2}$ ) of the resulting gastric homogenates in sterile BHI.  
Note: Dilutions should be decided based on the typical bacterial loads obtained for a given *H. pylori* strain used for infection, as well as the duration of infection. Undiluted samples can also be used.
  4. Divide pre-dried HBA plates (see Note 2.6 above) into three or four segments. Using an adaptation of the Miles and Misra technique, add 10-100  $\mu$ l of each dilution onto a segment of the agar plate and spread using sterile plastic loops<sup>16</sup>.
  5. Allow the plates to dry and then place them in an inverted position (lid side down) in anaerobe gas jars. To maintain humidity in the jars, include a Petri dish containing water.
  6. Incubate jars at 37 °C until colonies form (typically 4–7 days).
  7. Enumerate segment(s) containing between 10 and 100 isolated colonies.
  8. Calculate the bacterial loads as (CFU/g of tissue), using the following formula:  
[(Average number of colonies counted)  $\times$  (dilution factor)  $\times$  (volume plated)]/(stomach weight).
2. Detection of *H. felis* Infection in Gastric Tissues by the Polymerase Chain Reaction (PCR).
1. Extract DNA from mouse stomachs using standard DNA isolation protocols, or a commercially available kit.
  2. Determine the DNA concentration of samples using the Qubit™ fluorometric quantitation technique.
  3. Set up PCR reactions targeting a 342-base pairs (bp) fragment of the *H. felis* urease B gene (*ureB*). Each reaction should contain: 100 ng of genomic DNA; 1  $\mu$ M each of forward (5'-AAA ATC CAC GAA GAC TGG GG-3') and reverse (5'-CTT TTA TCC AAG TGG TGG CAC ACC-3') primers; 200  $\mu$ M dNTPs; 0.5 unit Taq Polymerase and the appropriate amounts of buffer and nuclease-free water.  
Note: This oligonucleotide pair has been designed to recognise and bind to homologous sequences in both *H. pylori* and *H. felis ureB* genes but when subjected to the PCR conditions below, not those present in the *ureB* genes of enterohepatic *Helicobacter* spp.
  4. Perform PCR amplification using the following thermal profile: heating at 94°C for 5 min, followed by 35 cycles of 94°C for 30 sec, 61°C for 30 sec and 72°C for 1 min, before holding at 20°C.
  5. Run PCR products on a 2% agarose gel for 30 min at 100 V.

## 5. Histological analyses of *Helicobacter*-infected mouse stomach sections.

1. Processing of Stomach Tissues
  1. Remove stomach tissues from formalin and place in clean Petri dishes.
  2. Cut stomach tissues with a scalpel into several equal-sized longitudinal strips (each 2-3 mm thick) and place in labelled embedding cassettes containing foam padding.
  3. Fix stomach tissue by placing embedding cassettes in a jar filled with 80% ethanol.

Note: Stomachs can be processed immediately or stored for up to 1-2 days prior to proceeding to the next step.

4. Stomachs are then processed on an automated tissue processor, programmed with the following settings:
  1. Dehydration: 70% ethanol - 1 cycle, 20 mins; 90% ethanol - 1 cycle, 20 mins; 100% ethanol - 2 cycles, 20 mins each + 1 cycle, 40 mins + 1 cycle, 1 hr.
  2. Clearing: xylene - 2 cycles, 30 mins each + 1 cycle, 45 mins.
  3. Impregnation: paraffin wax at 60°C - 1 cycle, 45 mins + 1 cycle, 1 hr + 1 cycle, 1.25 hrs.
5. Remove the processed samples from the machine and store at room temperature for paraffin embedding.

## 2. Paraffin Embedding of Processed Gastric Tissues.

1. Place stainless steel base moulds on the stage of the embedding unit to warm the bases of the moulds.

Note: Embedding machine should be set at 60°C for efficient paraffin embedding.
2. Place waxed cassettes containing the samples into a warm wax bath/hot plate area of the embedding unit until wax fully dissolves.

Note: It is recommended that the sample be embedded shortly after wax dissolves. This ensures that hardening of tissues does not occur.
3. Fill half of the stainless steel moulds with paraffin wax. Using warm forceps, remove stomach tissue strips from the cassettes and gently push the stomach strips through the paraffin to the base of the moulds. Carefully orientate tissue strips at a right angle to the base of the moulds so that their sliced ends are facing upwards.

Note: The following steps should be performed as quickly as possible to avoid hardening and separation of the paraffin layers within embedded blocks. The proper orientation of stomach tissues is critical for downstream analyses.
4. Place moulds on the cold plate of the embedding unit to fix the specimens in place and re-orientate tissues if necessary.

Note: If the tissues become dislodged and the paraffin begins to harden, place moulds back onto the hot plate to melt the wax and re-embed tissues in moulds.
5. Place half of the labelled embedding cassettes (which were used for the tissue processing) on to the top of the moulds and gently fill with warm wax. Do not allow paraffin to overflow.
6. Gently place moulds on to a cold plate and allow to cool.
7. Once the paraffin has fully set, separate the embedded blocks from moulds. Clean excess paraffin wax on cassette edges using a hot plate (set above 80°C) or a scraper. Blocks can be stored at room temperature until sectioning is performed.

## 3. Sectioning of Tissues.

1. Chill paraffin-embedded tissue blocks on ice and heat a water bath filled with ultrapure water to 40-45°C.

2. Secure the blade in the holder of the microtome and set the clearance angle between  $1^{\circ}$ - $5^{\circ}$  to prevent contact between the block face and knife facet, before inserting paraffin blocks.  
Note: Ensure blocks are clear of excess paraffin acquired from the embedding, as this may hinder the fit of the block.
  3. Orientate the blade for a straight cut across the block. Gently cut 2-3 thin sections to ensure correct positioning of the block.
  4. Trim blocks by a thickness of approximately 10-30  $\mu\text{m}$ . This step ensures that a maximal surface area of each tissue strip will be cut.
  5. Cut 10  $\mu\text{m}$  sections and discard any that contain holes caused by trimming.
  6. Carefully pick up sections using tweezers and float them in the water bath for flattening. Use tweezers to separate each section.
  7. Collect sections from the water bath and place onto charged SuperFrost Plus™ glass slides.
  8. Store slides upright in a slide rack and place in an incubator at  $37^{\circ}\text{C}$ . Dry sections overnight.
  9. Store sections at room temperature indefinitely for subsequent analyses.
4. Haematoxylin and Eosin (H&E) Staining of Stomach Tissues.
1. Dewax slides using 3 washes of xylene for 5 mins each, followed by 3 washes in 100% ethanol, for 3 mins each. Ensure fresh solutions are used at each stage.
  2. Rinse slides in tap water for 30 sec-1 min.
  3. Remove excess water by gently tapping the bottom of the slides on a paper towel. Stain with filtered Haematoxylin for 3 mins. Ensure that sections are sufficiently covered with the solution.
  4. Rinse slides under running tap water until water runs clear.
  5. Dip slides in Scott's Tap water for 8-10 sec. Slides should not be exposed to the solution for over 10 sec as this will result in darker and intense stains. Staining of sections can be viewed under a microscope. Efficient staining at this stage will result in a 'baby blue' colour.  
Note: Prepare Scott's Tap water by dissolving 2 g sodium hydrogen carbonate ( $\text{NaHCO}_3$ ) and 20 g magnesium sulphate ( $\text{MgSO}_4$ ) in 1 L of distilled water.
  6. Rinse slides in tap water for 30 sec-1 min.
  7. Remove excess water as described in step 3, then stain with filtered 1% aqueous Eosin for 3 mins.
  8. Rinse slides under running tap water until water runs clear.  
Note: Staining can be assessed using a light microscope. If staining is too dark, slides can be dehydrated in 100% ethanol for longer than the specified time. If darker staining is required, slides can be stained with Eosin for 1-2 minutes longer, prior to proceeding to subsequent steps.
  9. Dehydrate slides using 3 washes of 100% ethanol for 30 sec each, followed by 3 washes of xylene for 2 mins each. Ensure fresh solutions are used at each stage.



10. Mount slides with DPX or equivalent mounting medium. Add a drop of DPX in the centre of a clean coverslip prior to gently placing slide on top with sections facing downwards.

Note: Do not dry slides prior to cover slipping.

11. Place slides on a flat surface and allow to air dry. Slides can also be dried in a fume hood to accelerate drying time.

#### 5. Giemsa Staining of Stomach Tissues.

1. Dewax slides using 2 washes of histolene for 5 mins each, followed by 2 washes of 100% ethanol for 3 mins each and then a final wash in 70% ethanol for 3 mins. Ensure fresh solutions are used for each wash.
2. Rinse slides in tap water for 30 sec-1 min.
3. Prepare Giemsa solution by mixing 20% Giemsa stain with 80% distilled water. Stain slides with Giemsa solution for 1 h.
4. Place slides in 100 ml distilled water containing 3-4 drops of acetic acid for 2-3 sec.  
Note: Solution must be mixed well prior to use. At this stage, slides should appear pale blue in colour.
5. Wash slides in 96% ethanol for 30 sec.
6. Wash slides in 3 baths of isopropanol for 2 mins each, followed by 3 baths of histolene for 2 mins each. Use fresh isopropanol histolene for each wash.
7. Coverslip slides with DPX mounting medium, as described earlier.

#### REPRESENTATIVE RESULTS:

This protocol describes an oral gavage technique to achieve intragastric infection with *H. pylori* or *H. felis* in murine mouse models (**Figure 1**). Following euthanasia, stomachs are removed, weighed and divided into 2 equal halves comprising the antrum, body and non-glandular regions of gastric tissues (**Figure 2**). The non-glandular region is removed prior to performing any analyses.

Successful colonisation of animals is typically confirmed by performing viable counting on *H. pylori*-infected gastric homogenates, and subsequently enumerating individual colonies on HBA plates (**Figure 3**). Alternatively, PCR is employed to verify infection with *H. felis* using specific, validated primers directed at a 342-bp region of the *H. felis* and *H. pylori ureB* genes (**Figure 4**).

Gastric tissues are processed, embedded and sectioned for downstream histological applications. The H&E staining technique is used to assess the histopathology in *Helicobacter*-infected mice. In the current example, WT C57BL/6 mice display moderate signs of inflammation, including hyperplasia (enlarged mucosa) and gland atrophy at 6 months' post-infection with *H. felis*. The presence of cellular infiltrates can also be observed in the sub-mucosa. Interestingly, however, more severe inflammation is observed in KO mice at the same time point, with the additional presence of lymphoid follicles located in close proximity to cellular infiltrates (**Figure 5**). Finally, *H. felis* bacteria are observed in Giemsa-stained sections of infected mouse stomachs (**Figure 6**).

#### FIGURE LEGENDS:

**Figure 1: Image demonstrating the oral gavage technique.** A disposable 1 ml syringe and flexible catheter are used to deliver  $\geq 10^5$  CFU of bacterial inocula to a mouse via the intragastric route. The mouse was anaesthetised using methoxyflurane and held in a firm grip at the neck, allowing for access of the catheter to the stomach via the oesophagus.

**Figure 2: Harvesting of mouse stomachs post-infection.** Mouse stomachs were harvested post-euthanasia and their contents removed by scraping with a scalpel and washing in sterile PBS. The tissues were then weighed and flattened on a cotton sheet to reveal 2 equal halves, each comprising the gastric antrum, body and non-glandular regions.

**Figure 3: Viable counts on *H. pylori*-infected mouse stomachs.** Mice on the C57BL/6 background were inoculated with  $10^7$  CFU of *H. pylori* SS1 and left for 8 weeks. Bacterial loads post-infection were assessed by enumerating 10-100 individual colonies per sample (A). HBA plates containing >100 individual colonies were not analysed (B). HBA plates may display some fungal and/or bacterial contamination which can make the counting of *H. pylori* colonies difficult (C).

**Figure 4: PCR detection of *H. felis* infection in gastric biopsies using oligonucleotides targeting the *ureB* gene.** A specific oligonucleotide pair was designed to recognise and bind to homologous sequences in both *H. felis* and *H. pylori ureB* genes. These primers were validated using genomic DNA from *H. pylori* SS1 (lane 2) or *H. felis* (lane 3). Deionized water was included as a negative control (lane 1).

**Figure 5: Representative images of H&E-stained stomach sections from WT and KO mice at 6 months' post-infection with *H. felis*.** Paraffin-embedded tissue sections were stained with H&E. WT samples were moderately inflamed compared with stomachs from KO mice, which display signs of severe inflammation. Tissue sections from KO mice contain the presence of mucosal lymphoid follicles (\*), cellular infiltrates (→), gland atrophy (►) and hyperplasia. Magnification = 10 X; Scale bar = 100  $\mu$ m.

**Figure 6: Representative images of Giemsa-stained gastric sections from C57BL/6 WT mice at 3 months' post-infection with *H. felis*.** Paraffin-embedded tissue sections were stained with Giemsa. Arrows indicate the presence of *H. felis* in the gastric glands. Magnification = 50 X; Scale bar = 200  $\mu$ m.

#### DISCUSSION:

This protocol describes the use of an *in vivo* mouse model for *Helicobacter* infection. The critical steps of the procedure are the: 1) preparation of *Helicobacter* inocula containing viable and motile bacteria; 2) delivery of the appropriate numbers of bacteria to the mouse via intragastric gavage; 3) detection of bacterial infection by colony counting and/or PCR; and 4) processing of gastric tissues to enable the assessment of histopathology in infected stomachs. Further



suggestions for modifications, troubleshooting and technical considerations are discussed below.

The method of growing *Helicobacter* spp. using Blood Agar Base no. 2 (Oxoid) supplemented with horse blood has been well established in our laboratory. However, alternate agar bases such as Brucella agar and Columbia blood agar can also be used<sup>21</sup>. It is important to ensure that only sterile glassware which is free of detergent is used to prepare the growth medium. Furthermore, moist agar plates should be used while subculturing bacteria to attain optimal growth. When preparing *Helicobacter* spp. inocula for infection, it is vital to subculture *H. pylori* and *H. felis* strains every 1-1.5 or 2 days, respectively, to ensure bacterial viability. At every subculture, bacteria should be assessed for their viability and motility by phase contrast microscopy. A urease assay can also be routinely employed to discriminate between gastric *Helicobacter* spp. and other bacteria<sup>22</sup>, however, it is important to realise that this assay detects both viable and non-viable *Helicobacter* bacteria. Following inoculation of animals, viable counts on *Helicobacter* suspensions must be performed to quantitate numbers of viable bacteria used for infection. As *H. felis* does not reproducibly form isolated colonies on agar medium<sup>16</sup>, estimation of bacterial numbers is performed using phase contrast microscopy. Quantification of bacterial numbers by optical density measurement ( $A_{600}$ ) is inaccurate as this method does not discriminate between viable and non-viable bacteria. This method should not be used in *Helicobacter* research.

When performing *Helicobacter* infection studies, it is crucial to consider the optimal mouse and *Helicobacter* strain, as well as the length of infection, to suit the purpose of the experiment. It is also essential to regularly confirm that the animals used for experimentation are indeed *Helicobacter*-free using genus-specific PCR primers<sup>23</sup>. The presence of other enteric *Helicobacter* species, such as *Helicobacter bilis*, *Helicobacter hepaticus* or *Helicobacter muridarum*, may alter the disease susceptibility of mice and introduce confounding factors into *in vivo* studies<sup>24,25</sup>. It is also advisable to include a mock treatment control group of animals (*i. e.* fed broth only) in initial screening experiments to investigate the effects of the normal microbiota on *Helicobacter* colonisation and pathogenesis.

Post-euthanasia, *H. pylori* colonisation in murine stomachs can be measured by viable counting. HBA plates used for colony counts should be supplemented with bacitracin and naladixic acid in addition to the modified Skirrow's selective supplement, to restrict the growth of bacterial species from the normal gastric microbiota and hence prevent contamination<sup>26</sup>. *H. felis* does not always form colonies, but instead tends to form swarming growth on agar plates<sup>14,16</sup>. Therefore, PCR and qPCR are normally employed to determine the presence and levels of *H. felis* colonisation, respectively<sup>27</sup>. In section 4.2, we introduced a simple and quick PCR method to confirm colonisation by *H. felis* in the murine stomach using a pair of primers, which have been validated to target a 342-bp region of *H. felis* and *H. pylori ureB* genes. Using the PCR conditions described above, it is possible to discriminate between infection by these gastric *Helicobacter* spp. and urease-producing enterohepatic *Helicobacters*. Other genes that have been validated for PCR detection of gastric *Helicobacter* infection include the 16s rRNA and flagellin B (*flaB*) genes<sup>16,27,28</sup>.

Finally, we have described the use of two powerful staining techniques: H&E staining, to assess histopathological changes in the stomach post-infection; and Giemsa staining, to detect *H. felis* infection. To obtain optimal staining, it is essential to ensure that tissues have been preserved, processed and embedded in the correct orientation. Additionally, only freshly prepared solutions and filtered stains must be used during the process. Tissue sections can be stored indefinitely and utilised for more specific analysis of gastric pathology via immunofluorescence or immunohistochemistry. Some other common measures of gastric inflammation and disease include: immune cell recruitment (anti-CD45 staining); mucosal thickening/destruction (Periodic Acid Schiff/Alcian blue staining); epithelial cell proliferation (proliferating cell nuclear antigen, PCNA/Bromodeoxyuridine, BrDU staining); or cellular apoptosis (TUNEL staining). The lymphoid follicles observed in the H&E-stained tissues of *H. felis*-infected mice can be confirmed by immunohistochemistry, using antibodies directed against B (B220<sup>+</sup>) and T cell (CD3<sup>+</sup>) antigens<sup>29</sup>.

In summary, animal models of bacterial disease provide valuable tools in the field of infection biology. The protocols of intragastric gavage and processing of stomach tissues provided here may be adapted to mouse infection models involving other enteric pathogens.

**ACKNOWLEDGEMENTS:** The authors would like to thank Ms. A. De Paoli for technical assistance. The laboratory is supported by funding from the National Health and Medical Research Council (NHMRC) to RLF (APP1079930, APP1107930). RLF is supported by a Senior Research Fellowship from the NHMRC (APP1079904). KD and MC are both supported by Monash Graduate Scholarships. KD is also supported by the Centre for Innate Immunity and Infectious Diseases, Hudson Institute of Medical Research, while MC has an International Postgraduate Scholarship from the Faculty of Medicine, Nursing and Health Sciences, Monash University. Research at the Hudson Institute of Medical Research is supported by the Victorian Government's Operational Infrastructure Support Program.

**DISCLOSURE:** The authors have nothing to disclose.

## REFERENCES:

- 1 Goh, K.-L., Chan, W.-K., Shiota, S. & Yamaoka, Y. Epidemiology of *Helicobacter pylori* Infection and Public Health Implications. *Helicobacter*. **16** (0 1), 1-9, doi:10.1111/j.1523-5378.2011.00874.x, (2011).
- 2 Montecucco, C. & Rappuoli, R. Living dangerously: how *Helicobacter pylori* survives in the human stomach. *Nat Rev Mol Cell Biol*. **2** (6), 457-466 (2001).
- 3 Tomb, J. F. *et al.* The complete genome sequence of the gastric pathogen *Helicobacter pylori*. *Nature*. **388** (6642), 539-547, doi:10.1038/41483, (1997).
- 4 Peek, R. M., Jr., Fiske, C. & Wilson, K. T. Role of innate immunity in *Helicobacter pylori*-induced gastric malignancy. *Physiol Rev*. **90** (3), 831-858, doi:10.1152/physrev.00039.2009, (2010).



- 5 O'Rourke, J. L. & Lee, A. Animal models of *Helicobacter pylori* infection and disease. *Microbes and Infection*. **5** (8), 741-748, doi:http://dx.doi.org/10.1016/S1286-4579(03)00123-0, (2003).
- 6 Sakagami, T. *et al.* Atrophic gastric changes in both *Helicobacter felis* and *Helicobacter pylori* infected mice are host dependent and separate from antral gastritis. *Gut*. **39** (5), 639-648, (1996).
- 7 Correa, P. *Helicobacter pylori* and gastric carcinogenesis. *Am J Surg Pathol*. **19** (1), S37-43 (1995).
- 8 Enno, A. *et al.* MALToma-like lesions in the murine gastric mucosa after long-term infection with *Helicobacter felis*. A mouse model of *Helicobacter pylori*-induced gastric lymphoma. *The American Journal of Pathology*. **147** (1), 217-222 (1995).
- 9 Lee, A. *et al.* A standardized mouse model of *Helicobacter pylori* infection: introducing the Sydney strain. *Gastroenterology*. **112** (4), 1386-1397 (1997).
- 10 Grubman, A. *et al.* The innate immune molecule, NOD1, regulates direct killing of *Helicobacter pylori* by antimicrobial peptides. *Cell Microbiol*. **12** (5), 626-639, doi: 10.1111/j.1462-5822.2009.01421.x, (2010).
- 11 Israel, D. A. *et al.* *Helicobacter pylori* strain-specific differences in genetic content, identified by microarray, influence host inflammatory responses. *J Clin Invest*. **107** (5), 611-620, doi:10.1172/jci11450, (2001).
- 12 Fox, J. G. *et al.* *Helicobacter pylori*-induced gastritis in the domestic cat. *Infect Immun*. **63** (7), 2674-2681 (1995).
- 13 Lee, A., Hazell, S. L., O'Rourke, J. & Kouprach, S. Isolation of a spiral-shaped bacterium from the cat stomach. *Infect Immun*. **56** (11), 2843-2850 (1988).
- 14 Viala, J. *et al.* Nod1 responds to peptidoglycan delivered by the *Helicobacter pylori* cag pathogenicity island. *Nat Immunol*. **5** (11), 1166-1174, doi:10.1038/ni1131, (2004).
- 15 Ferrero, R. L., Thiberge, J. M., Huerre, M. & Labigne, A. Immune responses of specific-pathogen-free mice to chronic *Helicobacter pylori* (strain SS1) infection. *Infect Immun*. **66** (4), 1349-1355 (1998).
- 16 Ferrero, R. L., Wilson, J. E. & Sutton, P. Mouse models of *Helicobacter*-induced gastric cancer: use of cocarcinogens. *Methods Mol Biol*. **921** 157-173, doi:10.1007/978-1-62703-005-2\_20, (2012).
- 17 Ferrero, R. L. & Labigne, A. Cloning, expression and sequencing of *Helicobacter felis* urease genes. (0950-382X (Print)).
- 18 Kim, J.-S., Chang, J.-H., Chung, S.-I. & Yum, J.-S. Importance of the host genetic background on immune responses to *Helicobacter pylori* infection and therapeutic vaccine efficacy. *FEMS Immunology & Medical Microbiology*. **31** (1), 41-46, doi:10.1111/j.1574-695X.2001.tb01584.x, (2001).
- 19 Nedrud, J. G. *et al.* Lack of Genetic Influence on the Innate Inflammatory Response to *Helicobacter* Infection of the Gastric Mucosa. *Frontiers in Immunology*. **3** 181, doi:10.3389/fimmu.2012.00181, (2012).
- 20 Cai, X. *et al.* *Helicobacter felis* eradication restores normal architecture and inhibits gastric cancer progression in C57BL/6 mice. *Gastroenterology*. **128** (7), 1937-1952 (2005).

- 21 Stevenson, T. H., Castillo, A., Lucia, L. M. & Acuff, G. R. Growth of *Helicobacter pylori* in various liquid and plating media. *Lett Appl Microbiol.* **30** (3), 192-196 (2000).
- 22 Uotani, T. & Graham, D. Y. Diagnosis of *Helicobacter pylori* using the rapid urease test. *Annals of Translational Medicine.* **3** (1), 9, doi:10.3978/j.issn.2305-5839.2014.12.04, (2015).
- 23 Riley, L. K., Franklin, C. L., Hook, R. R., Jr. & Besch-Williford, C. Identification of murine helicobacters by PCR and restriction enzyme analyses. *J Clin Microbiol.* **34** (4), 942-946 (1996).
- 24 Chaouche-Drider, N. *et al.* A commensal *Helicobacter* sp. of the rodent intestinal flora activates TLR2 and NOD1 responses in epithelial cells. *PLoS One.* **4** (4), e5396, doi:10.1371/journal.pone.0005396, (2009).
- 25 Fox, J. G. *Helicobacter bilis*: bacterial provocateur orchestrates host immune responses to commensal flora in a model of inflammatory bowel disease. *Gut.* **56** (7), 898-900, doi:10.1136/gut.2006.115428, (2007).
- 26 McGee, D. J. *et al.* Cholesterol enhances *Helicobacter pylori* resistance to antibiotics and LL-37. *Antimicrob Agents Chemother.* **55** (6), 2897-2904, doi:10.1128/aac.00016-11, (2011).
- 27 Ng, G., Every, A., McGuckin, M. & Sutton, P. Increased *Helicobacter felis* colonization in male 129/Sv mice fails to suppress gastritis. *Gut Microbes.* **2** (6), 358-360, doi:10.4161/gmic.19143, (2011).
- 28 Kong, L. *et al.* A sensitive and specific PCR method to detect *Helicobacter felis* in a conventional mouse model. *Clinical and Diagnostic Laboratory Immunology.* **3** (1), 73-78 (1996).
- 29 Ferrero, R. L., *et al.* Outbred mice with long-term *Helicobacter felis* infection develop both gastric lymphoid tissue and glandular hyperplastic lesions. *Journal of Pathology.* **191** (3), 333-340 (2000).

**Figure 1:**

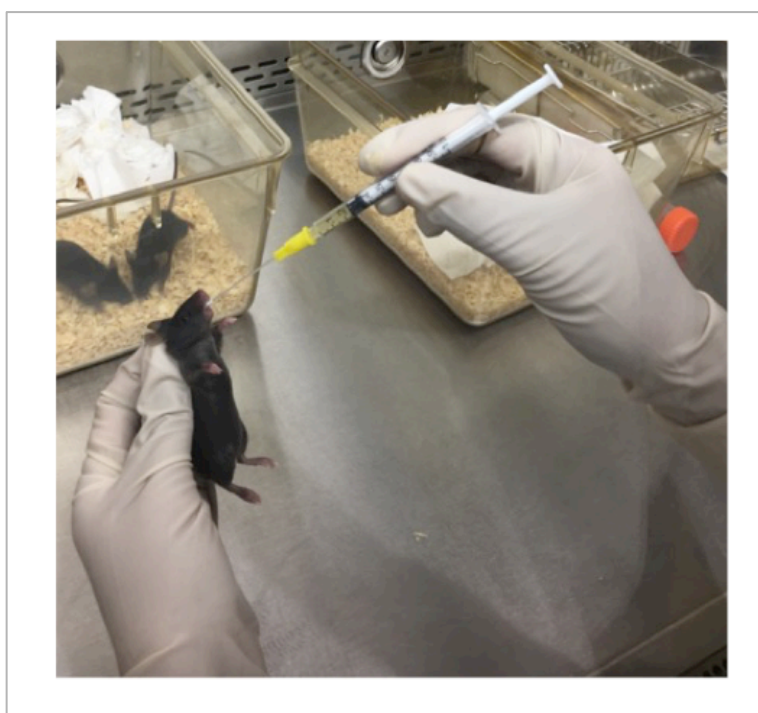


**Figure 2:**

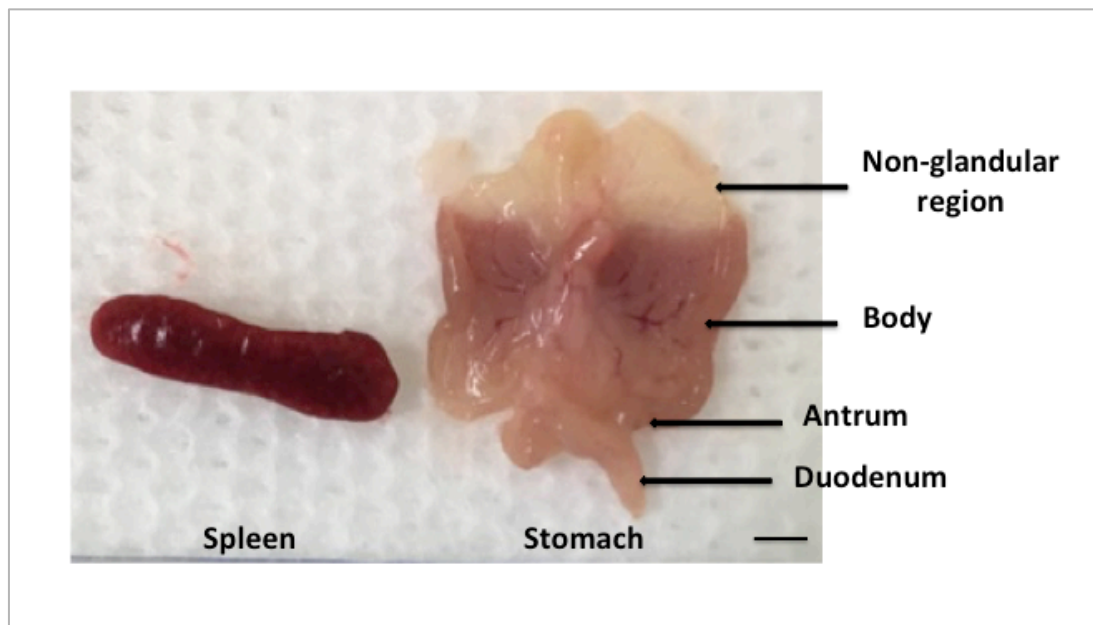


**Figure 3:**

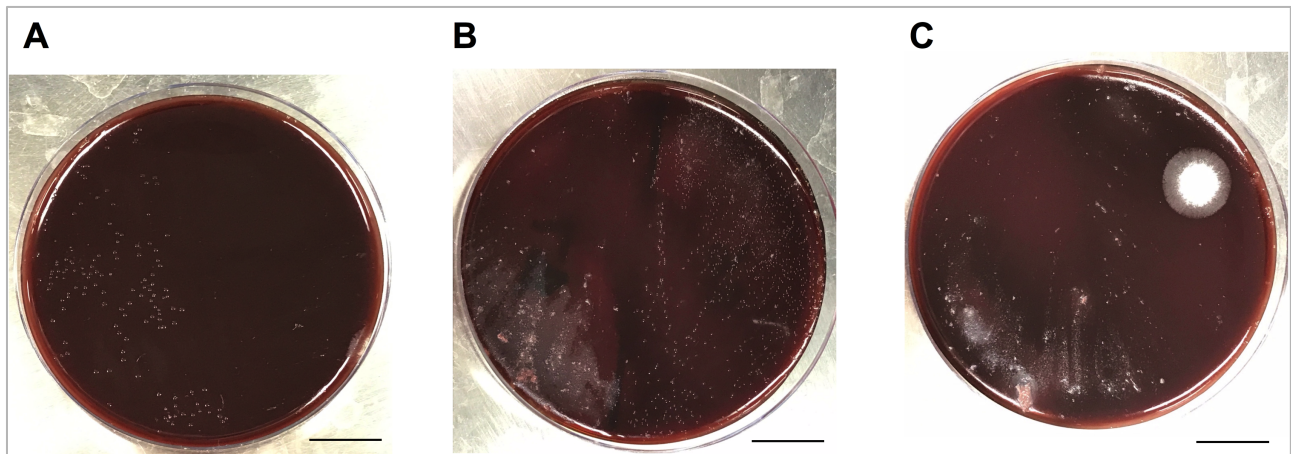




**Figure 4:**

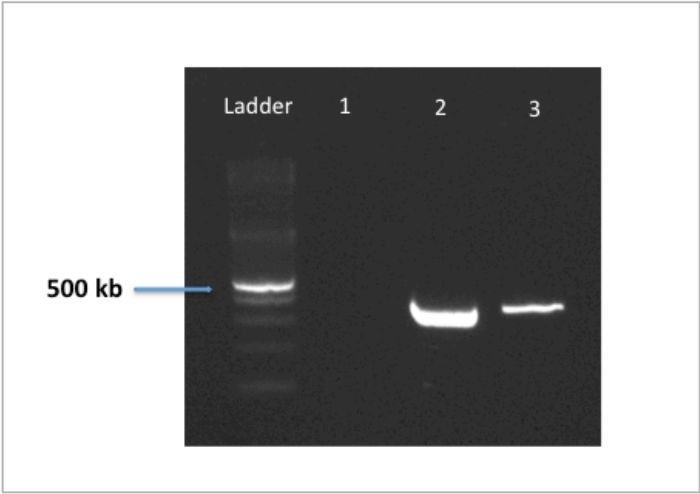


**Figure 5:**

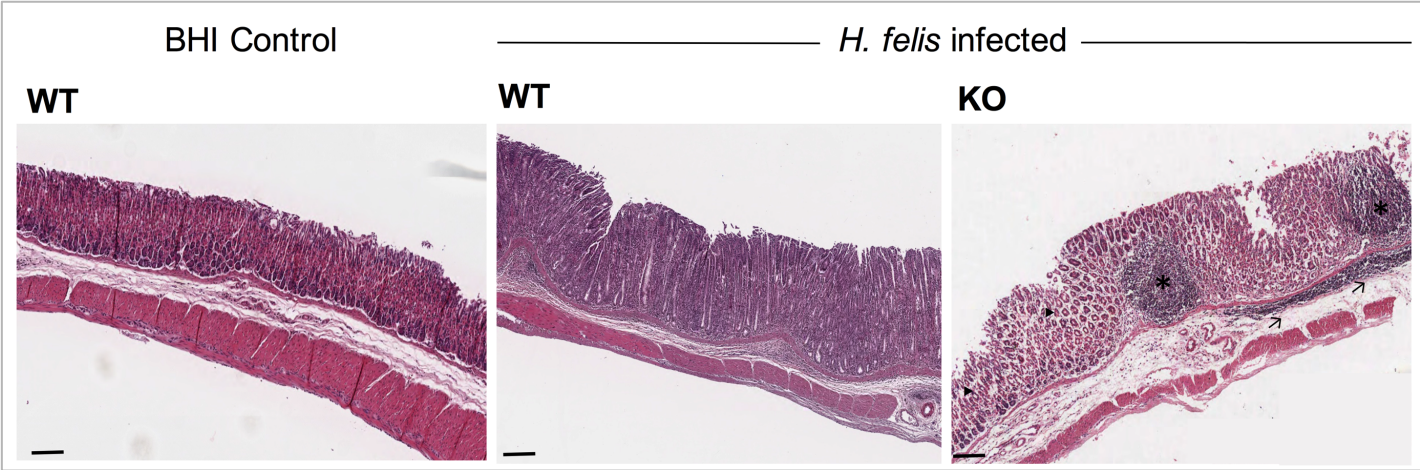
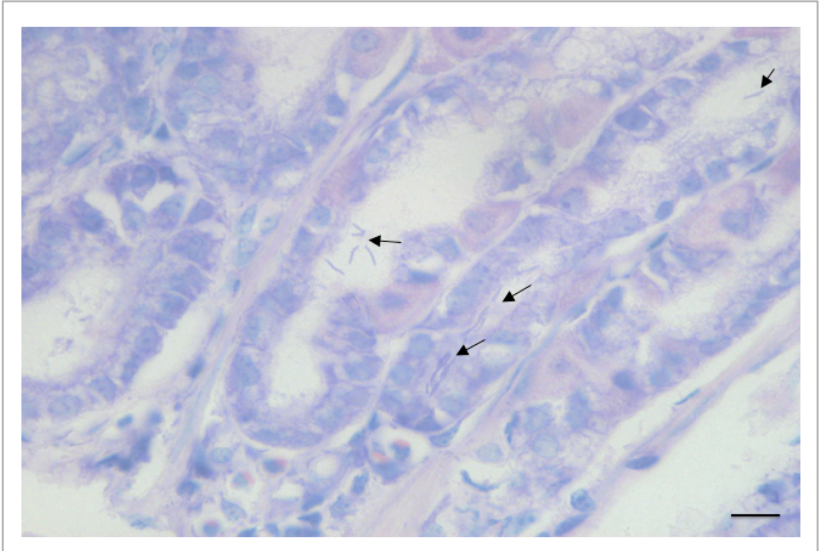


**Figure 6:**



## NOD1 is required for *Helicobacter pylori* induction of IL-33 responses in gastric epithelial cells

Le Son Tran<sup>1</sup> | Darren Tran<sup>1</sup> | Amanda De Paoli<sup>1</sup> | Kimberley D'Costa<sup>1</sup> | Sarah J. Creed<sup>2</sup> | Garrett Z. Ng<sup>3,4</sup> | Lena Le<sup>1</sup> | Philip Sutton<sup>3,4,5</sup> | J. Silke<sup>6,7</sup> | U. Nachbur<sup>6,7</sup> | Richard L. Ferrero<sup>1,8</sup> 

<sup>1</sup>Centre for Innate Immunity and Infectious Diseases, The Hudson Institute of Medical Research, Monash University, Clayton, Victoria, Australia

<sup>2</sup>Monash Micro Imaging, The Hudson Institute of Medical Research, Monash University, Clayton, Victoria, Australia

<sup>3</sup>Murdoch Children's Research Institute, The Royal Children's Hospital, Parkville, Victoria, Australia

<sup>4</sup>School of Veterinary and Agricultural Science, The University of Melbourne, Parkville, Victoria, Australia

<sup>5</sup>Department of Paediatrics, The University of Melbourne, Parkville, Victoria, Australia

<sup>6</sup>Division of Cell Signalling and Cell Death, The Walter and Eliza Hall Institute, Parkville, Victoria, Australia

<sup>7</sup>Department of Medical Biology, The University of Melbourne, Parkville, Victoria, Australia

<sup>8</sup>Biomedicine Discovery Institute, Department of Microbiology, Monash University, Clayton, Victoria, Australia

### Correspondence

Dr Le Son Tran, Centre for Innate Immunity and Infectious Diseases, The Hudson Institute of Medical Research, Monash University, 27-31 Wright Street, Clayton, Victoria, Australia. Email: lesan.tran@hudson.org.au

Dr Richard Ferrero, Centre for Innate Immunity and Infectious Diseases, The Hudson Institute of Medical Research, Monash University, 27-31 Wright Street, Clayton, Victoria, Australia. Email: richard.ferrero@hudson.org.au

### Funding information

National Health and Medical Research Council, Grant/Award Numbers: APP1079904 and APP1079930; Faculty of Medicine, Nursing and Health Sciences, Monash University, Grant/Award Number: International Postgraduate Scholarship; National Health and Medical Research Council (NHMRC), Grant/Award Numbers: APP1079904 and APP1079930

### Abstract

*Helicobacter pylori* (*H. pylori*) causes chronic inflammation which is a key precursor to gastric carcinogenesis. It has been suggested that *H. pylori* may limit this immunopathology by inducing the production of interleukin 33 (IL-33) in gastric epithelial cells, thus promoting T helper 2 immune responses. The molecular mechanism underlying IL-33 production in response to *H. pylori* infection, however, remains unknown. In this study, we demonstrate that *H. pylori* activates signalling via the pathogen recognition molecule Nucleotide-Binding Oligomerisation Domain-Containing Protein 1 (NOD1) and its adaptor protein receptor-interacting serine-threonine Kinase 2, to promote production of both full-length and processed IL-33 in gastric epithelial cells. Furthermore, IL-33 responses were dependent on the actions of the *H. pylori* Type IV secretion system, required for activation of the NOD1 pathway, as well as on the Type IV secretion system effector protein, CagA. Importantly, *Nod1*<sup>+/+</sup> mice with chronic *H. pylori* infection exhibited significantly increased gastric IL-33 and splenic IL-13 responses, but decreased IFN- $\gamma$  responses, when compared with *Nod1*<sup>-/-</sup> animals. Collectively, our data identify NOD1 as an important regulator of mucosal IL-33 responses in *H. pylori* infection. We suggest that NOD1 may play a role in protection against excessive inflammation.



## 1 | INTRODUCTION

Chronic inflammation caused by infection with the Gram-negative bacterium *Helicobacter pylori* is an essential precursor to gastric carcinogenesis (Peek & Crabtree, 2006). Upon infection, *H. pylori* interacts with host cells within the gastric mucosa, resulting in activation of multiple innate immune signalling pathways that shape host adaptive immune responses (Tran, Chonwerawong, & Ferrero, 2017). Innate immune recognition of *H. pylori* results in T helper (Th) 1 and 17 responses which promote the development of gastric immunopathologies (Hitzler, Kohler, Engler, Yazgan, & Muller, 2012; Sayi et al., 2009). It has been shown, however, that *H. pylori* can limit excessive gastric inflammation and promote bacterial persistence through the induction of Th2 immune responses (Berg, Lynch, Lynch, & Lauricella, 1998; Chen, Shu, & Chadwick, 2001; Smythies et al., 2000).

The IL-1 cytokine family comprises 11 members and has been described as important drivers of the host adaptive cytokine profile (Lopetuso, Chowdhry, & Pizarro, 2013). A recently identified member of this family, IL-33, has been shown to act as an alarmin and be associated with Th2 signature cytokine production (e.g., IL-4, IL-5, and IL-13) by Group 2 innate lymphoid cells and Th2 lymphocytes during allergic inflammation or parasite infection (Liew, Girard, & Tumquist, 2016). In addition, IL-33 was shown to promote the proliferation of regulatory T cells and to function as an anti-inflammatory cytokine mediating tissue repair (Martin & Martin, 2016; Molofsky, Savage, & Locksley, 2015).

A recent study reported upregulated IL33 gene expression in human gastric mucosa in response to *H. pylori* infection (Shahi et al., 2015). Buzzelli et al (Buzzelli et al., 2015) demonstrated increased IL-33 responses in the gastric mucosa of *H. pylori*-infected mice in the acute phase of infection, whereas its expression was reduced during chronic infection. Despite the observed association between IL33 expression and *H. pylori* infection, the upstream signalling mechanism underlying *H. pylori* regulated IL-33 production remains elusive.

We have previously reported that the cytosolic receptor Nucleotide-Binding Oligomerisation Domain-Containing Protein 1 (NOD1) is an important pathogen recognition receptor regulating host epithelial cell responses to *H. pylori* (Viala et al., 2004). NOD1 was shown to sense Gram-negative peptidoglycan (PG), delivered into the cytoplasm of host cells via the *H. pylori* Type IV secretion system (T4SS), encoded by the *cag* pathogenicity island (CagPAI; Allison, Kufer, Kremmer, Kaparakis, & Ferrero, 2009; Boonyanugomol et al., 2013; Viala et al., 2004). In addition to the T4SS, *H. pylori* can activate the NOD1 pathway via the actions of outer membrane vesicles (OMVs) which function as a transport mechanism for bacterial PG into the host cell cytosol (Irving et al., 2014; Kaparakis et al., 2010; Olofsson et al., 2010). Upon recognition of PG, NOD1 undergoes self-oligomerisation, leading to the recruitment of the scaffolding kinase protein, receptor-interacting serine-threonine kinase 2 (RIPK2; also known as RIP2, RICK, or CARDIAK; Allison et al., 2009; Baker et al., 2017; Hasegawa et al., 2008; Olofsson et al., 2010). This leads to activation of nuclear factor-kappa B (NF- $\kappa$ B) and mitogen-activated protein kinases signalling pathways and the subsequent transcriptional activation of multiple pro-inflammatory cytokine genes (Allison et al., 2009).

Given that IL-33 is downstream of the NF- $\kappa$ B signalling pathway (Farias & Rousseau, 2015; Kobori et al., 2010), we hypothesised that NOD1 sensing of *H. pylori* infection may regulate IL-33 responses in the stomach. Here, we show that NOD1 is required for *H. pylori* upregulation of IL-33 gene expression, synthesis, and processing in gastric epithelial cells (GECs) in vitro and in vivo. Furthermore, NOD1 regulation of IL-33 production was shown to be associated with the development of Th2-type immune responses in mice with chronic *H. pylori* infection, suggesting a protective role for NOD1 against excessive inflammation.

## 2 | RESULTS

### 2.1 | NOD1 sensing of *H. pylori* mediates IL-33 responses in GECs

It has been shown that IL-33 production is mediated by NF- $\kappa$ B signalling and that sensing of *H. pylori* infection by NOD1 leads to the activation of NF- $\kappa$ B signalling in GECs (Allison et al., 2009; Farias & Rousseau, 2015; Kobori et al., 2010; Viala et al., 2004). In order to initially investigate the link between NOD1 signalling and IL-33 regulation in response to *H. pylori*, we used the mouse GSM06 gastric epithelial cell line. To block NOD1 signalling in GSM06 cells, we pretreated cells with the NOD1-specific inhibitor ML130 (Correa et al., 2011). As expected, inactivation of NOD1 signalling by treatment with ML130 significantly attenuated the production of keratinocyte chemoattractant (KC), a cytokine downstream of *H. pylori* induced NOD1 activation (Figure 1a;  $p < .05$ ). Likewise, the stimulation of cells with *H. pylori* bacteria induced upregulated IL33 gene expression and this was significantly reduced in cells pretreated with ML130 (Figure 1b;  $p < .05$ ). Consistent with the gene expression data, full-length IL-33 (33 kDa) production was increased in the lysates of GSM06 cells in response to *H. pylori* stimulation, whereas the levels were reduced when NOD1 signalling was inhibited by ML130 treatment (Figure 1c). Furthermore, we detected higher levels of processed IL-33 (22 kDa) in the lysates and cultured supernatants of GSM06 cells following *H. pylori* stimulation as compared with ML130-treated cells (Figure 1c). Lower levels of total IL-33 were also detected in the culture supernatants of ML130-treated GSM06 cells, as compared with control cells (Figure S1a). These data showed that NOD1 promotes both gene transcription and protein production of IL-33 in mouse GECs. To further investigate the contribution of NOD1 in IL-33 regulation, we isolated primary mouse GECs from *Nod1*<sup>+/+</sup> or *Nod1*<sup>-/-</sup> mice. The purity of the GEC preparations was confirmed by immunofluorescence staining with an antibody to the epithelial cell-specific marker, EpCAM (Figure S1b,c). The reduction in KC and macrophage inflammatory protein 2 (MIP2) production in *Nod1*<sup>-/-</sup> GECs further confirmed the important role of NOD1 in activation of NF- $\kappa$ B in response to *H. pylori* stimulation (Figure S1d,e). The GECs were then co-cultured with the *H. pylori* clinical Strain 10700 or its mouse-adapted variant, Sydney Strain 1 (SS1). Consistent with findings in GSM06 cells, the levels of full-length and processed IL-33 were markedly lower in *Nod1*<sup>-/-</sup> GECs as compared with *Nod1*<sup>+/+</sup> cells in response to either 10700 or SS1 stimulation (Figure 1d). To extend our findings, we used



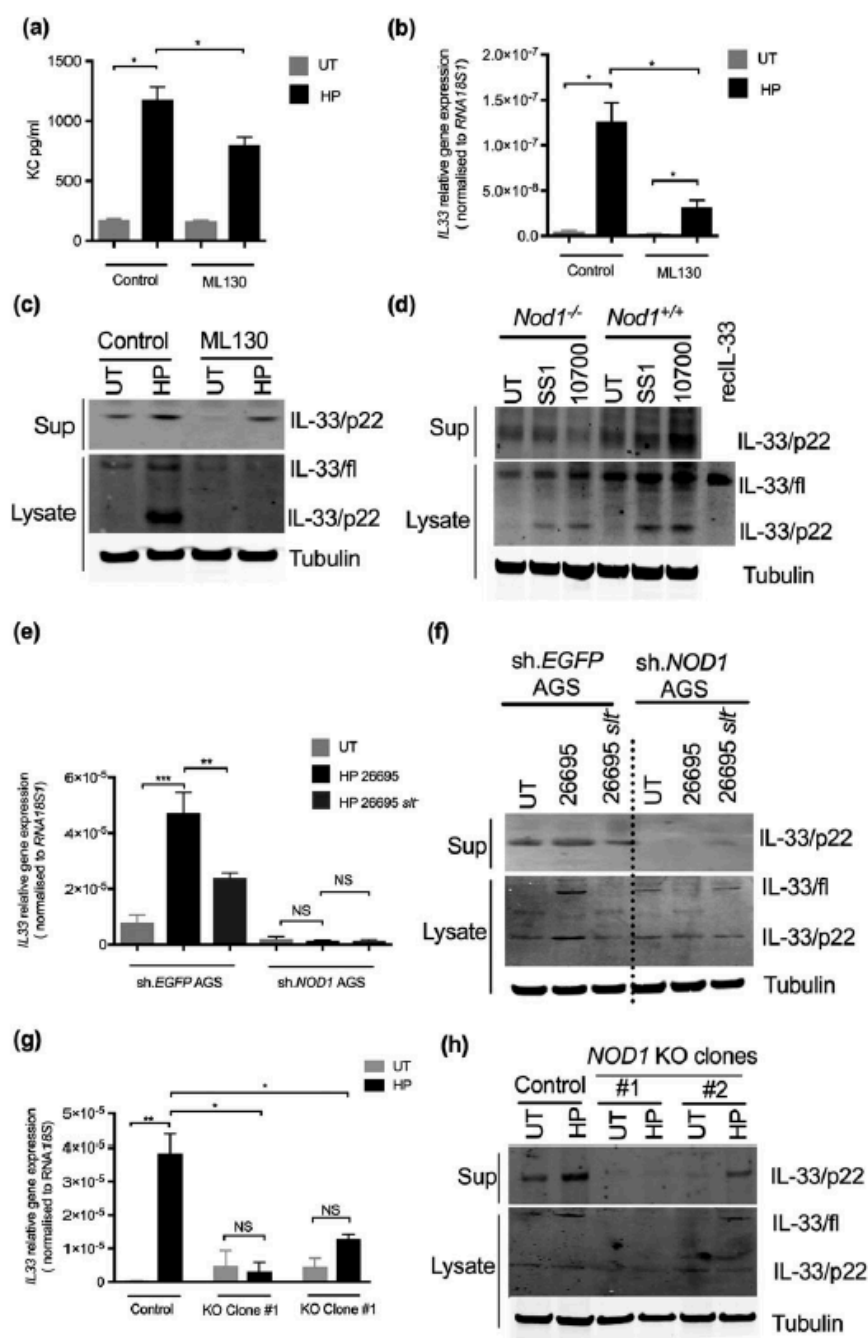


**FIGURE 1** NOD1 sensing of *H. pylori* promotes both full-length and mature IL-33 production in mouse and human GECs. (a) KC production, (b) IL33 gene expression, and (c) IL-33 protein synthesis in GSM06 mouse GECs pretreated with NOD1-specific inhibitor ML130 (5  $\mu$ M), followed by *H. pylori* (HP) stimulation for 6 hr. (d) Full-length (fl) and processed IL-33 (p22) in primary mouse GECs isolated from *Nod1*<sup>+/+</sup> or *Nod1*<sup>-/-</sup> mice infected with *H. pylori* 10700 or SS1. Commercial recombinant IL-33 protein (recIL-33) served as an antibody-specific control. Tubulin was used as a loading control for cell lysates. (e) IL33 gene expression, (f) full-length and processed IL-33 in human AGS cells expressing control (sh.EGFP) or NOD1-specific shRNA (sh.NOD1) stimulated with wild type (26695) or an isogenic mutant (26695 *slt*<sup>-</sup>) at an MOI = 10 for 24 hr. (g) IL33 gene expression and (h) IL-33 protein production in control or NOD1 knockout AGS cell lines. Data in (a), (b), (e), and (g) are presented as means  $\pm$  SEM and are representative of at least two independent experiments ( $n > 2$ ). \* $p < .05$ , \*\* $p < .01$ , \*\*\* $p < .001$ , and NS = not significant

human AGS GEC lines, stably expressing an shRNA specific for NOD1 or an irrelevant gene EGFP (hereafter referred to as sh.NOD1 AGS or sh. EGFP, respectively [Grubman et al., 2010]). Increased levels of IL33 gene expression, as well as full-length IL-33 synthesis and processing, were observed in sh.EGFP AGS cells in response to stimulation with *H. pylori* 26695 bacteria (Figure 1e,f). In contrast, these responses were

completely ablated in sh.NOD1 AGS cells (Figure 1e,f). To investigate the role of NOD1 sensing of bacterial PG in IL-33 responses, we stimulated AGS cells with wild type or isogenic mutant bacteria that lack the lytic transglycosylase, Slt (HP0645). These *slt*<sup>-</sup> mutant bacteria release less NOD1 ligand and therefore also have a reduced capacity to activate the NOD1 signalling pathway (Viala et al., 2004). AGS cells that were co-

cultured with *H. pylori* *slt* bacteria exhibited reduced IL-33 responses when compared with the parental strain (Figure 1e,f). Furthermore, *H. pylori* OMVs harbouring PG induced higher levels of full-length and processed IL-33 in sh.EGFP AGS cells when compared with sh.NOD1 cells (Figure S2). These findings confirm the importance of NOD1 sensing of *H. pylori* PG for IL-33 responses in GECs.

To confirm our findings, we generated NOD1 knockout (KO) AGS cells using CRISPR/Cas9 technology to target the CARD domain of NOD1, which is required for its interaction with downstream adaptor molecules and activation of NF- $\kappa$ B signalling (Inohara et al., 1999). The isolated NOD1 KO clone#1 and clone#2 were shown to carry 71-bp and 31-bp deletions, respectively, introducing premature stop codons that resulted in truncated proteins (Figure S3a,b). As expected, the two KO clones displayed undetectable levels of NOD1 gene expression (Figure S3c) and attenuated IL-8 production in response to NOD1 agonist C12-EDAP or *H. pylori* stimulation (Figure S3d). Importantly, both NOD1 KO AGS clones express significantly lower levels of *IL33* gene expression (Figure 1g;  $p < .05$ ) and produce less full-length and mature IL-33 protein than control AGS cells (Figure 1h). Taken together, these findings show that activation of NOD1 signalling by *H. pylori* enhances IL-33 production in both mouse and human GECs.

In addition to NOD1, recent studies have reported that the host tumour necrosis factor receptor-associated factor (TRAF)-interacting protein with forkhead-associated domain (TIFA) drives NF- $\kappa$ B activation upon detection of heptose-1,7-bisphosphate, an intermediate product of lipopolysaccharide biosynthesis (Gall, Gaudet, Gray-Owen, & Salama,

2017; Gaudet et al., 2017; Stein et al., 2017). To address the contribution of TIFA in *H. pylori*-induced IL-33 production, we "knocked down" its expression by transfecting AGS cells with TIFA-specific siRNA prior to bacteria stimulation. Transfection with TIFA siRNA resulted in significant reductions in TIFA gene expression and IL-8 responses (Figure S4a,b), yet the levels of both full-length and mature forms of IL-33 in the lysates of *H. pylori*-stimulated cells remained unchanged (Figure S4c). Interestingly, AGS cells in which TIFA expression was reduced by siRNA treatment secreted lower levels of mature IL-33 into the culture supernatants, as compared with control AGS cells (Figure S4c). These data suggest that unlike NOD1, TIFA is required for IL-8 production and proteolytic processing of full-length IL-33 but is dispensable for IL-33 synthesis.

## 2.2 | RIPK2 is required for NOD1-mediated production and processing of IL-33

RIPK2 has been described to be a central down-stream mediator of NOD1 signalling (Hasegawa et al., 2008). To test the role of RIPK2 in *H. pylori*-mediated IL-33 responses, AGS cells were either transfected with RIPK2-specific siRNA or pretreated with the RIPK2 inhibitor, WEHI-345, prior to *H. pylori* stimulation (Nachbur et al., 2015). siRNA-mediated knock down of RIPK2 expression was confirmed by qPCR (Figure 2a;  $p < .05$ ). Additionally, inhibition of RIPK2 function was confirmed by measuring IL-8 responses as the production of this chemokine in response to *H. pylori* stimulation is known to be

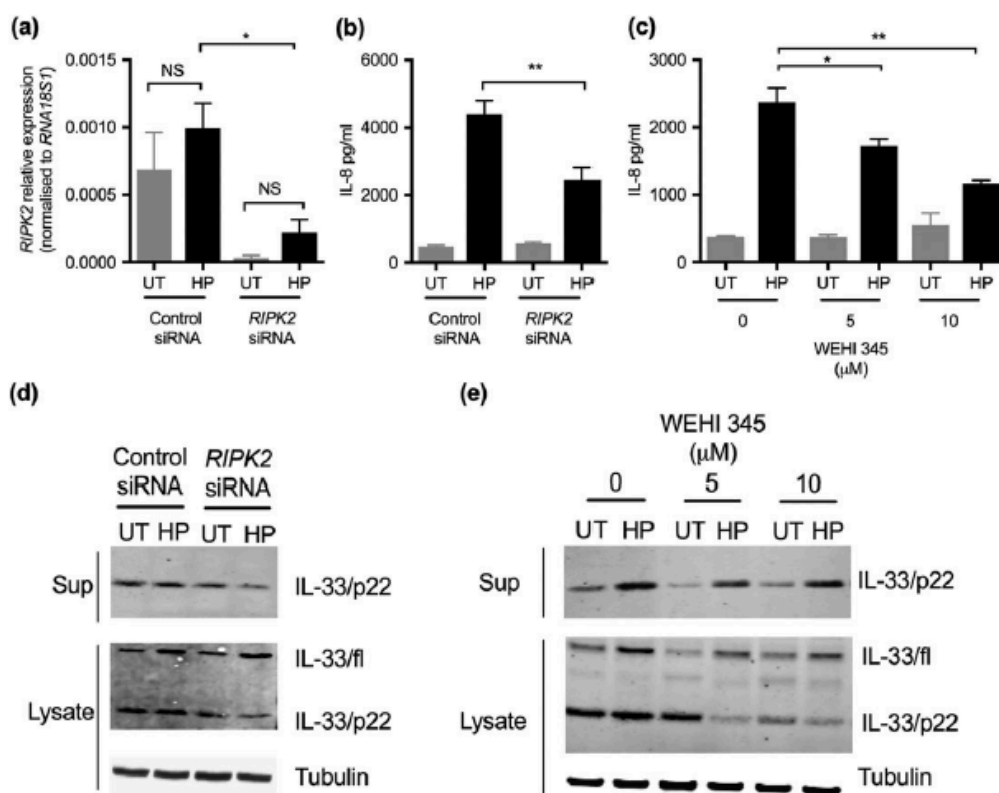


**FIGURE 2** NOD1-mediated IL-33 production and processing in response to *H. pylori* infection are dependent on the NOD1 adaptor molecule, RIPK2. (a) RIPK2 gene expression, (b and c) IL-8, and (d and e) IL-33 (full-length and mature form) production in AGS cells transfected with control siRNA or RIPK2 specific siRNA or pretreated with RIPK2-specific kinase inhibitor WEHI 345 prior to *H. pylori* stimulation. Data are presented as means  $\pm$  SEM and are representative of two independent experiments (a–c). \* $p < .05$ , \*\* $p < .01$  and NS = not significant. Western blot images (d and e) are representative of three independent experiments ( $n = 3$ ). Tubulin served as a loading control

NOD1-dependent (Figure 2b,c). Importantly, RIPK2 inhibition resulted in reduced levels of IL-33 production and processing (Figure 2d,e). These data show that classical NOD1/RIPK2 signalling is important in mediating the IL-33 responses induced by *H. pylori*.

### 2.3 | Loss of nuclear localisation of IL-33 in response to *H. pylori* stimulation is NOD1-dependent

It has been reported that under basal conditions, IL-33 predominantly resides in the nucleus of epithelial cells, whereas loss of its nuclear location is associated with enhanced release of IL-33 and induction of inflammatory responses (Kuchler et al., 2008; Moussion, Ortega, & Girard, 2008). Consistent with the published literature, IL-33 expression was predominantly localised within the nucleus of unstimulated control and NOD1 KO AGS cells (Figure 3a,b). *H. pylori* stimulation promoted the relocalisation of IL-33 from the nucleus to the cytoplasm in control cells, but not in NOD1 KO AGS cells, which instead displayed a predominantly nuclear localisation for IL-33 similar to that in non-stimulated cells (Figure 3c,d). This observation was further confirmed by a significant reduction in the ratio of nuclear to cytoplasmic IL-33 in control cells but not in NOD1 KO AGS cells after stimulation with *H. pylori* (Figure 3e;  $p < .001$ ). These data indicate that NOD1 is involved in promoting the nuclear release of IL-33. Thus, NOD1 not only promotes the synthesis of IL-33 protein but also release of this cytokine, which may allow host epithelial cells to activate other immune cell subsets and shape the downstream immune responses to *H. pylori* infection.

### 2.4 | The *H. pylori* T4SS and CagA are required for induction of IL-33 in human GECs

The *H. pylori* T4SS is one mechanism by which bacteria can deliver their PG into the cytoplasm of host cells, leading to the activation of

NOD1 signalling (Viala et al., 2004). Therefore, we addressed whether bacterial T4SS plays a role in NOD1-mediated IL-33 responses by co-culturing human AGS cells with wild type *H. pylori* 251 or isogenic mutant strains having either defective T4SSs (i.e.,  $\Delta\text{cagPAI}$  and  $\Delta\text{cagM}$ ) or lacking the T4SS effector protein, CagA ( $\Delta\text{cagA}$ ). These mutant *H. pylori* bacteria induced significantly reduced levels of IL-8 production when compared with wild type bacteria (Figure 4a;  $p < .01$  and  $p < .05$ , respectively). *H. pylori* mutant bacteria with defective T4SSs also induced significantly lower levels of IL33 expression (Figure 4b;  $p < .05$ ), as well as reduced production of both full-length and processed IL-33 (Figure 4c,d;  $p < .05$ ). Interestingly, *H. pylori*  $\Delta\text{cagA}$  bacteria also induced significantly reduced IL-33 responses in AGS cells (Figure 4c,d;  $p < .05$ ). Taken together, our data show that T4SS, which is required for the activation of NOD1 signalling, as well as for translocation of the CagA oncoprotein, contributes to *H. pylori* induced IL-33 production in human GECs.

### 2.5 | NOD1 drives IL-33 production and Th2 cytokine responses during chronic *H. pylori* infection in vivo

To study the role of NOD1 in IL-33 production in vivo, *Nod1*<sup>+/+</sup> and *Nod1*<sup>-/-</sup> mice were inoculated with *H. pylori* and left for 1 or 8 weeks, respectively. At 1 week post-infection, we observed no significant changes in *Il33* gene expression (Figure 5a) or IL-33 production (Figure 5b) in the stomachs of either *H. pylori*-infected *Nod1*<sup>+/+</sup> or *Nod1*<sup>-/-</sup> mice, when compared with control uninfected animals. In contrast, at 8 weeks post-infection, *Nod1*<sup>-/-</sup> animals displayed significantly down-regulated levels of *Il33* gene expression (Figure 5a;  $p < .05$ ) and protein production (Figure 5b;  $p < .001$ ), when compared with *H. pylori*-infected *Nod1*<sup>+/+</sup> animals. The former also exhibited lower levels of both full-length and processed IL-33 forms (Figure 5c). Thus,

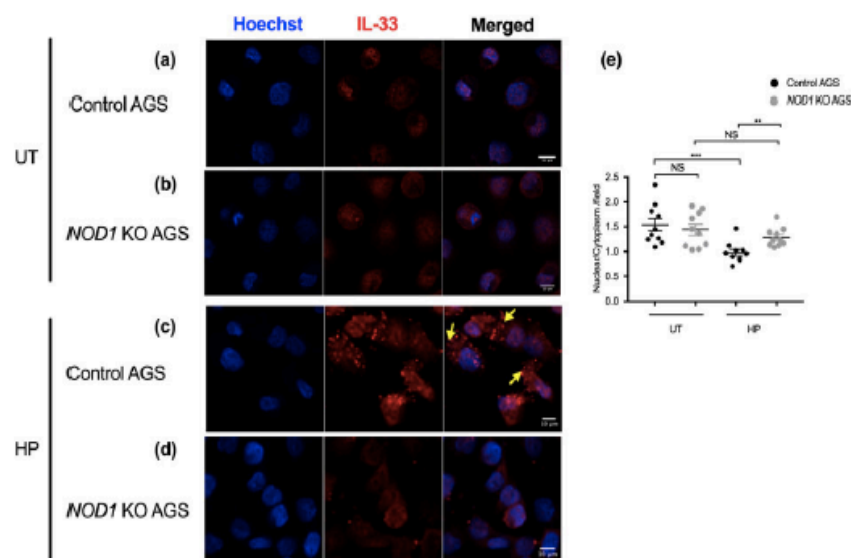


**FIGURE 3** NOD1 mediates loss of nuclear location of IL-33 in human GECs in response to *H. pylori* stimulation. (a)–(d) Cell nuclei were stained with Hoechst 33342 (blue) and IL-33 (red) detected by immunostaining in control AGS or NOD1 knockout (KO) AGS cells left untreated (a and b) or stimulated with *H. pylori* (c and d) for 24 hr. Arrows indicate cells displaying loss of nuclear IL-33. Data are representative images of two independent experiments. Images were acquired on a confocal microscope with 200X magnification (scale bar, 10  $\mu\text{m}$ ). (e) The nuclear to cytoplasmic ratios of IL-33 staining per field were calculated as described in the experimental procedures section. Data are presented as means  $\pm$  SEM and representative of two independent experiments. In each experiment, images were acquired from 10 different fields per treatment group \*\*  $p < .01$ , \*\*\*  $p < .001$  and NS = not significant



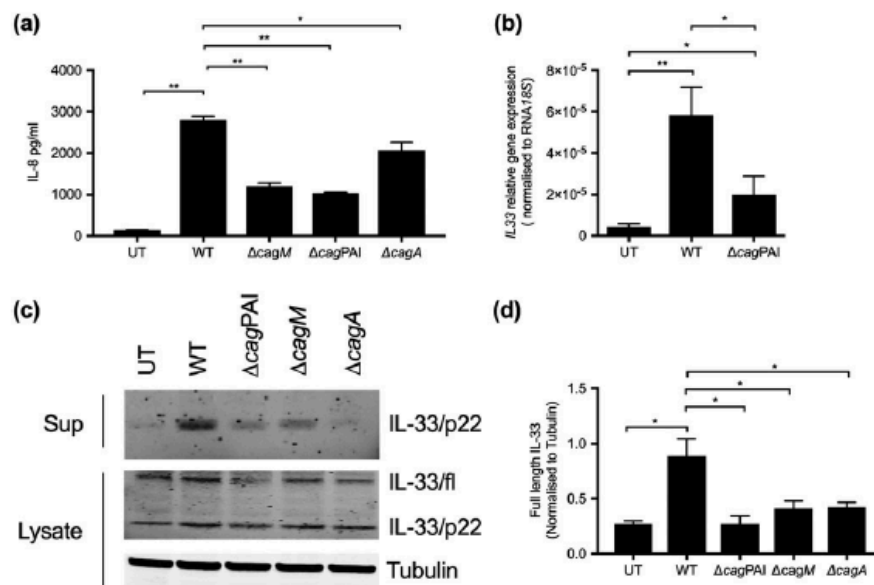


**FIGURE 4** *H. pylori* T4SS and CagA are required for the induction of IL-33 responses in human GECs. (a) IL-8 production and (b) IL33 gene expression in AGS cells stimulated with an *H. pylori* wild type strain (WT) or isogenic mutant strains lacking a functional T4SS ( $\Delta cagPAI$ ,  $\Delta cagM$ ) or CagA ( $\Delta cagA$ ). Data are presented as means  $\pm$  SEM and are representative of three independent experiments ( $n = 3$ ). (c) Full-length or processed IL-33 in AGS cells stimulated with *H. pylori* wild type strain or isogenic mutant strains. (d) Densitometry analysis of blot images in B shows the relative level of full-length IL-33 normalised to Tubulin. Images are representative of results from at least three independent experiments ( $n > 3$ ), and data are presented as the mean  $\pm$  SEM. \* $p < .05$  and \*\* $p < .01$

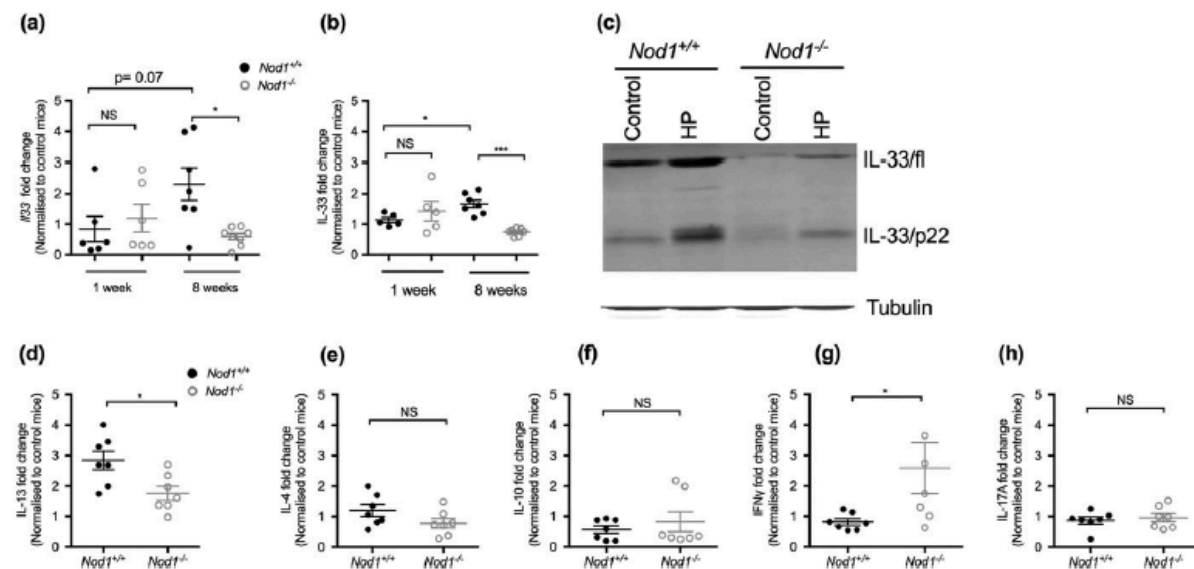


**FIGURE 5** *Nod1*<sup>-/-</sup> mice display reduced IL-33 production associated with down-regulated IL-13 but up-regulated IFN- $\gamma$  responses in response to chronic *H. pylori* infection. (a) Fold changes in IL33 gene expression and (b) total IL-33 protein levels in gastric homogenates of *Nod1*<sup>+/+</sup> or *Nod1*<sup>-/-</sup> mice administered either broth or *H. pylori* for 1 or 8 weeks. (c) Full-length and mature IL-33 production in the gastric homogenates of *Nod1*<sup>+/+</sup> or *Nod1*<sup>-/-</sup> mice at 8 weeks' post-infection. Tubulin was used as a loading control. (d) IL-13, (e) IL-4, (f) IL-10, (g) IFN- $\gamma$ , and (h) IL-17A in the culture supernatants of ConA-stimulated splenic cells isolated from mice at 8 weeks' post-infection. Data in (a) and (b) and (d)–(h) were normalised to control animals and presented as the means  $\pm$  SEM. Data are representative of two independent experiments. In each experiment, four–seven animals per groups per were used ( $n = 4$ –7). \* $p < .05$ , \*\* $p < .01$ , \*\*\* $p < .001$ , and NS = not significant

consistent with our in vitro data, NOD1 mediates IL-33 production during chronic infection with *H. pylori*.

Given that IL-33 is a key driver of Th2 immunity in a wide range of inflammatory settings, we next investigated the cytokine profiles of

splenocytes isolated from *Nod1*<sup>+/+</sup> or *Nod1*<sup>-/-</sup> mice at 8 weeks post-infection. Although splenocytes from *Nod1*<sup>+/+</sup> and *Nod1*<sup>-/-</sup> mice produced similar levels of the Th2 cytokines, IL-4 and IL-10, significant differences were observed for another Th2 cytokine, IL-13 (Figure 5d-f;  $p < .05$ ). Conversely, the splenocytes from *Nod1*<sup>-/-</sup> mice produced significantly higher levels of the Th1 cytokine IFN- $\gamma$ , as compared with *Nod1*<sup>+/+</sup> splenocytes (Figure 5g;  $p < .05$ ). No differences were observed for the Th-17 cytokine, IL-17 (Figure 5h). Thus, during chronic infection with *H. pylori*, NOD1 is involved in IL-33 production thereby shaping host adaptive immune responses towards a Th2-dominant phenotype.

### 3 | DISCUSSION

IL-33 is well established as an important mediator of both innate and adaptive immune responses (Martin & Martin, 2016). Although recent studies have revealed an association between mucosal IL-33 production and *H. pylori* infection, the underlying mechanism by which the bacterium drives IL-33 production remains unknown (Buzzelli et al., 2015; Shahi et al., 2015). In this study, we show that *H. pylori* activation of the innate immune molecule NOD1 promotes IL33 gene expression and processing in GECs.

It has recently been reported that IL-33 induction is driven by NF- $\kappa$ B signalling in epithelial cells in response to bacterial infection and inflammation (Farias & Rousseau, 2015; Kobori et al., 2010). This led us to hypothesise that in response to *H. pylori* infection, NOD1 may regulate IL-33 production in epithelial cells. Consistent with this hypothesis, we showed that disruption of NOD1 signalling by either pharmacological inhibition, siRNA knockdown or CRISPR/Cas9 gene targeting resulted in attenuation of both classical NF- $\kappa$ B-dependent cytokine production and IL-33 responses. Furthermore, we showed that blockade of RIPK2, a critical downstream mediator of NOD1 signalling responsible for NF- $\kappa$ B activation (Inohara et al., 2000), resulted in decreased IL-33 production. Thus, these findings suggest that NOD1 sensing of *H. pylori* promotes IL-33 production via activation of the NF- $\kappa$ B signalling pathway.

It is thought that IL-33 possesses a nuclear localisation sequence within its N terminus and is thus normally stored in the nucleus in order to be protected from cleavage and inappropriate release (Carriere et al., 2007; Gautier et al., 2016). In this study, we observed that NOD1 activation by *H. pylori* caused loss of nuclear IL-33 and enhanced secretion of processed IL-33 in the culture supernatants of control AGS cells but not those from NOD1 KO cells (Figure 3). Thus, it is possible that NOD1 mediates the release of IL-33 via cleavage of an N-terminal nuclear localisation signal required for tethering IL-33 in the nucleus. However, the mechanism(s) whereby these processed forms are secreted into the extracellular compartment remain(s) largely unknown. The processed form of IL-33 may be biologically active or inactive, depending on the proteases mediating the cleavage (Martin & Martin, 2016). In common with other members of the IL-1 cytokine family, IL-33 was initially reported to become active after processing by caspase-1 (Schmitz et al., 2005). However, subsequent studies showed that caspase-1 and other apoptotic caspases, including caspases-3 and -7, could cleave IL-33 into an inactive form (Cayrol & Girard, 2009). IL-33 can also be processed by neutrophil proteases,

resulting in highly active forms (Lefrancais et al., 2012). Thus, future studies are needed to assess the protease(s) responsible for the processing of IL-33 in GECs, the secretion mechanism involved in release of the processed form, as well as the role of NOD1 in IL-33 processing and its impact on *H. pylori*-induced pathology.

The turnover and release of PG, mediated by the lytic transglycosylase Slt, has been shown to be important for *H. pylori* to activate NOD1 signalling (Viala et al., 2004). In the present study, we show that AGS cells stimulated with *H. pylori* slt deficient bacteria induced significantly lower levels of IL-33 mRNA and protein than those stimulated with wild type bacteria (Figure 1e,f). These data suggest the importance NOD1 sensing of PG in IL-33 responses. Consistent with this suggestion, *H. pylori* OMVs induced IL-33 responses via a NOD1-dependent mechanism (Figure S2). In addition, *H. pylori* mutant bacteria lacking a functional T4SS system, which is required to activate NOD1 signalling via the delivery of PG into host cells (Viala et al., 2004), were affected in their ability to induce IL-33 responses in human GECs (Figure 4). It is also noteworthy that we observed higher levels of processed IL-33 in the culture supernatants of mouse GECs after stimulation with the clinical isolate 10700, which has a functional T4SS, when compared with those from cells stimulated its mouse-adapted variant (Strain SS1), which lacks a functional T4SS (Philpott et al., 2002; Figure 1d). Although the T4SS is not essential for *H. pylori* induction of NF- $\kappa$ B-dependent responses in mouse GECs (Ferrero et al., 2008), it is possible that this secretion system may be required for maximal IL-33 responses in GECs of murine origin. Altogether, these data suggest that the metabolism and delivery of PG into host cells are crucial for *H. pylori* activation of NOD1-driven IL-33 responses in GECs.

The induction of both IL-8 and IL-33 production was not completely abrogated in GECs in which NOD1 signalling had been dampened by either pharmacological inhibition, shRNA knockdown or gene deletion (Figure 1), suggesting the potential involvement of a NOD1-independent mechanism in these responses. Although the contribution of CagA in *H. pylori* induced NF- $\kappa$ B responses remains controversial, we found that *H. pylori*  $\Delta$ cagA bacteria induced less IL-8 production compared with wild type bacteria and, moreover, these responses were not completely abolished in shNOD1 AGS cells (Figure 5a). Additionally, we showed that *H. pylori*  $\Delta$ cagA bacteria induced lower levels of IL-33 production and processing (Figure 4c, d), suggesting that CagA may act independently of NOD1 signalling to drive IL-33 production. Although beyond the scope of the current study, the mechanism whereby *H. pylori* CagA regulates IL-33 responses warrants further investigation.

Unlike NOD1, we found that TIFA is dispensable for the production of full-length IL-33 in cell lysates. IL-33 is known as an "alarmin" which is released rapidly during the early phase of infection to alert the host immune system to the presence of bacteria (Molofsky et al., 2015). We speculate that NOD1 is the first sensor recruited to the cell membrane upon initial contact with *H. pylori*, hence predominantly mediating a rapid response. This speculation is supported by a recent study by Gaudet et al. (Gaudet et al., 2017) showing that NOD1 and TIFA independently contribute to NF- $\kappa$ B activation by the invasive Gram-negative bacterium, *Shigella flexneri*, and that the activation of NOD1 pathway precedes TIFA. In contrast, however, Gall et al. (Gall et al., 2017) claimed that in *H. pylori* infection, TIFA is activated prior to the



NOD1 response. Nevertheless, there is currently no experimental evidence to support this sequential activation of NOD1 and TIFA during *H. pylori* infection. Future studies are therefore required to delineate the links between NOD1 and TIFA activation during *H. pylori* stimulation. Interestingly, a reduction in the levels of mature IL-33 was observed in the culture supernatants of cells in which TIFA had been knocked down using siRNA (Figure S4c). Thus, the involvement of both NOD1 and TIFA in IL-33 processing indicates that these proteins might be components of a protein complex that mediates proteolytic cleavage of IL-33 at later phases of infection.

To establish the in vivo significance of NOD1-mediated IL-33 production, we assessed IL-33 production in both the acute and chronic phases of infection (1 and 8 weeks' post-infection). In line with a recent clinical study that reported a strong correlation between chronic *H. pylori* infection and IL33 gene expression in human gastric biopsies (Shahi et al., 2015), we found enhanced IL-33 production in the chronic phase of infection (Figure 5a–c). A recent study by Buzzelli et al. (Buzzelli et al., 2015), however, reported that IL33 gene expression was increased in the early phase of infection (1 week) but reduced after long term infection. This discrepancy could be attributed to differences in the *H. pylori* strains used in the two studies. Indeed, Buzzelli et al. used the *H. pylori* SS1 strain that was previously shown to have lost its T4SS functions during in vivo colonisation (Philpott et al., 2002). In contrast, we used the *H. pylori* 245 m3 strain (Philpott et al., 2002) in our study which has an intact *cagPAI* and still possesses a functional T4SS (L. S. Tran, K. D'Costa, unpublished data). It is possible that this allows the bacterium to sustain IL-33 production during long term infection.

Importantly, the levels of gastric IL-33 mRNA and protein were significantly higher in *Nod1*<sup>+/+</sup> than *Nod1*<sup>-/-</sup> mice (Figure 5a,b). These IL-33 responses were associated with up-regulation of IL-13 and down-regulation of IFN- $\gamma$  in splenic lymphocytes (Figure 5d,g). Based on previous findings (Sawai et al., 1999; Sayi et al., 2009), these responses would be expected to attenuate the development of gastric inflammation and affect bacterial clearance. One possible mechanism underlying the beneficial effects of IL-33 is that this cytokine can drive the generation of regulatory T cells which was reported to limit inflammatory responses and reduce bacterial loads in mice infected with *H. pylori* (Rad et al., 2006). In contrast, IL-33 was shown to elicit Th1 immune responses in tumour tissues by inducing IFN- $\gamma$  production in CD8<sup>+</sup> T cells and NK cells (Gao et al., 2015). Thus, future studies should explore the biological consequences of IL-33 production in the context of *H. pylori* infection and disease.

Collectively, in this work, we report for the first time that *H. pylori* infection promotes IL-33 secretion in GECs via a NOD1-dependent mechanism. Additionally, NOD1-driven IL-33 production during chronic *H. pylori* infection is associated with a Th2-type immune response, which may protect against excessive inflammatory responses and favour the persistence of *H. pylori* infection.

## 4 | EXPERIMENTAL PROCEDURES

### 4.1 | Cell lines, bacterial, and mouse strains

The mouse GSM06 GEC line (RCB1779) was obtained from Riken Cell Bank and grown as described previously (Ferrero et al., 2008). Briefly,

the cells were maintained in Dulbecco's modified Eagle medium–nutrient mixture/F-12 medium, supplemented with 10% foetal calf serum, 1% (w/v) insulin/transferrin/selenite (Gibco) and 10 ng/ml epidermal growth factor. Cells were grown in 5% CO<sub>2</sub> at the permissive temperature of 33 °C, then moved to 37 °C prior to experiments.

Human AGS gastric cancer cells stably expressing sh.RNA to either EGFP (sh.EGFP) or NOD1 (sh.NOD1) were generated as described previously (Grubman et al., 2010). These cells were maintained in complete RPMI medium supplemented with 10% (v/v) foetal calf serum, 1% (w/v) L-glutamine and 1% (w/v) penicillin/streptomycin (Gibco; ThermoFisher Scientific, VIC, Australia).

AGS cells harbouring CRISPR/Cas9 mediated NOD1 gene KO were generated by using a "Cas9 nickase" nuclease with pairs of guide RNAs (gRNAs) to introduce double-strand breaks (Ran et al., 2013). The following pair of gRNAs were designed to target the CARD domain of NOD1: gRNA1: GCTGAAGAATGACTACTTC and gRNA2: GCTTTTCAGTAATTGAATGT. These gRNAs were cloned into pSpCas9n(BB)-2A-GFP (PX461; Addgene plasmid # 48140) and pSpCas9n(BB)-2A-Puro (PX462; Addgene plasmid # 48141). The ligated vectors were transfected into AGS cells using Lipofectamine LTX (ThermoFisher Scientific), and then cells were selected with 1  $\mu$ g/ml puromycin. As a control, cells were transfected with PX461 and PX462 plasmids not carrying gRNAs. Limiting dilution was performed to obtain mutant clones derived from a single cell. Frame-shift KO clones were screened by polymerase chain reaction and pyrosequencing with primers flanking the target region: Fwd-GGCCACAGT GAGATGGAAAT and Rev-GGCAGGCACACAAATCTC. The KO status of NOD1 in AGS cells was further verified by measuring the levels of NOD1 gene expression and NOD1 induced IL-8 production in response to NOD1 agonist C12-IEDAP (10  $\mu$ g/ml, Invivogen).

*H. pylori* Strains 26695 (wild type, *slr*<sup>-</sup>; Viala et al., 2004), 251 (wild type, *cagM*<sup>+</sup>, *cagPAI*<sup>+</sup>, and *cagA*<sup>+</sup>; Allison et al., 2009), SS1 and 10700 (Lee et al., 1997) were used for in vitro experiments. A mouse-adapted, *cagPAI*<sup>+</sup> *H. pylori* strain (245 m3; Philpott et al., 2002) was employed for in vivo experiments. All bacterial strains were grown on Blood Agar Base No. 2 (Oxoid; Thermo Fisher Scientific), supplemented with 5% (v/v) whole horse blood (Australian Ethical Biologicals, VIC, Australia), Skirrow's selective supplement (155  $\mu$ g/ml Polymyxin B, 6.25  $\mu$ g/ml vancomycin, 3.125 mg/ml trimethoprim, and 1.25 mg/ml Amphotericin B; Sigma, MO, USA), at 37 °C under microaerobic conditions.

*Nod1*<sup>+/+</sup> and *Nod1*<sup>-/-</sup> C57BL/6 mice were maintained under specific pathogen-free conditions at the Animal Research Facility (Monash Medical Centre). All animal procedures complied with guidelines approved by Monash Medical Centre Animal Ethics Committee (MMCA/2015/43).

### 4.2 | Primary GEC isolation

Stomachs were removed from 4 to 5-week-old *Nod1*<sup>+/+</sup> or *Nod1*<sup>-/-</sup> mice and the gastric tissues excised and finely minced in 5 ml of Hank's Balanced Salt Solution without Ca<sup>2+</sup> and Mg<sup>2+</sup> (Gibco), supplemented with 0.125% (w/v) bovine serum albumin (Sigma), 0.072% (w/v) dispase (Roche Life Science, NSW, Australia), and 0.1% (w/v) Collagenase A (Roche). Tissues were digested by incubation for 2 hr at 37 °C, in 5% CO<sub>2</sub> and shaking at 150 rpm. Digested tissues were pelleted and

washed in DMEM/F12 medium by centrifugation at  $300 \times g$  for 5 min. Cells were plated at  $10^5$  cells/ml per well in 24-well plates coated with 2 mg/ml rat Tail Collagen I (ThermoFisher Scientific). The culture medium was changed every 2 days to remove fibroblasts and epithelial cells were grown for 5 days before performing co-culture assays. Epithelial cell purity was confirmed by immunofluorescence using the epithelial cell-specific marker, EpCAM (Abcam, Cambridge, UK, 1:200) and isotype control rabbit IgG (Dako).

#### 4.3 | OMV isolation

OMVs were purified from mid-exponential phase cultures that were pelleted at  $4,000 \times g$  for 40 min at  $4^\circ\text{C}$  (Kaparakis et al., 2010). Supernatant fractions were collected and filtered through 0.22- $\mu\text{m}$  filters (Merck Millipore, VIC, Australia). Filtered supernatants were subjected to ultracentrifugation as described previously (Kaparakis et al., 2010). Supernatants were discarded and the pellets resuspended in Brain Heart Infusion medium (Thermo Fisher Scientific). OMV protein concentrations were quantified using the Bradford Protein Assay (BioRad, CA, USA).

#### 4.4 | Inhibitor treatment

The small molecule inhibitor, ML130 (CID-1088438), was purchased from Tocris (Bristol, UK) and has been confirmed to selectively inhibit NOD1 signalling ( $\text{IC}_{50} = 0.56 \mu\text{M}$ ) with no cytotoxicity in previous studies (Correa et al., 2011). The RIPK2 selective inhibitor WEHI-345 was used as described previously (Nachbur et al., 2015). Briefly, cells were pretreated with ML130 ( $5 \mu\text{M}$ ) or WEHI-345 (0, 5, or  $10 \mu\text{M}$ ) for 1 hr prior stimulation with *H. pylori*, and then maintained in inhibitor-containing medium throughout the experiment.

#### 4.5 | siRNA transfection

TIFA or RIPK2-specific silencer and negative control siRNA ( $40 \mu\text{mol}$  of each; ThermoFisher Scientific) were diluted in Opti-MEM medium (Gibco) supplemented with  $2 \mu\text{l}$  of Lipofectamine® 2000 reagent (Thermo Fisher Scientific). The mixtures were incubated at room temperature for 20 min then added in a drop-wise manner to each well of 12-well plates containing  $10^5$  AGS cells. Transfected cells were incubated at  $37^\circ\text{C}$  for 24 hr prior to co-culture with bacteria.

#### 4.6 | Cell co-culture assay

*H. pylori* liquid cultures were obtained by growing bacteria in BHI containing 10% (v/v) heat-inactivated foetal calf serum (Thermo Fisher Scientific) and Skirrow's selective supplement, in a shaking incubator for 16–18 hr. Bacteria were pelleted and washed twice with phosphate-buffered saline (PBS) by centrifugation at  $4,000 \times g$  for 10 min at  $4^\circ\text{C}$  prior to resuspension in culture medium for co-culture assays. Viable counts were performed by serial dilution of bacterial suspensions on horse blood agar plates.

Cells were seeded in 12-well plates at  $1 \times 10^5$  cells/ml and allowed to grow overnight. The culture medium was removed and replaced with serum- and antibiotic-free medium prior to stimulation with bacteria. Cells were incubated with *H. pylori* wild type or isogenic mutant

strains at a multiplicity of infection of 10:1. The bacteria were removed after 1 hr. RNA extraction was performed at 4 hrs post-stimulation, whereas culture supernatants and lysates were collected at 24 hrs post-stimulation for ELISA and Western blot analyses.

#### 4.7 | qRT-PCR analyses

RNA was extracted using the PureLink® RNA mini kit (Thermo Fisher Scientific). cDNA was generated from  $500 \mu\text{g}$  of RNA using the Tetro cDNA synthesis kit (Bioline, NSW, Australia), as per the manufacturer's instructions. qPCR reactions consisted of  $4 \mu\text{l}$  of diluted synthesised cDNA (1:10),  $5 \mu\text{l}$  of SYBR® Green qPCR MasterMix (Thermo Fisher Scientific), and  $1 \mu\text{l}$  of oligonucleotide primers ( $1 \mu\text{M}$ ) for the tested genes. Oligonucleotide sequences were as follows: *Rn18s*, Fwd-GTAACCCGTTGAACCCATT and Rev-CCATCCAATCGGTAGT AGCG; *RNA18S1*, Fwd-CGGCTACCACATCCAAGGAA and Rev-GCTGGAATTACCGCGGCT; *IL33*, Fwd-TTCCAATCCAAGATTTC CC and Rev-CAGAACGGAGTCTCATGCAG; *IL33*, Fwd-AGTCTCAAC ACCCTCAAATG and Rev-CTTTGTAGGACTCAGGGTTACC; *RIPK2*, Fwd-GCCACCTGAAAACATGAACC and Rev-CTGCAAAGGATTGG TGACATC. *TIFA*, Fwd-TCGATTCCCTCGCTCTG and Rev-CCGTCA TCTGGAGACAAGTTAC. qPCR assays were performed in an Applied Biosystems™ 7900 Fast Real-Time PCR machine (Thermo Fisher Scientific; MHTP Medical Genomics Facility), using the following program:  $50^\circ\text{C}$ , 2 min, followed by  $95^\circ\text{C}$ , 10 min, then 40 successive cycles of amplification ( $95^\circ\text{C}$ , 15 s;  $60^\circ\text{C}$ , 1 min). Gene expression levels were determined by the Delta-Delta Ct method to measure relative gene expression levels to the 18S rRNA gene.

#### 4.8 | Western blot analyses

Cell culture supernatants were harvested and concentrated with StrataClean resin beads (Agilent Technologies, CA, USA), as per the manufacturer's instructions. Cell lysates were prepared using NP-40 lysis buffer (Thermo Fisher Scientific), supplemented with complete protease and phosphatase inhibitors (Roche). Fifty micrograms of total protein lysate, as determined using the Qubit™ fluorometer (Thermo Fisher Scientific), were resuspended in  $30 \mu\text{l}$  of Laemmli buffer (Thermo Fisher Scientific). All samples were heated at  $98^\circ\text{C}$  for 10 min, loaded onto NuPAGE® 4–12% gels and run at 120 V in 1 X MES buffer (Thermo Fisher Scientific). The separated proteins were transferred onto membranes using the iBlot® transfer system (Thermo Fisher Scientific), as per the manufacturer's instructions. The membranes were blocked using Odyssey® blocking buffer (Odyssey; LI-COR, NE, USA). Membranes were incubated with 0.5 ng/ml of goat-antihuman IL-33 antibody (clone AF3625; R&D Systems, MN, USA) overnight, at  $4^\circ\text{C}$ . Membranes were then washed in PBS-Tween 0.05% (v/v) and incubated for 2 hr with 0.67 ng/ml of rabbit-anti-goat secondary antibody-Alexa Fluor® 680 conjugate (Thermo Fisher Scientific). Membranes were washed and developed on the Odyssey Infrared Imaging System (LI-COR). As loading controls, lysate samples were probed with 0.9 ng/ml of rat-antihuman TUBULIN (Rockland, PA, USA), followed by 0.33 ng/ml of goat-antirat secondary antibody-Alexa Fluor® 800 conjugate (Thermo Fisher Scientific). The relative intensity figures for all blots are now presented in Table S1.



## 4.9 | Immunofluorescence

GECs were fixed with 4% (w/v) paraformaldehyde for 15 min, at room temperature. Cells were washed in PBS and incubated in blocking buffer (3% BSA [w/v] and 0.1% [w/v] saponin in PBS). After 1 hr, cells were incubated overnight, at 4 °C with 5 µg/ml of goat antihuman IL-33 primary (clone AF3625; R&D Systems). Samples were washed thrice with blocking buffer and incubated with anti-goat Alexa Fluor® 680-conjugated secondary antibody (1:500) for 1 hr. After washing, cell nuclei were stained with Hoechst 33342 (Thermo Fisher Scientific; 1:1,000) for 5 min before mounting. Imaging was performed on a confocal microscope (Nikon Instruments Inc., NY, USA; Monash Micro Imaging). Cytoplasmic to nuclear ratio measurements were carried out in the FIJI image analysis software on a single image plane extracted from the z-stacks captured by confocal microscopy. All images were captured using the same settings. Images of the cytoplasmic fractions were created by subtracting Hoechst-stained images from IL-33 stained images using the image calculator in FIJI. A threshold was applied to the stained area in the resulting cytoplasmic fraction image. The mean intensity was measured for the area under the threshold. After measuring the intensity, the threshold of the cytoplasmic fraction image was converted to a binary, which was then subtracted from the original IL-33 stained image, using the FIJI image calculator, to generate a nuclear fraction image. A threshold was then applied to the nuclear fraction image and mean intensity measured.

## 4.10 | ELISA

Human CXCL8 (BD Biosciences, NSW, Australia) and mouse KC, MIP-2 and IL-33 (DuoSet ELISA kit, R&D Systems) were quantified by ELISA, as per the manufacturers' instructions. Absorbance values were measured at 450 nm with a FLUOStar® Optima microplate reader (BMG Labtech, VIC, Australia). Cytokine levels were determined by linear or 4-parameter fit analysis.

## 4.11 | Mouse *H. pylori* infection

*Nod1*<sup>+/+</sup> and *Nod1*<sup>-/-</sup> mice (6–8-week old) were inoculated via oral gavage with 10<sup>8</sup> colony-forming units of *H. pylori* Strain 245 m3 (Philpott et al., 2002), using previously described techniques (Ferrero et al., 2012). Bacterial viability and numbers were determined by agar plate dilution (Ferrero et al., 2012). Stomachs and spleens were harvested from these animals at 1 and 8 weeks post-infection. Gastric tissues were subjected to homogenisation using a gentleMACS™ Dissociator (Miltenyi Biotec, NSW, Australia). Bacterial infection status was confirmed by bacteriological culture (Ferrero et al., 2012). Gastric homogenates were then centrifuged at 13,000 × g at 4 °C and the supernatants collected for analysis by the Qubit™ protein assay (Thermo Fisher Scientific), ELISA, and/or Western blotting.

## 4.12 | Cytokine production in splenocytes

Spleens were collected from euthanised mice. Single cell suspensions were obtained by grinding through 70 µm cell strainers. Splenocytes were recovered in RPMI complete medium and seeded at 2 × 10<sup>6</sup> cells/ml in 24-well plates. Cells were left untreated or stimulated with

5 µg/ml Concanavalin A (ConA; Sigma) then incubated for 3 days at 37 °C in 5% CO<sub>2</sub>.

ProcartaPlex Multiplex Immunoassays (eBioscience; Thermo Fisher Scientific) were performed according to the manufacturer's instructions to simultaneously quantify the levels of IL-4, IL-10, IL-13, IL-17, and IFN-γ in splenocyte culture supernatants. Briefly, culture supernatants (50 µl) or standards were mixed with 50 µl magnetic beads and incubated overnight at 4 °C. After washing thrice with washing buffer, 50 µl of streptavidin-PE was added and incubated with shaking for 30 min at RT. The mixtures were resuspended in 120 µl of reading buffer after washing thrice with wash buffer. Data were acquired on the Luminex® 100/200™ instrument (Bio-Rad, NSW, Australia). The concentrations of each cytokine were calculated using the ProcartaPlex® Analyst 1.0 Software (eBioscience).

## 4.13 | Statistical analyses

GraphPad Prism (GraphPad Software, CA, USA) was used for graph preparation and statistical analyses. For qPCR assays and ELISA, data were analysed by the Mann-Whitney test. Differences were considered statistically significant for *p* < .05.

## ACKNOWLEDGEMENTS

This project was funded by the National Health and Medical Research Council (NHMRC) to R. L. F. (project APP1079930). Research at the Hudson Institute of Medical Research, Murdoch Children's Research Institute, and Walter and Eliza Hall Institute is supported by the Victorian Government's Operational Infrastructure Support Program. R. L. F. is a Senior Research Fellow of the NHMRC (APP1079904). K. D. C. is supported by an International Postgraduate Scholarship (Monash University Faculty of Medicine, Nursing and Health Sciences) and funding from the Centre for Innate Immunity and Infectious Diseases.

## CONFLICT OF INTEREST

The authors have no conflict of interest to declare.

## ORCID

Richard L. Ferrero  <http://orcid.org/0000-0002-5382-3903>

## REFERENCES

- Allison, C. C., Kufer, T. A., Kremmer, E., Kaparakis, M., & Ferrero, R. L. (2009). *Helicobacter pylori* induces MAPK phosphorylation and AP-1 activation via a NOD1-dependent mechanism. *Journal of Immunology*, 183, 8099–8109.
- Baker, P. J., De Nardo, D., Moghaddas, F., Tran, L. S., Bachem, A., Nguyen, T., ... Masters, S. L. (2017). Posttranslational modification as a critical determinant of cytoplasmic innate immune recognition. *Physiological Reviews*, 97, 1165–1209.
- Berg, D. J., Lynch, N. A., Lynch, R. G., & Lauricella, D. M. (1998). Rapid development of severe hyperplastic gastritis with gastric epithelial dedifferentiation in *Helicobacter felis*-infected IL-10(−/−) mice. *The American Journal of Pathology*, 152, 1377–1386.
- Boonyanugomol, W., Chomvarin, C., Hahnvanjanawong, C., Sripan, B., Kaparakis-Liaskos, M., & Ferrero, R. L. (2013). *Helicobacter pylori* cag pathogenicity island (cagPAI) involved in bacterial internalization and IL-8 induced responses via NOD1- and MyD88-dependent mechanisms in human biliary epithelial cells. *PLoS One*, 8, e77358.



- Buzzelli, J. N., Chalinor, H. V., Pavlic, D. I., Sutton, P., Menheniott, T. R., Giraud, A. S., Judd, L. M. (2015). IL33 is a stomach alarmin that initiates a skewed Th2 response to injury and infection. *Cellular and Molecular Gastroenterology and Hepatology*, 1, 203–21.e3.
- Carriere, V., Roussel, L., Ortega, N., Lacorre, D. A., Americh, L., Aguilar, L., ... Girard, J. P. (2007). IL-33, the IL-1-like cytokine ligand for ST2 receptor, is a chromatin-associated nuclear factor in vivo. *Proceedings of the National Academy of Sciences of the United States of America*, 104, 282–287.
- Cayrol, C., & Girard, J. P. (2009). The IL-1-like cytokine IL-33 is inactivated after maturation by caspase-1. *Proceedings of the National Academy of Sciences of the United States of America*, 106, 9021–9026.
- Chen, W., Shu, D., & Chadwick, V. S. (2001). *Helicobacter pylori* infection: Mechanism of colonization and functional dyspepsia reduced colonization of gastric mucosa by *Helicobacter pylori* in mice deficient in interleukin-10. *Journal of Gastroenterology and Hepatology*, 16, 377–383.
- Correa, R. G., Khan, P. M., Askari, N., Zhai, D., Gerlic, M., Brown, B., ... Reed, J. C. (2011). Discovery and characterization of 2-aminobenzimidazole derivatives as selective NOD1 inhibitors. *Chemistry & Biology*, 18, 825–832.
- Farias, R., & Rousseau, S. (2015). The TAK1--IKKbeta-->TPL2-->MKK1/MKK2 signaling cascade regulates IL-33 expression in cystic fibrosis airway epithelial cells following infection by *Pseudomonas aeruginosa*. *Frontiers in Cell and Developmental Biology*, 3, 87.
- Ferrero, R. L., Ave, P., Ndiaye, D., Bambou, J. C., Huerre, M. R., Philpott, D. J., ... Memet, S. (2008). NF-kappaB activation during acute *Helicobacter pylori* infection in mice. *Infection and Immunity*, 76, 551–561.
- Ferrero, R. L., Wilson, J. E., & Sutton, P. (2012). Mouse models of *Helicobacter*-induced gastric cancer: Use of cocarcinogens. *Methods in Molecular Biology (Clifton, NJ)*, 921, 157–173.
- Gall, A., Gaudet, R. G., Gray-Owen, S. D., & Salama, N. R. (2017). TIFA signaling in gastric epithelial cells initiates the cag type 4 secretion system-dependent innate immune response to *Helicobacter pylori* infection. *MBio*, 8, e01168-17.
- Gao, X., Wang, X., Yang, Q., Zhao, X., Wen, W., Li, G., ... Lu, B. (2015). Tumoral expression of IL-33 inhibits tumor growth and modifies the tumor microenvironment through CD8+ T and NK cells. *Journal of Immunology*, 194, 438–445.
- Gaudet, R. G., Guo, C. X., Molinaro, R., Kottwitz, H., Rohde, J. R., Dangeard, A. S., ... Gray-Owen, S. D. (2017). Innate recognition of intracellular bacterial growth is driven by the TIFA-dependent cytosolic surveillance pathway. *Cell Reports*, 19, 1418–1430.
- Gautier, V., Cayrol, C., Farache, D., Roga, S., Monsarrat, B., Burlet-Schiltz, O., ... Girard, J. P. (2016). Extracellular IL-33 cytokine, but not endogenous nuclear IL-33, regulates protein expression in endothelial cells. *Scientific Reports*, 6, 34255.
- Grubman, A., Kaparakis, M., Viala, J., Allison, C., Badea, L., Karrar, A., ... Ferrero, R. L. (2010). The innate immune molecule, NOD1, regulates direct killing of *Helicobacter pylori* by antimicrobial peptides. *Cellular Microbiology*, 12, 626–639.
- Hasegawa, M., Fujimoto, Y., Lucas, P. C., Nakano, H., Fukase, K., Nunez, G., Inohara, N. (2008). A critical role of RICK/RIP2 polyubiquitination in Nod-induced NF-kappaB activation. *The EMBO Journal*, 27, 373–383.
- Hitzler, I., Kohler, E., Engler, D. B., Yazgan, A. S., & Muller, A. (2012). The role of Th cell subsets in the control of *Helicobacter* infections and in T cell-driven gastric immunopathology. *Frontiers in Immunology*, 3, 142.
- Inohara, N., Koseki, T., del Peso, L., Hu, Y., Yee, C., Chen, S., ... Núñez, G. (1999). Nod1, an Apaf-1-like activator of caspase-9 and nuclear factor-kappaB. *The Journal of Biological Chemistry*, 274, 14560–14567.
- Inohara, N., Koseki, T., Lin, J., del Peso, L., Lucas, P. C., Chen, F. F., ... Núñez, G. (2000). An induced proximity model for NF-kappa B activation in the Nod1/RICK and RIP signaling pathways. *The Journal of Biological Chemistry*, 275, 27823–27831.
- Irving, A. T., Mimuro, H., Kufer, T. A., Lo, C., Wheeler, R., Turner, L. J., ... Kaparakis-Liaskos, M. (2014). The immune receptor NOD1 and kinase RIP2 interact with bacterial peptidoglycan on early endosomes to promote autophagy and inflammatory signaling. *Cell Host & Microbe*, 15, 623–635.
- Kaparakis, M., Turnbull, L., Carneiro, L., Firth, S., Coleman, H. A., Parkinson, H. C., ... Ferrero, R. L. (2010). Bacterial membrane vesicles deliver peptidoglycan to NOD1 in epithelial cells. *Cellular Microbiology*, 12, 372–385.
- Kobori, A., Yagi, Y., Imaeda, H., Ban, H., Bamba, S., Tsujikawa, T., ... Andoh, A. (2010). Interleukin-33 expression is specifically enhanced in inflamed mucosa of ulcerative colitis. *Journal of Gastroenterology*, 45, 999–1007.
- Kuchler, A. M., Pollheimer, J., Balogh, J., Sponheim, J., Manley, L., Sorensen, D. R., ... Haraldsen, G. (2008). Nuclear interleukin-33 is generally expressed in resting endothelium but rapidly lost upon angiogenic or proinflammatory activation. *The American Journal of Pathology*, 173, 1229–1242.
- Lee, A., O'Rourke, J., De Ungria, M. C., Robertson, B., Daskalopoulos, G., & Dixon, M. F. (1997). A standardized mouse model of *Helicobacter pylori* infection: Introducing the Sydney strain. *Gastroenterology*, 112, 1386–1397.
- Lefrancais, E., Roga, S., Gautier, V., Gonzalez-de-Peredo, A., Monsarrat, B., Girard, J. P., ... Cayrol, C. (2012). IL-33 is processed into mature bioactive forms by neutrophil elastase and cathepsin G. *Proceedings of the National Academy of Sciences of the United States of America*, 109, 1673–1678.
- Liew, F. Y., Girard, J. P., & Turnquist, H. R. (2016). Interleukin-33 in health and disease. *Nature Reviews Immunology*, 16, 676–689.
- Lopetuso, L. R., Chowdhry, S., & Pizarro, T. T. (2013). Opposing functions of classic and novel IL-1 family members in gut health and disease. *Frontiers in Immunology*, 4, 181.
- Martin, N. T., & Martin, M. U. (2016). Interleukin 33 is a guardian of barriers and a local alarmin. *Nature Immunology*, 17, 122–131.
- Molofsky, A. B., Savage, A. K., & Locksley, R. M. (2015). Interleukin-33 in tissue homeostasis, injury, and inflammation. *Immunity*, 42, 1005–1019.
- Moussion, C., Ortega, N., & Girard, J. P. (2008). The IL-1-like cytokine IL-33 is constitutively expressed in the nucleus of endothelial cells and epithelial cells in vivo: A novel 'alarmin'? *PLoS One*, 3, e3331.
- Nachbur, U., Stafford, C. A., Bankovacki, A., Zhan, Y., Lindqvist, L. M., Fiil, B. K., ... Silke, J. (2015). A RIPK2 inhibitor delays NOD signalling events yet prevents inflammatory cytokine production. *Nature Communications*, 6, 6442.
- Olofsson, A., Vallstrom, A., Petzold, K., Tegtmeyer, N., Schleucher, J., Carlsson, S., ... Arnqvist, A. (2010). Biochemical and functional characterization of *Helicobacter pylori* vesicles. *Molecular Microbiology*, 77, 1539–1555.
- Peek, R. M. Jr., & Crabtree, J. E. (2006). *Helicobacter* infection and gastric neoplasia. *The Journal of Pathology*, 208, 233–248.
- Philpott, D. J., Belaid, D., Troubadour, P., Thiberge, J. M., Tankovic, J., Labigne, A., ... Ferrero, R. L. (2002). Reduced activation of inflammatory responses in host cells by mouse-adapted *Helicobacter pylori* isolates. *Cellular Microbiology*, 4, 285–296.
- Rad, R., Brenner, L., Bauer, S., Schwendy, S., Layland, L., da Costa, C. P., ... Prinz, C. (2006). CD25+/Foxp3+ T cells regulate gastric inflammation and *Helicobacter pylori* colonization in vivo. *Gastroenterology*, 131, 525–537.
- Ran, F. A., Hsu, P. D., Lin, C. Y., Gootenberg, J. S., Konermann, S., Trevino, A. E., ... Zhang, F. (2013). Double nicking by RNA-guided CRISPR Cas9 for enhanced genome editing specificity. *Cell*, 154, 1380–1389.
- Sawai, N., Kita, M., Kodama, T., Tanahashi, T., Yamaoka, Y., Tagawa, Y., ... Imanishi, J. (1999). Role of gamma interferon in *Helicobacter pylori*-induced gastric inflammatory responses in a mouse model. *Infection and Immunity*, 67, 279–285.
- Sayi, A., Kohler, E., Hitzler, I., Arnold, I., Schwendener, R., Rehrauer, H., Müller, A. (2009). The CD4+ T cell-mediated IFN-gamma response to *Helicobacter* infection is essential for clearance and determines gastric cancer risk. *Journal of Immunology*, 182, 7085–7101.
- Schmitz, J., Owyang, A., Oldham, E., Song, Y., Murphy, E., McClanahan, T. K., ... Kastelein, R. A. (2005). IL-33, an interleukin-1-like cytokine that

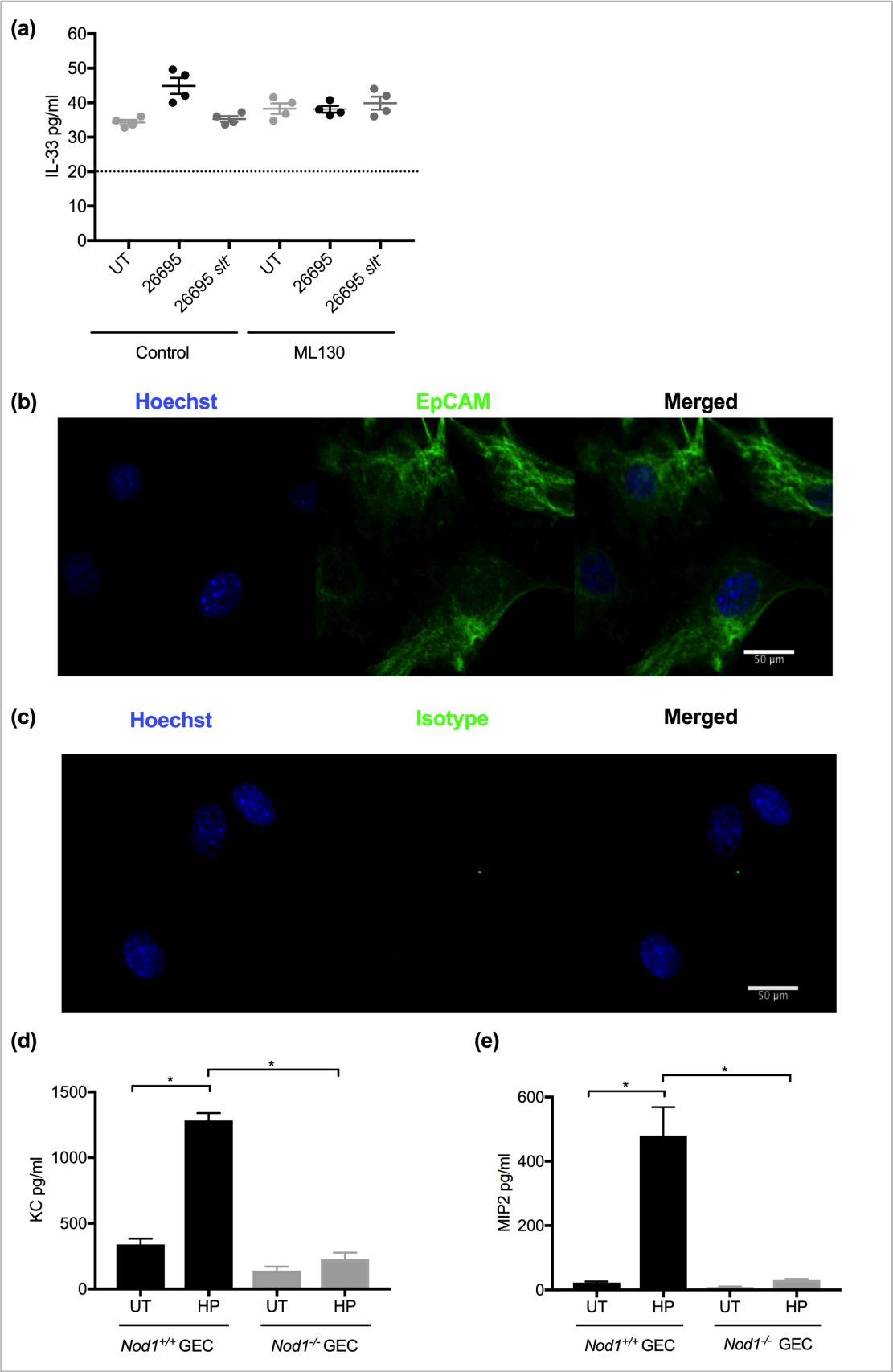
- signals via the IL-1 receptor-related protein ST2 and induces T helper type 2-associated cytokines. *Immunity*, 23, 479–490.
- Shahi, H., Reisi, S., Bahreini, R., Bagheri, N., Salimzadeh, L., & Shirzad, H. (2015). Association between *Helicobacter pylori* cagA, babA2 virulence factors and gastric mucosal Interleukin-33 mRNA expression and clinical outcomes in dyspeptic patients. *International Journal of Molecular and Cellular Medicine*, 4, 227–234.
- Smythies, L. E., Waites, K. B., Lindsey, J. R., Harris, P. R., Ghiara, P., & Smith, P. D. (2000). *Helicobacter pylori*-induced mucosal inflammation is Th1 mediated and exacerbated in IL-4, but not IFN- $\gamma$ , gene-deficient mice. *Journal of Immunology*, 165, 1022–1029.
- Stein, S. C., Faber, E., Bats, S. H., Murillo, T., Speidel, Y., Coombs, N., Josenhans, C. (2017). *Helicobacter pylori* modulates host cell responses by CagT4SS-dependent translocation of an intermediate metabolite of LPS inner core heptose biosynthesis. *PLoS Pathogens*, 13, e1006514.
- Tran, L. S., Chonwerawong, M., & Ferrero, R. L. (2017). Regulation and functions of inflammasome-mediated cytokines in *Helicobacter pylori* infection. *Microbes and Infection*, 19, 449–458.
- Viala, J., Chaput, C., Boneca, I. G., Cardona, A., Girardin, S. E., Moran, A. P., ... Ferrero, R. L. (2004). Nod1 responds to peptidoglycan delivered by the *Helicobacter pylori* cag pathogenicity island. *Nature Immunology*, 5, 1166–1174.

#### SUPPORTING INFORMATION

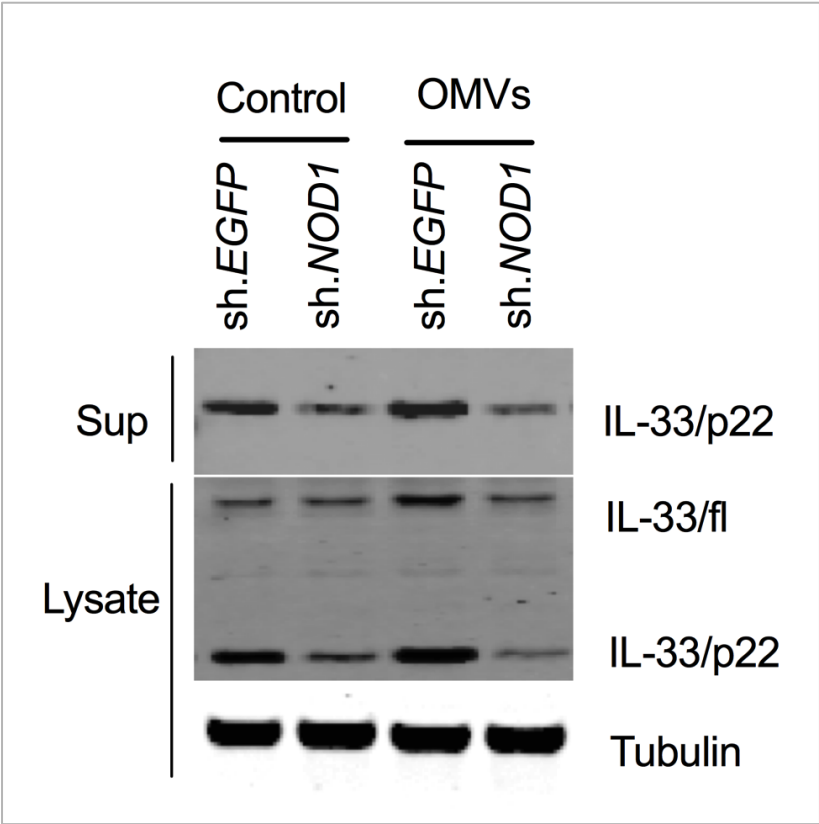
Additional Supporting Information may be found online in the supporting information tab for this article.

**How to cite this article:** Tran LS, Tran D, De Paoli A, et al. NOD1 is required for *Helicobacter pylori* induction of IL-33 responses in gastric epithelial cells. *Cellular Microbiology*. 2018;20:e12826. <https://doi.org/10.1111/cmi.12826>

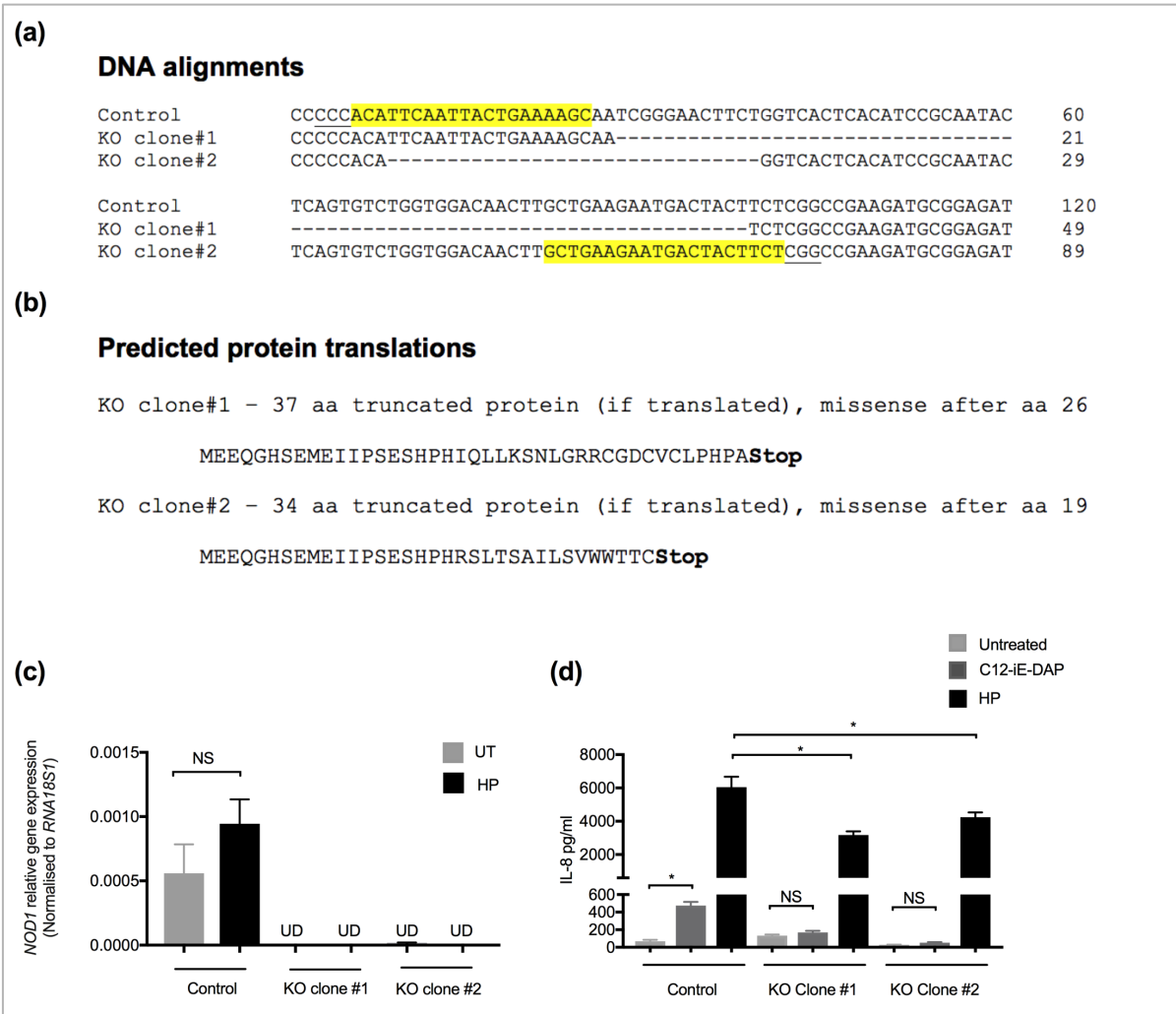
Supplementary Figure 1



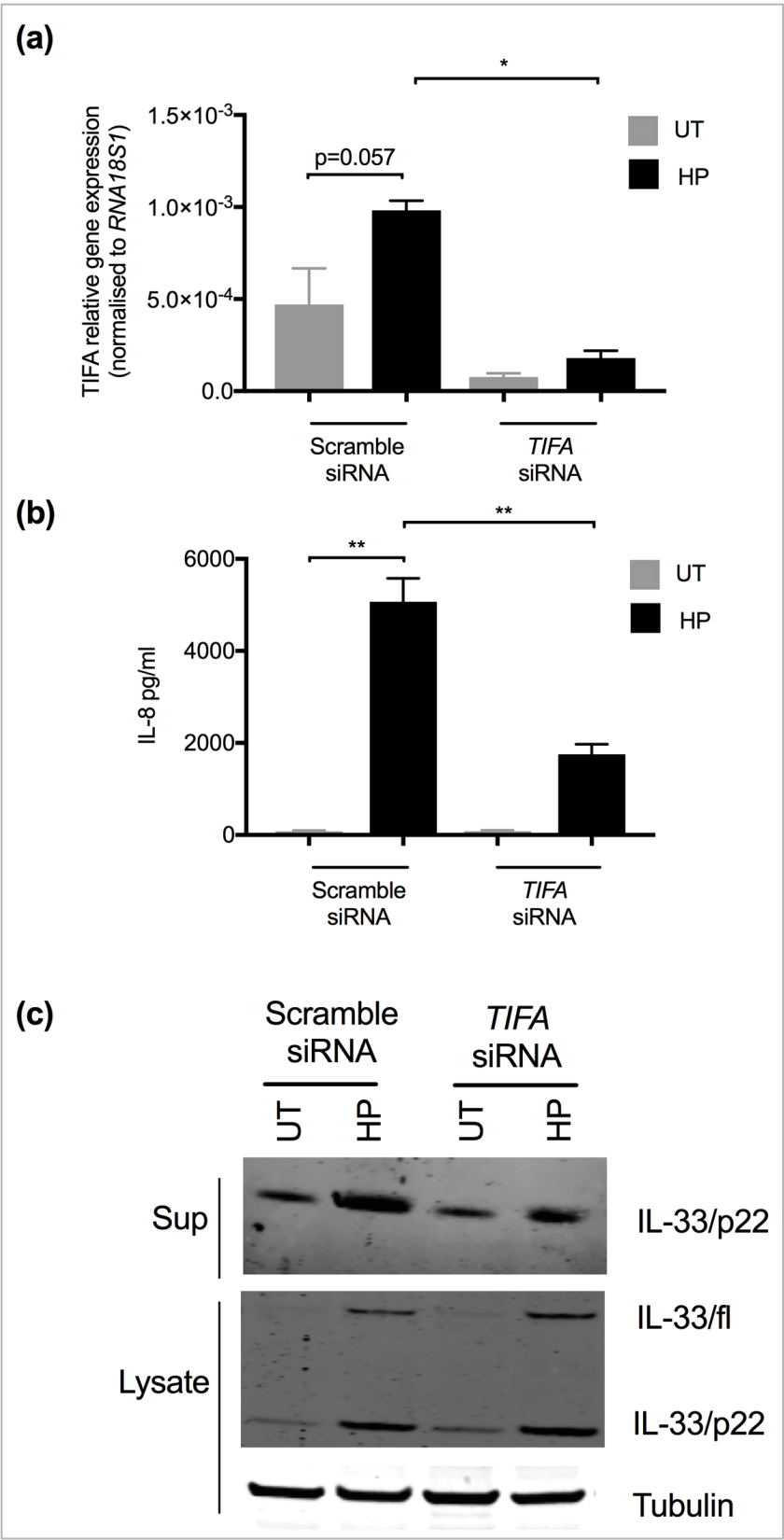
Supplementary Figure 2



Supplementary Figure 3



Supplementary Figure 4



**Supplementary Table 1:** The relative densitometry intensities calculated for each protein band and normalised to Tubulin.

Figure	Band	Lane					
		1	2	3	4	5	6
1c	SUP IL-33/p22	0.29	0.60	0.04	0.27		
	LYS IL-33/fl	0.30	0.69	0.28	0.20		
	LYS IL-33/p22	0.14	0.81	0.05	0.08		
1d	SUP IL-33/p22	0.19	0.21	0.15	0.27	0.32	0.53
	LYS IL-33/fl	0.16	0.21	0.29	0.40	0.43	0.56
	LYS IL-33/p22	0.10	0.19	0.24	0.25	0.39	0.40
1e	SUP IL-33/p22	0.39	0.59	0.40	0.02	0.02	0.13
	LYS IL-33/fl	0.16	0.43	0.06	0.20	0.19	0.27
	LYS IL-33/p22	0.19	0.32	0.12	0.16	0.26	0.15
1h	SUP IL-33/p22	0.36	0.66	0.11	0.12	0.15	0.28
	LYS IL-33/fl	0.25	0.58	0.17	0.31	0.27	0.33
	LYS IL-33/p22	0.15	0.30	0.18	0.17	0.41	0.25
2d	SUP IL-33/p22	0.49	0.63	0.36	0.23		
	LYS IL-33/fl	0.24	0.66	0.21	0.59		
	LYS IL-33/p22	0.16	0.34	0.25	0.29		
2e	SUP IL-33/p22	0.24	0.89	0.08	0.47	0.14	0.58
	LYS IL-33/fl	0.64	1.02	0.26	0.63	0.42	0.56
	LYS IL-33/p22	0.73	0.91	0.69	0.13	0.24	0.20
5c	IL-33/fl	0.69	1.21	0.04	0.44		
	IL-33/p22	0.28	1.27	0.19	0.53		

## **References**

1. Backhed, F., et al., *Gastric mucosal recognition of Helicobacter pylori is independent of Toll-like receptor 4*. J Infect Dis, 2003. **187**(5): p. 829-36.
2. Linz, B., et al., *An African origin for the intimate association between humans and Helicobacter pylori*. Nature, 2007. **445**(7130): p. 915-918.
3. Jiang, X. and M.P. Doyle, *Effect of environmental and substrate factors on survival and growth of Helicobacter pylori*. J Food Prot, 1998. **61**(8): p. 929-33.
4. Brown, L.M., *Helicobacter pylori: epidemiology and routes of transmission*. Epidemiol Rev, 2000. **22**(2): p. 283-97.
5. Necchi, V., et al., *Intracellular, intercellular, and stromal invasion of gastric mucosa, preneoplastic lesions, and cancer by Helicobacter pylori*. Gastroenterology, 2007. **132**(3): p. 1009-23.
6. Algood, H.M. and T.L. Cover, *Helicobacter pylori persistence: an overview of interactions between H. pylori and host immune defenses*. Clin Microbiol Rev, 2006. **19**(4): p. 597-613.
7. Hutton, M.L., M. Kaparakis-Liaskos, and R.L. Ferrero, *The use of AlbuMAX II(R) as a blood or serum alternative for the culture of Helicobacter pylori*. Helicobacter, 2012. **17**(1): p. 68-76.
8. Westblom, T.U., S. Gudipati, and B.R. Midkiff, *Enhanced growth of Helicobacter pylori using a liquid medium supplemented with human serum*. European Journal of Clinical Microbiology and Infectious Diseases, 1995. **14**(2): p. 155-156.
9. Henriksen, T.H., et al., *Rapid growth of Helicobacter pylori*. Eur J Clin Microbiol Infect Dis, 1995. **14**(11): p. 1008-11.
10. Montecucco, C. and R. Rappuoli, *Living dangerously: how Helicobacter pylori survives in the human stomach*. Nat Rev Mol Cell Biol, 2001. **2**(6): p. 457-66.
11. Polk, D.B. and R.M. Peek, Jr., *Helicobacter pylori: gastric cancer and beyond*. Nat Rev Cancer, 2010. **10**(6): p. 403-14.
12. Gisbert, J.P., *Helicobacter pylori-related diseases: dyspepsia, ulcers and gastric cancer*. Gastroenterol Hepatol, 2011. **34 Suppl 2**: p. 15-26.



13. Kraft, C. and S. Suerbaum, *Mutation and recombination in Helicobacter pylori: mechanisms and role in generating strain diversity*. Int J Med Microbiol, 2005. **295**(5): p. 299-305.
14. Björkholm, B., et al., *Mutation frequency and biological cost of antibiotic resistance in Helicobacter pylori*. Proceedings of the National Academy of Sciences of the United States of America, 2001. **98**(25): p. 14607-14612.
15. Suerbaum, S. and P. Michetti, *Helicobacter pylori infection*. N Engl J Med, 2002. **347**(15): p. 1175-86.
16. Pandeya, N. and D.C. Whiteman, *Prevalence and determinants of Helicobacter pylori sero-positivity in the Australian adult community*. J Gastroenterol Hepatol, 2011. **26**(8): p. 1283-9.
17. Trainor, E.A., et al., *Role of the HefC efflux pump in Helicobacter pylori cholesterol-dependent resistance to ceragenins and bile salts*. Infect Immun, 2011. **79**(1): p. 88-97.
18. Vakil, N. and F. Megraud, *Eradication therapy for Helicobacter pylori*. Gastroenterology, 2007. **133**(3): p. 985-1001.
19. McGee, D.J., et al., *Cholesterol enhances Helicobacter pylori resistance to antibiotics and LL-37*. Antimicrob Agents Chemother, 2011. **55**(6): p. 2897-904.
20. Peek, R.M., Jr., C. Fiske, and K.T. Wilson, *Role of innate immunity in Helicobacter pylori-induced gastric malignancy*. Physiol Rev, 2010. **90**(3): p. 831-58.
21. Ottemann, K.M. and A.C. Lowenthal, *Helicobacter pylori uses motility for initial colonization and to attain robust infection*. Infect Immun, 2002. **70**(4): p. 1984-90.
22. Rieder, G., W. Fischer, and R. Haas, *Interaction of Helicobacter pylori with host cells: function of secreted and translocated molecules*. Current opinion in microbiology, 2005. **8**(1): p. 67-73.
23. Mobley, H.L., L.T. Hu, and P.A. Foxal, *Helicobacter pylori urease: properties and role in pathogenesis*. Scand J Gastroenterol Suppl, 1991. **187**: p. 39-46.
24. Kong, L., et al., *A sensitive and specific PCR method to detect Helicobacter felis in a conventional mouse model*. Clinical and Diagnostic Laboratory Immunology, 1996. **3**(1): p. 73-78.

25. Tomb, J.F., et al., *The complete genome sequence of the gastric pathogen Helicobacter pylori*. Nature, 1997. **388**(6642): p. 539-47.
26. Clyne, M., B. Dolan, and E.P. Reeves, *Bacterial factors that mediate colonization of the stomach and virulence of Helicobacter pylori*. FEMS Microbiol Lett, 2007. **268**(2): p. 135-43.
27. Odenbreit, S., et al., *Translocation of Helicobacter pylori CagA into gastric epithelial cells by type IV secretion*. Science, 2000. **287**(5457): p. 1497-500.
28. Hatakeyama, M., *Oncogenic mechanisms of the Helicobacter pylori CagA protein*. Nat Rev Cancer, 2004. **4**(9): p. 688-94.
29. Kauser, F., et al., *The cag pathogenicity island of Helicobacter pylori is disrupted in the majority of patient isolates from different human populations*. J Clin Microbiol, 2004. **42**(11): p. 5302-8.
30. Crabtree, J.E., et al., *Helicobacter pylori induced interleukin-8 expression in gastric epithelial cells is associated with CagA positive phenotype*. J Clin Pathol, 1995. **48**(1): p. 41-5.
31. Yamaoka, Y., et al., *Helicobacter pylori cagA gene and expression of cytokine messenger RNA in gastric mucosa*. Gastroenterology, 1996. **110**(6): p. 1744-52.
32. Bourzac, K.M. and K. Guillemin, *Helicobacter pylori-host cell interactions mediated by type IV secretion*. Cell Microbiol, 2005. **7**(7): p. 911-9.
33. Kwok, T., et al., *Helicobacter exploits integrin for type IV secretion and kinase activation*. Nature, 2007. **449**(7164): p. 862-6.
34. Hutton, M.L., et al., *Helicobacter pylori exploits cholesterol-rich microdomains for induction of NF-kappaB-dependent responses and peptidoglycan delivery in epithelial cells*. Infect Immun, 2010. **78**(11): p. 4523-31.
35. Viala, J., et al., *Nod1 responds to peptidoglycan delivered by the Helicobacter pylori cag pathogenicity island*. Nat Immunol, 2004. **5**(11): p. 1166-74.
36. Backert, S. and M. Selbach, *Role of type IV secretion in Helicobacter pylori pathogenesis*. Cell Microbiol, 2008. **10**(8): p. 1573-81.
37. Gorrell, R.J., et al., *A novel NOD1- and CagA-independent pathway of interleukin-8 induction mediated by the Helicobacter pylori type IV secretion system*. Cell Microbiol, 2013. **15**(4): p. 554-70.

38. Wiedemann, T., et al., *Helicobacter pylori CagL dependent induction of gastrin expression via a novel alphavbeta5-integrin-integrin linked kinase signalling complex*. Gut, 2012. **61**(7): p. 986-96.
39. Sharma, S.A., et al., *Activation of IL-8 Gene Expression by Helicobacter pylori Is Regulated by Transcription Factor Nuclear Factor- $\kappa$ B in Gastric Epithelial Cells*. The Journal of Immunology, 1998. **160**(5): p. 2401.
40. Terradot, L. and G. Waksman, *Architecture of the Helicobacter pylori Cag-type IV secretion system*. FEBS Journal, 2011. **278**(8): p. 1213-1222.
41. Covacci, A., et al., *Molecular characterization of the 128-kDa immunodominant antigen of Helicobacter pylori associated with cytotoxicity and duodenal ulcer*. Proc Natl Acad Sci U S A, 1993. **90**(12): p. 5791-5.
42. Lai, C.H., et al., *Cholesterol depletion reduces Helicobacter pylori CagA translocation and CagA-induced responses in AGS cells*. Infect Immun, 2008. **76**(7): p. 3293-303.
43. Stein, M., R. Rappuoli, and A. Covacci, *Tyrosine phosphorylation of the Helicobacter pylori CagA antigen after cag-driven host cell translocation*. Proceedings of the National Academy of Sciences of the United States of America, 2000. **97**(3): p. 1263-1268.
44. Backert, S., N. Tegtmeyer, and W. Fischer, *Composition, structure and function of the Helicobacter pylori cag pathogenicity island encoded type IV secretion system*. Future Microbiol, 2015. **10**(6): p. 955-65.
45. Segal, E.D., et al., *Altered states: involvement of phosphorylated CagA in the induction of host cellular growth changes by Helicobacter pylori*. Proc Natl Acad Sci U S A, 1999. **96**(25): p. 14559-64.
46. Bagnoli, F., et al., *Helicobacter pylori CagA induces a transition from polarized to invasive phenotypes in MDCK cells*. Proc Natl Acad Sci U S A, 2005. **102**(45): p. 16339-44.
47. Mimuro, H., et al., *Helicobacter pylori Dampens Gut Epithelial Self-Renewal by Inhibiting Apoptosis, a Bacterial Strategy to Enhance Colonization of the Stomach*. Cell Host & Microbe, 2007. **2**(4): p. 250-263.
48. Crawford, H.C., et al., *Helicobacter pylori strain-selective induction of matrix metalloproteinase-7 in vitro and within gastric mucosa*. Gastroenterology. **125**(4): p. 1125-1136.

49. Peek, R.M., Jr., et al., *Helicobacter pylori cagA<sup>+</sup> strains and dissociation of gastric epithelial cell proliferation from apoptosis*. J Natl Cancer Inst, 1997. **89**(12): p. 863-8.
50. Naumann, M., et al., *Helicobacter pylori: A Paradigm Pathogen for Subverting Host Cell Signal Transmission*. Trends Microbiol, 2017. **25**(4): p. 316-328.
51. Woodhams, K.L., et al., *Peptidoglycan fragment release from Neisseria meningitidis*. Infect Immun, 2013. **81**(9): p. 3490-8.
52. Cloud-Hansen, K.A., et al., *Breaching the great wall: peptidoglycan and microbial interactions*. Nat Rev Microbiol, 2006. **4**(9): p. 710-6.
53. Burroughs, M., et al., *The biologic activities of peptidoglycan in experimental Haemophilus influenzae meningitis*. J Infect Dis, 1993. **167**(2): p. 464-8.
54. Luker, K.E., et al., *Bordetella pertussis tracheal cytotoxin and other muramyl peptides: distinct structure-activity relationships for respiratory epithelial cytopathology*. Proceedings of the National Academy of Sciences, 1993. **90**(6): p. 2365-2369.
55. Kaparakis, M., et al., *Bacterial membrane vesicles deliver peptidoglycan to NOD1 in epithelial cells*. Cell Microbiol, 2010. **12**(3): p. 372-85.
56. Kaparakis-Liaskos, M. and R.L. Ferrero, *Immune modulation by bacterial outer membrane vesicles*. Nat Rev Immunol, 2015. **15**(6): p. 375-87.
57. Fiocca, R., et al., *Release of Helicobacter pylori vacuolating cytotoxin by both a specific secretion pathway and budding of outer membrane vesicles. Uptake of released toxin and vesicles by gastric epithelium*. J Pathol, 1999. **188**(2): p. 220-6.
58. Renelli, M., et al., *DNA-containing membrane vesicles of Pseudomonas aeruginosa PAO1 and their genetic transformation potential*. Microbiology, 2004. **150**(Pt 7): p. 2161-9.
59. Kuehn, M.J. and N.C. Kesty, *Bacterial outer membrane vesicles and the host-pathogen interaction*. Genes Dev, 2005. **19**(22): p. 2645-55.
60. Irving, A.T., et al., *The immune receptor NOD1 and kinase RIP2 interact with bacterial peptidoglycan on early endosomes to promote autophagy and inflammatory signaling*. Cell Host Microbe, 2014. **15**(5): p. 623-35.
61. Girardin, S.E., et al., *Nod1 detects a unique muropeptide from gram-negative bacterial peptidoglycan*. Science, 2003. **300**(5625): p. 1584-7.

62. Inohara, N., et al., *An induced proximity model for NF-kappa B activation in the Nod1/RICK and RIP signaling pathways*. J Biol Chem, 2000. **275**(36): p. 27823-31.
63. Kobayashi, K., et al., *RICK/Rip2/CARDIAK mediates signalling for receptors of the innate and adaptive immune systems*. Nature, 2002. **416**(6877): p. 194-199.
64. Allison, C.C., et al., *Helicobacter pylori induces MAPK phosphorylation and AP-1 activation via a NOD1-dependent mechanism*. J Immunol, 2009. **183**(12): p. 8099-109.
65. Watanabe, T., et al., *NOD1 contributes to mouse host defense against Helicobacter pylori via induction of type I IFN and activation of the ISGF3 signaling pathway*. J Clin Invest, 2010. **120**(5): p. 1645-62.
66. Fan, Y.-H., et al., *Role of nucleotide-binding oligomerization domain 1 (NOD1) and its variants in human cytomegalovirus control in vitro and in vivo*. Proceedings of the National Academy of Sciences, 2016. **113**(48): p. E7818-E7827.
67. Grubman, A., et al., *The innate immune molecule, NOD1, regulates direct killing of Helicobacter pylori by antimicrobial peptides*. Cell Microbiol, 2010. **12**(5): p. 626-39.
68. Chaput, C., et al., *Role of AmiA in the morphological transition of Helicobacter pylori and in immune escape*. PLoS Pathog, 2006. **2**(9): p. e97.
69. Sycuro, L.K., et al., *Multiple peptidoglycan modification networks modulate Helicobacter pylori's cell shape, motility, and colonization potential*. PLoS Pathog, 2012. **8**(3): p. e1002603.
70. Yang, Y., et al. *Role of caspase-3/E-cadherin in helicobacter pylori-induced apoptosis of gastric epithelial cells*. Oncotarget, 2017. **8**, 59204-59216 DOI: 10.18632/oncotarget.19471.
71. Wang, G., et al., *Helicobacter pylori peptidoglycan modifications confer lysozyme resistance and contribute to survival in the host*. MBio, 2012. **3**(6): p. e00409-12.
72. Chaput, C., A. Labigne, and I.G. Boneca, *Characterization of Helicobacter pylori lytic transglycosylases Slt and MltD*. J Bacteriol, 2007. **189**(2): p. 422-9.

73. Roure, S., et al., *Peptidoglycan maturation enzymes affect flagellar functionality in bacteria*. Molecular Microbiology, 2012. **86**(4): p. 845-856.
74. Cover, T.L., *The vacuolating cytotoxin of Helicobacter pylori*. Mol Microbiol, 1996. **20**(2): p. 241-6.
75. Phadnis, S.H., et al., *Pathological significance and molecular characterization of the vacuolating toxin gene of Helicobacter pylori*. Infect Immun, 1994. **62**(5): p. 1557-65.
76. Atherton, J.C., et al., *Mosaicism in vacuolating cytotoxin alleles of Helicobacter pylori. Association of specific vacA types with cytotoxin production and peptic ulceration*. J Biol Chem, 1995. **270**(30): p. 17771-7.
77. Atherton, J.C., et al., *Clinical and pathological importance of heterogeneity in vacA, the vacuolating cytotoxin gene of Helicobacter pylori*. Gastroenterology, 1997. **112**(1): p. 92-9.
78. Cover, T.L., et al., *Divergence of genetic sequences for the vacuolating cytotoxin among Helicobacter pylori strains*. J Biol Chem, 1994. **269**(14): p. 10566-73.
79. Chung, C., et al., *Diversity of VacA intermediate region among Helicobacter pylori strains from several regions of the world*. J Clin Microbiol, 2010. **48**(3): p. 690-6.
80. Ricci, V., M. Romano, and P. Boquet, *Molecular cross-talk between Helicobacter pylori and human gastric mucosa*. World Journal of Gastroenterology : WJG, 2011. **17**(11): p. 1383-1399.
81. Jang, S., et al., *Epidemiological link between gastric disease and polymorphisms in VacA and CagA*. J Clin Microbiol, 2010. **48**(2): p. 559-67.
82. Rieder, G., W. Fischer, and R. Haas, *Interaction of Helicobacter pylori with host cells: function of secreted and translocated molecules*. Curr Opin Microbiol, 2005. **8**(1): p. 67-73.
83. Cover, T.L. and S.R. Blanke, *Helicobacter pylori VacA, a paradigm for toxin multifunctionality*. Nat Rev Microbiol, 2005. **3**(4): p. 320-32.
84. Gebert, B., et al., *Helicobacter pylori vacuolating cytotoxin inhibits T lymphocyte activation*. Science, 2003. **301**(5636): p. 1099-102.
85. Tombola, F., et al., *The Helicobacter pylori VacA toxin is a urea permease that promotes urea diffusion across epithelia*. J Clin Invest, 2001. **108**(6): p. 929-37.

86. Schoep, T.D., et al., *Surface properties of Helicobacter pylori urease complex are essential for persistence*. PLoS One, 2010. **5**(11): p. e15042.
87. Ansorg, R., et al., *Cholesterol binding of Helicobacter pylori*. Zentralbl Bakteriол, 1992. **276**(3): p. 323-9.
88. Inamoto, Y., et al., *Lipid composition and fatty acid analysis of Helicobacter pylori*. J Gastroenterol, 1995. **30**(3): p. 315-8.
89. Hirai, Y., et al., *Unique cholesteryl glucosides in Helicobacter pylori: composition and structural analysis*. J Bacteriol, 1995. **177**(18): p. 5327-33.
90. Wunder, C., et al., *Cholesterol glucosylation promotes immune evasion by Helicobacter pylori*. Nat Med, 2006. **12**(9): p. 1030-8.
91. Wang, H.J., et al., *Helicobacter pylori cholesteryl glucosides interfere with host membrane phase and affect type IV secretion system function during infection in AGS cells*. Mol Microbiol, 2012. **83**(1): p. 67-84.
92. Testerman, T.L., D.J. McGee, and H.L. Mobley, *Helicobacter pylori growth and urease detection in the chemically defined medium Ham's F-12 nutrient mixture*. J Clin Microbiol, 2001. **39**(11): p. 3842-50.
93. Trampenau, C. and K.-D. Müller, *Affinity of Helicobacter pylori to cholesterol and other steroids*. Microbes and infection, 2003. **5**(1): p. 13-17.
94. Simons, K. and R. Ehehalt, *Cholesterol, lipid rafts, and disease*. J Clin Invest, 2002. **110**(5): p. 597-603.
95. Hoshino, H., et al., *Membrane-associated activation of cholesterol alpha-glucosyltransferase, an enzyme responsible for biosynthesis of cholesteryl-alpha-D-glucopyranoside in Helicobacter pylori critical for its survival*. J Histochem Cytochem, 2011. **59**(1): p. 98-105.
96. Cox, J.V., et al., *Host HDL biogenesis machinery is recruited to the inclusion of Chlamydia trachomatis-infected cells and regulates chlamydial growth*. Cell Microbiol, 2012. **14**(10): p. 1497-512.
97. Schroeder, G.N. and H. Hilbi, *Cholesterol is required to trigger caspase-1 activation and macrophage apoptosis after phagosomal escape of Shigella*. Cell Microbiol, 2007. **9**(1): p. 265-78.
98. Guillemin, K., et al., *Cag pathogenicity island-specific responses of gastric epithelial cells to Helicobacter pylori infection*. Proceedings of the National Academy of Sciences, 2002. **99**(23): p. 15136-15141.

99. Simons, K. and E. Ikonen, *Functional rafts in cell membranes*. Nature, 1997. **387**(6633): p. 569-72.
100. Goluszko, P. and B. Nowicki, *Membrane cholesterol: a crucial molecule affecting interactions of microbial pathogens with mammalian cells*. Infect Immun, 2005. **73**(12): p. 7791-6.
101. Simons, K. and D. Toomre, *Lipid rafts and signal transduction*. Nat Rev Mol Cell Biol, 2000. **1**(1): p. 31-9.
102. Manes, S., G. del Real, and A.C. Martinez, *Pathogens: raft hijackers*. Nat Rev Immunol, 2003. **3**(7): p. 557-68.
103. Wang, X.Q. and A.S. Paller, *Lipid rafts: membrane triage centers*. J Invest Dermatol, 2006. **126**(5): p. 951-3.
104. Chatterjee, S. and S. Mayor, *The GPI-anchor and protein sorting*. Cell Mol Life Sci, 2001. **58**(14): p. 1969-87.
105. Lang, D.M., et al., *Identification of reggie-1 and reggie-2 as plasmamembrane-associated proteins which cocluster with activated GPI-anchored cell adhesion molecules in non-caveolar micropatches in neurons*. J Neurobiol, 1998. **37**(4): p. 502-23.
106. Langhorst, M.F., A. Reuter, and C.A. Stuermer, *Scaffolding microdomains and beyond: the function of reggie/flotillin proteins*. Cell Mol Life Sci, 2005. **62**(19-20): p. 2228-40.
107. Munro, S., *Lipid rafts: elusive or illusive?* Cell, 2003. **115**(4): p. 377-88.
108. Lopez, D. and R. Kolter, *Functional microdomains in bacterial membranes*. Genes Dev, 2010. **24**(17): p. 1893-902.
109. Donovan, C. and M. Bramkamp, *Characterization and subcellular localization of a bacterial flotillin homologue*. Microbiology, 2009. **155**(Pt 6): p. 1786-99.
110. Bach, J.N. and M. Bramkamp, *Flotillins functionally organize the bacterial membrane*. Mol Microbiol, 2013. **88**(6): p. 1205-17.
111. Mielich-Suss, B., J. Schneider, and D. Lopez, *Overproduction of flotillin influences cell differentiation and shape in Bacillus subtilis*. MBio, 2013. **4**(6): p. e00719-13.
112. Toledo, A., et al., *The lipid raft proteome of Borrelia burgdorferi*. Proteomics, 2015. **15**(21): p. 3662-75.



113. LaRocca, T.J., et al., *Cholesterol lipids of Borrelia burgdorferi form lipid rafts and are required for the bactericidal activity of a complement-independent antibody*. Cell Host Microbe, 2010. **8**(4): p. 331-42.
114. Zhang, H.M., et al., *An alkali-inducible flotillin-like protein from Bacillus halodurans C-125*. Protein J, 2005. **24**(2): p. 125-31.
115. Bramkamp, M. and D. Lopez, *Exploring the existence of lipid rafts in bacteria*. Microbiol Mol Biol Rev, 2015. **79**(1): p. 81-100.
116. Medzhitov, R., *Recognition of microorganisms and activation of the immune response*. Nature, 2007. **449**(7164): p. 819-26.
117. Fritz, J.H., et al., *Nod-like proteins in immunity, inflammation and disease*. Nat Immunol, 2006. **7**(12): p. 1250-7.
118. Salama, N.R., M.L. Hartung, and A. Muller, *Life in the human stomach: persistence strategies of the bacterial pathogen Helicobacter pylori*. Nat Rev Microbiol, 2013. **11**(6): p. 385-99.
119. Ko, G.H., et al., *Invasiveness of Helicobacter pylori into Human Gastric Mucosa*. Helicobacter, 1999. **4**(2): p. 77-81.
120. Perez-Perez, G.I., et al., *Activation of human THP-1 cells and rat bone marrow-derived macrophages by Helicobacter pylori lipopolysaccharide*. Infect Immun, 1995. **63**(4): p. 1183-7.
121. Gewirtz, A.T., et al., *Helicobacter pylori flagellin evades toll-like receptor 5-mediated innate immunity*. J Infect Dis, 2004. **189**(10): p. 1914-20.
122. Allen, L.-A.H., L.S. Schlesinger, and B. Kang, *Virulent Strains of Helicobacter pylori Demonstrate Delayed Phagocytosis and Stimulate Homotypic Phagosome Fusion in Macrophages*. The Journal of Experimental Medicine, 2000. **191**(1): p. 115-128.
123. Kaparakis, M., et al., *Macrophages are mediators of gastritis in acute Helicobacter pylori infection in C57BL/6 mice*. Infect Immun, 2008. **76**(5): p. 2235-9.
124. Suzuki, T., et al., *Localization of antigen-presenting cells in Helicobacter pylori-infected gastric mucosa*. Pathol Int, 2002. **52**(4): p. 265-71.
125. Wang, Y.H., J.J. Wu, and H.Y. Lei, *The autophagic induction in Helicobacter pylori-infected macrophage*. Exp Biol Med (Maywood), 2009. **234**(2): p. 171-80.

126. Zhou, Y.N., et al., *Regulation of cell growth during serum starvation and bacterial survival in macrophages by the bifunctional enzyme SpoT in Helicobacter pylori*. J Bacteriol, 2008. **190**(24): p. 8025-32.
127. Gobert, A.P., et al., *Helicobacter pylori arginase inhibits nitric oxide production by eukaryotic cells: a strategy for bacterial survival*. Proc Natl Acad Sci U S A, 2001. **98**(24): p. 13844-9.
128. Borlace, G.N., R.N. Butler, and D.A. Brooks, *Monocyte and macrophage killing of helicobacter pylori: relationship to bacterial virulence factors*. Helicobacter, 2008. **13**(5): p. 380-7.
129. Gobert, A.P., et al., *Helicobacter pylori heat shock protein 60 mediates interleukin-6 production by macrophages via a toll-like receptor (TLR)-2-, TLR-4-, and myeloid differentiation factor 88-independent mechanism*. J Biol Chem, 2004. **279**(1): p. 245-50.
130. Harris, P.R., et al., *Recombinant Helicobacter pylori urease activates primary mucosal macrophages*. J Infect Dis, 1998. **178**(5): p. 1516-20.
131. Kusugami, K., et al., *Mucosal macrophage inflammatory protein-1alpha activity in Helicobacter pylori infection*. J Gastroenterol Hepatol, 1999. **14**(1): p. 20-6.
132. Yamaoka, Y., et al., *Induction of various cytokines and development of severe mucosal inflammation by cagA gene positive Helicobacter pylori strains*. Gut, 1997. **41**(4): p. 442-451.
133. Crabtree, J.E., et al., *Mucosal tumour necrosis factor alpha and interleukin-6 in patients with Helicobacter pylori associated gastritis*. Gut, 1991. **32**(12): p. 1473-7.
134. Zhuang, Y., et al., *Helicobacter pylori-infected macrophages induce Th17 cell differentiation*. Immunobiology, 2011. **216**(1-2): p. 200-7.
135. Kanneganti, T.D., M. Lamkanfi, and G. Nunez, *Intracellular NOD-like receptors in host defense and disease*. Immunity, 2007. **27**(4): p. 549-59.
136. Motta, V., et al., *NOD-like receptors: versatile cytosolic sentinels*. Physiol Rev, 2015. **95**(1): p. 149-78.
137. Shimada, K., et al., *Oxidized mitochondrial DNA activates the NLRP3 inflammasome during apoptosis*. Immunity, 2012. **36**(3): p. 401-14.

138. Homer, C.R., et al., *A dual role for receptor-interacting protein kinase 2 (RIP2) kinase activity in nucleotide-binding oligomerization domain 2 (NOD2)-dependent autophagy*. J Biol Chem, 2012. **287**(30): p. 25565-76.
139. Magalhaes, J.G., et al., *Nucleotide oligomerization domain-containing proteins instruct T cell helper type 2 immunity through stromal activation*. Proc Natl Acad Sci U S A, 2011. **108**(36): p. 14896-901.
140. Inohara, N. and G. Nunez, *NODs: intracellular proteins involved in inflammation and apoptosis*. Nat Rev Immunol, 2003. **3**(5): p. 371-82.
141. Martinon, F., K. Burns, and J. Tschopp, *The inflammasome: a molecular platform triggering activation of inflammatory caspases and processing of proIL-beta*. Mol Cell, 2002. **10**(2): p. 417-26.
142. Schroder, K. and J. Tschopp, *The inflammasomes*. Cell, 2010. **140**(6): p. 821-32.
143. Schroder, K., et al., *Acute lipopolysaccharide priming boosts inflammasome activation independently of inflammasome sensor induction*. Immunobiology, 2012. **217**(12): p. 1325-9.
144. Strowig, T., et al., *Inflammasomes in health and disease*. Nature, 2012. **481**(7381): p. 278-86.
145. Pérez-Figueroa, E., et al., *Activation of NLRP3 inflammasome in human neutrophils by Helicobacter pylori infection*. Innate Immunity, 2015. **22**(2): p. 103-112.
146. Semper, R.P., et al., *Helicobacter pylori-induced IL-1beta secretion in innate immune cells is regulated by the NLRP3 inflammasome and requires the cag pathogenicity island*. J Immunol, 2014. **193**(7): p. 3566-76.
147. Koch, K.N. and A. Müller, *Helicobacter pylori activates the TLR2/NLRP3/caspase-1/IL-18 axis to induce regulatory T-cells, establish persistent infection and promote tolerance to allergens*. Gut Microbes, 2015. **6**(6): p. 382-387.
148. Benoit, B.N., et al., *Role of ASC in the mouse model of Helicobacter pylori infection*. J Histochem Cytochem, 2009. **57**(4): p. 327-38.
149. Yamauchi, K., et al., *Regulation of IL-18 in Helicobacter pylori infection*. J Immunol, 2008. **180**(2): p. 1207-16.

150. Hitzler, I., et al., *Caspase-1 has both proinflammatory and regulatory properties in Helicobacter infections, which are differentially mediated by its substrates IL-1beta and IL-18*. J Immunol, 2012. **188**(8): p. 3594-602.
151. Tran, L.S., M. Chonwerawong, and R.L. Ferrero, *Regulation and functions of inflammasome-mediated cytokines in Helicobacter pylori infection*. Microbes and Infection, 2017. **19**(9): p. 449-458.
152. Girardin, S.E., et al., *Peptidoglycan molecular requirements allowing detection by Nod1 and Nod2*. J Biol Chem, 2003. **278**(43): p. 41702-8.
153. Inohara, N., et al., *Nod1, an Apaf-1-like activator of caspase-9 and nuclear factor-kappaB*. J Biol Chem, 1999. **274**(21): p. 14560-7.
154. Inohara, N. and G. Nuñez, *The NOD: a signaling module that regulates apoptosis and host defense against pathogens*. Oncogene, 2001. **20**: p. 6473.
155. Girardin, S.E., et al., *Identification of the critical residues involved in peptidoglycan detection by Nod1*. J Biol Chem, 2005. **280**(46): p. 38648-56.
156. Chamaillard, M., et al., *An essential role for NOD1 in host recognition of bacterial peptidoglycan containing diaminopimelic acid*. Nat Immunol, 2003. **4**(7): p. 702-7.
157. Girardin, S.E., et al., *Nod2 is a general sensor of peptidoglycan through muramyl dipeptide (MDP) detection*. J Biol Chem, 2003. **278**(11): p. 8869-72.
158. Moreira, L.O. and D.S. Zamboni, *NOD1 and NOD2 Signaling in Infection and Inflammation*. Front Immunol, 2012. **3**: p. 328.
159. Magalhaes, J.G., et al., *Murine Nod1 but not its human orthologue mediates innate immune detection of tracheal cytotoxin*. EMBO Rep, 2005. **6**(12): p. 1201-7.
160. Zarantonelli, M.L., et al., *Penicillin resistance compromises Nod1-dependent proinflammatory activity and virulence fitness of neisseria meningitidis*. Cell Host Microbe, 2013. **13**(6): p. 735-45.
161. Sycuro, L.K., et al., *Peptidoglycan Crosslinking Relaxation Promotes Helicobacter pylori's Helical Shape and Stomach Colonization*. Cell, 2010. **141**(5): p. 822-833.
162. Wang, G., et al., *Peptidoglycan Deacetylation in Helicobacter pylori Contributes to Bacterial Survival by Mitigating Host Immune Responses*. Infection and Immunity, 2010. **78**(11): p. 4660-4666.

163. Bonis, M., et al., *A M23B family metallopeptidase of Helicobacter pylori required for cell shape, pole formation and virulence*. Mol Microbiol, 2010. **78**(4): p. 809-19.
164. Philpott, D.J., et al., *Reduced activation of inflammatory responses in host cells by mouse-adapted Helicobacter pylori isolates*. Cell Microbiol, 2002. **4**(5): p. 285-96.
165. Vegna, S., et al., *NOD1 Participates in the Innate Immune Response Triggered by Hepatitis C Virus Polymerase*. J Virol, 2016. **90**(13): p. 6022-35.
166. Finney, C.A., et al., *Disruption of Nod-like receptors alters inflammatory response to infection but does not confer protection in experimental cerebral malaria*. Am J Trop Med Hyg, 2009. **80**(5): p. 718-22.
167. Silva, G.K., et al., *Cutting edge: nucleotide-binding oligomerization domain 1-dependent responses account for murine resistance against Trypanosoma cruzi infection*. J Immunol, 2010. **184**(3): p. 1148-52.
168. Kestra, A.M., et al., *Manipulation of small Rho GTPases is a pathogen-induced process detected by NOD1*. Nature, 2013. **496**(7444): p. 233-237.
169. Kufer, T.A., et al., *The pattern-recognition molecule Nod1 is localized at the plasma membrane at sites of bacterial interaction*. Cell Microbiol, 2008. **10**(2): p. 477-86.
170. Uehara, A., et al., *Meso-diaminopimelic acid and meso-lanthionine, amino acids specific to bacterial peptidoglycans, activate human epithelial cells through NOD1*. J Immunol, 2006. **177**(3): p. 1796-804.
171. Fritz, J.H., et al., *Nod1-mediated innate immune recognition of peptidoglycan contributes to the onset of adaptive immunity*. Immunity, 2007. **26**(4): p. 445-59.
172. Shaw, P.J., et al., *Signaling via the RIP2 adaptor protein in central nervous system-infiltrating dendritic cells promotes inflammation and autoimmunity*. Immunity, 2011. **34**(1): p. 75-84.
173. Travassos, L.H., et al., *Nod1 and Nod2 direct autophagy by recruiting ATG16L1 to the plasma membrane at the site of bacterial entry*. Nat Immunol, 2010. **11**(1): p. 55-62.
174. Chen, G.Y., et al., *The innate immune receptor Nod1 protects the intestine from inflammation-induced tumorigenesis*. Cancer Res, 2008. **68**(24): p. 10060-7.

175. Millrud, C.R., et al., *Nod-like receptors in head and neck squamous cell carcinoma*. Acta Otolaryngol, 2013. **133**(12): p. 1333-44.
176. da Silva Correia, J., et al., *Nod1-dependent control of tumor growth*. Proc Natl Acad Sci U S A, 2006. **103**(6): p. 1840-5.
177. Yan, F., et al., *Epidermal growth factor receptor activation protects gastric epithelial cells from Helicobacter pylori-induced apoptosis*. Gastroenterology, 2009. **136**(4): p. 1297-1307, e1-3.
178. Toller, I.M., et al., *Prostaglandin E2 prevents Helicobacter-induced gastric preneoplasia and facilitates persistent infection in a mouse model*. Gastroenterology, 2010. **138**(4): p. 1455-67, 1467.e1-4.
179. Kim, E.J., et al., *Association between genetic polymorphisms of NOD 1 and Helicobacter pylori-induced gastric mucosal inflammation in healthy Korean population*. Helicobacter, 2013. **18**(2): p. 143-50.
180. Hofner, P., et al., *Genetic polymorphisms of NOD1 and IL-8, but not polymorphisms of TLR4 genes, are associated with Helicobacter pylori-induced duodenal ulcer and gastritis*. Helicobacter, 2007. **12**(2): p. 124-31.
181. Wang, P., et al., *Association of NOD1 and NOD2 genes polymorphisms with Helicobacter pylori related gastric cancer in a Chinese population*. World J Gastroenterol, 2012. **18**(17): p. 2112-20.
182. Necchi, V., et al., *In vivo accumulation of Helicobacter pylori products, NOD1, ubiquitinated proteins and proteasome in a novel cytoplasmic structure*. PLoS One, 2010. **5**(3): p. e9716.
183. Tsuji, Y., et al., *Sensing of Commensal Organisms by the Intracellular Sensor NOD1 Mediates Experimental Pancreatitis*. Immunity. **37**(2): p. 326-338.
184. Watanabe, T., et al., *Nucleotide-binding oligomerization domain 1 and gastrointestinal disorders*. Proc Jpn Acad Ser B Phys Biol Sci, 2017. **93**(8): p. 578-599.
185. Kutikhin, A.G., *Role of NOD1/CARD4 and NOD2/CARD15 gene polymorphisms in cancer etiology*. Human immunology, 2011. **72**(10): p. 955-968.
186. Yamaoka, Y., *Mechanisms of disease: Helicobacter pylori virulence factors*. Nat Rev Gastroenterol Hepatol, 2010. **7**(11): p. 629-41.

187. Salama, N.R., M.L. Hartung, and A. Muller, *Life in the human stomach: persistence strategies of the bacterial pathogen Helicobacter pylori*. Nat Rev Micro, 2013. **11**(6): p. 385-399.
188. Huang, Z. and E. London, *Cholesterol lipids and cholesterol-containing lipid rafts in bacteria*. Chemistry and physics of lipids, 2016. **199**: p. 11-16.
189. Liao, W.-C., et al., *Statin Decreases Helicobacter pylori Burden in Macrophages by Promoting Autophagy*. Frontiers in Cellular and Infection Microbiology, 2016. **6**: p. 203.
190. Lin, C.-J., et al., *Statins Attenuate Helicobacter pylori CagA Translocation and Reduce Incidence of Gastric Cancer: In Vitro and Population-Based Case-Control Studies*. PLoS ONE, 2016. **11**(1): p. e0146432.
191. Burroughs, M.H., et al., *Composition of the peptidoglycan of Haemophilus influenzae*. J Biol Chem, 1993. **268**(16): p. 11594-8.
192. Antignac, A., et al., *Detailed structural analysis of the peptidoglycan of the human pathogen Neisseria meningitidis*. J Biol Chem, 2003. **278**(34): p. 31521-8.
193. Liu, M., et al., *The Legionella pneumophila EnhC protein interferes with immunestimulatory muramyl peptide production to evade innate immunity*. Cell host & microbe, 2012. **12**(2): p. 166-176.
194. Blaser, M.J. and D.E. Berg, *Helicobacter pylori genetic diversity and risk of human disease*. Journal of Clinical Investigation, 2001. **107**(7): p. 767-773.
195. Kansau, I., et al., *Genotyping of Helicobacter pylori isolates by sequencing of PCR products and comparison with the RAPD technique*. Res. Microbiol., 1996. **147**(8): p. 661-669.
196. Hutton, M.L., et al., *A Helicobacter pylori Homolog of Eukaryotic Flotillin Is Involved in Cholesterol Accumulation, Epithelial Cell Responses and Host Colonization*. Frontiers in Cellular and Infection Microbiology, 2017. **7**: p. 219.
197. Lee, A., et al., *A standardized mouse model of Helicobacter pylori infection: introducing the Sydney strain*. Gastroenterology, 1997. **112**(4): p. 1386-97.
198. Ferrero, R.L., et al., *Immune Responses of Specific-Pathogen-Free Mice to Chronic Helicobacter pylori (Strain SS1) Infection*. Infection and Immunity, 1998. **66**(4): p. 1349-1355.

199. Lee, A., et al., *A standardized mouse model of Helicobacter pylori infection: introducing the Sydney strain*. Gastroenterology, 1997. **112**(4): p. 1386-1397.
200. Watanabe, K., et al., *Chemoattractants for neutrophils in lipopolysaccharide-induced inflammatory exudate from rats are not interleukin-8 counterparts but gro-gene-product/melanoma-growth-stimulating-activity-related factors*. Eur J Biochem. , 1993. **214**: p. 267-270.
201. Folkening, W.J., et al., *Structure of Bordetella pertussis peptidoglycan*. J Bacteriol, 1987. **169**(9): p. 4223-7.
202. Smart, J., et al., *Cag-delta (Cag3) protein from the Helicobacter pylori 26695 cag type IV secretion system forms ring-like supramolecular assemblies*. FEMS Microbiol Lett, 2017. **364**(1).
203. Pinto-Santini, D.M. and N.R. Salama, *Cag3 is a novel essential component of the Helicobacter pylori Cag type IV secretion system outer membrane subcomplex*. J Bacteriol, 2009. **191**(23): p. 7343-7352.
204. Aihara, E., et al., *Motility and Chemotaxis Mediate the Preferential Colonization of Gastric Injury Sites by Helicobacter pylori*. PLoS Pathogens, 2014. **10**(7): p. e1004275.
205. Ferrero, R.L., J.E. Wilson, and P. Sutton, *Mouse models of Helicobacter-induced gastric cancer: use of cocarcinogens*. Methods Mol Biol, 2012. **921**: p. 157-73.
206. Bolger, A.M., M. Lohse, and B. Usadel, *Trimmomatic: a flexible trimmer for Illumina sequence data*. Bioinformatics, 2014. **30**(15): p. 2114-2120.
207. Li, H. and R. Durbin, *Fast and accurate long-read alignment with Burrows-Wheeler transform*. Bioinformatics, 2010. **26**(5): p. 589-595.
208. Li, H., *A statistical framework for SNP calling, mutation discovery, association mapping and population genetical parameter estimation from sequencing data*. Bioinformatics, 2011. **27**(21): p. 2987-2993.
209. Rohde, M., et al., *A novel sheathed surface organelle of the Helicobacter pylori cag type IV secretion system*. Mol Microbiol., 2003. **49**(1): p. 219-234.
210. Glauner, B., *Separation and quantification of muropeptides with high-performance liquid chromatography*. Analytical Biochemistry, 1988. **172**(2): p. 451-464.



211. Keenan, J., et al., *A role for the bacterial outer membrane in the pathogenesis of Helicobacter pylori infection*. FEMS Microbiol Lett, 2000. **182**(2): p. 259-264.
212. Ferrero, R.L., et al., *NF- $\kappa$ B Activation during Acute Helicobacter pylori Infection in Mice*. Infection and Immunity, 2008. **76**(2): p. 551-561.
213. Schirm, M., et al., *Structural, genetic and functional characterization of the flagellin glycosylation process in Helicobacter pylori*. (0950-382X (Print)).
214. Suarez, G., et al., *Modification of Helicobacter pylori Peptidoglycan Enhances NOD1 Activation and Promotes Cancer of the Stomach*. Cancer Res, 2015. **75**(8): p. 1749-59.
215. Allison, C.C. and R.L. Ferrero, *Role of virulence factors and host cell signaling in the recognition of Helicobacter pylori and the generation of immune responses*. Future Microbiol, 2010. **5**(8): p. 1233-55.
216. Shimada, K., et al., *The NOD/RIP2 pathway is essential for host defenses against Chlamydomydia pneumoniae lung infection*. PLoS Pathog, 2009. **5**(4): p. e1000379.
217. Mosa, A., et al., *Nonhematopoietic cells control the outcome of infection with Listeria monocytogenes in a nucleotide oligomerization domain 1-dependent manner*. Infect Immun, 2009. **77**(7): p. 2908-18.
218. Shi, Y., et al., *Helicobacter pylori-induced Th17 responses modulate Th1 cell responses, benefit bacterial growth, and contribute to pathology in mice*. J Immunol, 2010. **184**(9): p. 5121-9.
219. Allison, C.C., et al., *Nucleotide oligomerization domain 1 enhances IFN- $\gamma$  signaling in gastric epithelial cells during Helicobacter pylori infection and exacerbates disease severity*. J Immunol, 2013. **190**(7): p. 3706-15.
220. Bertin, J., et al., *Human CARD4 protein is a novel CED-4/Apaf-1 cell death family member that activates NF- $\kappa$ B*. J Biol Chem, 1999. **274**(19): p. 12955-8.
221. Girardin, S.E., et al., *CARD4/Nod1 mediates NF- $\kappa$ B and JNK activation by invasive Shigella flexneri*. EMBO Rep, 2001. **2**(8): p. 736-42.
222. Yoo, N.J., et al., *Nod1, a CARD protein, enhances pro-interleukin-1 $\beta$  processing through the interaction with pro-caspase-1*. Biochemical and Biophysical Research Communications, 2002. **299**(4): p. 652-658.

223. Ashida, H., et al., *Cell death and infection: a double-edged sword for host and pathogen survival*. J Cell Biol, 2011. **195**(6): p. 931-42.
224. Ferrero, R.L., et al., *Outbred mice with long-term Helicobacter felis infection develop both gastric lymphoid tissue and glandular hyperplastic lesions*. J Pathol, 2000. **191**(3): p. 333-40.
225. Sutton, P., et al., *A genetic basis for atrophy: dominant non-responsiveness and helicobacter induced gastritis in F(1) hybrid mice*. Gut, 1999. **45**(3): p. 335-40.
226. Chonwerawong, M., et al., *Interferon-gamma promotes gastric lymphoid follicle formation but not gastritis in Helicobacter-infected BALB/c mice*. Gut Pathog, 2016. **8**: p. 61.
227. Ritchie, M.E., et al., *limma powers differential expression analyses for RNA-sequencing and microarray studies*. Nucleic Acids Res, 2015. **43**(7): p. e47.
228. Masumoto, J., et al., *Nod1 acts as an intracellular receptor to stimulate chemokine production and neutrophil recruitment in vivo*. J Exp Med, 2006. **203**(1): p. 203-13.
229. Caruso, R., et al., *NOD1 and NOD2: Signaling, Host Defense, and Inflammatory Disease*. Immunity, 2014. **41**(6): p. 898-908.
230. Travassos, L.H., et al., *Nod1 participates in the innate immune response to Pseudomonas aeruginosa*. J Biol Chem, 2005. **280**(44): p. 36714-8.
231. Fox, J.G., et al., *High-salt diet induces gastric epithelial hyperplasia and parietal cell loss, and enhances Helicobacter pylori colonization in C57BL/6 mice*. Cancer Res, 1999. **59**(19): p. 4823-8.
232. Touati, E., et al., *Chronic Helicobacter pylori infections induce gastric mutations in mice*. Gastroenterology, 2003. **124**(5): p. 1408-1419.
233. Algood, H.M., et al., *Regulation of gastric B cell recruitment is dependent on IL-17 receptor A signaling in a model of chronic bacterial infection*. J Immunol, 2009. **183**(9): p. 5837-46.
234. Nakajima, S., et al., *Mast cell involvement in gastritis with or without Helicobacter pylori infection*. Gastroenterology, 1997. **113**(3): p. 746-54.
235. Bimczok, D., et al., *Human primary gastric dendritic cells induce a Th1 response to H. pylori*. Mucosal Immunology, 2010. **3**: p. 260.
236. McGee, D.J. and H.L. Mobley, *Pathogenesis of Helicobacter pylori infection*. Curr Opin Gastroenterol, 2000. **16**(1): p. 24-31.

237. Sawai, N., et al., *Role of gamma interferon in Helicobacter pylori-induced gastric inflammatory responses in a mouse model*. Infect Immun, 1999. **67**(1): p. 279-85.
238. Yamaoka, Y., et al., *Natural History of Gastric Mucosal Cytokine Expression in Helicobacter pylori Gastritis in Mongolian Gerbils*. Infection and Immunity, 2005. **73**(4): p. 2205-2212.
239. Kao, J.Y., et al., *Helicobacter pylori immune escape is mediated by dendritic cell-induced Treg skewing and Th17 suppression in mice*. Gastroenterology, 2010. **138**(3): p. 1046-1054.
240. Fernandez, N., et al., *Mannan and peptidoglycan induce COX-2 protein in human PMN via the mammalian target of rapamycin*. Eur J Immunol, 2007. **37**(9): p. 2572-82.
241. Lappas, M., *NOD1 expression is increased in the adipose tissue of women with gestational diabetes*. J Endocrinol, 2014. **222**(1): p. 99-112.
242. Oshima, H., et al., *Prostaglandin E(2) signaling and bacterial infection recruit tumor-promoting macrophages to mouse gastric tumors*. Gastroenterology, 2011. **140**(2): p. 596-607.e7.
243. Lu, Y., et al., *PAC1 Deficiency in a Murine Model Induces Gastric Mucosa Hypertrophy and Higher Basal Gastric Acid Output*. Journal of Molecular Neuroscience, 2011. **43**(1): p. 76-84.
244. Le, S.V., et al., *PAC1 and PACAP expression, signaling, and effect on the growth of HCT8, human colonic tumor cells*. Regul Pept, 2002. **109**(1-3): p. 115-25.
245. Seaborn, T., et al., *Protective effects of pituitary adenylate cyclase-activating polypeptide (PACAP) against apoptosis*. Curr Pharm Des, 2011. **17**(3): p. 204-14.
246. Calam, J., *Helicobacter pylori modulation of gastric acid*. The Yale Journal of Biology and Medicine, 1999. **72**(2-3): p. 195-202.
247. El - Omar, E.M., *Mechanisms of increased acid secretion after eradication of Helicobacter pylori infection*. Gut, 2006. **55**(2): p. 144-146.
248. Takashima, M., et al., *Effects of <em>Helicobacter pylori</em> infection on gastric acid secretion and serum gastrin levels in Mongolian gerbils*. Gut, 2001. **48**(6): p. 765.

249. Crew, K.D. and A.I. Neugut, *Epidemiology of gastric cancer*. World Journal of Gastroenterology : WJG, 2006. **12**(3): p. 354-362.
250. Blaser, M.J., et al., *Infection with Helicobacter pylori strains possessing cagA is associated with an increased risk of developing adenocarcinoma of the stomach*. Cancer Res, 1995. **55**(10): p. 2111-5.
251. Franco, A.T., et al., *Activation of beta-catenin by carcinogenic Helicobacter pylori*. Proc Natl Acad Sci U S A, 2005. **102**(30): p. 10646-51.
252. Thompson, L.J., et al., *Chronic Helicobacter pylori Infection with Sydney Strain 1 and a Newly Identified Mouse-Adapted Strain (Sydney Strain 2000) in C57BL/6 and BALB/c Mice*. Infection and Immunity, 2004. **72**(8): p. 4668-4679.
253. Nagy, T.A., et al., *Helicobacter pylori regulates cellular migration and apoptosis by activation of PI3K signaling*. The Journal of infectious diseases, 2009. **199**(5): p. 641-651.
254. Patel, S.R., et al., *Helicobacter pylori downregulates expression of human  $\beta$ -defensin 1 in the gastric mucosa in a type IV secretion-dependent fashion*. Cellular Microbiology, 2013. **15**(12): p. 2080-2092.
255. Sycuro, L.K., et al., *Flow cytometry-based enrichment for cell shape mutants identifies multiple genes that influence Helicobacter pylori morphology*. Mol Microbiol, 2013. **90**(4): p. 869-83.
256. Kim, H.S., et al., *Structural basis for the recognition of muramyltripeptide by Helicobacter pylori Csd4, a D,L-carboxypeptidase controlling the helical cell shape*. Acta Crystallogr D Biol Crystallogr, 2014. **70**(Pt 11): p. 2800-12.
257. Kim, H.S., et al., *The Cell Shape-determining Csd6 Protein from Helicobacter pylori Constitutes a New Family of L,D-Carboxypeptidase*. J Biol Chem, 2015. **290**(41): p. 25103-17.
258. Frirdich, E., et al., *Peptidoglycan-Modifying Enzyme Pgp1 Is Required for Helical Cell Shape and Pathogenicity Traits in Campylobacter jejuni*. PLoS Pathogens, 2012. **8**(3): p. e1002602.
259. Ha, R., et al., *Accumulation of Peptidoglycan O-Acetylation Leads to Altered Cell Wall Biochemistry and Negatively Impacts Pathogenesis Factors of Campylobacter jejuni*. J Biol Chem, 2016. **291**(43): p. 22686-22702.

260. Stahl, M., et al., *The Helical Shape of Campylobacter jejuni Promotes In Vivo Pathogenesis by Aiding Transit through Intestinal Mucus and Colonization of Crypts*. Infect Immun, 2016. **84**(12): p. 3399-3407.
261. Gall, A., et al., *TIFA Signaling in Gastric Epithelial Cells Initiates the cag Type 4 Secretion System-Dependent Innate Immune Response to Helicobacter pylori Infection*. MBio, 2017. **8**(4).
262. Gaudet, R.G., et al., *Cytosolic detection of the bacterial metabolite HBP activates TIFA-dependent innate immunity*. Science, 2015. **348**(6240): p. 1251.
263. Gaudet, R.G. and S.D. Gray-Owen, *Heptose Sounds the Alarm: Innate Sensing of a Bacterial Sugar Stimulates Immunity*. PLoS Pathog, 2016. **12**(9): p. e1005807.
264. Gaudet, R.G., et al., *Innate Recognition of Intracellular Bacterial Growth Is Driven by the TIFA-Dependent Cytosolic Surveillance Pathway*. Cell Rep, 2017. **19**(7): p. 1418-1430.
265. Milivojevic, M., et al., *ALPK1 controls TIFA/TRAF6-dependent innate immunity against heptose-1,7-bisphosphate of gram-negative bacteria*. PLoS Pathog, 2017. **13**(2): p. e1006224.
266. Zimmermann, S., et al., *ALPK1- and TIFA-Dependent Innate Immune Response Triggered by the Helicobacter pylori Type IV Secretion System*. Cell Rep, 2017. **20**(10): p. 2384-2395.
267. Miampamba, M., et al., *Expression of pituitary adenylate cyclase-activating polypeptide and PACAP type 1 receptor in the rat gastric and colonic myenteric neurons*. Regul Pept, 2002. **105**(3): p. 145-54.
268. Fradinger, E.A., et al., *Characterization of four receptor cDNAs: PAC1, VPAC1, a novel PAC1 and a partial GHRH in zebrafish*. Mol Cell Endocrinol, 2005. **231**(1-2): p. 49-63.
269. Tennant, S.M., et al., *Influence of Gastric Acid on Susceptibility to Infection with Ingested Bacterial Pathogens*. Infection and Immunity, 2008. **76**(2): p. 639-645.
270. Kavathas, P.B., et al., *Nod1, but not the ASC inflammasome, contributes to induction of IL-1 $\beta$  secretion in human trophoblasts after sensing of Chlamydia trachomatis*. Mucosal immunology, 2013. **6**(2): p. 235-243.

271. Shimada, M., et al., *Helicobacter pylori* infection upregulates interleukin-18 production from gastric epithelial cells. European journal of gastroenterology & hepatology, 2008. **20**(12): p. 1144-1150.
272. Tomita, T., et al., *Expression of Interleukin-18, a Th1 cytokine, in human gastric mucosa is increased in Helicobacter pylori infection.* J Infect Dis, 2001. **183**(4): p. 620-7.
273. Yamauchi, K., et al., *Regulation of IL-18 in Helicobacter pylori Infection.* Journal of immunology (Baltimore, Md. : 1950), 2008. **180**(2): p. 1207-1216.
274. Duewell, P., et al., *NLRP3 inflammasomes are required for atherogenesis and activated by cholesterol crystals.* Nature, 2010. **464**: p. 1357.
275. Rajamaki, K., et al., *Cholesterol crystals activate the NLRP3 inflammasome in human macrophages: a novel link between cholesterol metabolism and inflammation.* PLoS One, 2010. **5**(7): p. e11765.
276. Le Bourhis, L., S. Benko, and S.E. Girardin, *Nod1 and Nod2 in innate immunity and human inflammatory disorders.* Biochem Soc Trans, 2007. **35**(Pt 6): p. 1479-84.
277. Correa, R.G., S. Milutinovic, and J.C. Reed, *Roles of NOD1 (NLRC1) and NOD2 (NLRC2) in innate immunity and inflammatory diseases.* Biosci Rep, 2012. **32**(6): p. 597-608.
278. McGovern, D.P., et al., *Association between a complex insertion/deletion polymorphism in NOD1 (CARD4) and susceptibility to inflammatory bowel disease.* Hum Mol Genet, 2005. **14**(10): p. 1245-50.
279. Hysi, P., et al., *NOD1 variation, immunoglobulin E and asthma.* Hum Mol Genet, 2005. **14**(7): p. 935-41.
280. Schertzer, J.D., et al., *NOD1 activators link innate immunity to insulin resistance.* Diabetes, 2011. **60**(9): p. 2206-15.
281. Chan, K.L., et al., *Circulating NOD1 Activators and Hematopoietic NOD1 Contribute to Metabolic Inflammation and Insulin Resistance.* Cell Rep, 2017. **18**(10): p. 2415-2426.
282. Cardenas, I., et al., *Nod1 activation by bacterial iE-DAP induces maternal-fetal inflammation and preterm labor.* J Immunol, 2011. **187**(2): p. 980-6.
283. Hildebrandt, E. and D.J. McGee, *Helicobacter pylori lipopolysaccharide modification, Lewis antigen expression, and gastric colonization are cholesterol-dependent.* BMC Microbiol, 2009. **9**: p. 258.

